IAEA-TECDOC-1719

IAEA TECDOC SERIES

IAEA-TECDOC-1719

Environmental Sensitivity in Nuclear Emergencies in Rural and Semi-natural Environments

Report of Working Group 8, Environmental Sensitivity of EMRAS II Topical Heading Approaches for Assessing Emergency Situations

Environmental Modelling for Radiation Safety (EMRAS II) Programme

IAEA
International Atomic Energy Agency

IAEA SAFETY STANDARDS AND RELATED PUBLICATIONS

IAEA SAFETY STANDARDS

Under the terms of Article III of its Statute, the IAEA is authorized to establish or adopt standards of safety for protection of health and minimization of danger to life and property, and to provide for the application of these standards.

The publications by means of which the IAEA establishes standards are issued in the **IAEA Safety Standards Series**. This series covers nuclear safety, radiation safety, transport safety and waste safety. The publication categories in the series are **Safety Fundamentals**, **Safety Requirements** and **Safety Guides**.

Information on the IAEA's safety standards programme is available at the IAEA Internet site

http://www-ns.iaea.org/standards/

The site provides the texts in English of published and draft safety standards. The texts of safety standards issued in Arabic, Chinese, French, Russian and Spanish, the IAEA Safety Glossary and a status report for safety standards under development are also available. For further information, please contact the IAEA at PO Box 100, 1400 Vienna, Austria.

All users of IAEA safety standards are invited to inform the IAEA of experience in their use (e.g. as a basis for national regulations, for safety reviews and for training courses) for the purpose of ensuring that they continue to meet users' needs. Information may be provided via the IAEA Internet site or by post, as above, or by email to Official.Mail@iaea.org.

RELATED PUBLICATIONS

The IAEA provides for the application of the standards and, under the terms of Articles III and VIII.C of its Statute, makes available and fosters the exchange of information relating to peaceful nuclear activities and serves as an intermediary among its Member States for this purpose.

Reports on safety and protection in nuclear activities are issued as **Safety Reports**, which provide practical examples and detailed methods that can be used in support of the safety standards.

Other safety related IAEA publications are issued as **Radiological Assessment Reports**, the International Nuclear Safety Group's **INSAG Reports**, **Technical Reports** and **TECDOCs**. The IAEA also issues reports on radiological accidents, training manuals and practical manuals, and other special safety related publications.

Security related publications are issued in the **IAEA Nuclear Security Series**.

The **IAEA Nuclear Energy Series** consists of reports designed to encourage and assist research on, and development and practical application of, nuclear energy for peaceful uses. The information is presented in guides, reports on the status of technology and advances, and best practices for peaceful uses of nuclear energy. The series complements the IAEA's safety standards, and provides detailed guidance, experience, good practices and examples in the areas of nuclear power, the nuclear fuel cycle, radioactive waste management and decommissioning.

ENVIRONMENTAL SENSITIVITY IN NUCLEAR EMERGENCIES IN RURAL AND SEMI-NATURAL ENVIRONMENTS

The following States are Members of the International Atomic Energy Agency:

AFGHANISTAN
ALBANIA
ALGERIA
ANGOLA
ARGENTINA
ARMENIA
AUSTRALIA
AUSTRIA
AZERBAIJAN
BAHRAIN
BANGLADESH
BELARUS
BELGIUM
BELIZE
BENIN
BOLIVIA
BOSNIA AND HERZEGOVINA
BOTSWANA
BRAZIL
BULGARIA
BURKINA FASO
BURUNDI
CAMBODIA
CAMEROON
CANADA
CENTRAL AFRICAN REPUBLIC
CHAD
CHILE
CHINA
COLOMBIA
CONGO
COSTA RICA
CÔTE D'IVOIRE
CROATIA
CUBA
CYPRUS
CZECH REPUBLIC
DEMOCRATIC REPUBLIC OF THE CONGO
DENMARK
DOMINICA
DOMINICAN REPUBLIC
ECUADOR
EGYPT
EL SALVADOR
ERITREA
ESTONIA
ETHIOPIA
FIJI
FINLAND
FRANCE
GABON
GEORGIA
GERMANY
GHANA
GREECE
GUATEMALA
HAITI
HOLY SEE
HONDURAS
HUNGARY
ICELAND
INDIA
INDONESIA
IRAN, ISLAMIC REPUBLIC OF
IRAQ
IRELAND
ISRAEL
ITALY
JAMAICA
JAPAN
JORDAN
KAZAKHSTAN
KENYA
KOREA, REPUBLIC OF
KUWAIT
KYRGYZSTAN
LAO PEOPLE'S DEMOCRATIC REPUBLIC
LATVIA
LEBANON
LESOTHO
LIBERIA
LIBYA
LIECHTENSTEIN
LITHUANIA
LUXEMBOURG
MADAGASCAR
MALAWI
MALAYSIA
MALI
MALTA
MARSHALL ISLANDS
MAURITANIA
MAURITIUS
MEXICO
MONACO
MONGOLIA
MONTENEGRO
MOROCCO
MOZAMBIQUE
MYANMAR
NAMIBIA
NEPAL
NETHERLANDS
NEW ZEALAND
NICARAGUA
NIGER
NIGERIA
NORWAY
OMAN
PAKISTAN
PALAU
PANAMA
PAPUA NEW GUINEA
PARAGUAY
PERU
PHILIPPINES
POLAND
PORTUGAL
QATAR
REPUBLIC OF MOLDOVA
ROMANIA
RUSSIAN FEDERATION
RWANDA
SAUDI ARABIA
SENEGAL
SERBIA
SEYCHELLES
SIERRA LEONE
SINGAPORE
SLOVAKIA
SLOVENIA
SOUTH AFRICA
SPAIN
SRI LANKA
SUDAN
SWAZILAND
SWEDEN
SWITZERLAND
SYRIAN ARAB REPUBLIC
TAJIKISTAN
THAILAND
THE FORMER YUGOSLAV REPUBLIC OF MACEDONIA
TOGO
TRINIDAD AND TOBAGO
TUNISIA
TURKEY
UGANDA
UKRAINE
UNITED ARAB EMIRATES
UNITED KINGDOM OF GREAT BRITAIN AND NORTHERN IRELAND
UNITED REPUBLIC OF TANZANIA
UNITED STATES OF AMERICA
URUGUAY
UZBEKISTAN
VENEZUELA
VIETNAM
YEMEN
ZAMBIA
ZIMBABWE

The Agency's Statute was approved on 23 October 1956 by the Conference on the Statute of the IAEA held at United Nations Headquarters, New York; it entered into force on 29 July 1957. The Headquarters of the Agency are situated in Vienna. Its principal objective is "to accelerate and enlarge the contribution of atomic energy to peace, health and prosperity throughout the world''.

IAEA-TECDOC-1719

ENVIRONMENTAL SENSITIVITY IN NUCLEAR EMERGENCIES IN RURAL AND SEMI-NATURAL ENVIRONMENTS

REPORT OF WORKING GROUP 8
ENVIRONMENTAL SENSITIVITY
OF EMRAS II TOPICAL HEADING
APPROACHES FOR ASSESSING EMERGENCY SITUATIONS

ENVIRONMENTAL MODELLING FOR
RADIATION SAFETY (EMRAS II) PROGRAMME

INTERNATIONAL ATOMIC ENERGY AGENCY
VIENNA, 2013

For further information on this publication, please contact:

Waste and Environment Safety Section
Assessment and Management of Environmental Releases Unit
International Atomic Energy Agency
Vienna International Centre
PO Box 100
1400 Vienna, Austria
Email: Official.Mail@iaea.org

Printed by the IAEA in Austria
November 2013

IAEA Library Cataloguing in Publication Data

Environmental sensitivity in nuclear emergencies in rural and semi-natural environments : report of Working Group 8, environmental sensitivity of EMRAS II topical heading approaches for assessing emergency situations ; Environmental Modelling for RAdiation Safety (EMRAS II) Programme. – Vienna : International Atomic Energy Agency, 2013.
p. ; 30 cm. – (IAEA-TECDOC series, ISSN 1011-4289
; no. 1719)
ISBN 978-92-0-112610-8
Includes bibliographical references.

1. Radiation – Mathematical models. 2. Ionizing radiation – Environmental aspects. 3. Radioisotopes – Environmental aspects. I. International Atomic Energy Agency. II. Series.

IAEAL 13-00852

FOREWORD

Environmental assessment models are used for evaluating the radiological impact of actual and potential releases of radionuclides to the environment. They are essential tools for use in the regulatory control of routine discharges to the environment and also in planning measures to be taken in the event of accidental releases. They are also used for predicting the impact of releases which may occur far into the future, for example, from underground radioactive waste repositories. It is important to verify, to the extent possible, the reliability of the predictions of such models by comparison with measured values in the environment or by comparing them with the predictions of other models.

The IAEA has been organizing programmes of international model testing since the 1980s. The programmes have contributed to a general improvement in models, in transfer data and in the capabilities of modellers in Member States. IAEA publications on this subject over the past three decades demonstrate the comprehensive nature of the programmes and record the associated advances which have been made.

From 2009 to 2011, the IAEA organized a programme entitled Environmental Modelling for RAdiation Safety (EMRAS II), which concentrated on the improvement of environmental transfer models and the development of reference approaches to estimate the radiological impacts on humans, as well as on flora and fauna, arising from radionuclides in the environment. The following topics were addressed in nine working groups:

Reference Approaches for Human Dose Assessment

- Working Group 1: Reference Methodologies for Controlling Discharges of Routine Releases
- Working Group 2: Reference Approaches to Modelling for Management and Remediation at NORM and Legacy Sites
- Working Group 3: Reference Models for Waste Disposal

Reference Approaches for Biota Dose Assessment

- Working Group 4: Biota Modelling
- Working Group 5: Wildlife Transfer Coefficient Handbook
- Working Group 6: Biota Dose Effects Modelling

Approaches for Assessing Emergency Situations

- Working Group 7: Tritium Accidents
- Working Group 8: Environmental Sensitivity
- Working Group 9: Urban Areas

This report describes the work of the Environmental Sensitivities Working Group. The work was partially supported by the FMO/EEA FM Grants through the EL0086 — NTUA

Scholarship and Mobility Program 2004–2011. The IAEA officer responsible for this publication was V. Berkovskyy of the Division of Radiation, Transport and Waste Safety.

ACKNOWLEDGEMENT

The work of the researcher L. Monte from ENEA institute and of J.E. Brittain from Oslo University is gratefully acknowledged with regard to their constant cooperation and scientific support throughout the modelling implementation. The contributions of the researchers P.A. Georgopoulos, C. Tsabaris, G. Korres, A. Paulidou, P. Drakopoulou, A. Machias, V. Kapsimalis and S. Kabbadas from HCMR and N. Maragos from NTUA, is acknowledged with regard to their contributions of unpublished data, scientific information, as well as fruitful and informative discussions. The IAEA also wishes to acknowledge the contribution made by the Working Group Leader, B. Tracy.

CONTENTS

SUMMARY

This report describes work undertaken by Working Group 8 of the IAEA's EMRAS II Programme to explore the concept of environmental sensitivity in rural and semi-natural environments following a nuclear emergency. Sensitivity was broadly defined as the effect *(Y)* to a set of conditions *(X)* for a given stress *(D)*. For the purposes of this report, *D* was taken to be radionuclide deposition per square meter, *Y* was the dose to an adult member of the critical group and *X* represented all the intervening environmental factors which modify the doses to the critical group. Lists of the factors most likely to affect sensitivity were compiled for each of several different kinds of environments.

A series of modelling exercises were carried out in order to explore the relative sensitivities of different environments and to understand the chief factors contributing to the sensitivity of each environment. Altogether 4 broad types of environments were considered:

- Temperate and alpine agricultural;
- Temperate forest and arctic tundra;
- Freshwater aquatic; and
- Shallow marine or coastal.

The agricultural environments included temperate zones in Canada and western Europe and also the alpine zone in central Europe. The temperate forest and arctic sites were all located in Canada, where indigenous peoples depend to a large degree on these environments for a major portion of their food supply. The freshwater aquatic scenarios involved widely-differing lakes in Italy, Norway, Ontario and northern Saskatchewan. The coastal marine settings involved 6 locations across northern Europe and 2 locations in the Mediterranean Sea.

Each environment was assumed to receive 1000 Bq/m^2 of each of the two long-lived radionuclides – ^{137}Cs and ^{90}Sr – and one short-lived radionuclide – ^{131}I. Modelers were asked to calculate the concentrations of these radionuclides in key environmental compartments as functions of time after the event and also to calculate the doses to an adult, a 10 year old child and a 1 year old infant living in a community that inhabits the environment under consideration and derives a major portion of its food resources from that environment.

The adult dose during the first year from ^{137}Cs has been shown to be a particularly useful indicator of sensitivity. The ^{137}Cs doses dominate in most environments, with the highest values obtained for agricultural settings, followed by temperate forests where the pathway lichens → grazing animals → humans dominates. The sensitivity is less in freshwater aquatic environments and least in marine environments. However, there are situations where consideration of other radionuclides can add additional information. For instance, ^{90}Sr and ^{131}I may have greater impacts on children and infants, particularly through the grass → cow → milk pathway. In certain scenarios, ^{90}Sr in water may be important, because of its persistence in the solution phase. In the coastal marine environments, ^{131}I uptake may be significant from edible seaweeds, whereas ^{239}Pu may be important from consumption of molluscs.

It must be emphasized that sensitivity is not only climate dependent but also depends on social and economic factors such as individual living habits, food consumption preferences and agricultural practices. Seasonal differences perhaps contribute the greatest degree of variability and uncertainty in all the environmental settings considered here except coastal marine. Depth of the water body is very important in both freshwater aquatic and shallow marine environments. In human dose assessments, the greatest variability factor is the assumed consumption rate of a contaminated food item. For this reason, radionuclide concentrations in major food items and drinking water should be used as supplementary indicators of sensitivity.

1. INTRODUCTION

The objective of Working Group 8 (WG8) of the EMRAS II Programme was to explore the concept of environmental sensitivity in rural and semi-natural environments after an emergency situation. The main tasks of the Working Group were to:

- Formulate the concept of environmental sensitivity;
- Compile a list of sensitivity factors;
- Design scenarios;
- Carry out modelling exercises based on these scenarios.

In the modelling exercises the approach taken by the Working Group was not so much to conduct an inter-comparison of different models, but rather to use the models as tools to explore the relative sensitivities of different environments and to understand the chief factors contributing to the sensitivity of each environment. Nonetheless, 3 independent models were run for each type of environment in order to give the results some degree of robustness.

Altogether 4 broad types of environments were considered:

- Temperate and alpine agricultural;
- Temperate forest and arctic tundra;
- Treshwater aquatic;
- Shallow marine or coastal.

The agricultural environments included temperate zones in Canada and Western Europe and also the alpine zone in central Europe. The temperate forest and arctic sites were all located in Canada, where indigenous peoples depend to a large degree on these environments for as major portion of their food supply. The freshwater aquatic scenarios involved widely-differing lakes in Italy, Norway, Ontario, and northern Saskatchewan. The coastal marine settings involved 6 locations across northern Europe and 2 locations in the Mediterranean Sea.

Each environment was assumed to receive 1000 Bq/m^2 of each of the 2 long-lived radionuclides – ^{137}Cs and ^{90}Sr – and 1 short-lived radionuclide – ^{131}I. Modelers were asked to calculate the concentrations of these radionuclides in key environmental compartments as functions of time after the event, and also to calculate the doses to human populations who receive most or all of their food intake from the respective environments.

The concept of environmental sensitivity is developed in Section 2. Lists of sensitivity factors applicable to different environments are compiled in Section 3. Section 4 sets forth the modelling exercises designed to assess the sensitivities of various rural and semi-natural environments. Results of the modelling exercises are presented in Sections 5–8. Section 9 contains a comparison and discussion of the results.

It is hoped that this report will prove useful in emergency planning and preparedness by identifying sensitive areas and developing emergency response plans appropriate to those areas. During the actual response to the emergency, the results can aid in setting priorities for the allocation of limited resources. The identification of vulnerable environments should prove valuable in planning the locations of new nuclear facilities.

2. THE CONCEPT OF ENVIRONMENTAL SENSITIVITY

2.1. A DEFINITION OF ENVIRONMENTAL SENSITIVITY

What is meant by environmental sensitivity? In everyday language the word sensitivity is somewhat ambiguous and unfortunately this ambiguity carries over into the scientific context. Among the various dictionary definitions, we find, for instance, that sensitivity is "the capacity of an organism or sense organ to respond to stimulation". A more insightful definition for our discussion states that "an object, whether animate or inanimate, is sensitive to a certain feature of the environment if it behaves differently according to the presence or absence of that feature". This notion of sensitivity assumes that the behaviour of the object depends on some features of the environment without any direct reference to the magnitude of the stimulus that produces the behaviour.

Particular interpretations of the meaning of the environmental sensitivity notion can be found in several radioecological studies:

- By analysing the sensitivity of the lacustrine environment, Håkanson et al. [1] remarked that "a given load (=fallout) of any substance to a given lake may cause very different concentrations in water and biota depending on the characteristics of the lake and its catchment".
- An environmental sensitivity analysis exercise performed by Aarkrog [2] was aimed at assessing how "the values of the time integrated activity concentrations of ^{137}Cs and ^{90}Sr in milk (Bq L^{-1} y) per Bq m^{-2} of radionuclide fallout depend on the geographic area where contamination occurred".
- A study from Howard [3] focused on "the individual and collective doses for a given radionuclide fallout in different regions".

The above definitions are particular instances of a more general principle:

Sensitivity is the effect (or set of effects) *Y* to a condition (or set of conditions) *X* for a given stress (or set of stresses) *D*.

According to this definition the notion of sensitivity is a triadic relationship among 3 elements: a set of effects or consequences, an independent set of conditions and a set of given stresses. If *X* and *D* can be expressed as mathematical functions of independent or dependent variables, then we can introduce the expression:

$$Y = S(X, D) \tag{1}$$

If *Y* is proportional to *D*, Equation (1) becomes:

$$Y = S(X) \cdot D \tag{2}$$

Thus the sensitivity *S(X)* is the ratio between an effect *(Y)* and a stress *(D)*·*S(X)* can be used to rank the conditions *X* according to their effects *Y*. For instance, the stress *D* could be a radionuclide deposition on a lake surface in Bq/m^2; the effect *Y* could be the radionuclide concentration in water; *X* could represent the set of parameters needed to characterize the lake environment. If there is a wide range of variability in *Y* for a particular parameter *X*, e.g. mean water residence time, then we can say that the radionuclide concentration in lake water is very sensitive to the mean water retention time.

TABLE 1. THE CATEGORICAL ELEMENTS IN THE GENERAL STRUCTURE OF THE SENSITIVITY CONCEPT IN RELATION TO DIFFERENT TYPES OF APPLICATIONS IN RADIOECOLOGICAL ASSESSMENTS

Approach	**Terms in sensitivity definition**		
	Effect *(Y)*	**Condition *(X)***	**Stress *(D)***
Håkanson et al. [1]	Environmental (radionuclides in water and biota)	Environmental (characteristics of the lacustrine system)	Environmental (radionuclide deposition)
Aarkrog [2]	Environmental (radionuclides in milk)	Environmental (type of geographic region)	Environmental (radionuclide deposition)
Howard [3]	Social (radiation dose)	Environmental (type of geographic region)	Environmental (radionuclide deposition)
Shaw et al. [4]	Social (radiation dose reduction)	Economic/environmental (economic and environmental features of countermeasure options)	Environmental (radionuclide contamination of forests)

The modelling exercises in this report were performed by accounting for such a definition of sensitivity. Even when the above formalism is not mentioned explicitly, the pragmatic character of the exercises insures that the reader will easily understand the practical meaning of the notion of sensitivity.

The above expression is consistent with the notion of "model sensitivity analysis" that aims at evaluating how the variations in the model parameters influence the model output for a given value of the input. The next step is to identify the *elements* of the above functions, namely, the sets of effects, conditions and stresses necessary for performing environmental sensitivity analyses. It seems natural to select these elements from 3 main categories – environmental, social and economic factors – which are of paramount importance in the decision process for the management of environmental emergencies.

Table 1 shows the 3 categorical elements (economic, social and environmental factors) according to environmental sensitivity analysis performed by Håkanson et al. [1], Aarkrog [2], Howard [3] and Shaw et al. [4].

In this report, the stresses are radionuclide depositions in Bq/m^2. The primary effects are doses to an adult, a 10 year old child and a 1 year old infant living in a community that lives in the environment under consideration and derives a major portion of its food resources from that environment. Admittedly, there are many other stresses that should have been considered, such as impacts on individual species, the local ecosystem, or on the local economy. However, this would have made the report too unwieldy and would not have facilitated the comparison of impacts in the different environments considered here. A more detailed evaluation of stresses on other systems must await a future study.

2.2. ALTERNATE DEFINITIONS OF SENSITIVITY

It is noteworthy that alternative definitions of environmental sensitivity are reported in the international literature, such as that suggested by Buckley [5]: "The environmental sensitivity of a given environment unit may usefully be defined as the relation between the response of that unit to a given stress, and the severity of the stress". Although the above definition is frequently adopted, it does not convey in full the meaning associated with the notion of environmental sensitivity that is commonly in radioecology.

On the other hand, the Buckley's definition seems to comply with the notion of environmental vulnerability that, according to the OECD glossary of statistical terms[1] is the "measure of the extent to which a community, structure, service or geographical area is likely to be damaged or disrupted, on account of its nature or location, by the impact of a particular disaster hazard" [6].

The definition of Buckley is somewhat conflicting with the notion of sensitivity that we have previously illustrated. However, we should recognize that the concept of "biological sensitivity" is often used in radioecology and is related to the intensity of the response of a species to radiation in agreement with the Buckley's definition.

It is useful to recall the notion of "susceptibility" in order to plainly understand the purport of the use of the different terms "sensitivity" and "vulnerability". The concept of "susceptibility" takes into account the risk of exposure to a stressor of a given environmental unit.

A more proper use of the above words can be helpful to avoid the previously mentioned conflict of meanings. Indeed, the "biological sensitivity" could be better defined "biological vulnerability of a species". On the other hand, the "ecological vulnerability of a species" could refer to the response of the species to the stressor when the ecological factors (trophic level, habitat, etc.) that determine the risk of exposure of the species to the stressor in the environment (susceptibility) are accounted for.

An obvious advantage of such a kind of terminology is the unequivocal use of appropriate terms to denote different concepts (vulnerability, susceptibility and sensitivity) by limiting the notion of sensitivity to the variability of the intensity of an effect as a function of certain conditions.

2.3. UNCERTAINTY AND SENSITIVITY ANALYSES

In assessing *radioecological sensitivity* and the related variability of radiation doses, model sensitivity and uncertainty analysis are commonly employed [3].

Uncertainty analysis is the process of estimating the uncertainties in model predictions that result from the uncertainties in model inputs. It provides an indication of where the greatest uncertainty lies in the model and which parameter estimates need to be improved in order to achieve better predictions. This involves a determination of the variations in the output results based upon variations in input parameters. Usually, an uncertainty analysis is done prior to a sensitivity analysis.

Knowledge of the uncertainties in the model predictions can be useful in 2 ways. It can be helpful in making decisions about countermeasures to apply in response to accidental releases of radionuclides. Second, it aids in deciding if efforts should be made to collect more data on input parameters in order to try to reduce the uncertainties. Since a model such as a food-chain model may have many input parameters, and reducing every input parameter distribution function (PDF) may require huge effort, it is important to prioritize efforts. This can be done through sensitivity analysis.

Sensitivity analysis is the process of estimating the sensitivity of the model predictions to changes in the input parameter values. It ascertains which environmental parameters are most

[1] See http://stats.oecd.org/glossary/detail.asp?ID=2886

"responsible" for ecosystem sensitivity and can thus lead to higher doses. This requires that the model includes the particular parameter or set of parameters as input variables, although there may be proxy variables that estimate the sensitive parameter. Sensitivity analysis helps ranking the input parameters based upon how much impact they have on the output end point.

The following is an example of the formal processes for performing uncertainty and sensitivity analysis of a particular model. The methods discussed are those implemented in the CHERPAC code (see Section 5.1.1) although they can be applied to any environmental code with appropriate modifications.

In CHERPAC, the uncertainty analysis is carried out using a numerical Monte Carlo approach [7, 8]. Probability density functions (PDFs) and correlations for many CHERPAC input parameters have been developed based on data from the literature and the judgment of qualified experts. Latin hypercube sampling of the input parameter PDFs is used to generate 1000 sets of input parameter values, which were used in 1000 model runs to produce distributions of model predictions. CHERPAC calculates the means and the 2.5^{th} and 97.5^{th} percentiles (95% confidence limits) of these distributions. The sampling of the input PDFs and analysis of the distributed predictions is carried out using coding developed at Sandia National Laboratories [9].

In CHERPAC, the sensitivity analysis is carried out statistically using the information generated during the uncertainty analysis described above and using coding developed at Sandia National Laboratories [10]. For each combination of distributed input parameter and output variable, the standardized regression and partial correlation coefficients can be calculated from the previously-determined distributed input and output values. Alternately, the coefficients can be determined from the ranks of the values, rather than the values themselves. The latter method is often better when nonlinear relationships are involved. The regression coefficients and correlation coefficients provide slightly different and complementary information on the response of the model to changes in a given parameter value. However, the relative magnitudes of values of either of these coefficients indicate the relative sensitivity of a model output to different input parameters.

The accuracy of the regression and correlation coefficients is dependent upon the number of distributed input parameters. Therefore, for cases involving a large number of distributed input parameters, it is generally recommended that an iterative analysis process be used to accurately identify the most important input parameters. Initially, all the potentially-distributed parameters should be treated as having uncertain values, and the regression and correlation coefficients calculated. For the next iteration, the least important parameters should be assigned deterministic values, and the coefficients re-calculated. The process should be repeated until only a few important input parameters are treated as having uncertain values.

3. ENVIRONMENTAL SENSITIVITY FACTORS

3.1. INTRODUCTION

The notion of sensitivity described in the previous chapter refers to the variability of the intensity of an effect as a function of certain conditions. With reference to the general principle (see Equation (1) above), sensitivity factors will be those variables *X* which determine the extent of effects *Y* due to a stress *D*.

In 2000, Howard divided the criteria affecting variation in exposure into 4 main categories: pathways, habits, location and habitats and communities. Working group participants agreed to focus on the doses to humans living in rural and semi natural environments, expressed as individual exposures, leaving other biota and ecosystem responses as well as collective doses to future exercises. In analogy to the critical group approach [3], the human populations were assumed to derive a major portion of their food resources from the contaminated environment and to spend long periods of time in contaminated areas.

A major goal of this exercise was to identify critical sensitivity factors in key environmental compartments that are responsible for the major radionuclide impacts on that environment. The range of environments considered here are not exhaustive but reflect the capabilities and interests of individual Working Group members. The main components of the environmental pathways and the underlying processes that can lead to accumulation of large amounts of specific radionuclides have been derived from previous modelling exercises and from environmental radioactivity measurements.

The following listing of sensitivity factors is based on a literature review [11, 12] as well as other published data. The sensitivity factors have been subsequently grouped and linked to the environments in focus. The sensitivity factors have been used to fine-tune the modelling exercises.

Sensitivity factors are radionuclide specific, time dependent, and spatially variable. Changes over time in the radionuclide activity concentrations in environmental compartments can be characterized by their biological or ecological half-lives [11]. The environmental sensitivity factors will be different under short term scenarios or mid-long term scenarios. Their influence will also vary depending on the scenario of an acute or a continuous release.

Climate is also an important factor of environmental sensitivity, connected to spatial variability [13]. Areas with high precipitation rates, for instance, received much higher amounts of global fallout than those areas which received little precipitation [14] (cited by Howard [3]). Animal nutritional requirements and stable/analogous element status in the feedstuff will affect absorption of radionuclides through the gastrointestinal tract. For instance, a low content of Ca will enhance absorption of Sr.

Interactions between environmental and agricultural practices are also important. For instance, in the model CHERPAC [15–17], the pasture activity decreases because of weathering. However, the activity in the feeding diet may increase when the feeding regime switches to the use of stored feed that has been harvested immediately after the deposition.

3.2. AGRICULTURAL ENVIRONMENT, INCLUDING ALPINE

The sensitivity of the agricultural environment depends on a series of factors whose importance changes with geographic, climatic and anthropic conditions. Among them, the development of the plant canopy and the gastrointestinal absorption of animals can be considered key factors of sensitivity in the short term [18, 19], while the time after contamination and radionuclide mobility in soil become sensitive factors in the longer term [20, 21].

The sensitivity of the alpine environment is linked to a retarded migration of radionuclides into deeper soil layers and a higher plant uptake and longer ecological half-lives in comparison to lowland ecosystems [22].

Sensitivity factors are first of all radionuclide specific. A list of element-specific parameters for the agricultural environment derived from the CHERPAC code [15] is summarized below. It is followed by a list of non-element-specific parameters for those components of the environment studied in the scenario.

3.2.1. List of element-specific parameters for the agricultural environment

- Dry deposition velocities (m s^{-1}) for iodine (elemental and organic) and particulates;
- Washout ratios (dimensionless) for iodine (elemental and organic) and particulates;
- Fraction of wet deposition retained on plants;
- Weathering half-life of the element on plants;
- Loss rate (d^{-1}) of the element from surface soil;
- Loss rate (d^{-1}) of the element from soil in the rooting zone;
- Translocation factors (m^2 kg^{-1}) for plants;
- Concentration ratios from soil to plants;
- Fraction of element retained from bovine ingestion;
- Transfer factors (d L^{-1}) from animal feed to raw food products;
- Loss rate (d^{-1}) of element during storage of raw food products;
- Processing factors, i.e. fraction of activity in 1 kg of processed product (e.g. cheese) compared with 1 kg of raw product (e.g. milk);
- Transfer factors (d kg^{-1}) from forage to meat (e.g. beef or pork);
- Loss rate (d^{-1}) of element from meat;
- Fraction of element absorbed by animal lung or gut;
- Processing reduction factors for plant and animal products.

TABLE 2. LIST OF NON-ELEMENT-SPECIFIC PARAMETERS FOR THE AGRICULTURAL ENVIRONMENT

Compartment or food item	Parameter
Soil	– Density of soil – Shallow seeding depth of vegetables – Deep seeding depth of grain – Fraction of bare soil where vegetables are not growing – Fraction of soil adhering to potatoes and root crops
Leafy vegetables	– Month in which leafy vegetables start to grow – First and last months for harvesting and eating fresh – Yield of leafy vegetables
Root crops and potato toes	– Month in which root crops start to grow – First and last months for harvested and eating fresh – # of days between harvesting and ingestion
Fodder and grain	– Month when grain starts to grow – Month when grain is harvested – # of days between harvest and ingestion of grain – Months of first and second cuts of hay – Yield of pasture
Fruit	– Month in which fruit starts to grow – First and last months that fruit is harvested and eaten fresh – Month that fruit is harvested and stored for eating
Cattle	– Husbandry and animal diet • month that cows are let onto pasture • month that cows are taken off pasture • pasture consumption by cows • stored forage consumption by cows – Soil ingestion by cows on pasture – Storage time • # of days between milking and ingestion of (processed) milk products • # of days between slaughter and ingestion of meat
Poultry	– Husbandry and animal diet • month that poultry is let outdoors • month that poultry is brought in for the winter • ingestion of grain by chickens – Ingestion of soil by free-range chickens – Storage time • # of days between laying and ingestion of eggs • # of days between slaughter and ingestion of poultry
Pork	– Animal diet • milk intake by pigs • grain intake by pigs – Weight of pig at slaughter – Storage time (# days between slaughter and ingestion)

3.3. TEMPERATE FOREST AND ARCTIC TUNDRA ENVIRONMENTS

Forest ecosystems differ in radionuclide biogeochemistry and exposure pathways from agricultural ecosystems. Mushrooms and forest berries, recognized as an important natural food, can accumulate radiocaesium to a significant degree in comparison with foodstuffs grown in agricultural systems. The radionuclide concentration in game animals depends on their feeding habits and complex diets, and reflects the soil and pasture conditions varying between locations and seasons [23]:

- Type of forest (deciduous, spruce forest, peat bogs, etc.);
- Soil type (clay, loam, sand, organic);
- Radionuclide distribution coefficients in soils;
- Aggregate transfer coefficients of radionuclides to berries and mushrooms;
- Dry matter content of mushrooms and berries;
- Aggregate transfer coefficients of radionuclides to large and small game;
- Biological half-times in plants and animals;
- Harvest quantities of wild plants and animals;
- Carcass weights of animals;
- First and last months that mushrooms are harvested and eaten fresh;
- Month that mushrooms are harvested and stored for eating;
- First month of berry season, (assumed to be 2 months long);
- First month of hunting season (assumed to be 3 months long) for big game;
- First month of hunting season (assumed to be 6 months long) for small game;
- Loss rate from soil rooting zone for mushrooms;
- Loss rate from wild berries;
- Processing reduction factors for mushrooms and wild berries;
- Processing factor for big and small game;
- Loss rate of element from big and small game.

Arctic ecosystems show a high sensitivity to contamination by radionuclides. The rates of biogeochemical processes are generally slower than in temperate regions. Contaminants can therefore reside for longer periods in the biota of arctic than of temperate ecosystems. The most sensitive arctic food pathway is considered the food chain: lichen → reindeer or caribou → human. However contamination in cow milk and lamb meat may be a larger problem in some Arctic areas. Mushrooms, freshwater fish and berries may also be important exposure pathways [24].

- Open tundra or boreal forest;
- Presence and depth of permafrost;
- Fraction of the year with snow and ice cover;
- Mass interception factor for lichens;
- Biological half-times in lichens.

3.4. FRESHWATER ECOSYSTEMS

A number of factors are crucial in determining the sensitivity of particular freshwater environments to contamination by radioactive isotopes. These can be either catchment characteristics or properties of the actual lake or river [1, 25–27]. Arctic and alpine freshwaters are often more sensitive on account of their low biomass, low ionic concentrations and high runoff over frozen ground in spring. Nevertheless, certain lowland lakes with long retention times can give rise to continued high activity concentrations in biota. In general rivers are less sensitive compared to lakes as the wave of contamination will have a relatively short residence time.

TABLE 3. LIST OF SENSITIVITY FACTORS IN FRESHWATER ECOSYSTEMS

Environmental sensitivity parameter	**Most sensitive**	**Comments**
Water retention time	Long retention times	Especially seepage lakes and lakes with retention times >10 years
Water volume	Small volume	
Ionic concentration	Low concentrations	Especially analogues, e.g. K for Cs and Ca for Sr
Sedimentation rate	Low sedimentation rate	Contaminated sediments are rapidly covered when sedimentation rates are high.
Catchment soils	Soils low in clays	Organic and sandy soils are particularly sensitive.
Catchment characteristics	Frozen ground	In Arctic and alpine areas spring runoff will be greater over frozen ground.
Seasonality	Contamination during production season	Most sensitive usually during spring and summer
Biomass	Low biomass	Biological dilution
Food chain characteristics	Long food chains with predatory fish	Accumulation of certain elements higher up in the food chain

3.5. SHALLOW MARINE OR COASTAL ENVIRONMENTS

Environmental marine modelling has to simultaneously describe the dispersion of radionuclides in water and sediment phases; bioaccumulation of radionuclides in biota and finally, dose assessments. It is obvious that such an approach comes up against the problem of complexity and the need for a large set of parameters. The sensitivity analysis of the model parameters can contribute to identifying important processes and parameters in a specific ecosystem.

The following parameters have been considered [28]:

- Depth and water volume;
- Residence time;
- Sedimentation rate;
- Suspended sediment load in the water column;
- Concentration factor to biota;
- Surface sediment thickness;
- Porosity of bottom sediment;
- Density of sediment material.

4. DESCRIPTION OF THE MODELLING EXERCISES

The modelers were given the following set of instructions:

4.1. SOURCE TERM

The source term consists of one instantaneous deposition of 1000 Bq/m^2 of each of the radionuclides ^{137}Cs, ^{90}Sr, and ^{131}I. Each deposition should be considered under dry conditions and heavy rainfall (20 mm/hour).

4.2. SEASONAL EFFECTS

Effects may vary greatly depending on season of the year. Each environment should be modeled under different seasonal conditions corresponding roughly to winter, spring, summer, and autumn. The exact dates of these seasons will vary, depending on climate conditions in the environment being studied. A rough guide to seasonal designation is given in Table 4.

Where applicable, the following soil types should be considered: clay, loam, sand, and organic.

4.3. RADIONUCLIDE CONCENTRATIONS IN SOIL, WATER, PLANTS AND ANIMALS

Calculate radionuclide concentrations in soils (terrestrial environments) or water (aquatic and marine environments. Calculate concentrations in plant and animal types consumed by humans, or as parts of food chains leading to human.

4.4. DIETARY INTAKES

Assume a human population which obtains all or nearly all of their food intake from the specified environment. This will require some judgment and may require some adjustment in later stages of the exercise. Specify the assumptions made in the dietary intake. During this phase of the exercise, do not assume that any countermeasures have been put in place.

4.5. DOSE CALCULATIONS

Use standard ingestion dose coefficients, e.g. from ICRP 72 [29]. Compute doses from a full year of consumption for adult, 10 year old child, 1 year old infant. Do this for the first year and the second year following the accident, and at later times if relevant. Results of the modelling exercises for the various environments are presented in Sections 5–8. Section 9 contains a comparison and discussion of the results.

TABLE 4. MODELLING FOR SEASONAL EFFECTS

Season	Approximate date in north temperate zone	Description
Winter	February	Ground is frozen and snow-covered; animals are on dry fodder and sheltered inside
Spring	May	Snow is gone; fields have been planted; animals are on pasture
Summer	August	Crops are mature and ready for harvest; animals are still on pasture
Autumn	November	Crops have been harvested, animals are on dry fodder and sheltered inside; ground is not yet frozen or snow-covered

TABLE 5. IMPORTANT BIOTIC COMPARTMENTS FOR FOOD CHAINS LEADING TO HUMANS

Scenario	Plants	Animals
Temperate agricultural	Fresh and dry forage, garden vegetables, fruits, root crops, grain, (rice).	Milk and milk products, beef, lamb (pork, chicken, eggs)
Alpine	Fresh and dry forage, berries, mushrooms.	Milk and milk products, (deer)
Temperate forest	Berries, mushrooms	Big game – deer, moose, elk; small game – rabbits, birds; fish
Arctic	Fresh and dry forage, lichens, berries, mushrooms	Reindeer or caribou, milk and milk products, (musk ox); fish
Shallow marine	Seaweed	Fish, shellfish – crustaceans, molluscs

Bracketed items are optional.

5. AGRICULTURAL AND ALPINE MODEL RESULTS

5.1. AGRICULTURAL SCENARIO, ONTARIO, CANADA LOCATION, CHERPAC CODE

5.1.1. Model description

The CHERPAC (CHalk River Environmental Research Pathways Analysis Code) code was developed by AECL to predict the time-dependent concentrations of radionuclides in environmental compartments and the resulting radiation dose to humans following an accidental release of radionuclides from a nuclear facility [15–17]. Its primary purpose is to calculate the ingestion dose to humans from terrestrial pathways following accidental atmospheric releases, but it has some additional capabilities. CHERPAC can be used for assessing long-term effects of nuclear accidents, both in the near-field and far-field.

CHERPAC was developed and enhanced through its usage in international model intercomparison studies using Chernobyl fallout data from European countries (e.g. Finland and Czech Republic). Some models in CHERPAC and parameter values for them were taken from the routine-release dose calculation methodology of CSA Standard N288.1-M87 [30] and adapted for simulating accidental releases.

The models are expressed in terms of simple analytical equations that require no special mathematical or numerical methods to solve. Concentrations and doses are calculated at discrete points in time, using in a time-stepping approach.

CHERPAC can be used to make either deterministic predictions or stochastic predictions (means and 2.5th and 97.5th percentiles) using a Latin hypercube sampling (LHS) method [9]. For stochastic predictions, the input parameters can follow any of a wide variety of probability distribution functions or PDFs (e.g. normal, lognormal, uniform, triangular, and user-defined) and parameter correlations can be taken into account. CHERPAC can also perform sensitivity analysis using partial correlation and standardized regression coefficients methods [10].

Predictions can be made for any 1 of 25 radionuclides (^{51}Cr, ^{54}Mn, ^{59}Fe, ^{58}Co, ^{60}Co, ^{65}Zn, ^{89}Sr, ^{90}Sr, ^{95}Zr, ^{95}Nb, ^{99}Mo, ^{103}Ru, ^{106}Ru, ^{132}Te, ^{131}I, ^{132}I, ^{133}I, ^{134}I, ^{135}I, ^{134}Cs, ^{136}Cs, ^{137}Cs, ^{140}Ba, ^{141}Ce and ^{144}Ce) released to the atmosphere.

The calculations are based on input values of daily-average measured ground-level air concentration of radionuclide and daily rainfall at the location of the receptor. The code predicts radionuclide concentrations in soil, forage grass, leafy and non-leafy above-ground vegetables, potatoes, other root crops, fruits, winter and spring grains, wild berries and mushrooms, milk, cheese, beef, pork, eggs, chicken, and small and large game. It predicts radiation doses to a man, woman and 10 year old child as a result of ingestion, inhalation, cloudshine and groundshine; and also predicts the human body burden resulting from ingestion and inhalation. CHERPAC also has a limited capability for calculating human dose and body burden from the ingestion of fish. The code accounts for seasonality and is capable of handling an accident occurring at any time of year. It accounts for the time between the harvest of food products and their ingestion and also for other losses resulting from food processing. Pathways modelled in CHERPAC are shown in Figure 1.

Most of the default parameter values (e.g. diet, growing season, yield, animal diets and concentration ratios) provided with the code are specific to Ontario, Canada, but the code can be used for other regions by proper adjustment of the parameters.

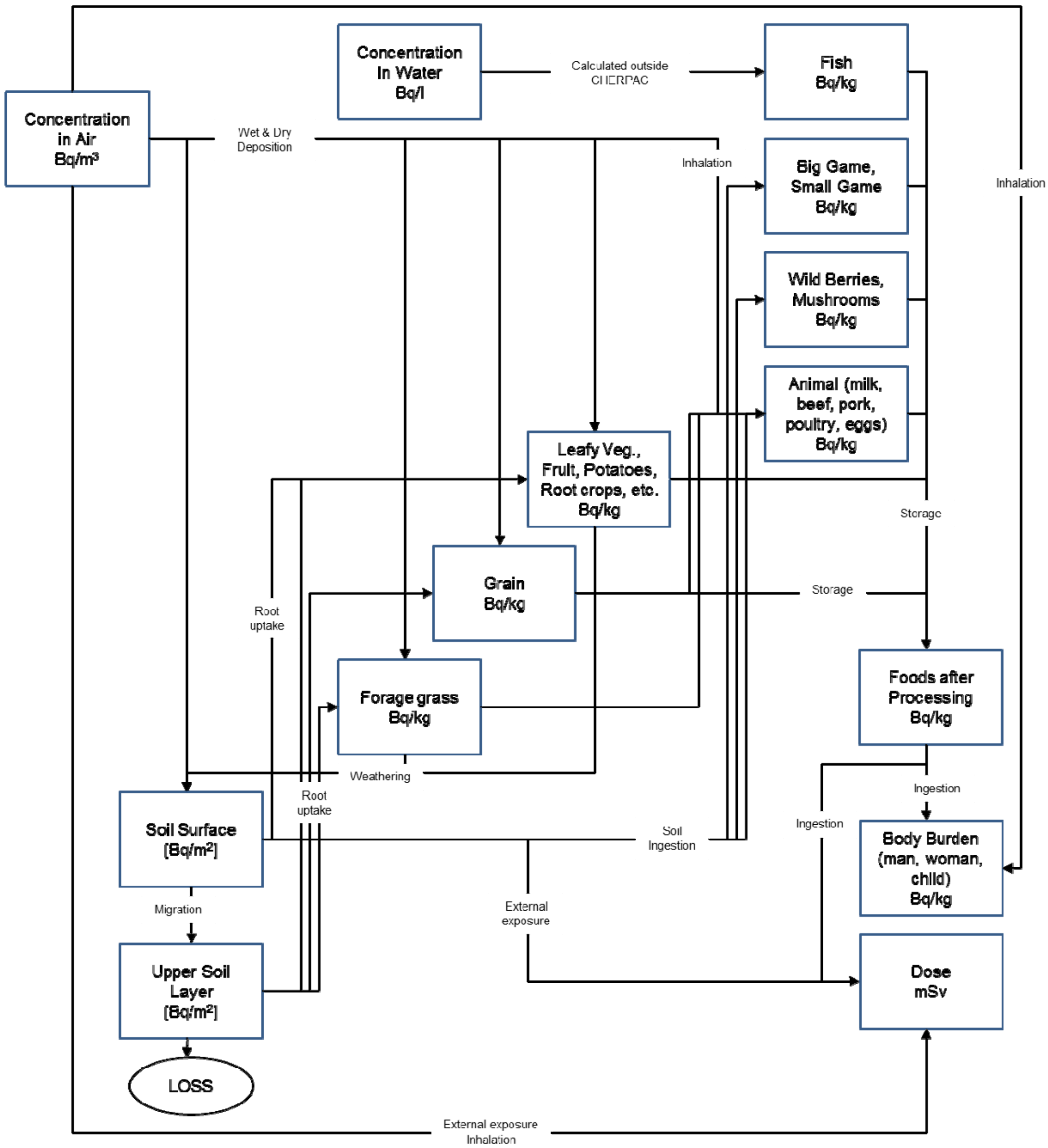

FIG. 1. Pathways modelled in CHERPAC.

5.1.2. Scenario description

In this scenario, it was assumed that 1000 Bq m^{-2} of ^{137}Cs, ^{90}Sr and ^{131}I were deposited instantaneously in an agricultural ecosystem. It was also assumed that people living in this ecosystem were self-sufficient with respect to the agricultural products included in this scenario and did not consume contaminated forest food products.

Cases of the deposition occurring under dry or heavy rainfall conditions were evaluated. Seasonal effects were evaluated by considering cases in which the deposition occurred in winter, spring, summer, or autumn. The concentrations in common food products and the ingestion and groundshine doses to an adult, a 10 year old child and a 1 year old infant were predicted for a 2 year period following the deposition.

5.1.3. Application of CHERPAC to the agricultural scenario

A 1 year old infant age class was added to CHERPAC. The calculations started with the air concentrations of radionuclides, which were calibrated to achieve the desired amount of deposited activity on grass and bare soil surfaces. The direct transfer from air to plant and products was disabled. Calculations were performed using CHERPAC's default parameter values. A clay soil type was assumed.

5.1.4. Results

Although detailed results were calculated for all cases, most of the discussion and figures presented here are for one case: the dry deposition of ^{137}Cs in summer (August). Many of the comments made here apply to other cases also. Some additional comments relating to other cases are also made.

5.1.4.1. Top mixed layer of soil covered with grass or grain

Figure 2 illustrates that the soil concentration builds up over the first few months because some deposited activity is initially retained by the plant leaves but then washes off and transfers to the soil. The soil concentration peaks at 4 months, and then decreases very slowly because of radioactive decay (30 year half-life for ^{137}Cs) and other losses from soil due to erosion, volatilization, leaching and crop removal (100 year half-time).

A larger fraction of activity is initially retained on the plants if the deposition occurs in dry conditions rather than during heavy rain, when large fractions of the radionuclides initially retained are immediately washed off. Soil activity is also sensitive to the timing of the deposition. For example, if deposition occurs close to harvest, then some deposited activity is removed by harvesting.

5.1.4.2. *Plant products*

Figure 3 shows that the plant product concentrations depend on many factors including plant uptake and retention characteristics, plant rooting depth, the timing of the deposition, the migration of activity through the soil and agricultural practices.

For deposition in summer, the concentration in all plants initially decreases because the activity deposited directly on the plants is washed off and removed by other processes (15 day half-life). Forage grass and leafy vegetables initially have the highest concentrations because these plants have parameter values that favour the uptake and retention of radionuclides. The forage grass concentrations shown here are for grass ingested by dairy cows. In Ontario dairy cows eat fresh grass from May to October and then eat grass harvested in August from November to April. Following an August deposition, the concentration in forage decreases during September and October, but in November it returns to its August value because the cows are now consuming grass that was harvested in August.

For dry deposition in summer, the greenhouse vegetables initially have the lowest concentrations. This is because greenhouses are partly open to the atmosphere, so the dry deposition inside is only a fraction of that outside. In the sixth month, the concentrations increase because some soil in the greenhouses is replaced with the outdoor soil, which is more heavily contaminated.

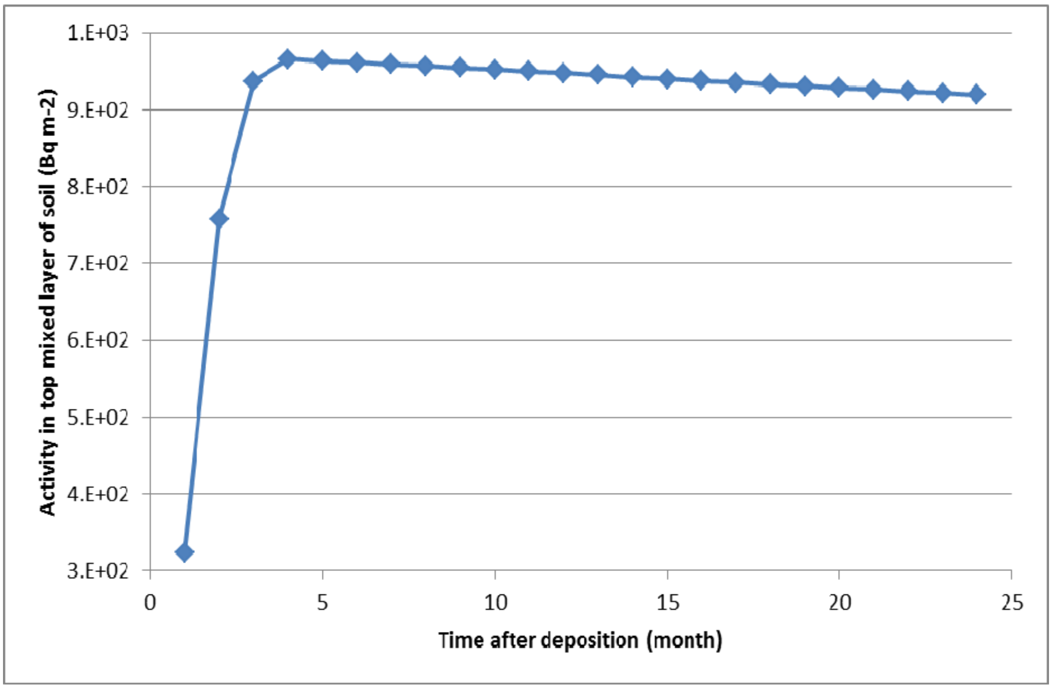

FIG. 2. CHERPAC-predicted activity in top mixed layer of soil covered with grass or grain: ^{137}Cs, dry deposition in summer (August).

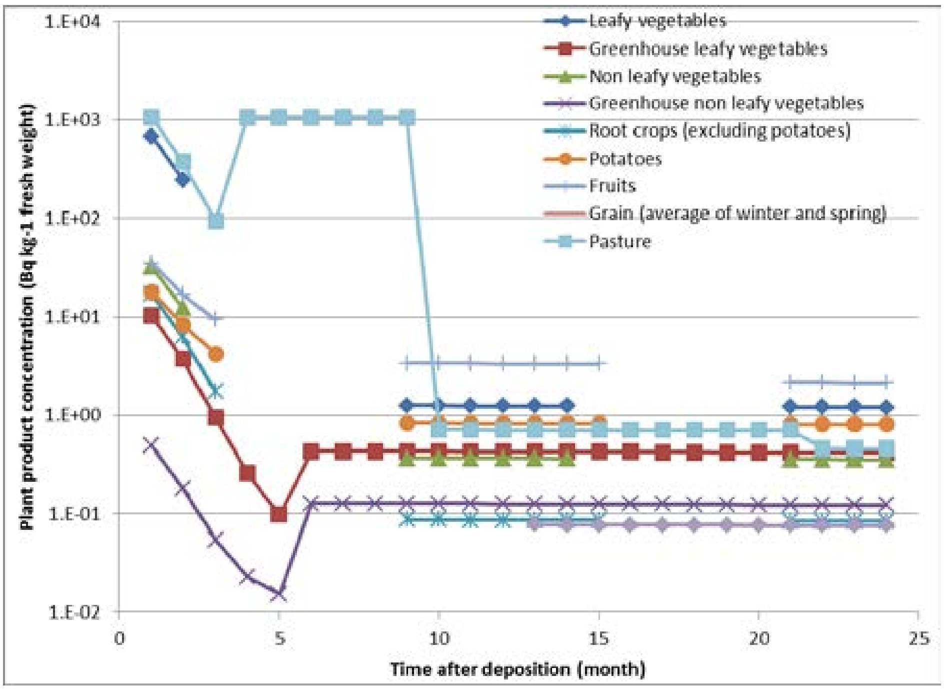

FIG. 3. CHERPAC-predicted concentrations in plant products: ^{137}Cs, dry deposition in summer (August). Except for forage grass, all values are in-field. Forage grass values are those at consumption.

5.1.4.3. Animal products

Figure 4 shows the animal product concentrations depend on many factors including animal uptake and retention characteristics, soil concentrations, grass and grain concentrations and agricultural practices. In general, concentrations are highest in beef and lowest in eggs.

For the first 2 months after deposition in summer, the concentration in beef is zero because the cattle are assumed to eat grass stored from the previous year. The concentration rises when they start eating grass harvested in the current year. Grass for beef cattle is harvested twice (June and August). Grass from the first harvest is fed to the cattle from July to September and grass from the second harvest is fed to them for the remaining months. The large decrease in beef concentration starting twelve months after deposition is because of the much lower grass and grain concentrations for the same period.

Dairy cows are assumed to eat fresh grass in the first 3 months after deposition in summer, so the concentrations in milk and cheese decrease with the decrease in grass concentration during this period. The predicted milk and cheese concentrations increase in November when the cows start eating stored grass.

For deposition in summer, the concentrations in chicken and eggs initially build up through soil ingestion only, because chickens are assumed to eat grain harvested before the deposition. When chickens are taken indoors in November, the concentration in eggs drops to zero immediately, and the concentration in chicken meat drops to zero over a 3-month period corresponding to the life span of the chickens.

The predictions for pigs are for Canadian animals that are kept indoors. It is assumed that they are slaughtered when they are 6 months old. For the first 2 months, pigs drink milk; and for all 6 months, they eat grain.

5.1.4.4. Doses to Humans from ^{137}Cs

Figure 5 illustrates the ingestion doses are about 2 orders of magnitude higher than the groundshine doses. The differences in ingestion doses for different age groups result from differences in intake rates and dose conversion factors (DCFs). The peak percentage contributions from various food products to monthly total ingestion dose to an adult are: milk, 86% in month 2; leafy vegetables, 32% in month 3; cheese, 6% in month 11; beef, 97% in month 13; fruits, 46% in month 22; and potatoes, 13% in month 23. The cumulative ingestion dose to adult at 1 year after the deposition event came 45% from milk, 45% from beef, and only 10% from the remaining food items.

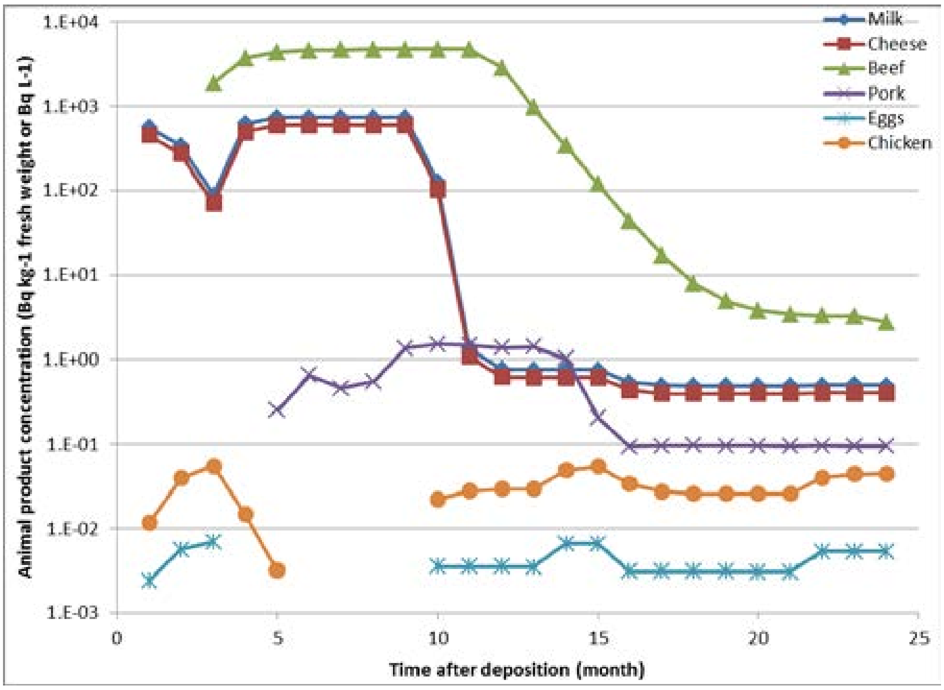

FIG. 4. CHERPAC-predicted concentrations in domestic animal products: ^{137}Cs, dry deposition in summer (August).

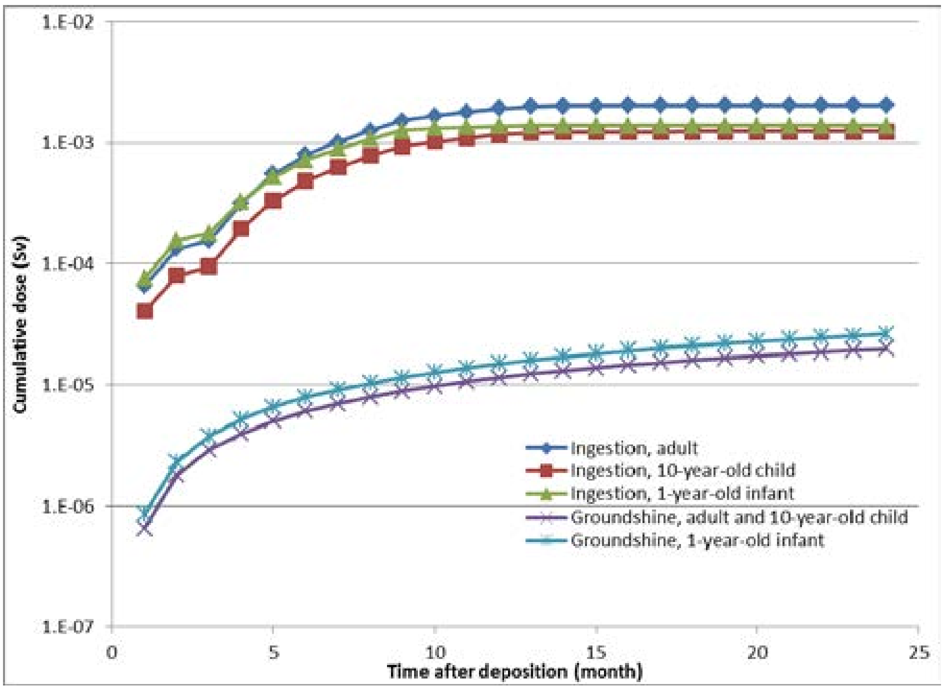

FIG. 5. CHERPAC-predicted cumulative doses to humans: ^{137}Cs, dry deposition in summer (August).

5.1.4.5. Cumulative doses from all radionuclides at 2 years after the deposition event

Figure 6 shows that the ingestion doses are highest if deposition occurs in summer (August), and lowest if it occurs in fall (November). For summer deposition, the plants are nearly ready to be harvested, whereas, for fall deposition, no plants are growing and much activity is lost from the soil before the ground is seeded in the spring. Groundshine doses are not dependent on the season of in which the deposition occurs.

The degree of variation in ingestion dose as a function of the timing of deposition is radionuclide dependent. For ^{131}I, which has a short half-life, the ingestion dose resulting from deposition in the fall or winter is significantly lower than that resulting from deposition in the spring or summer. For ^{137}Cs and ^{90}Sr, which have long half-lives, the ingestion doses are not as dependent on the season in which the deposition occurs.

The age group receiving the highest ingestion dose is also radionuclide dependent. The ingestion dose from ^{137}Cs is highest for adults, whereas the ingestion doses from ^{90}Sr and ^{131}I are highest for infants. This is because of the relative food product concentrations, intake rates and dose conversion factors (DCFs). The relative groundshine doses to different age groups depend mainly upon the relative DCFs.

If the deposition occurs in spring or summer, the ingestion dose under dry conditions is up to 3 times higher than that under heavy rainfall conditions; then the activity initially retained are largely immediately washed off.

5.1.5. Uncertainty/sensitivity analysis

An uncertainty analysis and a sensitivity analysis were performed only for the case of the cumulative ingestion dose to an adult resulting from the dry deposition of ^{137}Cs in summer (August).

5.1.5.1. Uncertainty analysis

In the uncertainty analysis, 184 input parameters were treated as having uncertain values. In Figure 7 it is shown that the 95% confidence limits for the predicted cumulative ingestion dose span greater than an order of magnitude. At the end of 2 years, the lower limit is about one-fifth of the deterministic best-estimate and the upper limit is over 6 times the best-estimate.

5.1.5.2. Sensitivity analysis

The sensitivity analysis was done based on the ranks of the input and output values, rather than the values themselves. Initially, all 184 input parameters were treated as having uncertain values, whereas in the final iteration, only 16 were treated as having uncertain values.

For the cumulative ingestion dose at 2 years after the deposition event, Table 6 lists the 5 most important input parameters and their partial rank correlation coefficients and standardized rank regression coefficients. The most important parameter is the transfer factor from beef cattle to beef.

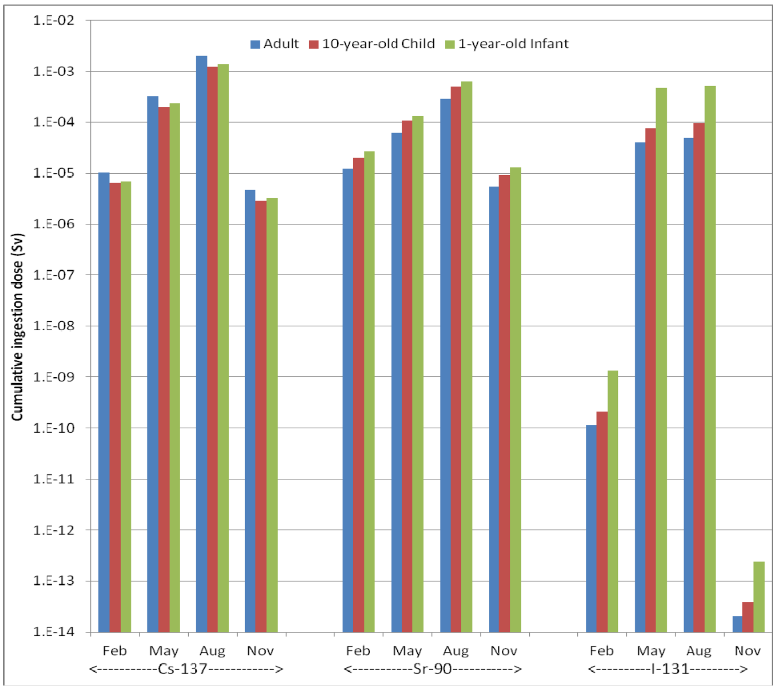

FIG. 6. CHERPAC-predicted cumulative ingestion dose at 2 years after the deposition event: dry deposition.

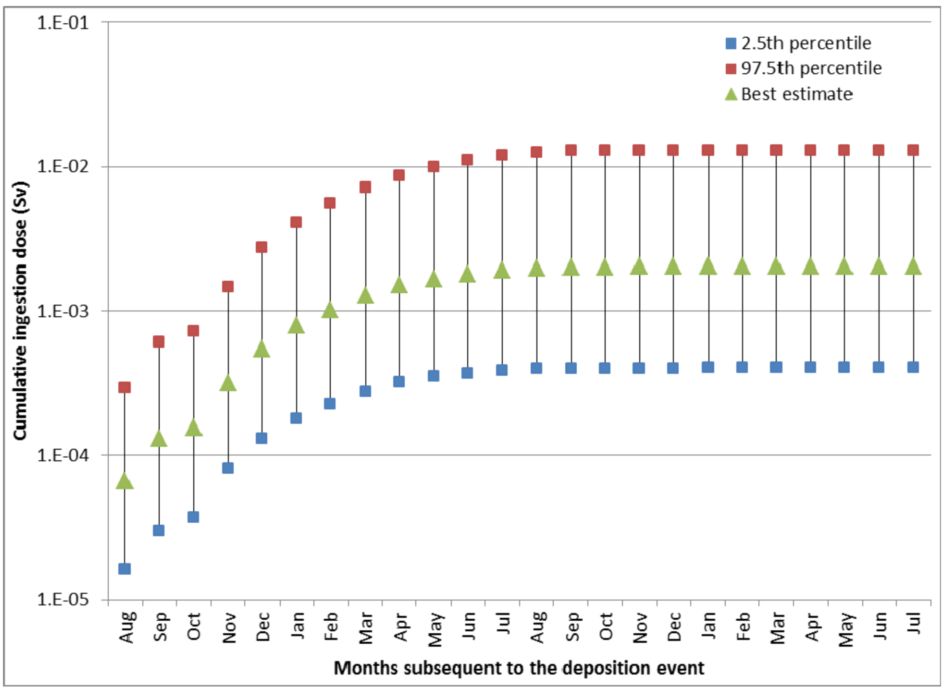

FIG. 7. CHERPAC-predicted cumulative ingestion dose to an adult resulting from the dry deposition of ^{137}Cs in summer (August).

TABLE 6. SENSITIVITY OF CUMULATIVE INGESTION DOSE TO AN ADULT AT 2 YEARS AFTER THE DRY DEPOSITION OF ^{137}CS IN SUMMER (AUGUST)

Input parameter (units)	Distribution type (range)	Rank	Partial rank correlation coefficient	Standardized rank regression coefficients
Transfer factor from beef cattle to beef (d kg^{-1})	Lognormal (3.74E-4, 0.467)	1	0.97	0.85
Yield of forage grass (kg fw m^{-2})	Lognormal (0.118, 3.77)	2	-0.90	-0.41
Intake rate of milk by man (kg d^{-1})	Lognormal (0.17, 1.08)	3	0.74	0.21
Removal half-life for all vegetables and fruits (d)	Lognormal (4.2, 53.5)	4	0.55	0.13
Forage grass consumption by dairy cattle (kg fw d^{-1})	Normal (48.5, 99.5)	5	0.41	0.09

5.1.6. Conclusions from CHERPAC modelling

This exercise provided a challenging test of CHERPAC's prediction and its ability to adapt to a particular scenario with certain conditions and assumptions, and CHERPAC performed well. Doses from agricultural products are highest from radionuclide deposition in summer because all plants are at their peak growth and are assumed to have been ingested fresh after the deposition event. The dose is higher if the deposition occurs in dry conditions rather than during heavy rain, because radionuclides adhere better to dry plant leaves. For ^{137}Cs, the ingestion dose is higher for adults than other age groups, but for ^{90}Sr and ^{131}I, the ingestion dose is highest for infants. This is a result of relative food product concentrations, intake rates and DCFs. The stochastic features of CHERPAC were found to be useful in estimating the magnitude of the uncertainty in predicted dose and also in ranking of the input parameters based upon their influence on the final dose.

5.2. AGRICULTURAL SCENARIO, CENTRAL EUROPE, JRODOS CODE

Scenario type: Agricultural
Scenario location: Europe temperate zone
Short name: Agri-Eur

5.2.1. Model description

Name of model: FDMT (Food chain and Dose Model) of RODOS (Real-time On-line DecisiOn Support system)

Brief description of the model: FDMT [31] is a dynamic terrestrial food chain and dose model integrated in the RODOS decision support system [32, 33]. This model is appropriate for agricultural settings in the temperate zone. It estimates the transfer of radioactive material in up to 35 food and up to 22 feeding products, raw and processed, and the doses from all relevant pathways (inhalation, ingestion, groundshine, cloudshine), similar to the radioecological model ECOSYS [34].

The main processes considered for the calculation of activity concentration in plant products are:

- Dry and wet deposition of radionuclides;
- Foliar uptake, with consideration of weathering effects (rain, wind), radioactive decay and growth dilution;
- Root uptake, with consideration of translocation into or from the root zone;
- Resuspension;
- Storage and processing of foodstuffs and feeding stuffs.

Contamination of stored plant products for human consumption is taken either as the activity of the last day of harvest (e.g. for cereals, potatoes, fruit), or as the average contamination during the whole harvest period (e.g. for root vegetables and fruit vegetables). There is one exception, leafy vegetables, which are assumed to be available all year round.

For the animal products the following processes are taken into consideration:

- Inhalation;
- Ingestion of contaminated feed;
- Kinetics of the radionuclide inside the animal (transfer of radionuclides to animal products, biological excretion, etc);
- Storage and processing.

To account for regional variability in e.g. soil characteristics, agricultural production regimes, the growing and harvesting periods and the human and animal diet, the model allows for different radioecological regions. Within each region relatively uniform radioecological conditions are assumed to prevail so that the same set of model parameters can be used anywhere in the region.

5.2.2. Application of the model to the EMRAS II WG8 Scenario

The FDMT model was applied for the basic EMRAS II WG8 Scenario in the following way. A release of 3 radionuclides was assumed: ^{131}I, ^{137}Cs and ^{90}Sr. All output quantities were scaled such as to correspond to a standard deposition of 1000 Bq/m^2.

The calculations reported here were performed for 2 types of soil: clay and sandy. Model parameters from the FDMT-RODOS database (typical for Central Europe), were used with the exception of soil to plant transfer factors and leaching rates. The soil to plant transfer factors used are based on the IAEA-TECDOC-1616 [12] and required customization of the RODOS radioecological database. The leaching rates were calculated based on Base and Sharp [35] with an infiltration rate typical for Belgium (100 mm/year), see Table 7 below.

Three deposition dates were considered: 1 May, 15 July and 20 November. Dry deposition was considered in all cases reported, unless otherwise stated. Wet deposition (with precipitation rate of 10 mm/h during 1 h after release) was considered in one case only and is reported in Section 5.2.3.4.

Model parameters from the FDMT-RODOS database (typical for Central Europe) were used in calculations, with the exception of soil to plant transfer factors and leaching rates. The soil-to-plant transfer factors used are based on IAEA-TECDOC-1616 [12]. The leaching rates were calculated based on Base and Sharp [35] with an infiltration rate typical for Belgium (100 mm/year), see Table 7 below.

TABLE 7. LEACHING RATES (A^{-1}) FROM SOIL FOR THE 3 RADIONUCLIDES

Radionuclide	Type of soil	Sand	Clay
^{137}Cs	Arable	4.19E-04	4.66E-05
	Pasture	8.38E-04	9.32E-05
^{90}Sr	Arable	1.00E-02	2.69E-03
	Pasture	2.01E-02	5.38E-03
^{131}I	Arable	5.23E-02	2.27E-02
	Pasture	1.05E-01	4.55E-02

The harvesting times were as follows (see page 40 of [31]):

- Grass: from 1 May to 31 October, with 70% of the hay collected in the first half of the interval;
- Winter wheat: 5 August;
- Potatoes: from 15 August to 24 September;
- Leafy vegetables: from 1 May to 31 October;
- Fruit vegetables: from 1 August to 15 October;
- Root vegetables: from 1 August to 31 October;
- Fruit: from 1 July to 15 October.

The growing season for the different plants is characterized as follows (FDMT database values, typical for Central Europe (for more details see page 41 of [31]):

- Grass: Beginning of growing season: 15 March, with peak of yield 15 May – 31 October;
- Winter wheat: Beginning of growing season: 25 October; LAI (leaf area index) increase gradually until the peak on 10 June, then decreases until harvest;
- Potatoes: Beginning of growing season: 20 May; leaves from 20 May to 15 September; peak of LAI between 1 July – 1 August;
- Leafy vegetables: Beginning of growing season: 10 March; constant LAI throughout the year, but no growth during winter;
- Root vegetables, fruit vegetables and fruit: Beginning of growing season: 15 April; leaves between 15 April – 1 November; maximal LAI from 1 July to 1 October.

Except for pasture grass (for which growth dilution is considered explicitly), growth dilution for plants consumed entirely is determined by relating the activity deposited on the leaves with the yield at harvest.

The dietary intakes assumed in the FDMT database are described in detail by Müller et al. [31] (see page 41). For some food products considered in this study these dietary intakes are given in Table 8. We also give for comparison similar data for the Belgian diet in Appendix II, Figures 64–68.

Note that certain seasonal dependencies are considered for the dietary habits, i.e. from May to October, a factor of 1.5, and from November to April a factor of 0.1 is applied to the consumption rates for leafy vegetables. This accounts for the fact that in winter time only a reduced fraction of leafy vegetables comes from outdoor crops.

TABLE 8. CONSUMPTION RATES IN THE FDMT DATABASE (BASED ON GERMAN DATA) AND AVERAGE CONSUMPTION RATES FOR BELGIUM

Food product	Diet RODOS- adult [kg/year]	Diet RODOS- child 1 year [kg/year]	Diet Adult Belgium [kg/year]
Cow's milk	84.0	204	75.0
Beef (bull)	20.1	1.10	18.2
Pork	39.4	1.42	11.7
Chicken	6.20	0.55	10.5
Lamb	0.22	0.00	3.60
Fruit Vegetables	17.2	4.38	19.4
Leafy Vegetables	34.3	21.2	23.7
Root Vegetables	12.0	7.67	5.30
Winterwheat (flour)	47.5	12.8	48.5

5.2.3. Results

5.2.3.1. Activity concentration in selected food and feeding products

The maximum and average concentrations of radionuclides in different foodstuffs and feeding stuffs are presented in the Tables 9 and 10 for sandy soil and a July release date, as this scenario produced (with few exceptions) the highest activity concentrations in food products. Results for May and November release dates and for clay as well as sandy soil types, are given in Appendix II.

For the same amount of ground deposition, ^{137}Cs generally leads to higher activity concentrations than 90Sr, which is especially evident in lamb, beef and milk.

5.2.3.2. Seasonal variations

The Figures 8–10 display some examples of seasonal variations in the activity concentrations in food products.

5.2.3.3. Doses

The Figures 11 and 12 depict effective ingestion doses due to ^{131}I, ^{90}Sr and ^{137}Cs for different age groups, in the first and second year after deposition, respectively. These doses have been calculated on the basis of default dietary intakes from the RODOS database (see Section 5.2.2.

5.2.3.4. Effect of precipitation

The effect of precipitation was considered for intensive precipitation of 10 mm/h during the first hour after the release. Figure 13 gives an example of this effect; care should be taken in interpreting these results since the deposition has been standardized to 1000 Bq/m^2 for both dry and wet deposition.

TABLE 9. MAXIMUM AND AVERAGE CONCENTRATIONS OF RADIONUCLIDES IN DIFFERENT FOODSTUFFS AND FEEDING STUFFS FOR YEAR 1, Bq/kg FRESH WEIGHT

(2a) Scenario: soil type: sandy; release date 15 July

Scenario: Sandy July; maximum and average activity concentrations						
	^{137}Cs		^{90}Sr		^{131}I	
Product	**Maximum Year 1**	**Average Year 1**	**Maximum Year 1**	**Average Year 1**	**Maximum Year 1**	**Average Year 1**
Cow's milk	1.53E+02	2.41E+01	9.08E+01	1.47E+01	2.40E+02	6.12E+00
Beef	1.74E+02	7.58E+01	3.24E+00	1.82E+00	2.54E+00	1.62E-01
Pork	8.53E+01	6.65E+01	3.38E-01	2.53E-01	7.97E-04	7.47E-05
Chicken	8.28E+01	6.49E+01	1.21E-01	9.81E-02	1.66E-03	6.63E-05
Lamb	1.01E+03	3.93E+02	2.95E+00	1.71E+00	1.97E+00	1.33E-01
Fruit Vegetables	1.87E+02	1.77E+02	2.17E+01	8.50E+00	4.94E+01	1.49E+00
Leafy Vegetables	1.41E+03	6.11E+01	1.41E+03	6.19E+01	1.61E+03	2.98E+01
Root Vegetables	1.40E+02	1.33E+02	9.91E-01	8.15E-01	3.71E+01	1.12E+00
Winter Wheat	2.50E+02	2.34E+02	5.24E+01	4.90E+01	6.48E+01	2.12E+00
Potatoes	1.40E+02	1.10E+02	3.94E-01	3.23E-01	6.23E+00	2.56E-01
GrassInt	1.12E+03	5.83E+01	1.12E+03	5.39E+01	1.64E+03	2.88E+01

TABLE 10. MAXIMUM AND AVERAGE CONCENTRATIONS OF RADIONUCLIDES IN DIFFERENT FOODSTUFFS AND FEEDING STUFFS FOR YEAR 2, Bq/kg FRESH WEIGHT

(3a) Scenario: soil type: sandy; release date 15 July

Scenario: Sandy July; maximum and average activity concentrations						
	^{137}Cs		^{90}Sr		^{131}I	
Product	**Maximum Year 2**	**Average Year 2**	**Maximum Year 2**	**Average Year 2**	**Maximum Year 2**	**Average Year 2**
Cow's milk	8.16E-01	5.73E-01	4.11E+00	2.69E+00	N/A	N/A
Beef	2.01E+01	3.39E+00	1.13E+00	6.25E-01	N/A	N/A
Pork	8.47E+01	1.78E+01	3.35E-01	8.31E-02	N/A	N/A
Chicken	8.16E+01	1.81E+01	1.19E-01	2.65E-02	N/A	N/A
Lamb	5.09E+01	8.52E+00	7.26E-01	2.58E-01	N/A	N/A
Fruit Vegetables	1.83E+02	3.48E-02	8.92E+00	4.55E-01	N/A	N/A
Leafy Vegetables	7.78E-02	7.36E-02	8.90E-01	8.59E-01	N/A	N/A
Root Vegetables	1.37E+02	6.62E-02	9.30E-01	9.14E-01	N/A	N/A
Winter Wheat	2.45E+02	2.25E-01	5.12E+01	7.92E-01	N/A	N/A
Potatoes	1.19E+02	1.58E-01	3.69E-01	3.63E-01	N/A	N/A
GrassInt	2.00E+00	1.29E+00	6.59E+00	6.32E+00	N/A	N/A

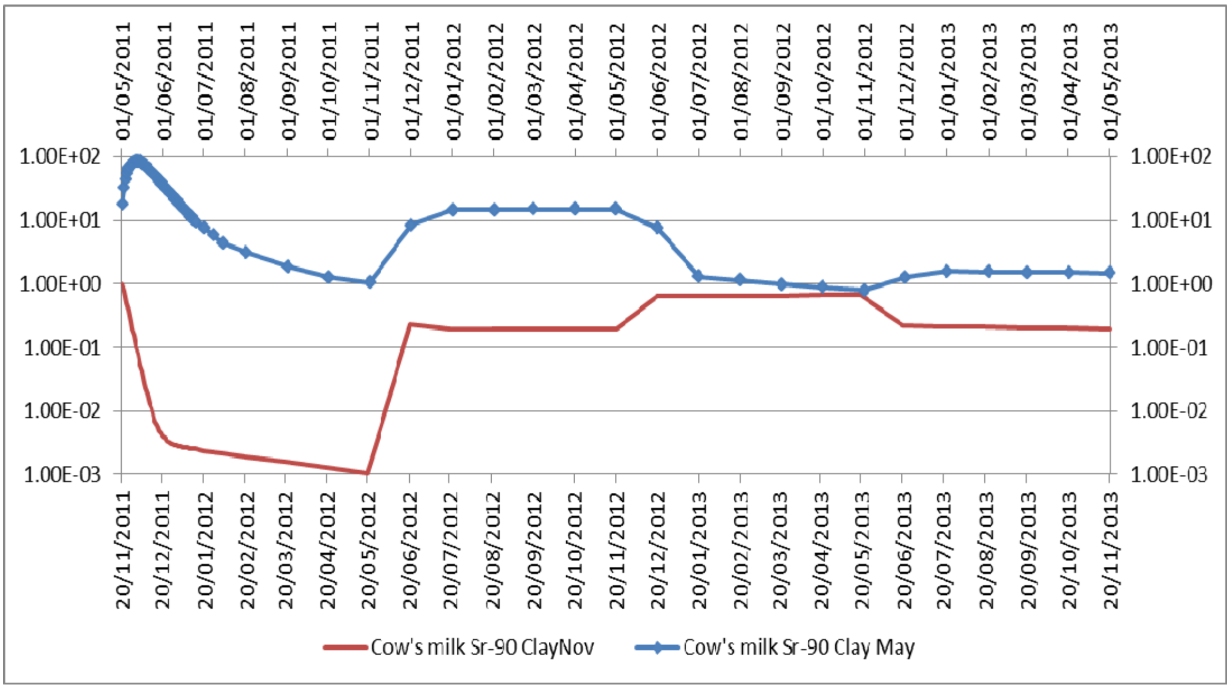

FIG. 8. Activity concentration of ^{90}Sr in cow's milk [Bq/kg] depending on the release date. The upper scale refers to a May and the lower scale to a November release.

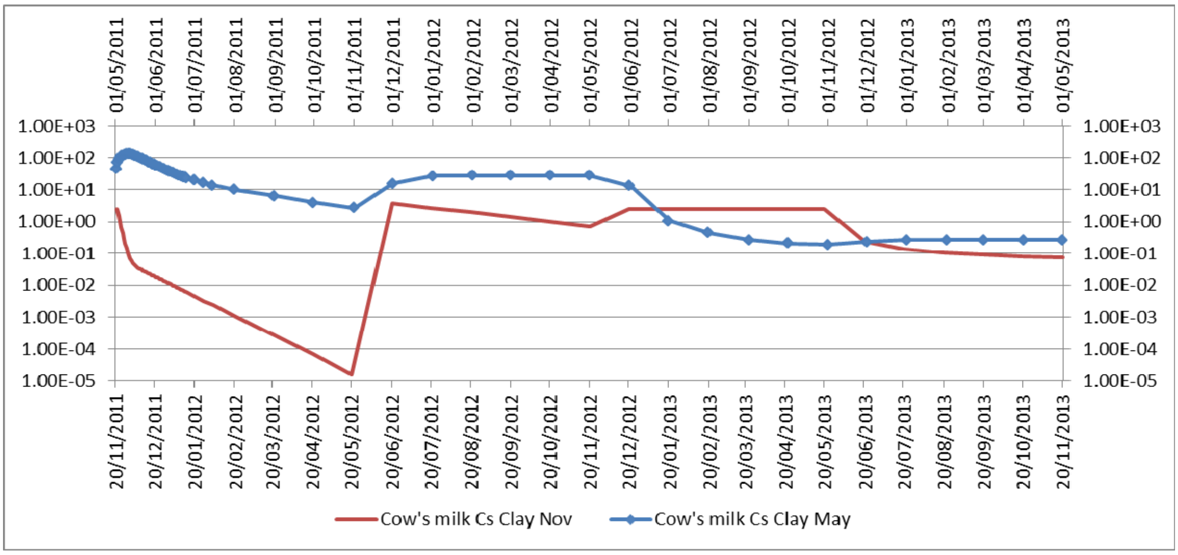

FIG. 9. Activity concentration of ^{137}Cs in cow's milk [Bq/kg] depending on the release date. The upper scale refers to a May and the lower scale to a November release.

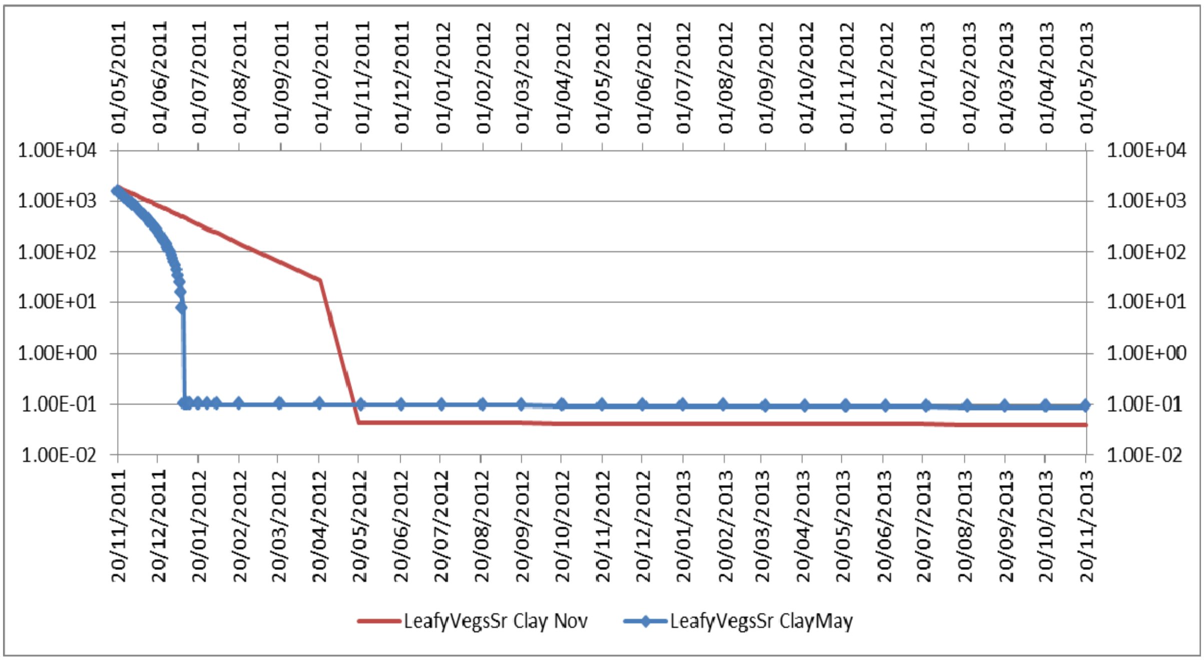

FIG. 10. Activity concentration of ^{90}Sr in leafy vegetables [Bq/kg] depending on the release date. The upper scale refers to a May and the lower scale to a November release.

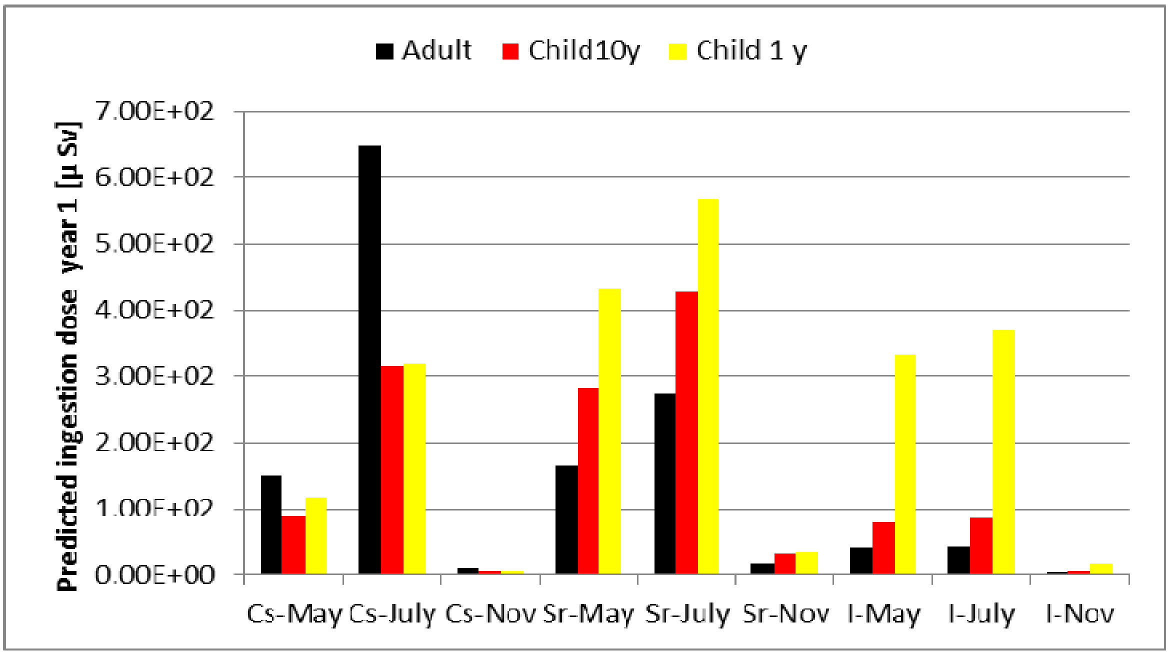

FIG. 11. Predicted ingestion dose [µSv], year 1, linear scale.

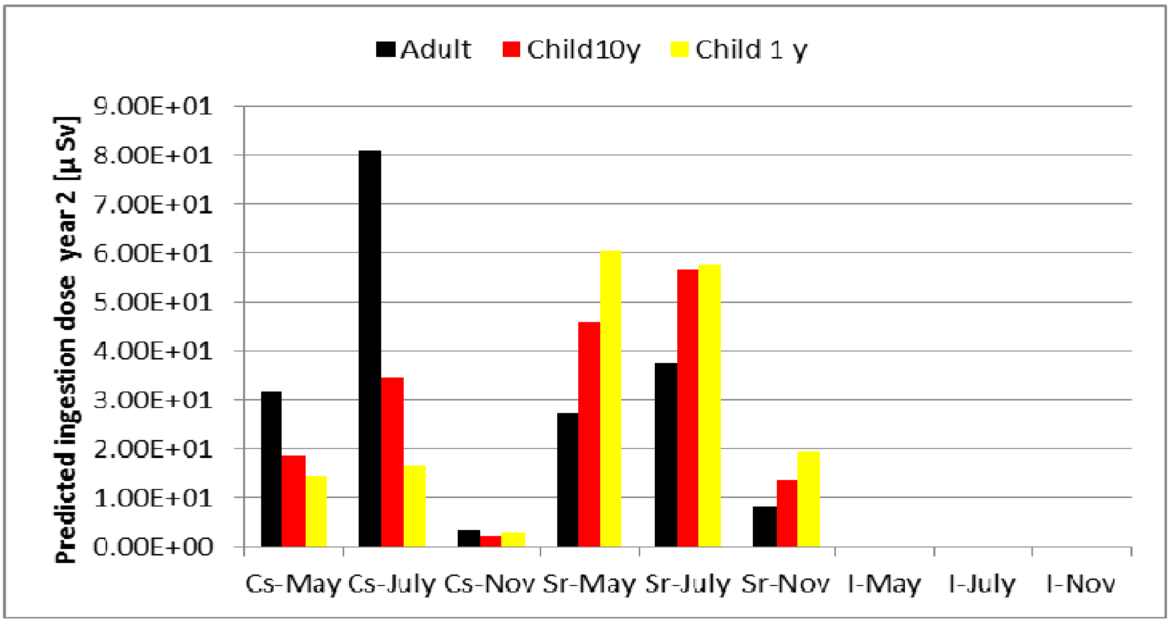

FIG. 12. Predicted ingestion dose [µSv], year 2, linear scale.

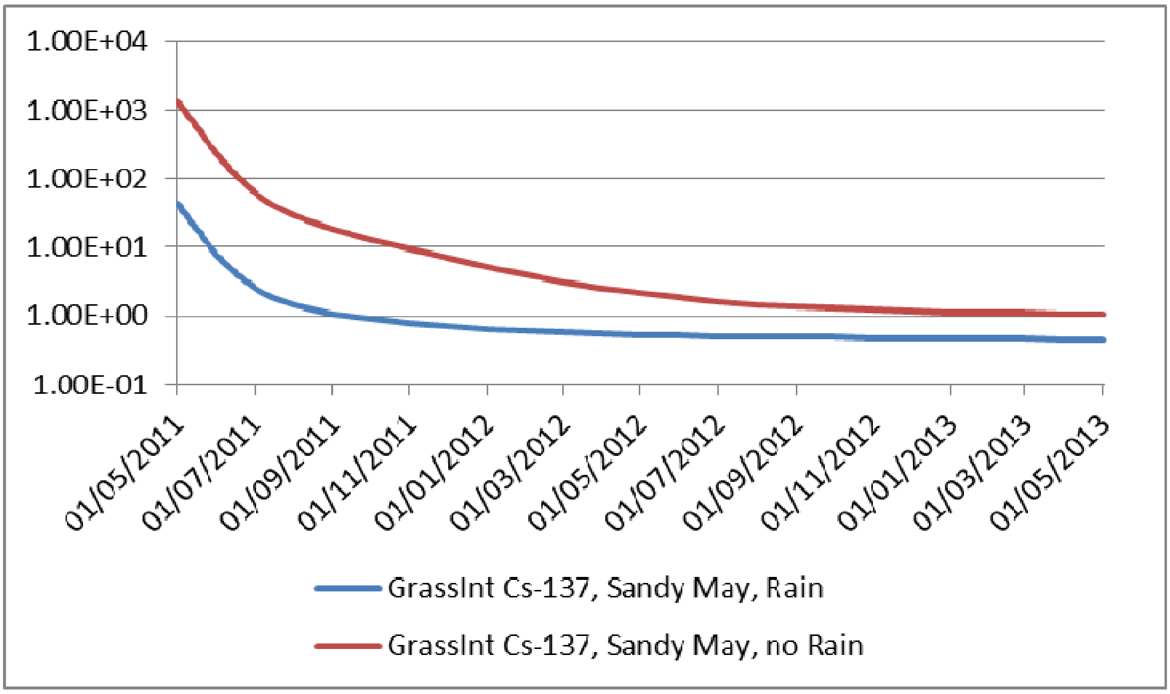

FIG. 13. Effect of rain (for standardized deposition of 1000 Bq/m^2).

5.2.4. Sensitivity/uncertainty analysis

The FDMT model is a complex model with hypotheses needing to be thoroughly considered during the application of the model and the interpretation of results. For instance, animal husbandry practices or plant harvesting may change under specific weather conditions (e.g. cows still on the fields in December due to mild weather) and these changes should be taken into account.

For releases during spring, the main contribution to the adult dose will most likely be due to milk products and leafy vegetables in case of ^{90}Sr or ^{131}I; and to milk, beef, leafy vegetables and possibly lamb in case of ^{137}Cs. For releases in mid-summer before the beginning of the harvest period, cereals, potatoes and fruit vegetables will bring an important contribution to the total dose for mobile elements such as ^{137}Cs. For releases in late autumn, the main contribution is due to leafy vegetables (conservatively assumed to be available all year round, although consumption is reduced during winter time).

The effect of the soil type is more pronounced for releases in late autumn and winter, when the contribution of direct deposition to activity concentrations in plant and animal products is less than during the vegetation period.

5.2.5. Discussion

^{137}Cs generally leads to higher activity concentrations than ^{90}Sr. A ground deposition of 1000 Bq/m^2 can cause high activity concentrations in leafy vegetables, lamb, milk and beef. Regional variations in the diet (e.g. higher consumptions of lamb) can cause significant increases in the ingestion dose.

It can be noticed that doses from ^{90}Sr are higher for infants in all scenarios considered, as compared to adults or 10 years old children. In case of ^{137}Cs, the doses for adults are slightly higher than for infants. Similar effects were observed with the CHERPAC model (Section 5.1) though resulting doses are higher in the latter case for all radionuclides.

For a standardized ground deposition, a high precipitation amount would lead to lower activity concentrations in plant products since large fractions of the radionuclides initially retained are immediately washed off.

5.3. AGRICULTURAL SCENARIO, CENTRAL EUROPE, ALPINE

Scenario type: Alpine
Scenario location: Europe temperate zone
Short name: Alpine-Eur

5.3.1. Model description

Name of model: Radioecological model for assessing the transfer of radionuclides to foodstuffs after deposition on agricultural land, and the radiation exposure of people via all relevant pathways (ECOSYS for Excel 1.4) and Food chain data customization for decision support systems in Austria (OECOSYS).

Brief description of the model: ECOSYS for Excel is a dynamic terrestrial food chain and dose model based on ECOSYS-87 [34] which is used in the European Real-time Decision Support System RODOS. It includes new programme modules as discussed in Müller et al. [36]. ECOSYS for Excel is a deterministic model, i.e. for each transfer parameter a definite value is input in the model, and for each result a definite number is given.

The following pathways are considered:

- Inhalation;
- Ingestion;
- External exposure from the plume;
- External exposure from deposited radionuclides (groundshine);
- External exposure from deposition to skin and clothes.

The considered transfer processes from wet and dry deposition to the processed foodstuffs are described in detail in Müller et al. [37] and are shown in Figure 14.

Model parameters (e.g. leaf area indices, growth periods) may depend on the region where the model is applied. The values of the standard set of parameters are considered to be representative for Southern Germany which belongs to the temperate zone in Central Europe. The model with this set of parameters is referred as “standard” in the following.

5.3.2. Application of the model to the Alpine scenario

For the conditions in Austria the parameters of ECOSYS for Excel were modified [38]. Austria was considered to be divided into 3 radioecological regions which account for the differences in climate and ingestion habits: Alpine region, foothills of the Alps and Pannonic region. These regions define areas with relatively uniform conditions for which the same set of model parameters can be used. The model with the parameters of the Alpine region is referred in the following as “Alpine”. Compared to the standard parameters the following major changes were made: the growing period and the time dependence of the leaf area index were adjusted to the vegetation periods at higher altitude; the adapted consumption habits take into account the major alpine products cow’s milk and milk products. The transfer factors were left unchanged [39].

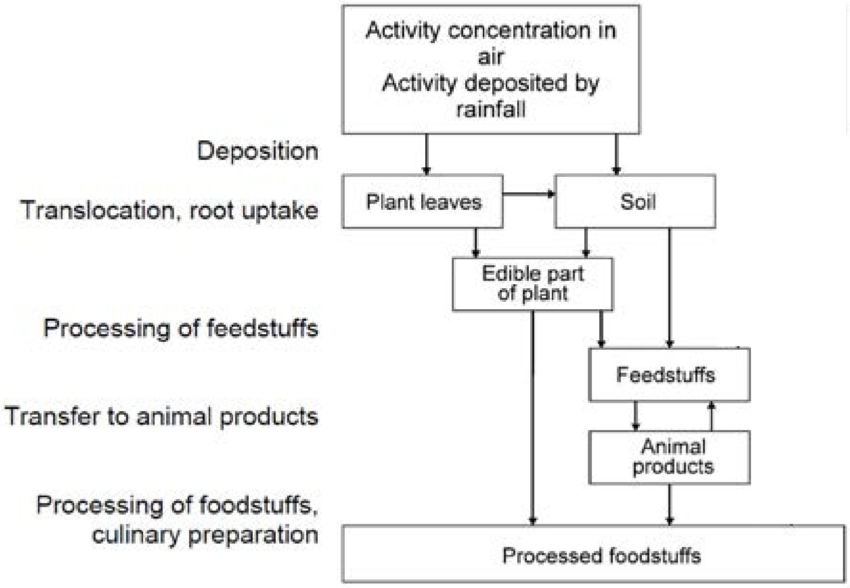

FIG. 14. Transfer processes included in the model (after Müller et al. [37]).

The basic EMRAS II WG8 Scenario was applied for ECOSYS for Excel with the standard parameter set ("Standard") and with the Alpine parameter set ("Alpine"). A release of the 3 radionuclides ^{137}Cs, ^{131}I and ^{90}Sr was assumed, leading to a uniform deposition of 1000 Bq/m^2 either by dry deposition or wet deposition (at a precipitation event of 20 mm) for both parameter sets.

For the radionuclide ^{137}Cs 4 dates of deposition were considered: winter conditions were assumed on 1 February, spring conditions on 15 May, summer conditions on 1 August, autumn conditions on 1 November, always in respect to Alpine climate. The radionuclides ^{131}I and ^{90}Sr were considered for the deposition date 1 August (summer conditions), expecting the highest impact on pasture on that date. The begin of the growing season for pasture was assumed to be on 15 March (standard) and 1 April (alpine), harvest period between 20 April – 10 November (standard) and 15 May – 20 October (alpine), respectively.

For Iodine the relation of particulate, elemental and organic bound was assumed to be 0.5: 0.3: 0.2. The other nuclides were assumed to be only particulate bound.

Besides the standard pathways (see Figure 14), special attention was given to the foodstuffs leafy vegetables, berries, cow's milk and cheese produced by rennet coagulation (usual alpine cheese), all preferred products in the Alpine region. The different consumption habits for cow's milk are given in Table 11.

TABLE 11. CONSUMPTION OF MILK (LITRES PER YEAR) FOR DIFFERENT AGE CLASSES IN THE STANDARD AND THE ALPINE SCENARIO

Age	1 year old	10 years old	Adult
Milk standard 1/a	201.4	65.7	84.0
Milk alpine 1/a	175.9	99.7	130.3

Doses for the different exposure pathways were calculated for the 3 age groups adult, child (10 years old) and infant (1 year old).

5.3.3. Results

5.3.3.1. Activity concentration in selected foodstuffs

The maximum and average concentrations of radionuclides in different foodstuffs are presented in Table 12 (year 1) and Table 13 (year 2) for the alpine and standard scenario during dry conditions. In addition, the concentrations of grass and hay (both from intensive cultivation) are given. As date of release the 1 August is assumed.

In the first year the mean contamination of foodstuffs is in general higher in the alpine case, but winter wheat is more contaminated in the standard scenario with ^{90}Sr and ^{131}I. Milk and cheese are more contaminated in the alpine region, in the first and as well in the second year. Milk products are on average most contaminated with ^{137}Cs, but the peak contamination is with ^{131}I.

In Tables 14 and 15 the contamination of the same food products during wet deposition is listed. Compared to dry deposition the contamination is on average significant less for both scenarios. This is mainly due to restricted interception and direct contamination of the soil during the shower (20 mm) in the deposition event. In the considered food products the average contamination is higher in the alpine region.

5.3.3.2. Seasonal variation

In Figure 15 the seasonal variation of ^{137}Cs contaminated foodstuffs is shown for the alpine and the standard scenario. Deposition date is 1 August; wet and dry deposition are considered separately. In the early stage, the direct contamination of leafy vegetables causes the highest contamination, after the harvest of these directly contaminated vegetables the next generation with root uptake of ^{137}Cs is much less contaminated. Due to the change of cow's feeding from grass to hay, again an increase of the contamination of milk and cheese in winter/spring is observed. Because of the shorter vegetation period in the Alpine region, the contaminated hay of the first year is used longer, causing contaminated milk and milk products at high levels over a longer period compared to the standard scenario. Contaminated berries of the first year are available longer because the new fruits of the second year appear later, keeping the contamination longer at high level. Due to losses by interception, leafy vegetables, grass and hay are less contaminated in the case of wet deposition causing less contaminated foodstuffs mainly in the first year after deposition.

Contamination with the radionuclides ^{90}Sr and ^{131}I and other release dates (1 February, 15 May and 1 November) are shown in Appendix III. Comparing alpine and standard scenario, contamination in August of milk and cheese with ^{90}Sr is higher in the Alpine region, whereas for iodine no difference is predicted. A deposition event in spring (15 May) or autumn (1 November) causes in general less contamination of food products in the alpine region because of the less developed vegetation. In the case of autumn deposition, milk and cheese are in the first year only slightly contaminated due to inhalation (dry deposition) or not at all, because feeding of grass has already stopped in the Alpine area.

TABLE 12. MAXIMUM AND AVERAGE CONCENTRATIONS OF RADIONUCLIDES IN DIFFERENT FOODSTUFFS AND FEEDING STUFFS FOR YEAR 1 AFTER THE DATE OF RELEASE, 1 AUGUST, Bq/kg FRESH WEIGHT

(a) Scenario: alpine, dry deposition only

Table (2a)	**^{137}Cs**		**^{90}Sr**		**^{131}I**	
Product	**MAXIMA year 1**	**AVERAGE year 1**	**MAXIMA year 1**	**AVERAGE year 1**	**MAXIMA year 1**	**AVERAGE year 1**
Cow's milk	6.46E+01	1.21E+01	3.86E+01	8.11E+00	7.17E+01	2.06E+00
Cheese	3.87E+01	7.20E+00	2.31E+02	4.79E+01	3.54E+00	8.54E-02
Beef	1.34E+02	9.65E+01	8.81E-01	5.93E-01	1.58E+00	7.11E-02
Winter Wheat	6.56E+01	5.42E+01	2.14E+01	9.56E+00	3.62E-01	1.32E-02
Leafy Vegetables	4.67E+02	2.28E+01	4.67E+02	2.36E+01	4.48E+02	1.02E+01
Berries	8.15E+01	7.71E+01	1.07E+01	4.51E+00	2.35E+01	7.94E-01
Grass	4.75E+02	2.50E+01	4.75E+02	2.39E+01	5.41E+02	1.18E+01
Hay	2.76E+02	2.29E+02	2.64E+02	2.21E+02	9.39E+01	5.85E+00

(b) Scenario: standard; dry deposition only

Table (2b)	**^{137}Cs**		**^{90}Sr**		**^{131}I**	
Product	**MAXIMA year 1**	**AVERAGE year 1**	**MAXIMA year 1**	**AVERAGE year 1**	**MAXIMA year 1**	**AVERAGE year 1**
Cow's milk	6.46E+01	9.73E+00	3.83E+01	6.00E+00	6.97E+01	1.92E+00
Cheese	3.87E+01	5.78E+00	2.29E+02	3.56E+01	3.44E+00	7.86E-02
Beef	7.73E+01	6.12E+01	5.48E-01	4.02E-01	1.19E-02	8.61E-04
Winter Wheat	3.90E+01	3.36E+01	3.19E+01	2.74E+01	6.56E-01	2.27E-02
Leafy Vegetables	4.67E+02	2.17E+01	4.67E+02	2.25E+01	4.47E+02	1.01E+01
Berries	8.15E+01	6.60E+01	1.63E+01	6.51E+00	2.58E+01	1.68E+00
Grass	4.75E+02	2.58E+01	4.75E+02	2.44E+01	5.41E+02	1.18E+01
Hay	2.19E+02	1.66E+02	2.08E+02	1.60E+02	6.75E+01	4.33E+00

TABLE 13. MAXIMUM AND AVERAGE CONCENTRATIONS OF RADIONUCLIDES IN DIFFERENT FOODSTUFFS AND FEEDING STUFFS FOR YEAR 2 AFTER THE DATE OF RELEASE, 1 AUGUST, Bq/kg FRESH WEIGHT

(a) Scenario: alpine, dry deposition only

Table (3a)	**^{137}Cs**		**^{90}Sr**		**^{131}I**	
Product	**MAXIMA year 2**	**AVERAGE year 2**	**MAXIMA year 2**	**AVERAGE year 2**	**MAXIMA year 2**	**AVERAGE year 2**
Cow's milk	2.49E-01	1.59E-01	1.37E+00	8.72E-01	5.72E-15	2.05E-16
Cheese	3.16E-01	1.09E-01	9.28E+00	5.64E+00	6.04E-15	1.98E-16
Beef	4.82E+01	1.15E+01	3.85E-01	1.70E-01	2.41E-15	8.97E-17
Winter Wheat	6.43E+01	9.73E+00	1.12E+01	2.14E+00	1.00E-12	3.90E-14
Leafy Vegetables	4.79E-02	4.67E-02	8.72E-01	8.55E-01	3.19E-15	1.25E-16
Berries	7.98E+01	2.24E+00	4.77E+00	3.97E-01	1.25E-12	2.82E-14
Grass	7.55E-01	2.21E-01	3.92E+00	1.59E+00	1.71E-14	6.49E-16
Hay	4.47E+00	3.87E+00	1.97E+01	1.93E+01	9.59E-14	3.72E-15

(b) Scenario: standard; dry deposition only

Table (3b)	**^{137}Cs**		**^{90}Sr**		**^{131}I**	
Product	**MAXIMA year 2**	**AVERAGE year 2**	**MAXIMA year 2**	**AVERAGE year 2**	**MAXIMA year 2**	**AVERAGE year 2**
Cow's milk	1.80E-01	1.41E-01	7.27E-01	5.54E-01	N/A	N/A
Cheese	1.61E-01	9.20E-02	4.73E+00	3.47E+00	N/A	N/A
Beef	7.73E+01	2.10E+01	5.55E-01	2.05E-01	N/A	N/A
Winter Wheat	3.82E+01	4.76E+00	3.12E+01	4.32E+00	N/A	N/A
Leafy Vegetables	4.79E-02	4.65E-02	8.72E-01	8.53E-01	N/A	N/A
Berries	5.99E-02	5.87E-02	2.79E-01	2.74E-01	N/A	N/A
Grass	6.93E-01	2.54E-01	3.36E+00	1.80E+00	N/A	N/A
Hay	4.67E+00	3.76E+00	1.70E+01	1.65E+01	N/A	N/A

TABLE 14. MAXIMUM AND AVERAGE CONCENTRATIONS OF RADIONUCLIDES IN DIFFERENT FOODSTUFFS AND FEEDING STUFFS FOR YEAR 1 AFTER THE DATE OF RELEASE, 1 AUGUST, Bq/kg FRESH WEIGHT

(a) Scenario: alpine, wet deposition only (20 mm)

Table (4a)	^{137}**Cs**		^{90}**Sr**		^{131}**I**	
Product	**MAXIMA year 1**	**AVERAGE year 1**	**MAXIMA year 1**	**AVERAGE year 1**	**MAXIMA year 1**	**AVERAGE year 1**
Cow's milk	4.92E+00	9.55E-01	5.90E+00	1.41E+00	2.40E+00	6.99E-02
Cheese	2.95E+00	5.64E-01	3.53E+01	8.15E+00	1.19E-01	2.91E-03
Beef	1.03E+01	7.49E+00	1.37E-01	1.00E-01	5.30E-02	2.42E-03
Winter Wheat	3.78E+00	3.13E+00	2.61E+00	1.30E+00	9.56E-03	3.53E-04
Leafy Vegetables	2.86E+01	1.44E+00	5.73E+01	3.61E+00	1.21E+01	2.77E-01
Berries	5.05E+00	4.77E+00	7.31E-01	4.74E-01	6.51E-01	2.25E-02
Grass	3.63E+01	2.06E+00	7.25E+01	4.89E+00	1.81E+01	4.00E-01
Hay	2.13E+01	1.79E+01	4.23E+01	3.76E+01	3.15E+00	1.99E-01

(b) Scenario: standard, wet deposition only (20 mm)

Table (4b)	^{137}**Cs**		^{90}**Sr**		^{131}**I**	
Product	**MAXIMA year 1**	**AVERAGE year 1**	**MAXIMA year 1**	**AVERAGE year 1**	**MAXIMA year 1**	**AVERAGE year 1**
Cow's milk	4.92E+00	7.77E-01	5.85E+00	1.10E+00	2.34E+00	6.50E-02
Cheese	2.95E+00	4.59E-01	3.50E+01	6.35E+00	1.15E-01	2.68E-03
Beef	3.23E+00	2.55E+00	5.03E-02	3.64E-02	2.20E-04	1.60E-05
Winter Wheat	2.24E+00	1.92E+00	3.69E+00	3.17E+00	1.68E-02	5.80E-04
Leafy Vegetables	2.86E+01	1.38E+00	5.72E+01	3.48E+00	1.20E+01	2.72E-01
Berries	5.05E+00	4.08E+00	2.00E+00	9.52E-01	7.14E-01	4.68E-02
Grass	3.63E+01	2.14E+00	7.25E+01	5.15E+00	1.81E+01	3.99E-01
Hay	1.69E+01	1.32E+01	3.34E+01	2.87E+01	2.27E+00	1.47E-01

TABLE 15. MAXIMUM AND AVERAGE CONCENTRATIONS OF RADIONUCLIDES IN DIFFERENT FOODSTUFFS AND FEEDING STUFFS FOR YEAR 2 AFTER THE DATE OF RELEASE, 1 AUGUST, Bq/kg FRESH WEIGHT

(a) Scenario: alpine, wet deposition only (20 mm)

Table (5a)	^{137}**Cs**		^{90}**Sr**		^{131}**I**	
Product	**MAXIMA year 2**	**AVERAGE year 2**	**MAXIMA year 2**	**AVERAGE year 2**	**MAXIMA year 2**	**AVERAGE year 2**
Cow's milk	1.01E-01	9.29E-02	6.64E-01	6.07E-01	N/A	N/A
Cheese	7.29E-02	5.72E-02	4.09E+00	3.69E+00		
Beef	4.05E+00	1.50E+00	8.27E-02	6.21E-02		
Winter Wheat	3.71E+00	6.07E-01	1.53E+00	6.80E-01		
Leafy Vegetables	4.70E-02	4.58E-02	8.55E-01	8.39E-01		
Berries	4.93E+00	1.91E-01	4.93E-01	2.74E-01		
Grass	4.52E-01	1.75E-01	3.85E+00	1.56E+00		
Hay	2.33E+00	2.23E+00	1.94E+01	1.89E+01		

(b) Scenario: standard, wet deposition only (20 mm)

Table (5b)	^{137}**Cs**		^{90}**Sr**		^{131}**I**	
Product	**MAXIMA year 2**	**AVERAGE year 2**	**MAXIMA year 2**	**AVERAGE year 2**	**MAXIMA year 2**	**AVERAGE year 2**
Cow's milk	8.46E-02	7.98E-02	4.85E-01	4.60E-01	N/A	N/A
Cheese	5.49E-02	4.87E-02	2.96E+00	2.78E+00		
Beef	3.23E+00	9.26E-01	5.09E-02	2.27E-02		
Winter Wheat	2.19E+00	3.21E-01	3.61E+00	9.11E-01		
Leafy Vegetables	4.70E-02	4.57E-02	8.55E-01	8.37E-01		
Berries	5.88E-02	5.76E-02	2.73E-01	2.69E-01		
Grass	3.91E-01	1.98E-01	3.30E+00	1.77E+00		
Hay	2.07E+00	1.94E+00	1.66E+01	1.62E+01		

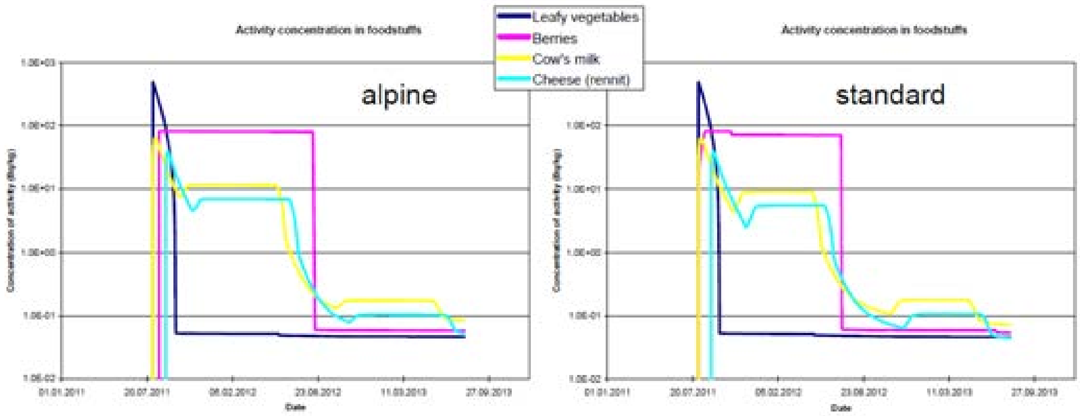

(a)

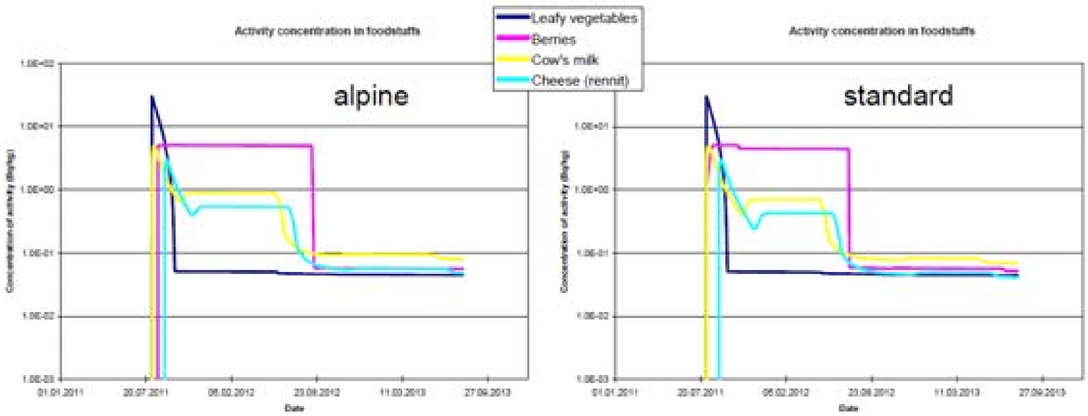

(b)

FIG. 15. ^{137}Cs contamination of selected foodstuff: (a) dry deposition only; (a) wet deposition only.

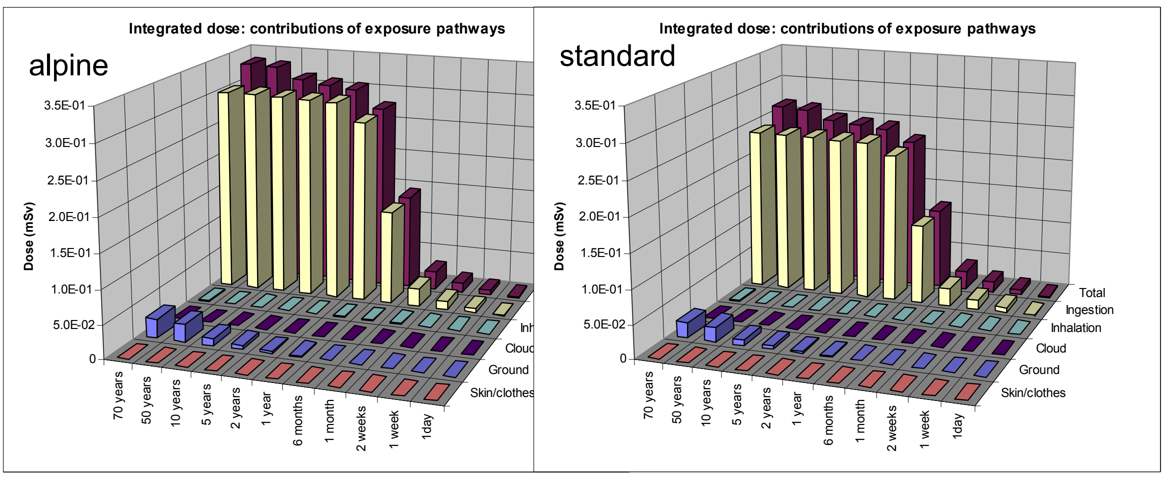

FIG. 16. Contribution of the different exposure pathways to total dose for dry deposition of ^{137}Cs in summer time (August) for adults.

5.3.3.3. *Doses for humans*

In the vegetation period (August) the total dose is significantly higher in the alpine scenario. The highest contribution to dose is resulting from ingestion (Figure 16), the second important source is ground shine for ^{137}Cs and inhalation for ^{90}Sr and ^{131}I (Appendix III). About 80% of the total dose is delivered in the first year for ^{137}Cs, about 70% for ^{90}Sr and about 100% for ^{131}I.

In the alpine scenario milk and milk products and meat contribute more to the ingestion dose compared to the standard scenario (Figure 17).

Resulting effective doses are shown for the alpine and the standard scenario in Figure 18 for the first year, in Figure 19 for the second year after deposition. In August the total dose resulting from ^{137}Cs is highest for the Alpine scenario for all 3 age groups. For other deposition dates and radionuclides, the standard scenario will lead to higher doses. In the second year, again the Alpine August ^{137}Cs dose is the highest. The other dose values are very close for both scenarios.

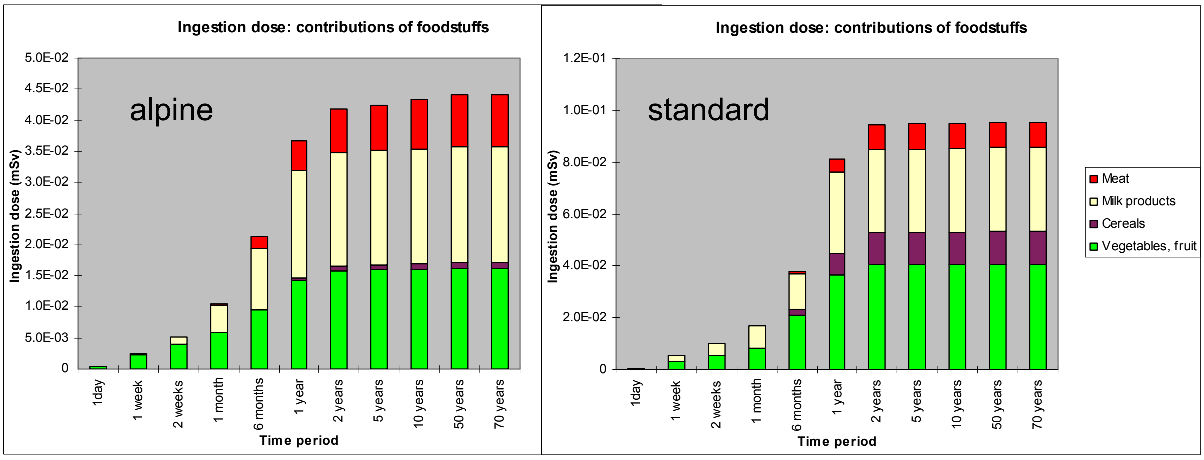

FIG. 17. Contribution of food stuffs to the ingestion dose (deposition date 15 May, dry deposition, 1 year old infant).

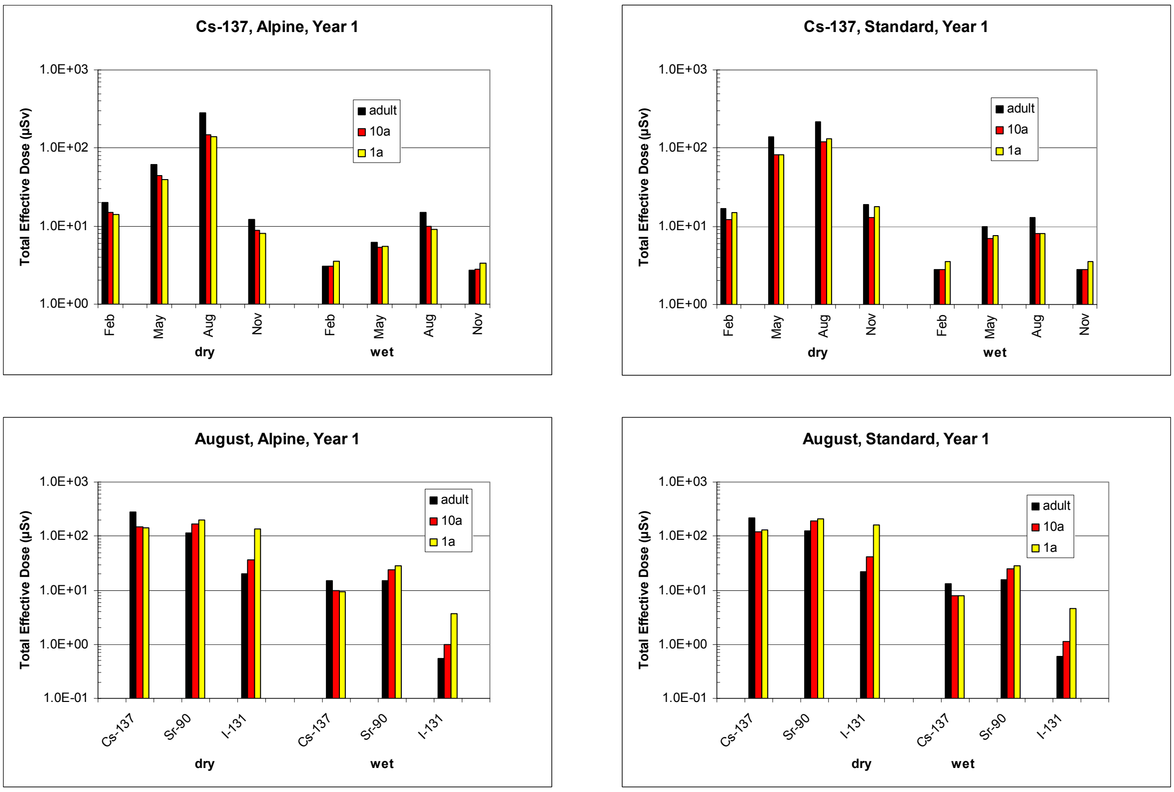

FIG. 18. Total effective dose for the alpine and the standard scenario for the first year after deposition.

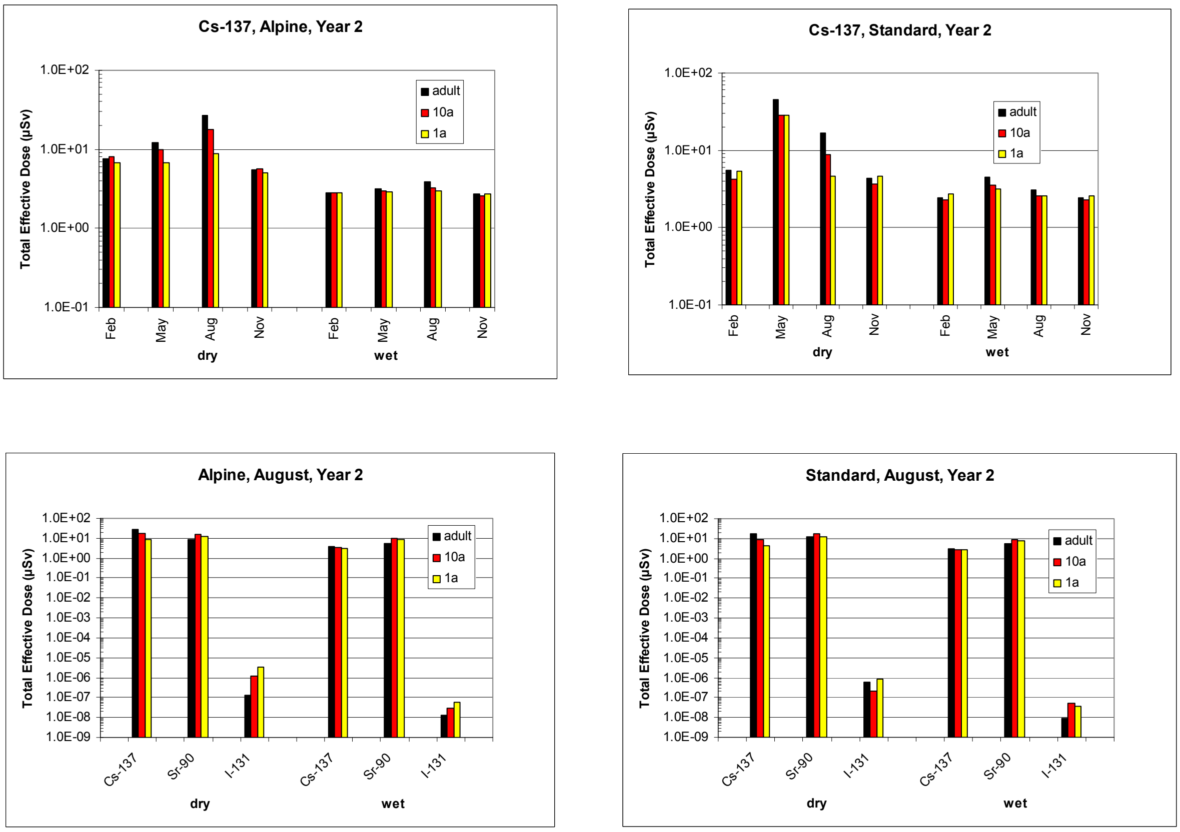

FIG. 19. Total effective dose for the alpine and the standard scenario for the second year after deposition.

6. TEMPERATE FOREST AND ARCTIC TUNDRA MODEL RESULTS

6.1. TEMPERATE FOREST SCENARIO, ONTARIO CANADA LOCATION, CHERPAC CODE

6.1.1. Model description

See Section 5.1.1.

6.1.2. Scenario description

In this scenario, it was assumed that 1000 Bq m^{-2} each of ^{137}Cs, ^{90}Sr, and ^{131}I were deposited instantaneously in a forest ecosystem. It was also assumed that people living in this ecosystem were self-sufficient with respect to the forest food products included in this scenario and did not consume contaminated agricultural and aquatic products.

Cases of the deposition occurring under dry or heavy rainfall conditions were evaluated. Seasonal effects were evaluated by considering cases in which the deposition occurred in winter, spring, summer, or autumn. The concentrations in common food products and the ingestion and groundshine doses to an adult, a 10 year old child and a 1 year old infant were predicted for a 2 year period following the deposition.

6.1.3. Application of CHERPAC to the Temperate Forest Scenario

Most of the information in Section 5.1.3 for the agricultural scenario is also applicable here. However, some additional steps were taken in order to use CHERPAC for modelling the forest scenario. CHERPAC originally considered the intake of contaminated food by humans from both the agricultural and the forest pathways, with the rates of intake of forest products being much lower than those of agricultural products. For the current exercise, enhanced rates of intake of forest products were assumed, based on the assumption that people living closer to the forest consume relatively more forest food.

Originally, bulk transfer factors for forest food products were available for ^{137}Cs only and were based on observations after the Chernobyl accident. Transfer factors for ^{90}Sr were derived by comparing ^{137}Cs and ^{90}Sr concentrations in fruits and forest plants, and in beef and forest animal products. Transfer factors for ^{131}I were derived considering its 8 day half-life for radioactive decay.

6.1.4. Results

Although detail results were calculated for all cases, the discussion and figures presented here are for one case: the dry deposition of ^{137}Cs in summer (August). Many of the comments made here apply to other cases also.

The soil model used for the forest environment is same as the one used for the agricultural environment (Section 5.1.4).

6.1.4.1. Plants products

Figure 20 shows the concentration in mushrooms increases slightly for first 2 years and then levels off and drops as the activity passes through the root zone. For deposition in summer (August), there is no activity predicted in wild berries for the next 10 months because deposition occurred after the assumed time of berry harvest. If the deposition had occurred before the berry harvest, then the concentration in berries would have a similar pattern to that in mushrooms.

6.1.4.2. Animal products

Figure 21 shows the differences in the concentrations in big game (e.g. deer) and small game (e.g. birds) are due to differences in the food they consume.

6.1.4.3. Doses from ^{137}Cs

Figure 22 shows the ingestion doses to an adult and 10 year old child are an order of magnitude lower than the groundshine doses. Adult ingestion doses are higher than those for children and infants because of the higher rates of intake of forest food products by adults.

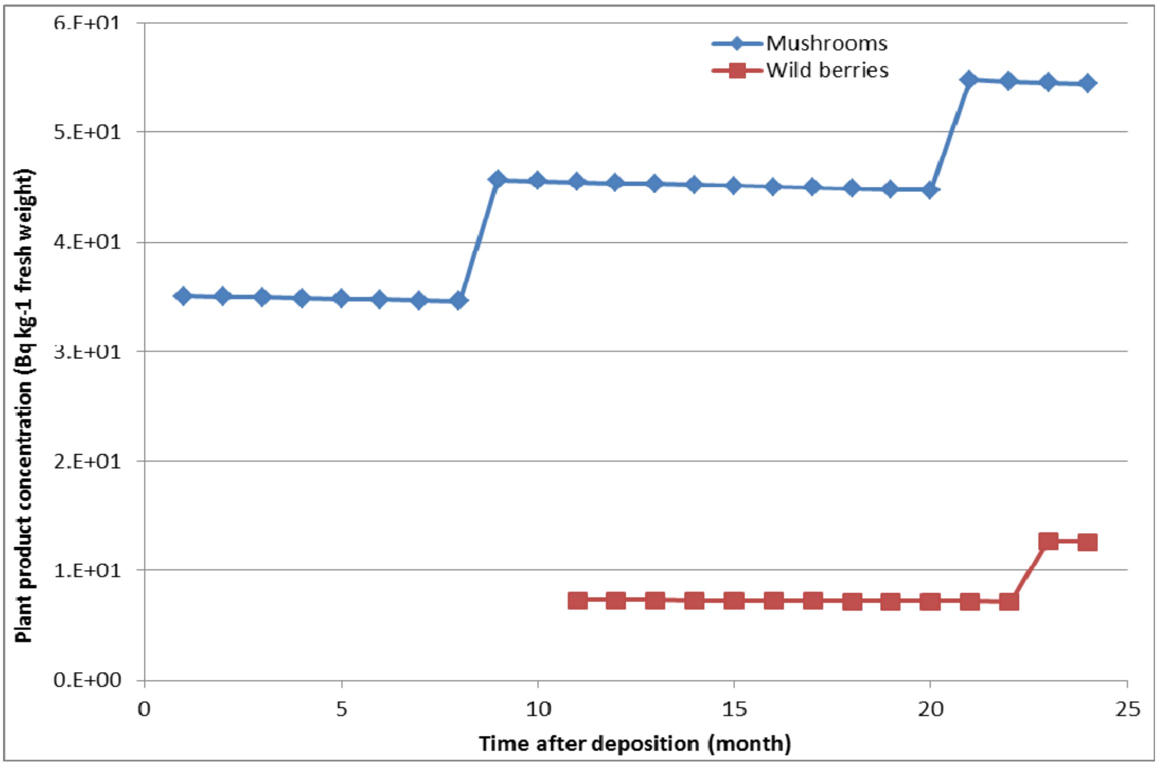

FIG. 20. CHERPAC-predicted concentrations in forest plant products at consumption: ^{137}Cs, dry deposition in summer (August).

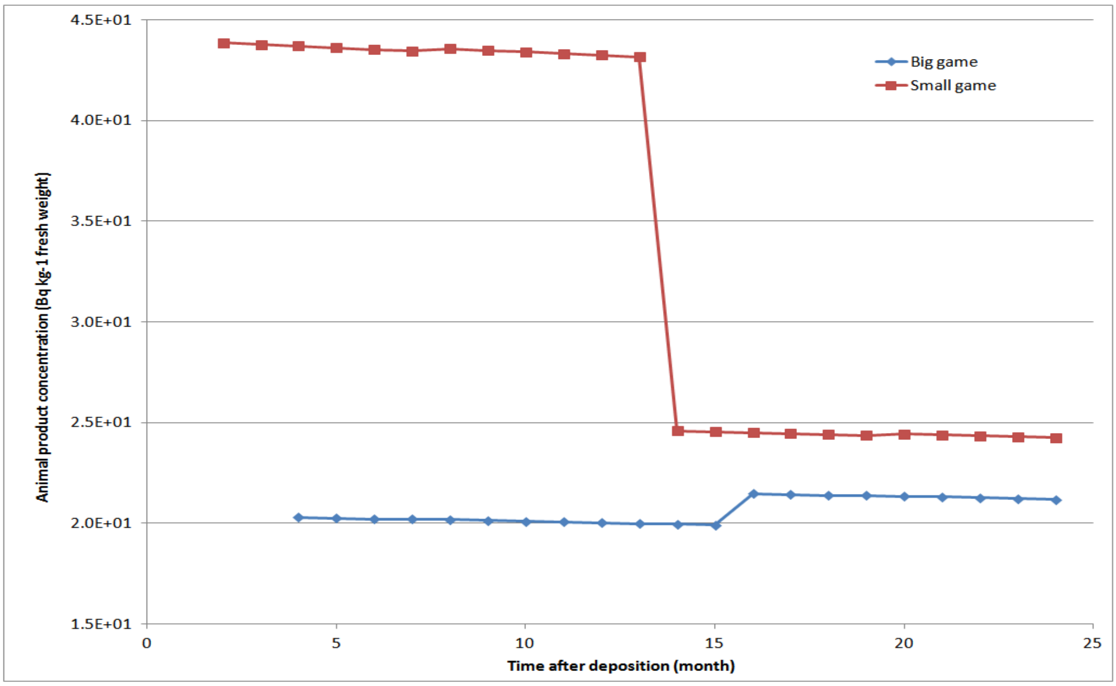

FIG. 21. CHERPAC-predicted concentrations in forest animal products at consumption: ^{137}Cs, dry deposition in summer (August).

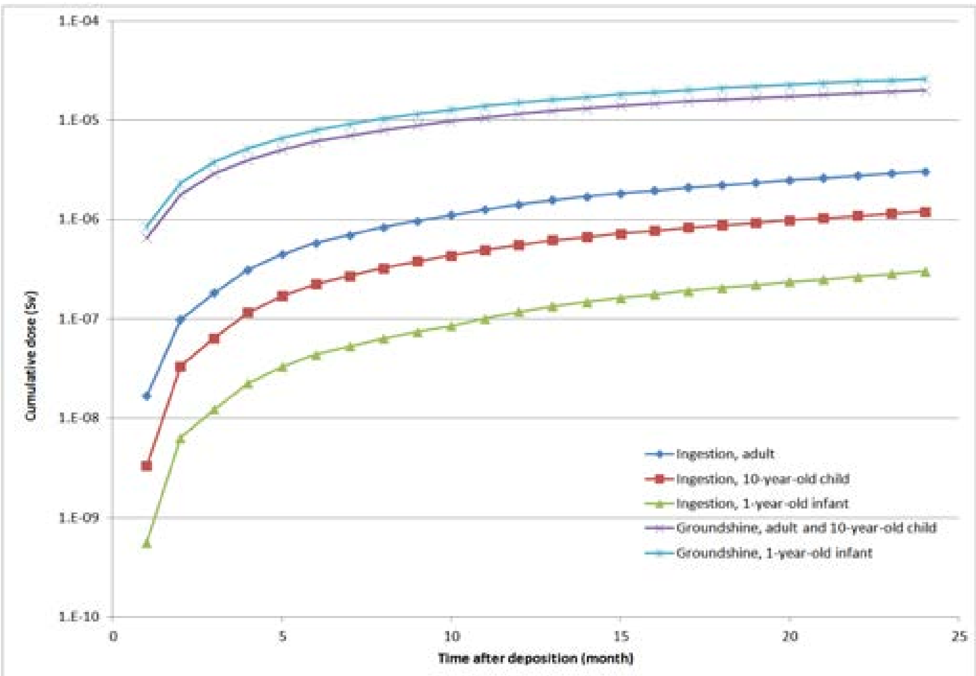

FIG. 22. CHERPAC-predicted cumulative doses to humans: ^{137}Cs, dry deposition in summer (August) in forest environment.

6.2. TEMPERATE FOREST SCENARIO, SASKATCHEWAN CANADA LOCATION, IMPACT CODE

Scenario type: Temperate Forest
Scenario location: Northern Canada
Short name: Temp-Can

6.2.1. Model description

IMPACT (Integrated Model for the Probabilistic Assessment of Contaminant Transport) is a recognized Canadian environmental pathways and exposure modelling tool which provides a wide range of answers for the environmental management of industrial activities. It has been serving Canadian government agencies and the nuclear industry for decades and is a standard tool for radiation dose calculation and for Derived Release Limit (DRL) calculation following Canadian Standard CSA N288.1 [40]. The Canadian Standard CSA N288.1, Guidelines for calculating derived release limits for radioactive material in airborne and liquid effluents for normal operation of nuclear facilities, is comparable with the IAEA's Safety Reports Series No. 19 [41] and NCRP Report No. 123 [42].

IMPACT is a modelling tool, created, maintained and supported by EcoMetrix Incorporated (formerly Beak International Inc.). It was originally developed in 1993 as part of research projects funded by the Atomic Energy Control Board (now the Canadian Nuclear Safety Commission). Since the initial development, IMPACT has been continuously updated to improve the interface to integrate various operating systems, and most importantly to embody an up-to-dated understanding of the fate, transport and toxicity of metals, radionuclides, and other constituents released to the environment. The IMPACT 5.4.4 version was tailored to align with the guidance for Derived Release Limits (DRLs) that is referred to in the Canadian Standards Association (CSA) standard N288.1-08 and supporting documentation [43].

The IMPACT model is a customizable tool that allows the user to assess the transport and fate of constituents of potential concern (COPCs) through a user-specified environment. It calculates the concentrations of COPCs in a range of media and enables the quantification of potential radiation doses and hazard quotients (HQs) for human receptors, and aquatic and terrestrial ecological receptors. The graphical user interface (GUI) features make it possible to create or modify scenarios quickly without the need to change the programming code. Thus, users can construct complex models to predict potential environmental effects in a wide variety of natural environments without the need for programming skills or the use of multiple and complex model interfaces. IMPACT has also given focused consideration to the determination of derived release limits (DRLs) for radioactive contaminants.

The pathways IMPACT considers are given in Figure 23.

6.2.2. Application of the Model to the EMRAS II WG8 Scenario

For the model scenario, it was assumed that 1000 Bq/m^2 each of ^{137}Cs, ^{131}I and ^{90}Sr were deposited in a temperate forest ecosystem in northern Saskatchewan. The deposition was assumed to be distributed uniformly over a soil mixing depth of 10 cm. The soil type chosen for this scenario was sand.

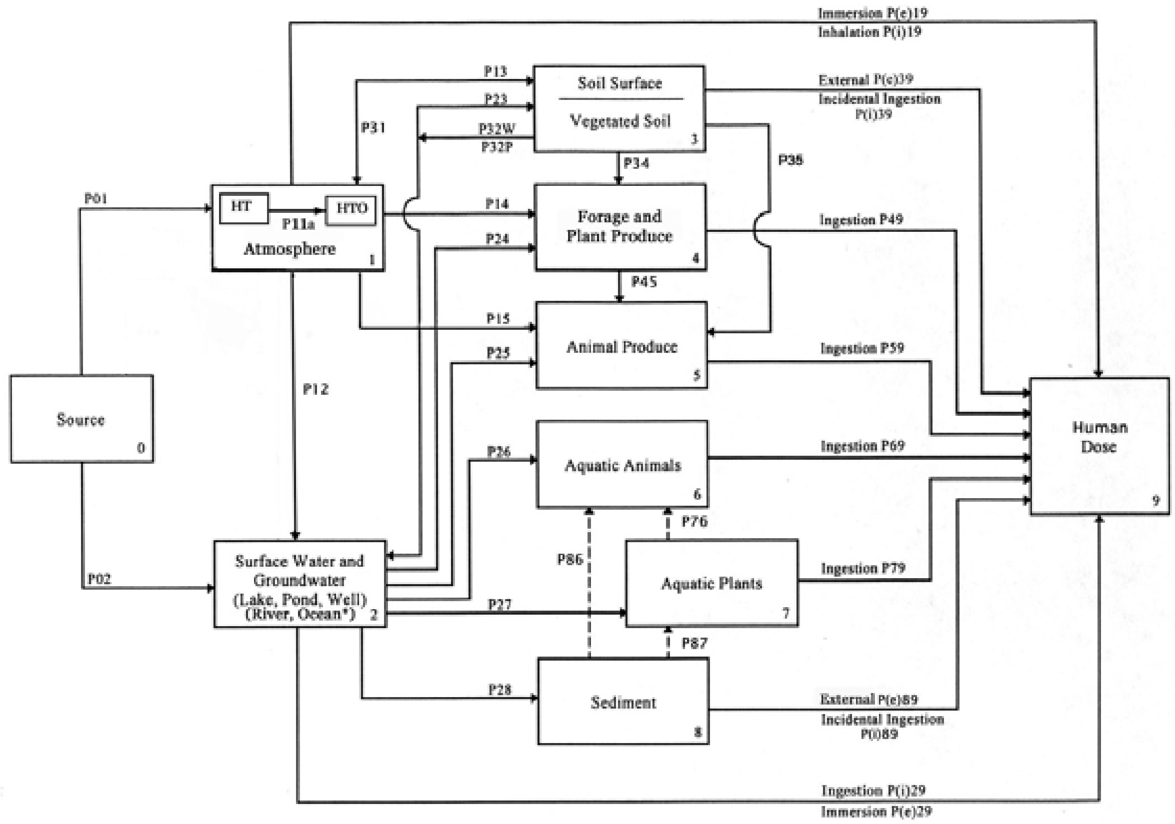

* For ocean water, pathways P23, P24, P25 and P(i)29 are not used.

FIG. 23. Environmental transport model for IMPACT.

The temperate forest scenario also included a lake with a surface area of 2.4 km^2 and a depth of 1.5 m. Environment Canada flow measurements for the November 1973 to December 2010 at the Wheeler River Station, were averaged on a monthly basis and these monthly averages were scaled based on drainage area to estimate flows at points of interest. Average monthly flows allowed the assessment of seasonal variations in flow rates. Over the total monitoring period (1973 to 2010), the average annual precipitation rate of 451 mm/a was used in the model based on measurements for the 1970 to 2000 period at the Key Lake monitoring station [44].

The scenario did not consider the groundwater and soil runoff pathways. Soil re-suspension and air deposition were included (Figure 23).

To simply the modelling scenario, it was assumed that all background nuclide concentrations in both freshwater and sediment were zero before the fallout event.

The IMPACT model developed for this scenario utilized an EcoMetrix database developed to assess temperate regions in Northern Saskatchewan. The parameters describing the transfer of COPCs in the environment were derived from regional data, including water-to-sediment partitioning coefficients, bioaccumulation factors for aquatic biota, and transfer factors from food to animal tissue [45, 46]. Information from published literature and expert judgment with similar environments were used to quantify physical parameters that are conceptual or not measured directly, such as sediment interface thickness. Aquatic and terrestrial dietary intakes are assumed to be 100% local food sources.

Two human age groups, an adult and a 1 year old infant, were considered in this scenario. All parameter values were taken from CSA N288.1 [40] and dose conversion factors from ICRP 72 values [29].

Human receptors were exposed to radiological COPCs through various exposure pathways, such as consumption of local country foods and drinking water. Resource use and dietary assumptions were developed from regional and site-specific information where possible. Food consumption rates were based on previous studies completed by EcoMetrix and are specific to Northern Saskatchewan (45, 46). The proportional distribution of food types in the country food diet of human receptor groups are presented in Table 16. The total adult food intake was estimated from the survey to be 702 kg/year.

The total radiological dose is the sum of doses from external exposure to gamma radiation and internal radiation dose due to intake of radionuclides from the following pathways:

- Inhalation of air;
- External exposure to air;
- Ingestion of drinking water;
- External exposure to drinking water;
- Incidental ingestion of soil;
- External exposure to soil; and;
- Ingestion of food.

The various pathways and model components included in the scenario are presented in Table 17.

6.2.3. Scenario results

Results presented here focus on the predicted exposures to human receptors following the fallout event. Environmental concentrations and human doses for the first and second year after exposure are summarized in the following sections.

6.2.3.1. Soil

Soil was estimated to have an initial concentration of 7.35 Bq/kg (dry weight) within a 10 cm mixing depth based on an initial deposition of 1000 Bq/m^2 and a bulk density of 1600 kg/m^3 and a water content of 15%. Within the first 0.1 years (36 days), the soil concentration of ^{131}I was predicted to rapidly decrease to 1 Bq/kg as a result of radiological decay. After a period of 0.2 years, concentrations of ^{131}I in soil were predicted to be negligible.

Concentrations of ^{137}Cs and ^{90}Sr in soil were predicted to exhibit similar trends in soil over time, resulting from similar decay half-life values (Figure 24). As ^{137}Cs is associated with a higher partition coefficient, concentrations in soil are predicted to be persistent with time and decrease to 7 Bq/kg after a 2.5 year time period.

TABLE 16. PROPORTIONAL DISTRIBUTION OF FOOD TYPES IN THE COUNTRY FOOD DIET OF HUMAN RECEPTOR GROUPS

Food source	Local food intake fraction (%)	
	Adult	**1 year old infant**
Beaver	0.16	0.12
Mallard	0.28	0.21
Caribou	31.81	23.54
Grouse	0.20	0.14
Moose	0.84	0.63
Store food*	66.72	75.36
Total	**100**	**100**

* The store bought foods do not contribute to human doses.

TABLE 17. PATHWAYS AND MODEL COMPONENTS INCLUDED IN THE SCENARIO

No.	Source media	Recptor media	Process	Receptor types
1	Outdoor air	Terrestrial plant	Air deposition	Browse, Labrador tea, lichen, blueberries, rose hips
		Terrestrial animal	Inhalation and exposure	Moose, caribou, hare,beaver, loon, muskrat, vole, scaup, mallard, lunx, mink, wolf
		Human	Inhalation and dermal exposure	Adult, infant (1 year old)
2	Soil	Outdoor air	Soil resuspension	Outdoor air
		Terrestrial plant	Plant uptake	Browse, Labrador tea, lichen, blueberries, rose hips
		Terrestrial animal	Ingestion	Moose, caribou, hare,beaver, loon, muskrat, vole, scaup, mallard, lunx, mink, wolf
		Human	Incidental ingestion and groundshine	Adult, infant (1 year old)
3	Water	Sediment	Diffusion, deposition, etc.	Small waterbodes sediment
		Aquatic plant	Equilibrium	Aquatic plants
		Aquatic animal	Equilibrium	Freshwater fish, aquatic invertebrate, clam
		Terrestrial animal	Ingestion	Moose, caribou, hare,beaver, loon, muskrat, vole, scaup, mallard, lunx, mink, wolf
		Human	Ingestion	Adult, infant (1 year old)
4	Sediment	Terrestrial animal	Incidental ingestion	Moose, caribou, hare,beaver, loon, muskrat, vole, scaup, mallard, lunx, mink, wolf
5	Aquatic plant	Terrestrial animal	Ingestion	Moose, caribou, ,beaver, muskrat, scaup, mallard, mink
6	Aquatic animal	Terrestrial animal	Ingestion	Loon, mink
		Human	Ingestion	Adult, infant (1 year old)
7	Terrestrial plant	Terrestrial animal	Ingestion	Lynx, mink, wolf
		Human	Ingestion	Adult, infant (1 year old)
8	Terrestrial animal	Human	Ingestion	Adult, infant (1 year old)

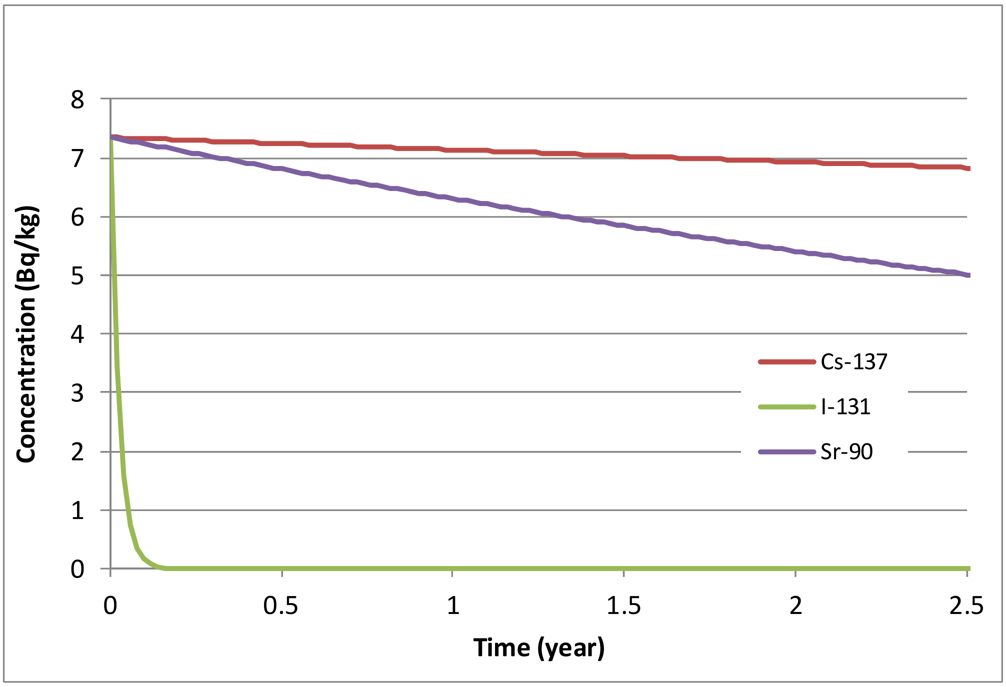

FIG. 24. Predicted concentrations of ^{137}Cs, ^{131}I and ^{90}Sr in soil after the fallout event.

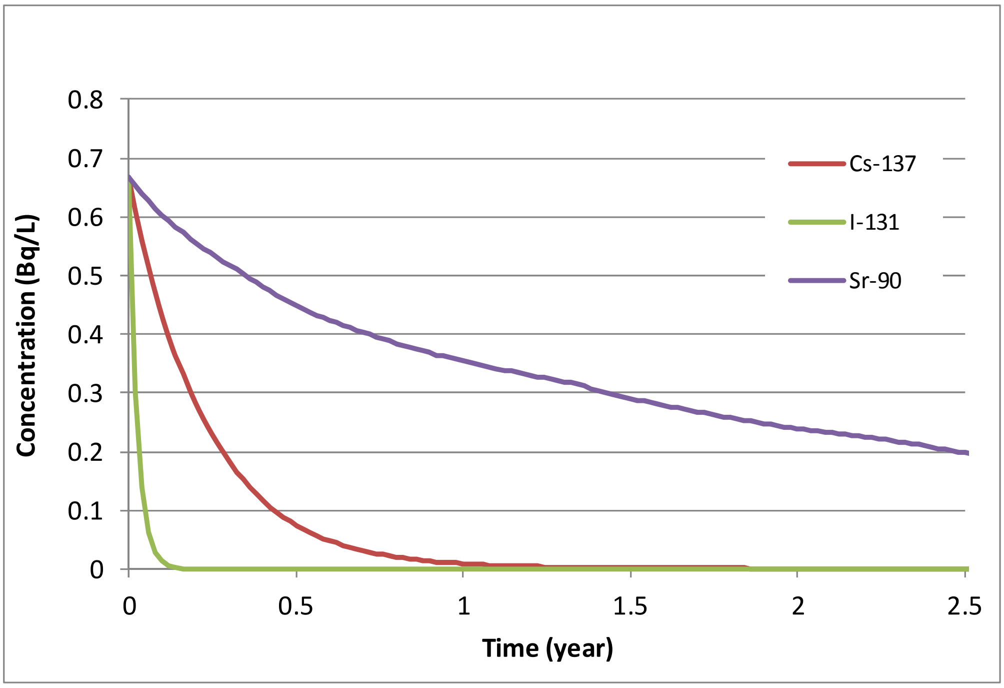

FIG. 25. Predicted concentrations of ^{137}Cs, ^{131}I and ^{90}Sr in water after the fallout event.

6.2.3.2. Water

Initial water concentrations were estimated to be 0.67 Bq/L, based on an initial deposition of 1000 Bq/m^2 and an average lake depth of 1.5 meters. Concentrations are predicted to decrease with time as a result of ambient water dilution and sediment interaction (Figure 25). Within the first 0.2 years, the concentration of ^{131}I in water was predicted to rapidly decrease as a result of the very short half-life of 8 days. Concentrations of ^{137}Cs in water were predicted to decrease over time and are reflective of a high partition coefficient with sediment of 22 000 L/kg. Concentrations of ^{90}Sr were predicted to decrease less rapidly with time, owing to a smaller sediment partition coefficient of 100 L/kg.

6.2.3.3. 6.2.3.3 Ecological receptors

The maximum concentrations of ^{137}Cs, ^{131}I and ^{90}Sr in each of the ecological receptors are presented in Table 18.

6.2.3.4. Human dose

Two human age groups were considered in this scenario, an adult and a 1 year old infant. At the end of 1 year of the deposition event, predicted committed effective doses were approximately 0.51 mSv for the adult and 0.27mSv for the 1 year old infant. At the end of the second year, the committed doses were predicted to be 0.55mSv and 0.3mSv for the adult and the 1 year old infant respectively (Figure 26).

To better demonstrate dose contributions over time from all pathways, dose rates are used instead of committed doses. Figures 27 and 28 represent the dose rates to the human receptor groups and the various pathways for the initial time period following deposition and the end of the first year following deposition. Immediately following the fallout event, the intake of terrestrial and aquatic animals was predicted to be the most important pathways for the human receptor dose. The most important nuclide for human dose was ^{137}Cs (Figures 27 and 28).

The pathways contributing to human dose following the first year of exposure are presented in Figures 29 and 30. At the end of the first year of exposure, the intake of terrestrial and aquatic animals was predicted to remain an important pathway for human dose. In addition, groundshine and the ingestion of water contribute significant pathways to human dose. The most important nuclide contributing to human dose was ^{137}Cs. Water ingestion of ^{90}Sr was also predicted to represent an important pathway in human dose after the first year of exposure.

TABLE 18. PREDICTED MAXIMUM CONCENTRATIONS OF ^{137}CS, ^{131}I AND ^{90}SR IN ECOLOGICAL RECEPTORS

Media	Units	Maximum concentration between 0 and 1 year			Concentration at 1 year			Concentrations at 2 years		
		^{137}Cs	^{131}I	^{90}Sr	^{137}Cs	^{131}I	^{90}Sr	^{137}Cs	^{131}I	^{90}Sr
Soil	Bq/kg	7.35	7.35	7.35	7.14	<0.01	6.31	6.93	<0.01	5.41
Air	Bq/m^3	<0.01	<0.01	<0.01	<0.01	<0.01	<0.01	<0.01	<0.01	<0.01
Water	Bq/L	0.67	0.67	0.67	<0.01	<0.01	0.35	<0.01	<0.01	0.24
Sediment	Bq/kg	251	2.73	44	250	<0.01	42	231	<0.01	30
Fish	Bq/kg	2335	4.00	1.33	34	<0.01	0.71	6.10	<0.01	0.48
Blueberry	Bq/kg	0.07	0.07	1.21	0.07	<0.01	1.04	0.07	<0.01	0.89
Labrador tea	Bq/kg	0.07	0.07	1.21	0.07	<0.01	1.04	0.07	<0.01	0.89
Caribou	Bq/kg	281	0.26	0.34	5.73	<0.01	0.28	2.24	<0.01	0021
Moose	Bq/kg	20	0.22	0.05	0.49	<0.01	0.04	0.25	<0.01	0.03
Mallard	Bq/kg	557	0.24	0.03	15	<0.01	0.03	7.49	<0.01	0.02
Beaver	Bq/kg	20 689	0.75	0.43	446	<0.01	0.33	188	<0.01	0.26
Grouse	Bq/kg	0.34	0.07	0.01	0.19	<0.01	<0.01	0.18	<0.01	<0.01

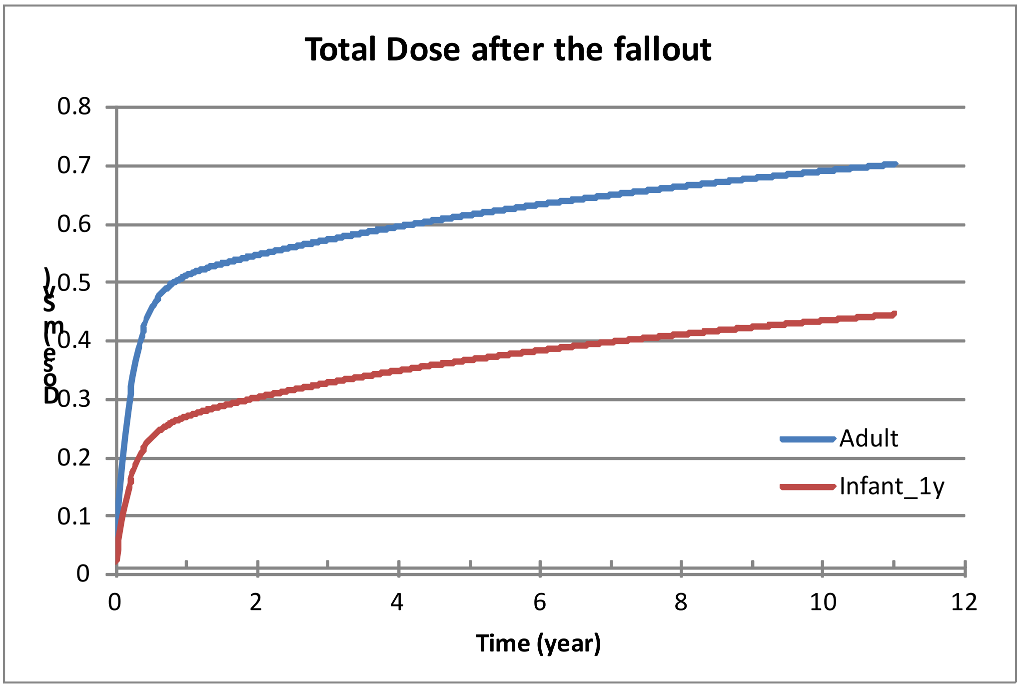

FIG. 26. Predicted total dose to human receptors after the fallout event.

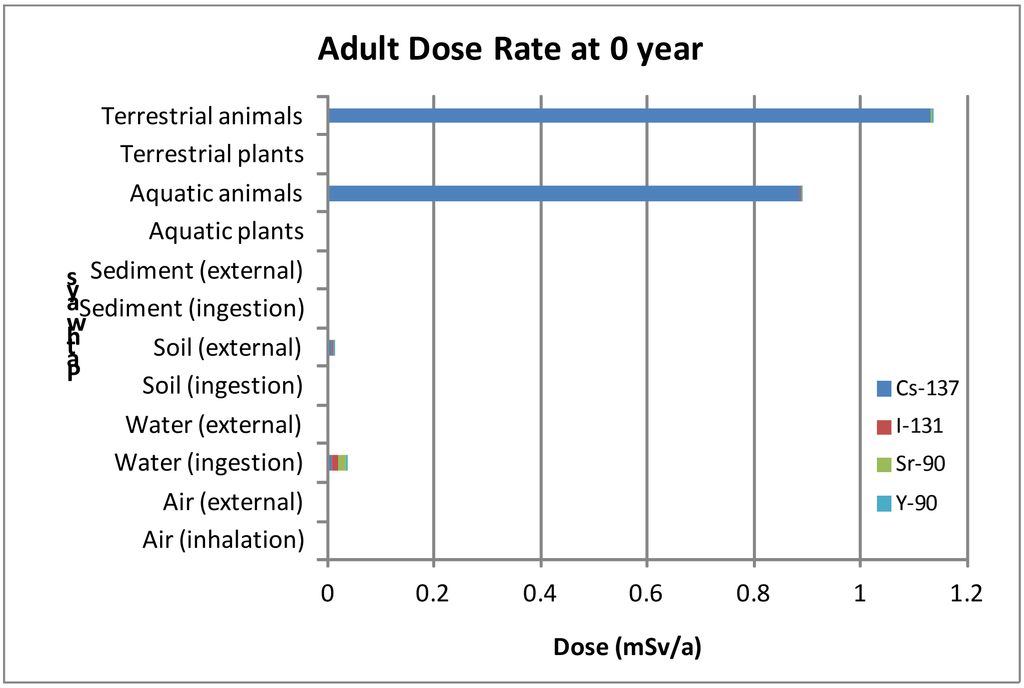

FIG. 27. Pathways contributing to the adult dose immediately after the fallout event.

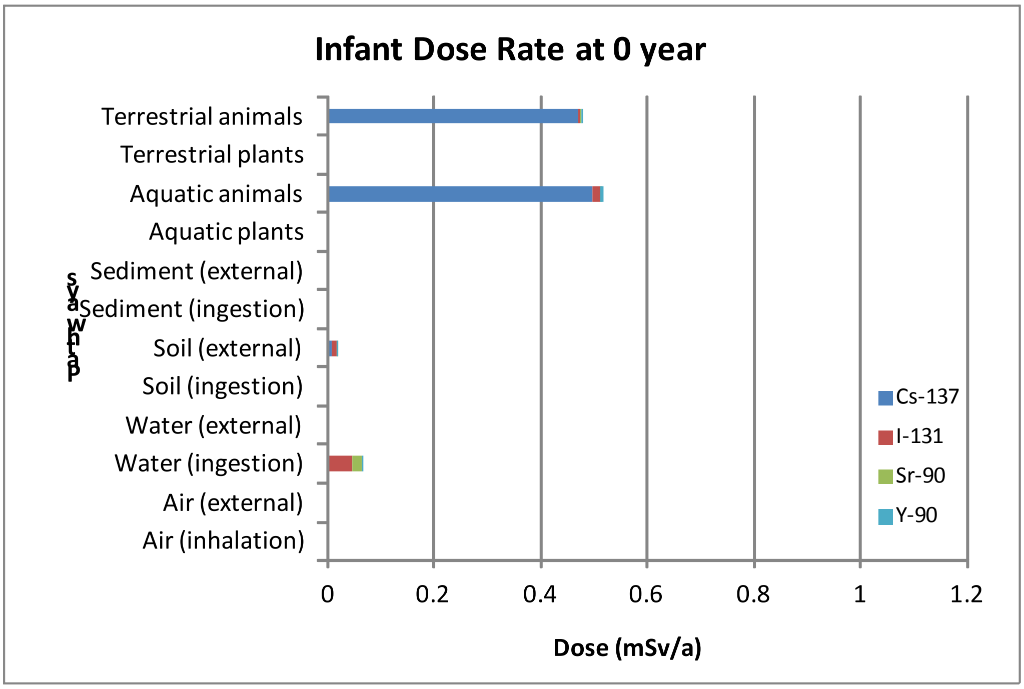

FIG. 28. Pathways contributing to the 1 year old infant dose immediately after the fallout event.

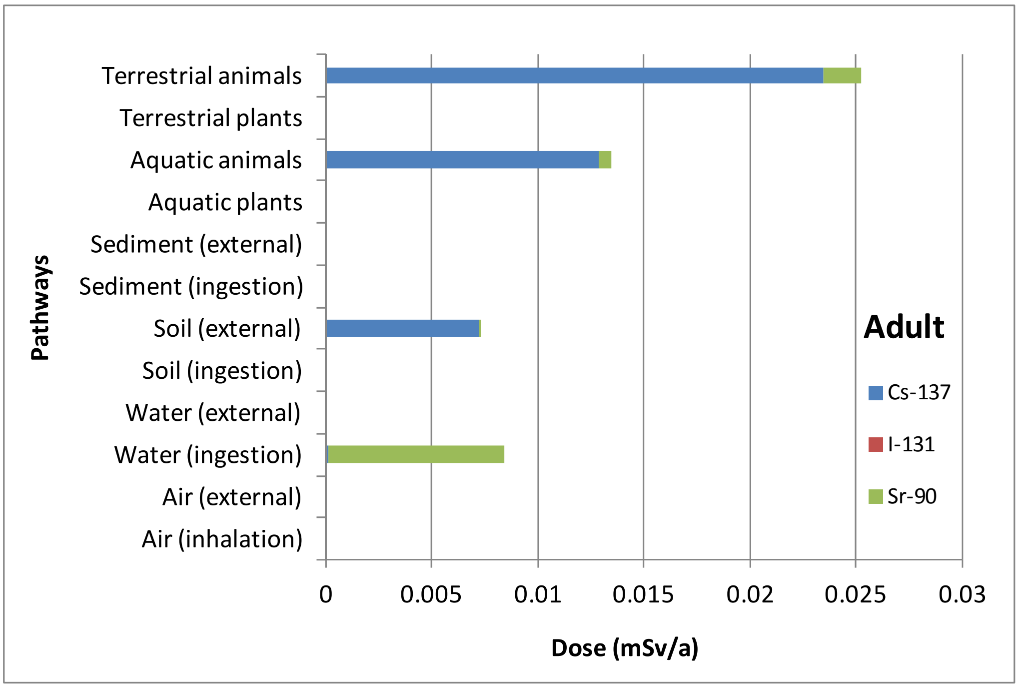

FIG. 29. Pathways contributing to the adult dose 1 year after the fallout event.

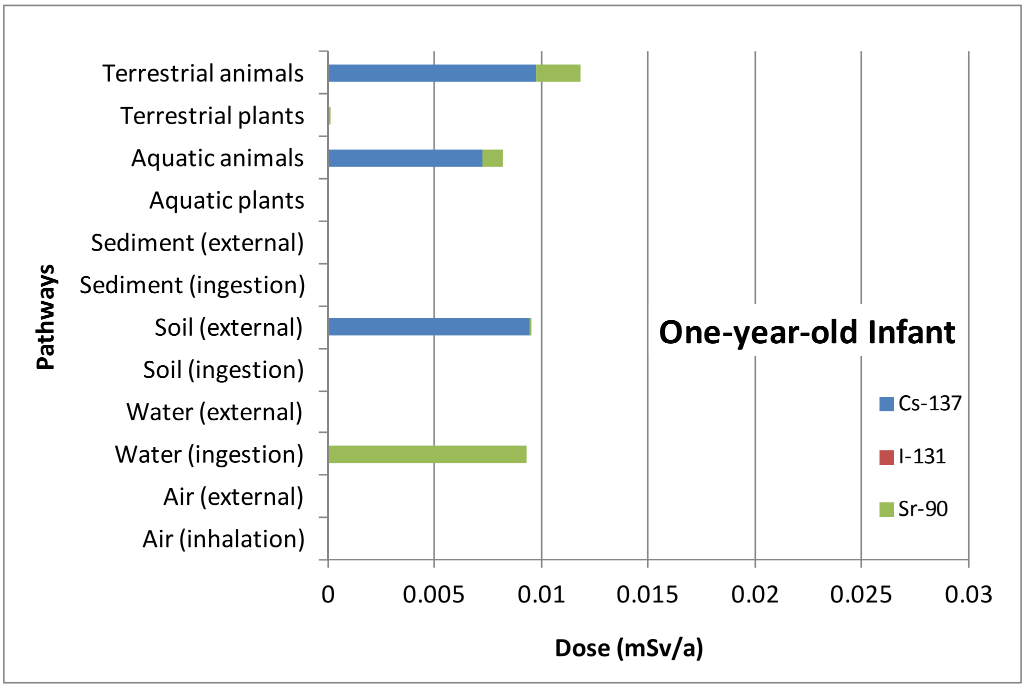

FIG. 30. Pathways contributing to the 1 year old infant dose 1 year after the fallout event.

6.3. ARCTIC TUNDRA, NORTHERN CANADA

Scenario type: Arctic tundra
Scenario location: Canada, north of the tree-line
Short name: Caribou model

6.3.1. Model description

This model focuses on the lichen → caribou → human pathway, which is by far the largest contributor to human doses in the Canadian Arctic. This is particular true for ^{137}Cs, which is developed in detail here. Other pathways for this radionuclide will give much smaller doses, which can be estimated by the use of aggregated transfer coefficients from the literature. ^{90}Sr has not been included due to a lack of available data for this radionuclide in arctic environments. The impact of ^{90}Sr is expected to be less than that of ^{137}Cs because it is not bio-accumulated to any significant degree in arctic food chains. Because of its short half-life ^{131}I also does not accumulate significantly in northern food chains. Furthermore, there is no milk production and little cultivation of leafy vegetables in the Canadian Arctic, pathways that would lead to significant uptake of ^{131}I in temperate climates.

The model for the uptake of ^{137}Cs is carried out in 3 stages:

- Uptake by lichens;
- Uptake by caribou or reindeer;
- Dose to humans.

6.3.1.1. Uptake by lichens

The direct uptake of radioactivity by lichens is one step removed from deposition. In this case, we can use a simple aggregated transfer factor from the literature:

$$C_L = D_{Cs} \bullet T_L \tag{3}$$

where:

C_L is the concentration of ^{137}Cs in lichens (Bq/kg dw);
D_{Cs} is the deposition density of ^{137}Cs (Bq/m^2). Assumed here to be 1000 Bq/m^2; and
T_L is the aggregated transfer factor for fallout ^{137}Cs to lichens (m^2/kg).

6.3.1.2. Uptake by caribou or reindeer

The concentration of ^{137}Cs in caribou or reindeer meat as a result of lichen consumption can be expressed as follows:

$$C_A = C_L \bullet F_L \bullet A_{Cs} \bullet T_{½} /\{ \ln(2) \bullet M_A \} \tag{4}$$

where:

C_A is the concentration of ^{137}Cs in the tissue of the animal (Bq/kg);
F_L is the lichen forage rate (kg dw/day);
A_{Cs} is the ^{137}Cs absorption factor in the animal gut (dimensionless);
$T_{½}$ is the biological halftime of ^{137}Cs in the body of the animal (days); and
M_A is the mass of animal (kg).

Please note that $T_{½}$/ln Equ. (4) is the mean residence time of ^{137}Cs in the body of the animal. It is assumed here that ^{137}Cs becomes uniformly distributed throughout the body of the animal.

6.3.1.3. Dose to humans

The dose to an adult human consuming caribou or reindeer meat can be expressed as follows:

$$H_I = C_A \bullet F_H \bullet DC(^{137}Cs) \tag{5}$$

where:

H_I is the dose (µSv/year) to an adult human during the first year following the event;
F_H is the annual consumption rate of the animal by humans (kg/year); and
$DC(^{137}Cs)$ is the adult ingestion dose coefficient for ^{137}Cs (µSv/Bq).

6.3.2. Application to the northern Canadian scenario

The values of the various parameters used in Equations (3)–(5) have been gathered from the literature and are summarized in Table 19. The last column is a weighted judgment of the best literature value.

TABLE 19. PARAMETERS USED TO CALCULATE DOSES FROM ^{137}CS IN THE ARCTIC MODEL

Parameter	Symbol	Units	Literature values	References	Value selected here
Aggregate transfer factor to lichens	T_L	m^2/kg	0.3–0.5 1.0 1.0 1.4 0.4–2.0	From data of Hansen [47] Ramsaev et al [48] Default value CSA [40] IAEA [11] From data of Hofmann et al [49]	1.0
Lichen forage rate	F_L	kg/day dw	2–5 2 2.5 4–5	Dietrich and Morton [50] Åhman [51] Holleman et al [52] From data of Hansen [47]	2.5
Absorption factor in animal gut	A_{Cs}	none	0.25 0.35 0.65 1.00	Holleman et al [52] Skuterud [53] Åhman [51] Value for humans	0.65
Half time in animal	$T_{½}$	days	17† 17.8 20–33	Holleman et al [52] Skuterud [53] IAEA [11]	20
Mass of animal	M_A	kg			80
Human consumption rate	F_H	kg/y	23.7‡	Tracy and Kramer [54]	23.7
Ingestion dose coefficient	DC(^{137}Cs)	µSv/Bq	1.3×10^{-2}	ICRP [29]	1.3×10^{-2}

† Winter value. The corresponding half-time in summer is 6.7 days.
‡ Highest value measured in 1989 survey.

TABLE 20. ^{137}CS ADULT DOSES

Pathway	^{137}Cs adult doses (µSv/year)			Method of calculation
	Year 1	Year 2	Year 10	
Caribou	181	161	64	Caribou model
Moose	1.6	1.4	0.57	Aggregated transfer coefficient†
Fruit and berries	2.1	1.9	0.67	Aggregated transfer coefficient
Groundshine	4.4	3.9	1.6	Groundshine dose factor‡
Total	**189**	**168**	**67**	

† From IAEA [11].
‡ From CSA [40].

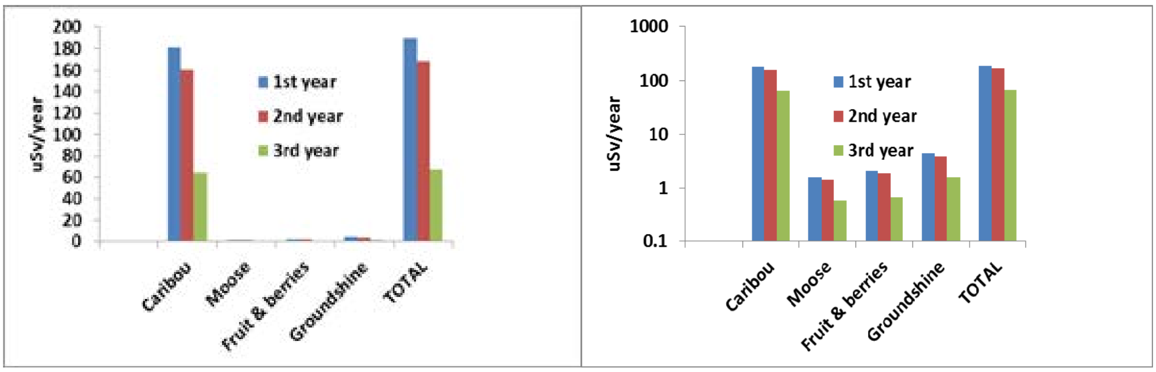

FIG. 31. ^{137}Cs adult doses. Linear scale on left graph; log scale on right graph.

6.3.3. Results

Assuming a ^{137}Cs deposition of 1000 Bq/m^2 and utilizing the parameters from Table 19, we obtain the following:

— ^{137}Cs concentration in lichens: **1000 Bq/kg**
— ^{137}Cs concentration in caribou meat: **586 Bq/kg**

Table 20 gives the adult doses from ^{137}Cs from caribou ingestion and other pathways after the first, second and tenth years. Doses from subsequent years have been derived from a simple ecological half-time of 6 years for ^{137}Cs in arctic environments [55]. Doses for infants and children have not been calculated. They will be much less, due to a lower consumption of caribou meat and other traditional foods by children. The milk pathway, which is so important for children in temperate zones, does not play role here as there is no milk production in the Canadian tundra.

Figure 31 presents the same results graphically, on both linear and logarithmic scales to facilitate comparisons.

6.3.4. Uncertainty analysis and discussion

As a reality check at the midpoint of this model calculation, we note that measurements in Finnish reindeer herds [11] taken during the winter following the Chernobyl accident (when lichen feeding would have been greatest) showed aggregated transfer coefficients for ^{137}Cs to reindeer of 0.15 to 0.84 m^2/kg, with a geometric mean of 0.46 m^2/kg. If this value is applied to our given deposition of 1000 Bq/m^2, then the concentration in reindeer meat would be 460 Bq/kg, close to our model estimate of 586 Bq/kg.

The dose calculations in Table 20 and Figure 31 are highly sensitive to the assumed human consumption of caribou and other traditional foods. The caribou consumption of 24 kg/y in Table 19 are based on the highest value obtained in a whole-body counting survey during the winter of 1989 [54]. This quantity can vary greatly with location and time, and from one person to the next. Values up to 100 kg/year or more have been assumed in some assessments.

The results for ^{137}Cs assume that the deposition occurs in late winter or early spring when caribou are still feeding on lichens and uptake from lichens is at a maximum. They also assume that, by the time of harvest, the caribou have been feeding long enough (several half-times) for their body burdens to have reached equilibrium. Furthermore, it is assumed that these concentrations are maintained in the animals for the entire year. This is not an unreasonable assumption, since northern Canadian residents often freeze the meat from a good harvest and consume it over an entire year.

7. FRESHWATER AQUATIC MODEL RESULTS

7.1. EUROPEAN LAKES

Scenario type: freshwater aquatic
Scenario location: Europe: lakes Øvre Heimdalsvatn (Norway) and Bracciano (Italy)
Short name: Lakes – Eur

7.1.1. Model description

Name of model: MOIRA-PLUS – MOdel-based computerized system for management support to Identify optimal remedial strategies for Restoring radionuclide contaminated Aquatic ecosystems and drainage areas.

Brief description of the model: The computerized decision support system MOIRA-PLUS [56] was used in the present exercise. MOIRA-PLUS is based on:

(a) Validated models to evaluate the behaviour of radionuclides in contaminated water bodies and biota and to assess the effect of countermeasures on contamination levels;
(b) Models to assess: (i) the radiation dose to people and biota (fish) by relevant exposure pathways; (ii) the effect of countermeasures and the associated economic impact;
(c) A Multi-Attribute value Analysis (MAA) module to evaluate the effectiveness of different countermeasure strategies by accounting for the social, ecological and economic detriments and costs in relation to their benefits;
(d) A software system consisting of: (i) software formulation of the mathematical models; (ii) a GIS (Geographic Information System) and associated databases to select the aquatic system of interest and, if necessary, the default environmental data required to run the models; (iii) a graphical user interface; (iv) an operating system connecting all the above parts.

MOIRA-PLUS allows one to make predictions for complex water body systems comprising lakes, reservoirs and rivers (MOIRA-RIVER). In particular, MOIRA-PLUS LAKES can evaluate the ecological impact of selected countermeasures on the basis of the so-called LEI (Lake Ecosystem Index) [57, 58].

Unless otherwise specified in Tables 21–25, default values were used for the migration parameters in the model [56, 59].

The radionuclide transfer models implemented in MOIRA-PLUS accounts for the dynamics of the following processes occurring in the fresh water environment:

- Water transport;
- Partition of radionuclide between dissolved and particulate forms;
- Radionuclide sedimentation;
- Direct interaction of dissolved radionuclide in the water column with bottom sediments;
- Radionuclide re-mobilisation from bottom sediments;
- Re-suspension of contaminated sediment;
- Sediment burial;
- Migration to water bodies of radionuclide deposited onto catchments.

7.1.2. Application of the model to the particular scenario

7.1.2.1. Scenario description

This modelling exercise involves two contrasting lakes, one in the mountains of southern Norway and one in the lowlands of central Italy. The lakes were chosen to represent different environmental and socio-economic conditions, in order to explore the concept of environmental sensitivity through predictive modelling. There is also a considerable amount of empirical data available for these lakes, thus reducing the dependence on default values. Most of the lake and catchment characteristics used in the modelling are based on actual field values, although a few parameters were added or modified in order to create an appropriate scenario for modelling purposes and to obtain the maximum information on the environmental sensitivity of such freshwater ecosystems.

7.1.2.2. Lake Øvre Heimdalsvatn

The lake, Øvre Heimdalsvatn, is situated in the Jotunheimen Mountains of central southern Norway (61°25’ N, 8°54’ E; elevation 1090 m). It is a small subalpine lake with a mean depth of 4.7 m, maximum depth 13 m, a surface area of 0.78 km^2 and a catchment area of 23.6 km^2. The highest point of the catchment is 1843 m. The water residence time varies from 2 days at the peak of the spring spate up to more than 400 days in winter (yearly average value 60–70 days) [60].

Øvre Heimdalsvatn is an oligotrophic lake and the concentrations of potassium and calcium in the lake water are 0.4 and 1.7 mg L^{-1}, respectively. Brown trout (*Salmo trutta*) and the European minnow (*Phoxinus phoxinus*) are the only 2 species of fish living in the lake.

There is no permanent settlement within the catchment, but a scientific field station is located on the lake, with an occupancy of about 600 man·days per year. Traditionally, herdsmen also look after cows and sheep during the summer months (70 man·days). These people will use the lake for drinking water in addition to anglers and tourists during the summer months (estimated at 100–200 man days).

The lake is located in the municipality of Øystre Slidre. This municipality has a population of 3216–1597 men and 1619 women. Age distribution: 0-5 years: 212; 6–15 years: 397; >15 years: 2607 persons. Dietary studies have been undertaken and a critical group in Øystre Slidre was identified [61]. Freshwater fish consumption for this group is estimated to be of the order of 5 kg y^{-1}.

The fish yield from Heimdalsvatn has varied over the years. In the 1960s and 1970s, it was about 600 kg y^{-1}, but due to the introduction of the European minnow and subsequent changes in habitat and food resources for the brown trout, this has been reduced to about 230 kg y^{-1}.

7.1.2.3. Lake Bracciano

The volcanic lake Bracciano (42°07’ N, 12°14’ E; elevation 164 m; depth 165 m) is located in central Italy (north Latium) in an area with a typical Mediterranean climate. The water discharge from the lake is approximately 1.2 $m^3 s^{-1}$ (mean water residence time ~137 years). The concentrations of potassium and calcium in the lake water are 40 and 17 mg L^{-1}, respectively. The lake waters show a stratified thermal structure during the period May–November. The epilimnion reaches a thickness of 20–25 m.

The lake is periodically stocked with whitefish (*Coregonus* hybrids). Fish productivity is of the order of 100 000 kg y^{-1}. The population living around the lake was estimated to be 25 492 in 1986 (0–5 years: 1758; 6–15 years: 3916; >15 years: 19 818). The freshwater fish consumption for this population can be approximately estimated of the order of 4 kg y^{-1}. The whitefish are planktonic and during the stratification prefer the cooler waters of the hypolimnion [60].

The first step of the present exercise was the calibration of MOIRA models by accounting for the available data of radiocaesium contamination of the lakes, Bracciano and Øvre Heimdalsvatn, following the Chernobyl accident. The calibration assures that the results of the present exercise can be deemed realistic evaluations of the environmental sensitivity of lacustrine systems to ^{137}Cs contamination. As similar empirical data were not available for ^{90}Sr, the results of the analysis for this latter radionuclide are estimates obtained by models making use of generic values for contaminant transfer parameters.

Considerations of the uncertainty of results from generic aquatic models have been presented and discussed in depth in Monte et al. [62]. The ^{90}Sr results should be assigned an uncertainty of about a factor 2 for concentrations in water, although it may be even greater for the contamination in fish. On the other hand, lower levels of uncertainty should be expected for ^{137}Cs in view of the preliminary model calibration.

The environmental sensitivity analysis was performed assuming an instantaneous deposition of 1000 Bq m^{-2} of ^{137}Cs and ^{90}Sr occurring under different seasonal conditions (winter, spring, summer and autumn). However, due to the particular input-output structure of MOIRA-PLUS, it was assumed that the deposition occurred over a period of 1 month at constant rate, with no distinction for wet or dry deposition.

7.1.3. Results

The environmental sensitivity was calculated as the ratios of the time integrated concentrations of radionuclides in water and fish and of the dose to fish divided by the deposition, at time 1 year, 2 years and 10 years following the pulse contamination event. Furthermore, similar calculations were performed for the doses to critical groups of individuals due to: a) the aquatic pathway alone (water and fish ingestion, external irradiation from contaminated water and sediment); b) the aquatic pathway with the addition the ingestion of crops and animal products contaminated by irrigation from the lakes.

The site specific values of the model parameters for ^{137}Cs obtained by model calibration are reported in Table 21. Tables 22, 23, 24 and 25 report the socioeconomic data used for the calculations of doses. In particular, Table 24 shows the annual consumptions of animal products and crops available in various literature [60, 61, 63] and assumed to be representative of the situations for both lacustrine environments. Tables 26, 27, 28, 29, 30 and 31 report the results of MOIRA-PLUS and of the environmental sensitivity analysis. Figures 32–37 report the dose rates released to the critical groups and to the fish.

7.1.4. Discussion

The time behavior of the integrated radionuclide concentrations in the lakes (Table 26 and 27) can be explained by accounting for: a) the different lake depths that imply, in the short term, a higher dilution of radionuclides in volcanic lake, Bracciano compared to Øvre Heimdalsvatn; and b) the significant difference between the mean water retention times of the 2 lakes. Indeed, in the long term, the high value of the water residence time (c. 137 years,) is responsible for persistent levels of water contamination in Bracciano. This is reflected in higher values of time integrated concentrations in water for Bracciano versus Øvre Heimdalsvatn after 10 years.

The significant differences between the time integrated concentrations of radiocaesium and radiostrontium in fish the 2 lakes can be explained by the high contents of K and Ca in waters of Bracciano (40 and 17 mg L^{-1}, respectively) compared to the Norwegian lake (0.4 mg L^{-1} of K and 1.7 mg L^{-1} of Ca).

In nearly all cases the indices in Tables 30 and 31 indicate that Øvre Heimdalsvatn is clearly more sensitive to the radioactive contamination than Bracciano. However, because of the peristence of radionuclide contamination in the volcanic lake, the time integrated concentrations of ^{137}Cs in water and the doses to critical individuals in Bracciano will exceed the corresponding values for Øvre Heimdalsvatn after 10 years. The "dose to critical individuals" was calculated by accounting for the contamination caused by the use of irrigation water from the lake. However, it is important to note that such an agricultural practice is not well documented for Bracciano and that the water used for irrigation purposes is probably not directly extracted from this lake. In reality, waters from Øvre Heimdalsvatn are also not used for irrigation, although irrigation may be employed in neighbouring agricultural catchments during summer.

The effects of an accident are more marked in spring and summer for the Norwegian lake. It was assumed that almost 70% of radionuclides deposited onto the ice covering the lake from October until June is released to the water body during the melting of the lake ice (June), although a major part this will be transported out of the lake during the period with high flow through rate during the spring snowmelt [64].

The case of Bracciano deserves some more attention. The model used here does not account for thermal stratification in this lake. Except for stratification, no other parameter can cause marked seasonal behaviour of radionuclides in the lake. Thermal stratification is responsible for enhanced levels of surface water contamination for accidents occurring from the end of spring to the end of autumn. Consequently, the concentration of radionuclide in surface water can be up to 4 times higher than the value estimated assuming an homogeneous distribution in the whole water column. This will cause an increase of the time integrated concentration in fish of 50% during the first year, 25% in the second and less than 5% after 10 years. It should be noted that whitefish show a marked preference for deep cold water that are contaminated with negligible amount of radionuclide during the stratification period. This behaviour implies a reduced contamination of fish even when high concentrations of radionuclides occur in the surface layers of lake water.

The doses to individuals and populations are not directly associated with the environmental conditions as they depend on factors of social and economic nature such as the population living habits, food consumption preferences, and agricultural practices. It is worthwhile to note that the doses to critical individuals from water and fish ingestion reflect the behaviour of the radionuclides in water and fish and therefore, in this respect, lake Øvre Heimdalsvatn is more sensitive than Bracciano. However, if we consider the doses to critical individuals accounting for the terrestrial pathway, due to the particular assumed agricultural practises, the doses released to the critical group living in Bracciano area are, in general, higher than those released to the corresponding group of lake Øvre Heimdalsvatn. However, particular seasonal conditions in summer imply higher doses to critical individuals during the first and the second years following the deposition in the Norwegian lake. Nevertheless, the Norwegian lake is, in any case, more sensitive to ^{90}Sr deposition than the Italian lake.

TABLE 21. CALIBRATED VALUES OF MODEL PARAMETERS FOR ^{137}CS IN THE 2 LAKES

Parameter	Øvre Heimdalsvatn	Bracciano
Transfer coefficient from catchment to water body (m^{-1})	0.0068	Default (0.06)
Sedimentation velocity (m $month^{-1}$)	Negligible	Default (0.6)
Bioaccumulation factor (trout) (m^3 kg^{-1})	5.34	–
Bioaccumulation factor (prey) (m^3 kg^{-1})	Default (calculated from potassium concentration in water and suspended matter)	0.30 (whitefish)
Bioaccumulation factor (pike) (m^3 kg^{-1})	–	0.29
Biological transfer rate from fish ($month^{-1}$)	0.03 (trout)	Default (0.35)

TABLE 22. POPULATION AGE CLASS STRUCTURES FOR THE MUNICIPALITIES SURROUNDING THE 2 LAKES

Age class (years)	Øystre Slidre	Municipalities of Anguillara Sabazia, Bracciano, Manziana and Trevignano Romano, Italy (in 1986)
0–5	212	1758
6–15	397	3916
>15	2607	19 818
Total	**3216**	**25 492**

TABLE 23. POPULATION HABITS FOR THE POPULATIONS LIVING NEAR THE 2 LAKES

Age group	Øvre Heimdalsvatn			Bracciano		
	0–5 years	6–15 years	>15 years	0–5 years	6–15 years	>15 years
Fraction time boating	0	0.0005	0.0005	0	0.001	0.001
Fraction time on shore	0.005	0.007	0.005	0.01	0.015	0.01
Fraction time swimming	0.002	0.003	0.003	0.004	0.006	0.006

TABLE 24. CONSUMPTION OF ANIMAL PRODUCTS AND CROPS

Product	Consumption (kg $year^{-1}$ – liter $year^{-1}$)
Cow's milk	230
Cow's meat	15
Fish (fresh water)	5
Vegetables, grain, potatoes, fruit	260

TABLE 25. FURTHER SOCIOECONOMIC DATA FOR THE LAKES AND THEIR CACHMENTS

Time of year	Lake Øvre Heimdalsvatn	Lake Bracciano
Period of fishing	June–September	Almost the entire year
Beginning of growing season for crops	May	March
Time of harvest	September	July
Month irrigation starts	June	June
Month irrigation ends	August	September

TABLE 26. TIME INTEGRATED CONCENTRATIONS OF ^{137}CS

Season	Years following the accident	Lake Øvre Heimdalsvatn		Lake Bracciano		
		Water (Bq·month/m^3)	Trout (Bq·month/kg)	Water (Bq·month/m^3)	Whitefish (Bq·month/kg)	Pike (Bq·month/kg)
Winter	1 year	189.03	121.77	113.34	22.15	8.16
	2 years	255.68	435.95	219.89	50.11	26.80
	10 years	300.33	1359.58	880.78	222.83	201.25
Spring	1 year	273.36	243.94	113.34	22.15	8.16
	2 years	323.41	621.97	219.89	50.11	26.80
	10 years	366.10	1664.99	880.78	222.83	201.25
Summer	1 year	473.54	469.92	113.34	22.15	8.16
	2 years	544.97	1098.64	219.89	50.11	26.80
	10 years	606.57	2780.92	880.78	222.83	201.25
Autumn	1 year	138.20	53.27	113.34	22.15	8.16
	2 years	236.52	345.60	219.89	50.11	26.80
	10 years	286.68	1293.15	880.78	222.83	201.25

TABLE 27. TIME INTEGRATED CONCENTRATIONS ^{90}SR

Season	Years following the accident	Lake Øvre Heimdalsvatn		Lake Bracciano		
		Water (Bq·month/m^3)	Trout (Bq·month/kg)	Water (Bq·month/m^3)	Whitefish (Bq·month/kg)	Pike (Bq·month/kg)
Winter	1 year	935.57	6.24	127.21	<0.12	<0.12
	2 years	1305.65	20.81	25.87	0.15	0.15
	10 years	3079.28	170.21	1074.51	3.20	3.20
Spring	1 year	2916.75	27.23	127.21	<0.12	<0.12
	2 years	3324.76	66.61	252.87	0.15	0.15
	10 years	5280.05	327.17	1074.51	3.20	3.20
Summer	1 year	970.72	8.11	127.21	<0.12	<0.12
	2 years	1303.27	22.46	252.87	0.15	0.15
	10 years	3064.58	170.49	1074.51	3.20	3.20
Autumn	1 year	523.15	2.28	127.21	<0.12	<0.12
	2 years	884.09	11.35	252.87	0.15	0.15
	10 years	2605.05	136.30	1074.51	3.20	3.20

TABLE 28. DOSE RATES FROM ^{137}CS

Season	Years following the accident	Lake Øvre Heimdalsvatn			Lake Bracciano		
		Dose to critical individuals (mSv/year)	Maximum dose to fish (mGy/year)	Dose to critical individuals from ingestion of fish and water (mSv/year)	Dose to critical individuals (mSv/year)	Maximum dose to fish (mGy/year)	Dose to critical individuals from ingestion of fish and water (mSv/year)
Winter	1 year	9.3×10^{-4}	9.8×10^{-2}	3.1×10^{-4}	1.5×10^{-3}	7.1×10^{-3}	1.2×10^{-4}
	2 years	1.6×10^{-3}	7.7×10^{-2}	1.0×10^{-3}	2.1×10^{-3}	9.9×10^{-3}	1.4×10^{-4}
	10 years	4.2×10^{-4}	1.5×10^{-2}	3.6×10^{-4}	1.6×10^{-3}	9.5×10^{-3}	1.2×10^{-4}
Spring	1 year	1.3×10^{-3}	1.6×10^{-1}	3.9×10^{-4}	2.0×10^{-3}	7.1×10^{-3}	1.2×10^{-4}
	2 years	1.9×10^{-3}	6.3×10^{-2}	1.2×10^{-3}	2.1×10^{-3}	9.9×10^{-3}	1.4×10^{-4}
	10 years	5.0×10^{-4}	1.8×10^{-2}	4.4×10^{-4}	1.6×10^{-3}	9.5×10^{-3}	1.2×10^{-4}
Summer	1 year	2.9×10^{-3}	2.9×10^{-1}	1.6×10^{-3}	4.1×10^{-4}	7.1×10^{-3}	1.2×10^{-4}
	2 years	2.4×10^{-3}	8.7×10^{-2}	1.9×10^{-3}	2.1×10^{-3}	9.9×10^{-3}	1.4×10^{-4}
	10 years	6.8×10^{-4}	2.9×10^{-2}	6.2×10^{-4}	1.6×10^{-3}	9.5×10^{-3}	1.2×10^{-4}
Autumn	1 year	8.3×10^{-4}	5.3×10^{-2}	2.6×10^{-4}	8.5×10^{-4}	7.1×10^{-3}	1.2×10^{-4}
	2 years	1.5×10^{-3}	1.1×10^{-1}	9.9×10^{-4}	2.1×10^{-3}	9.9×10^{-3}	1.4×10^{-4}
	10 years	4.0×10^{-4}	1.6×10^{-2}	3.5×10^{-4}	1.6×10^{-3}	9.5×10^{-3}	1.2×10^{-4}

TABLE 29. DOSE RATES FROM ^{90}SR

Season	Years following the accident	Lake Øvre Heimdalsvatn: Dose to critical individuals (mSv/y)	Lake Øvre Heimdalsvatn: Maximum dose to fish (mGy/y)	Lake Øvre Heimdalsvatn: Dose to critical individuals from ingestion of fish and water (mSv/y)	Lake Bracciano: Dose to critical individuals (mSv/y)	Lake Bracciano: Maximum dose to fish (mGy/y)	Lake Bracciano: Dose to critical individuals from ingestion of fish and water (mSv/y)
Winter	1 year	1.7×10^{-1}	7.5×10^{-3}	2.2×10^{-4}	1.4×10^{-2}	6.3×10^{-4}	2.5×10^{-5}
	2 years	8.5×10^{-2}	1.7×10^{-2}	1.7×10^{-4}	1.6×10^{-2}	1.8×10^{-3}	2.6×10^{-5}
	10 years	5.7×10^{-2}	2.1×10^{-2}	1.7×10^{-4}	1.4×10^{-2}	4.3×10^{-3}	2.3×10^{-5}
Spring	1 year	4.2×10^{-1}	3.2×10^{-2}	6.7×10^{-4}	1.5×10^{-2}	6.3×10^{-4}	2.5×10^{-5}
	2 years	1.4×10^{-1}	4.6×10^{-2}	3.4×10^{-4}	1.6×10^{-2}	1.8×10^{-3}	2.6×10^{-5}
	10 years	7.1×10^{-2}	3.7×10^{-2}	2.7×10^{-4}	1.4×10^{-2}	4.3×10^{-3}	2.3×10^{-5}
Summer	1 year	1.2×10^{-1}	9.6×10^{-3}	2.5×10^{-4}	4.2×10^{-3}	6.3×10^{-4}	2.5×10^{-5}
	2 years	6.5×10^{-2}	1.7×10^{-2}	1.6×10^{-4}	1.6×10^{-2}	1.8×10^{-3}	2.6×10^{-5}
	10 years	5.2×10^{-2}	2.1×10^{-2}	1.6×10^{-4}	1.4×10^{-2}	4.3×10^{-3}	2.3×10^{-5}
Autumn	1 year	9.6×10^{-2}	2.8×10^{-3}	1.3×10^{-4}	7.3×10^{-3}	6.3×10^{-4}	2.5×10^{-5}
	2 years	7.0×10^{-2}	1.1×10^{-2}	1.4×10^{-4}	1.6×10^{-2}	1.8×10^{-3}	2.6×10^{-5}
	10 years	5.2×10^{-2}	1.8×10^{-2}	1.5×10^{-4}	1.4×10^{-2}	4.3×10^{-3}	2.3×10^{-5}

TABLE 30. ENVIRONMENTAL SENSITIVITY ANALYSIS; RESULTS FOR ^{137}CS

Measure of the effect	Seasonal conditions of the accident	Sensitivity=Measure of the effect/1000 Bq m^{-2}					
		Lake Øvre Heimdalsvatn			Lake Bracciano		
		1 year	2 years	10 years	1 year	2 years	10 years
Time integrated concentration in water (Bq m^{-3}·month)	Winter	***1.9×10^{-1}***	***2.6×10^{-1}***	3.0×10^{-1}	1.1×10^{-1}	2.2×10^{-1}	***8.8×10^{-1}***
	Spring	***2.7×10^{-1}***	***3.2×10^{-1}***	3.7×10^{-1}	1.1×10^{-1}	2.2×10^{-1}	***8.8×10^{-1}***
	Summer	***4.7×10^{-1}***	***5.4×10^{-1}***	6.1×10^{-1}	1.1×10^{-1}	2.2×10^{-1}	***8.8×10^{-1}***
	Autumn	***1.4×10^{-1}***	***2.4×10^{-1}***	2.9×10^{-1}	1.1×10^{-1}	2.2×10^{-1}	***8.8×10^{-1}***
Time integrated concentration in fish (Bqkg^{-1}·month)	Winter	***1.2×10^{-1}***	***4.4×10^{-1}***	***1.4***	2.2×10^{-2}	5.0×10^{-2}	2.2×10^{-1}
	Spring	***2.4×10^{-1}***	***6.2×10^{-1}***	***1.7***	2.2×10^{-2}	5.0×10^{-2}	2.2×10^{-1}
	Summer	***4.7×10^{-1}***	***1.1***	***2.8***	2.2×10^{-2}	5.0×10^{-2}	2.2×10^{-1}
	Autumn	***5.3×10^{-2}***	***3.5×10^{-1}***	***1.3***	2.2×10^{-2}	5.0×10^{-2}	2.2×10^{-1}
Dose rate to fish (mGy y^{-1})	Winter	***9.8×10^{-5}***	***7.7×10^{-5}***	***1.5×10^{-5}***	7.1×10^{-6}	9.9×10^{-6}	9.3×10^{-6}
	Spring	***1.6×10^{-4}***	***6.3×10^{-5}***	***1.8×10^{-5}***	7.1×10^{-6}	9.9×10^{-6}	9.3×10^{-6}
	Summer	***2.9×10^{-4}***	***8.7×10^{-5}***	***2.9×10^{-5}***	7.1×10^{-6}	9.9×10^{-6}	9.3×10^{-6}
	Autumn	***5.3×10^{-5}***	***1.1×10^{-4}***	***1.6×10^{-5}***	7.1×10^{-6}	9.9×10^{-6}	9.3×10^{-6}
Dose rate to critical individuals (mSv y^{-1})	Winter	9.3×10^{-7}	1.6×10^{-6}	4.2×10^{-7}	***1.5×10^{-6}***	***2.1×10^{-6}***	***1.6×10^{-6}***
	Spring	1.3×10^{-6}	1.9×10^{-6}	5.0×10^{-7}	***2.0×10^{-6}***	***2.1×10^{-6}***	***1.6×10^{-6}***
	Summer	***2.9×10^{-6}***	***2.4×10^{-6}***	6.8×10^{-7}	4.1×10^{-7}	2.1×10^{-6}	***1.6×10^{-6}***
	Autumn	8.3×10^{-7}	1.5×10^{-6}	4.0×10^{-7}	***8.5×10^{-7}***	***2.1×10^{-6}***	***1.6×10^{-6}***
Dose rate to critical individuals from ingestion of fish and water (mSv y^{-1})	Winter	***3.1×10^{-7}***	***1.0×10^{-6}***	***3.6×10^{-7}***	1.2×10^{-7}	1.4×10^{-7}	1.2×10^{-7}
	Spring	***3.9×10^{-7}***	***1.2×10^{-6}***	***4.4×10^{-7}***	1.2×10^{-7}	1.4×10^{-7}	1.2×10^{-7}
	Summer	***1.6×10^{-6}***	***1.9×10^{-6}***	***6.2×10^{-7}***	1.2×10^{-7}	1.4×10^{-7}	1.2×10^{-7}
	Autumn	***2.6×10^{-7}***	***9.9×10^{-7}***	***3.5×10^{-7}***	1.2×10^{-7}	1.4×10^{-7}	1.2×10^{-7}

NOTE: The maximum value for each lake, condition and time period is in ***italics***.

TABLE 31. ENVIRONMENTAL SENSITIVITY ANALYSIS; RESULTS FOR ^{90}SR

Measure of the effect	Seasonal conditions of the accident	Sensitivity=Measure of the effect/1000 Bq m^{-2}					
		Lake Øvre Heimdalsvatn			Lake Bracciano		
		1 year	2 years	10 years	1 year	2 years	10 years
Time integrated concentration in water (Bq m^{-3}·month)	Winter	*9.4×10^{-1}*	*1.3*	*3.1*	1.3×10^{-1}	2.5×10^{-1}	1.1
	Spring	*2.9*	*3.3*	*5.3*	1.3×10^{-1}	2.5×10^{-1}	1.1
	Summer	*9.7×10^{-1}*	*1.3*	*3.1*	1.3×10^{-1}	2.5×10^{-1}	1.1
	Autumn	*5.2×10^{-1}*	*8.8×10^{-1}*	*2.6*	1.3×10^{-1}	2.5×10^{-1}	1.1
Time integrated concentration in fish (Bqkg^{-1}·month)	Winter	*6.2×10^{-3}*	*2.1×10^{-2}*	*1.7×10^{-1}*	$<1.2 \times 10^{-4}$	1.5×10^{-4}	3.2×10^{-3}
	Spring	*2.7×10^{-2}*	*6.7×10^{-2}*	*3.3×10^{-1}*	$<1.2 \times 10^{-4}$	1.5×10^{-4}	3.2×10^{-3}
	Summer	*8.1×10^{-3}*	*2.2×10^{-2}*	*1.7×10^{-1}*	$<1.2 \times 10^{-4}$	1.5×10^{-4}	3.2×10^{-3}
	Autumn	*2.3×10^{-3}*	*1.1×10^{-2}*	*1.4×10^{-1}*	$<1.2 \times 10^{-4}$	1.5×10^{-4}	3.2×10^{-3}
Dose rate to fish (mGy y^{-1})	Winter	*7.5×10^{-6}*	*1.7×10^{-5}*	*2.1×10^{-5}*	6.3×10^{-7}	1.8×10^{-6}	4.3×10^{-6}
	Spring	*3.2×10^{-5}*	*4.6×10^{-5}*	*3.7×10^{-5}*	6.3×10^{-7}	1.8×10^{-6}	4.3×10^{-6}
	Summer	*9.6×10^{-6}*	*1.7×10^{-5}*	*2.1×10^{-5}*	6.3×10^{-7}	1.8×10^{-6}	4.3×10^{-6}
	Autumn	*2.8×10^{-6}*	*1.1×10^{-5}*	*1.8×10^{-5}*	6.3×10^{-7}	1.8×10^{-6}	4.3×10^{-6}
Dose rate to critical individuals (mSv y^{-1})	Winter	*1.7×10^{-4}*	*8.5×10^{-5}*	*5.7×10^{-5}*	1.4×10^{-5}	1.6×10^{-5}	1.4×10^{-5}
	Spring	*4.2×10^{-4}*	*1.4×10^{-4}*	*7.1×10^{-5}*	1.5×10^{-5}	1.6×10^{-5}	1.4×10^{-5}
	Summer	*1.2×10^{-4}*	*6.5×10^{-5}*	*5.2×10^{-5}*	4.2×10^{-6}	1.6×10^{-5}	1.4×10^{-5}
	Autumn	*9.6×10^{-5}*	*7.0×10^{-5}*	*5.2×10^{-5}*	7.3×10^{-6}	1.6×10^{-5}	1.4×10^{-5}
Dose rate to critical individuals from ingestion of fish and water (mSv y^{-1})	Winter	*2.2×10^{-7}*	*1.7×10^{-7}*	*1.7×10^{-7}*	2.5×10^{-8}	2.6×10^{-8}	2.3×10^{-8}
	Spring	*6.7×10^{-7}*	*3.4×10^{-7}*	*2.7×10^{-7}*	2.5×10^{-8}	2.6×10^{-8}	2.3×10^{-8}
	Summer	*2.5×10^{-7}*	*1.6×10^{-7}*	*1.6×10^{-7}*	2.5×10^{-8}	2.6×10^{-8}	2.3×10^{-8}
	Autumn	*1.3×10^{-7}*	*1.4×10^{-7}*	*1.5×10^{-7}*	2.5×10^{-8}	2.6×10^{-8}	2.3×10^{-8}

NOTE: The maximum value for each lake, condition and time period is in italics.

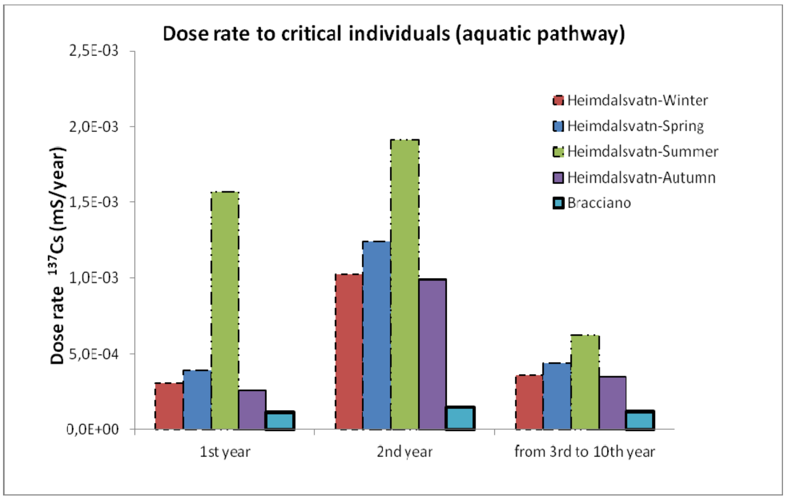

FIG. 32. Dose rates to critical individuals from ^{137}Cs due to the aquatic pathway.

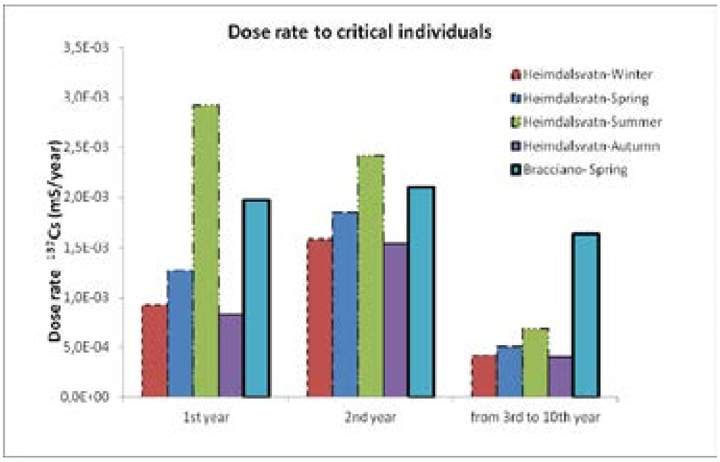

FIG. 33. Dose rates to critical individuals from ^{137}Cs due to both the aquatic and the terrestrial pathways, assuming that the lake waters are used for irrigation.

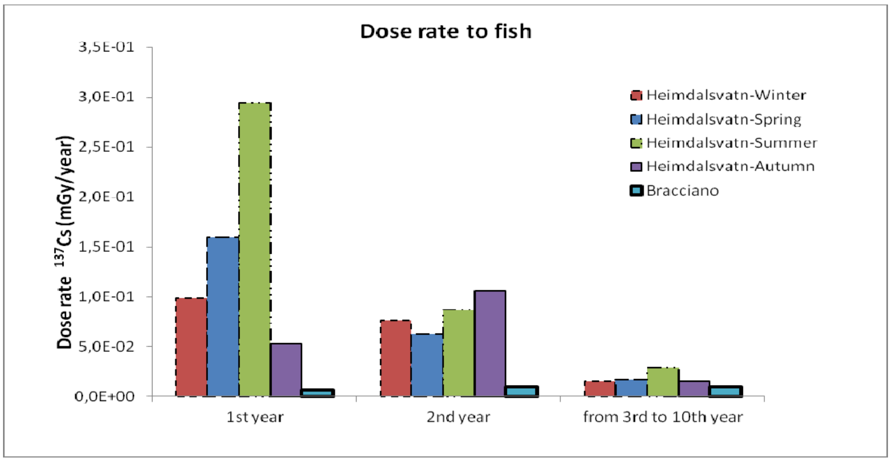

FIG. 34. Dose rates to fish from ^{137}Cs.

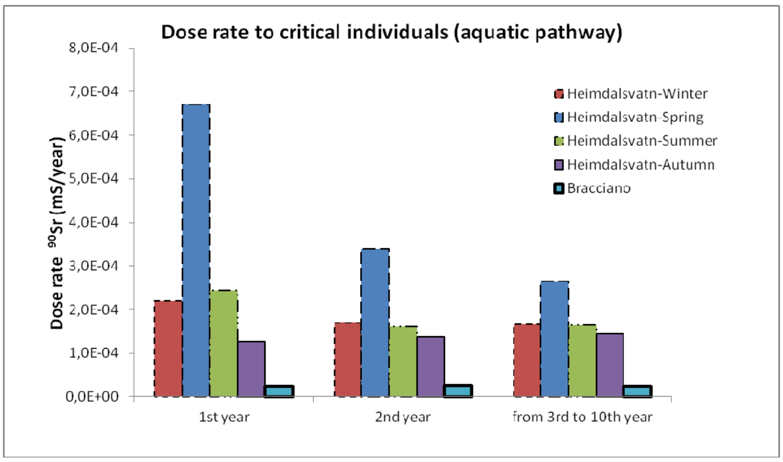

FIG. 35. Dose rates to critical individuals from ^{90}Sr due to the aquatic pathway.

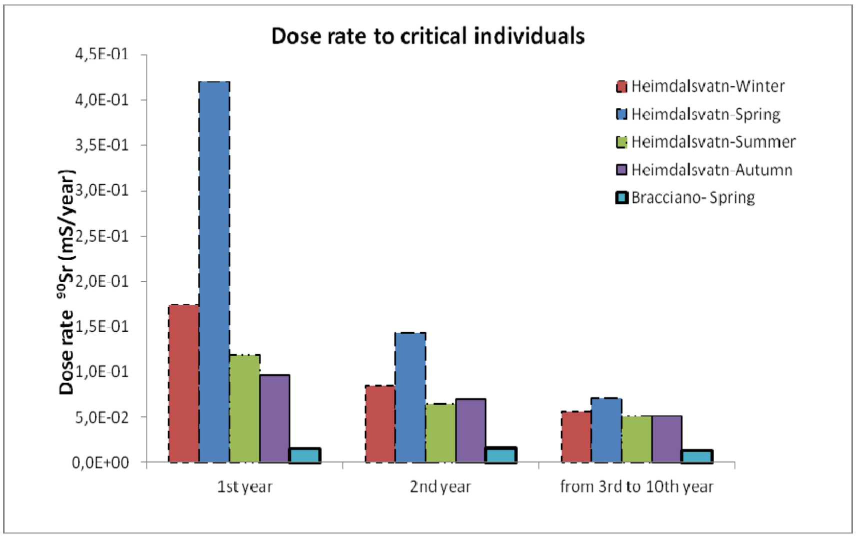

FIG. 36. Dose rates to critical individuals from ^{90}Sr due to the aquatic and to the terrestrial pathways assuming that the lake waters are used for irrigation.

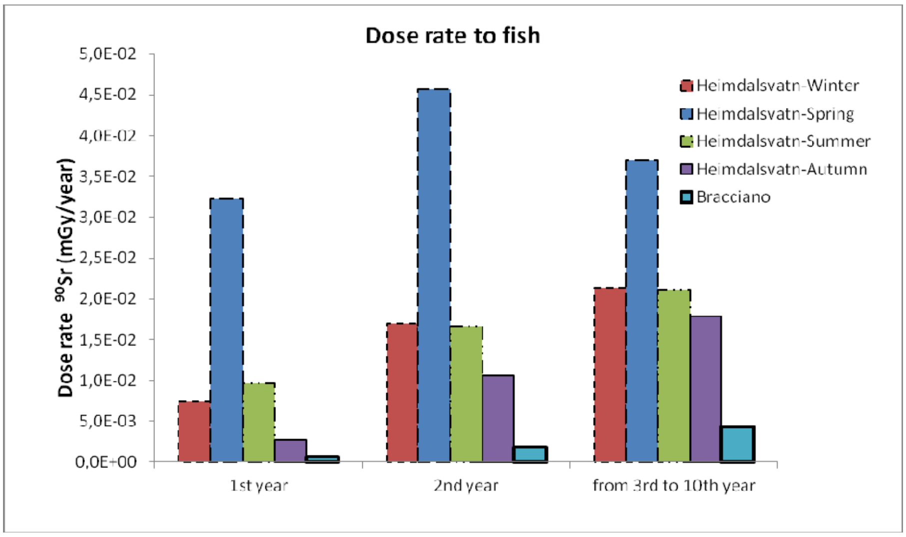

FIG. 37. Dose rates to fish from ^{90}Sr.

7.2. A SHALLOW LAKE IN ONTARIO CANADA

7.2.1. Model description

CHERPAC Code (See Section 5.1.1.)

7.2.2. Scenario description

In this scenario, it was assumed that 1000 Bq m^{-2} of ^{137}Cs, ^{90}Sr, and ^{131}I were deposited instantaneously in an aquatic freshwater ecosystem (a shallow lake, 5 m deep). It was also assumed that people living in this ecosystem were self-sufficient with respect to fish ingestion included in this scenario and did not consume contaminated agricultural/forest products, and did not drink water from that lake.

Cases of the deposition occurring under dry or heavy rainfall conditions were evaluated. Seasonal effects were evaluated by considering cases in which the deposition occurred in winter, spring, summer, or autumn. The concentration in fish and the ingestion and groundshine doses to an adult, a 10 year old child and a 1 year old infant were predicted for a 2 year period following the deposition.

7.2.3. Application to the Freshwater Aquatic Scenario

Most of the information in Section 5.1.1.3 for the agricultural scenario is also applicable here. However, some additional steps were taken in order to use CHERPAC for modelling this scenario.

CHERPAC has neither a lake model, nor a lake-to-fish transfer model. It actually takes monthly concentrations in fish as input values and accounts for the timing of the fishing season and for radioactive decay. To complete these calculations, a 5 m deep lake was modelled outside CHERPAC. After initial deposition on that lake, monthly water concentrations for ^{137}Cs were reduced using observed data from some lakes in Europe after Chernobyl fallout. For ^{90}Sr, it was done using pond model of CSA Guideline N288.1-08 [40]. For ^{131}I, it was done simply by using radioactive decay, because it is a short lived radionuclide. A model for accumulating ^{137} Cs in fish from lake water (previously used as a pre-processor for CHERPAC) was also used in this scenario. This model was adapted for ^{90}Sr by considering the water concentrations and BAF of ^{90}Sr, and the dynamics and BAF of ^{137}Cs. For ^{131}I, fish concentrations were calculated based on the water concentration and BAF.

7.2.4. Results

Although detailed results were calculated for all cases, the discussion and figures presented here are for 1 case: the dry deposition of ^{137}Cs in summer (August). Many of the comments made here apply to other cases also.

7.2.4.1. Fish

Figure 38 shows the concentration of ^{137}Cs in fish increases to a peak at about 9 months after deposition occurred, then decreases slowly.

7.2.4.2. Doses from ^{137}Cs

Figure 39 shows the ingestion doses to an adult and 10 year old child are of similar order of magnitude to the groundshine doses. Adult ingestion doses are higher than those for children and infants because of the higher rates of intake of fish by adults.

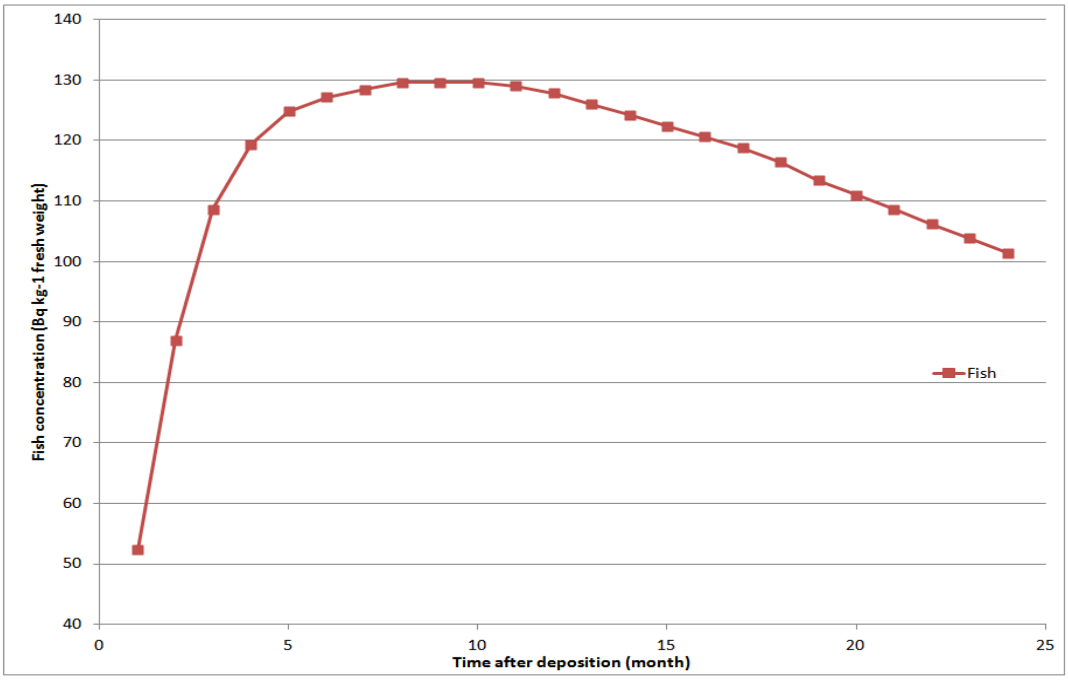

FIG. 38. CHERPAC-predicted concentrations in freshwater fish at consumption: ^{137}Cs, dry deposition in summer (August).

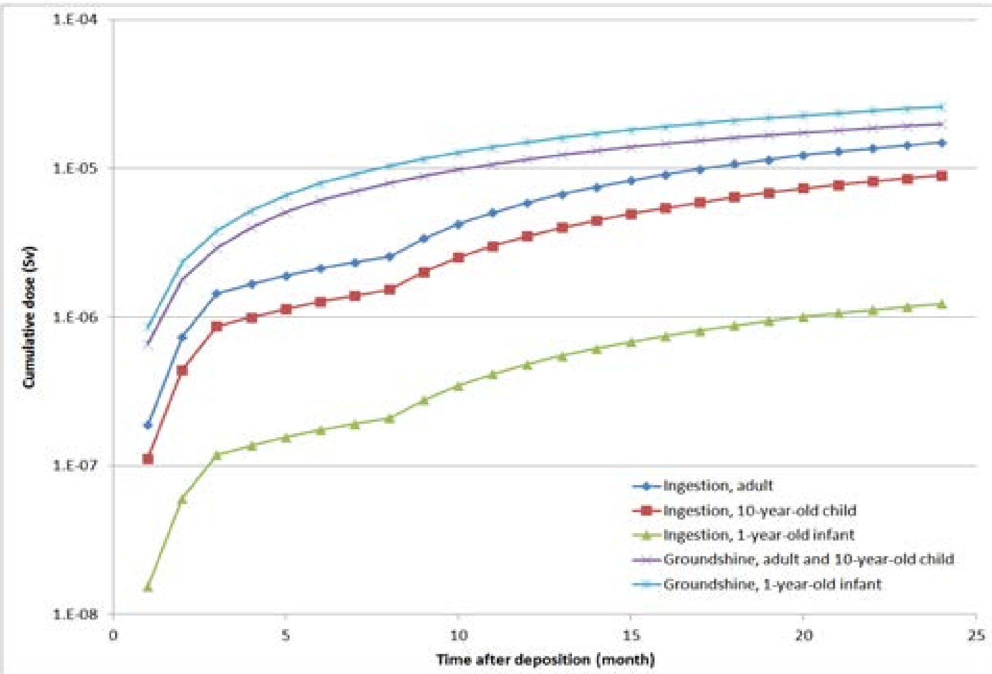

FIG. 39. CHERPAC-predicted cumulative doses to humans: ^{137}Cs, dry deposition in summer (August) in freshwater aquatic environment.

8. SHALLLOW MARINE AND COASTAL MODEL RESULTS

8.1. NORTHEAST AEGEAN SEA, GREECE

8.1.1. Model description

Name of model: NTUA-School of Chemical Engineering

Brief description of the model:

- General deterministic model developed to simulate the time-dependent behaviour of ^{137}Cs and heavy metals (Cu, Ni, Mn) in the NE Aegean Sea;
- Full Navier-Stokes equations for transient, 3-dimensional turbulent flow, heat and mass transfer;
- Computational Fluid Dynamics (CFD) code: PHOENICS (Parabolic Hyperbolic Or Elliptic Numerical Integration Code Series);
- Hydrodynamic dispersion and turbulence diffusion (sea surface, water column) of ^{137}Cs (activity concentrations Bq•m^{-3}, winter and summer);
- Activity concentrations in organisms based on activity concentration in sea water;
- External dose rate estimations based on sediment and sea water activity concentrations and on the habitat of the studied biota;
- Internal dose rate estimations based on radionuclide concentrations in generic biota;
- External, internal dose rates (human);
- Heavy metals concentrations (fish, human).

Details of the model can be found in Psaltaki et al. [65–68]. Further discussions on methodology and other applications are available in Papadimitrakis et al. [69, 70].

The full Navier-Stokes equation for transient, 3-dimensional turbulent flow, heat and mass transfer is presented in general form here. It is solved by the finite volume method.

$$\partial\left(r_i \rho_i \phi_i\right) / \partial t + div\left(r_i \vec{V}_i \rho_i \phi_i - \Gamma_{\phi_i} grad\left(r_i \phi_i\right)\right) = S_{\phi_i} \qquad (6)$$

The dose rates (μGy d^{-1}) in the areas of the marine ecosystem under consideration here:

Sediment

$$D = 9.58 \times 10^{-14} As(^{137}Cs)\ Gy/s \qquad (7)$$

where:

As(^{137}Cs) is the Activity Concentration of ^{137}Cs in sediment (Bq/kg).

Sediment – sea water intermediate phase

$$D = 4.79 \times 10^{-14} [As(A)^{137}Cs + As(B)^{137}Cs]\ Gy/s \qquad (8)$$

where:

As(A)^{137}Cs is the Activity Concentration of ^{137}Cs in seawater (Bq/l); and
As(B)^{137}Cs is the Activity Concentration of ^{137}Cs in sediment (Bq/kg).

Sea water

$$D = 9.58 \times 10^{-14} As(^{137}Cs)\ Gy/s \qquad (9)$$

where:

$As(^{137}Cs)$ is the Activity Concentration of ^{137}Cs in sea water (Bq/l)

Internal dose rates (human consumption of fish)

$$D = 0.5 \cdot \sum_{j=1}^{m} DCF_j \cdot CF_j \sum_{i=1}^{n} A_i \int_0^T C_{ij}(t)dt, \qquad (10)$$

where:

[0, T] is the time interval (y);
DCF_j *(Sv/Bq)* is the dose conversion factor for radionuclide *j* (*j* = 1,2,…, m);
CF_j *(m³/t)* is the concentration factor for radionuclide *j* in fish;
A_i *(t/y)* is the catch of fish in the model compartment *i* (*i* = 1,2,…,n);
C_{ij} *(Bq/m³)* is the concentration of radionuclide *j* in filtered seawater in model compartment *i*; and
0.5 is the edible fraction for fish.

Heavy metals concentrations

$$C_f = C_{tc}/C_e \qquad (11)$$

where:

C_f is the concentration factor;
C_{tc} is the metal concentration in a trophic component; and
C_e is the metal concentration of abiotic environment.

8.1.2. Application of the model to this particular scenario

- Scenario description: ^{137}Cs and heavy metals in marine ecosystems – Doses and concentrations;
- Location: NE Aegean Sea, off Lemnos Island;
- Interaction with Black Sea water through the Dardanelles Strait;
- Adaptations of the model to suit this scenario: Use of Polikarpov model as conceptual model, use of Erica Tool for comparisons;
- Annual fish consumption of 26.5 Bq/kg.

8.1.3. Results

TABLE 32. RESULTS FOR ^{137}Cs IN FIRST YEAR AFTER RELEASE

Quantity calculated	**Release in summer**	**Release in winter**
Concentration in food product leading to highest dose in humans (Bq/kg)	3.52	1.92
Dose to humans during the first year (μSv/year)	1.21	0.68

The results for the second year were similar.

8.1.4. Discussion

The effects of the dose rates received by marine biota depend on the radiosensitivity of the exposed organism. In terms of the conceptual model of organism response to the environmental pollutants and their possible effects, the estimated dose rates lie to the "uncertainty zone", that means no detected effects.

8.2. MEDITERRANEAN COASTAL WATERS

Scenario type: coastal waters
Scenario location: Thermaikos Gulf, North Aegean, Greece
Short name: Cost-Med

8.2.1. Introduction

The Gulf of Thermaikos, located in the North Aegean Sea, was selected for the modelling exercise of radiological sensitivity in a typical coastal Mediterranean environment. The selected region is the coastal zone of Thessaloniki, the second most populated urban centre in Greece, with intensive fishing and significant mussel cultivation and production. The scenario is enhanced by the fact that it is realistic, as 2 operating nuclear plants in Cernavoda (Romania) and Kozloduy (Bulgaria) are located 360 km and 580 km, respectively, from the studied area. The impact of Chernobyl nuclear accident in the region was significant [71–73], even though that it was located far away (~ 1200 km).

The Thermaikos Gulf is a semi-enclosed bay located in the northeastern Mediterranean (40.20º N, 23.00º E) covering approximately 3630 km^2. The Gulf is a rather shallow coastal region with depths varying from 10 to 150 m, bordered on 3 sides by land and widely open (~45 km) to the Aegean Sea towards the south. The hydrology of the region is strongly affected by Black Sea water and large rivers inflows associated with wide catchments, while 2 of the largest rivers in Greece (Axios and Aliakmonas) discharge into the northern part of the Gulf. The topographical features of the North Aegean contribute to the formation of specific coastal currents and permanent eddies with shifting direction through time, resulting in high homogenization of the water masses throughout the Gulf [74].

Despite the fact that the North Aegean Sea ecosystem is an oligotrophic region, it is among the most productive areas in the Eastern Mediterranean mainly due to the influence of nutrient rich, low saline, Black Sea waters and the local river flows. Small pelagic fish (mainly anchovies, *Engraulis encrasicolus*, and sardines*, Sardina pilchardus*) dominate catches, while the productivity of the European hake (*Merluccius merluccius*), red mullets (*Mullus barbatus*), commercial shrimp (*Parapenaeus longirostris*), and cephalopods (such as *Octopus vulgaris* and *Eledone spp.*) is significant [75]. Moreover, according to the data of the Greek Ministry of Agriculture in 2002, the Thermaikos Gulf hosted 70% of the entire Greek production of the *bivalve mollusc* species, mainly mussels and oysters. The annual fish catch and mussel production within the Gulf is of the order of 23 and 10 tonnes y^{-1}, respectively, considering that the fishing period lasts almost the entire year (January–October).

Five municipalities share the Thermaikos Gulf coastline. The total number of inhabitants living in this area, according the census of 2001, is 1 589 327, with age distribution: 0–5 years: 131 096; 6–15 years: 90 281; >15 years: 1 367 950 persons. The diet and the recreational habits of the population are considered to be typical Mediterranean characterized by high fish consumption (16 kg y^{-1}), boating, beach visits and swimming (0.3 man days $month^{-1}$).

The implemented model consists of the main morphological, hydrological and essential environmental-sociological characteristics of the area. These were retrieved from the literature, unpublished scientific data or directly calculated from site specific models. Standard values for the radionuclides parameters referring to their behavior towards the abiotic and biotic elements of the environment were also selected, while mean or slightly modified values were partially used for reducing the model's complexity and maximizing the efficiency of the modelling prediction.

8.2.2. Model description

Name of model: MOIRA-PLUS (MOdel-based computerized system for management support to Identify optimal remedial strategies for Restoring radionuclide contaminated Aquatic ecosystems and drainage areas) [56, 76]. MOIRA-PLUS is specifically designed for assisting managers, as well as experts in assessing the appropriateness of suitable strategies for the management of aquatic ecosystems contaminated by radionuclides.

Brief description of the model: MOIRA-PLUS employs a box-parameterization model based on quantitative evaluations and balances of radionuclide activity concentrations in the water system compartments (surface water, deep water, surface sediment, bottom sediment) and accounts for radionuclide transfer among the compartments. It includes predictive, user-friendly and simple models, driven by a small number of readily accessible environmental parameters, which simulate [77]:

- The time behavior of the hydrological, morphologic and environmental quantities and of the migration parameters of contaminants through aquatic ecosystems;
- The migration of pollutants from the catchment to the aquatic system;
- The migration of pollutants through the abiotic components of the aquatic system;
- The migration of pollutants from the abiotic components to fishes species;
- The effect of selected countermeasures to reduce the contamination levels of the water bodies and the radiological doses to man and biota.

Further sub-models are used to evaluate some significant environmental processes that influence the migration of contaminants (thermal water stratification, dynamics of chemicals and nutrients in water, biomass dynamics, etc.).

The processes of sedimentation, radioactive decay, radionuclide migration from water to sediment (diffusion/adsorption) and from sediment to water (re-suspension/re-mobilization), radionuclide burial to passive sediment, radionuclide migration from catchment and radionuclide transport through the compartments chain are considered in the elementary compartment activity concentration calculations. The fish contamination in water bodies with spatial and time-dependent pollution levels is based on the principles of first-order dynamics and the correlation of bioconcentration factors to the concentration of K and Ca [78], derived from the water salinity. The doses to fish and to the critical individuals, as well as the collective dose are calculated based on the standard assessment equations, taking into account the dietary and costal recreational habits of the population [79].

For the model implementation in the present scenario, appropriate modifications of the migration models had to be made to allow for two-way water fluxes between different portions of the aquatic system and for current circulations, which are typical of the marine environment. These modifications make possible the simulation of the movement of water masses through all adjoining segments, included in the latest version of MOIRA-PLUS (release 4.1.2) [80].

8.2.3. Application of the model to the particular scenario

Single, instantaneous depositions of 1000 Bq m^{-2} of ^{137}Cs and ^{90}Sr respectively have been assumed as the start-point radiological stress on the study area. The short-lived radionuclide ^{131}I and the different initial seasonal conditions were not taken into account, because of their negligible effect to the doses as only the marine aquatic pathway has been included in the analysis. The initial fallout was simulated as a constant rate deposition for a period of 1 month though out the region's compartments (catchment areas, marine and river compartments), due to model input limitation.

The study area was characterized by 5 box segments representing the main rivers that exit into the Gulf and another 5 marine compartments. Mean annual river fluxes, calculated catchment run off, precipitation and evaporation values from the last decade were used for hydrological modelling, while mean monthly values of fluxes between the marine segments were calculated in order to simulate Black Sea water input and circulation and mixing processes in the Gulf. The model's default values for reservoir-type segments were used for the migration constants [59], while all other parameters where extracted either from site specific data or estimated from relevant literature [29, 81].

Radionuclide concentrations as functions of time were simulated in sea water, seabed sediment, fish and mussels. Consequently, radiation doses have been calculated for 3 different age groups of the population (0–5 years; 6–15 years; >16 years) during the first, second and tenth years after the releases of the radionuclides, assuming that all of their food intake from the marine pathway comes from the local environment.

8.2.4. Results

In order to verify the functionality and maximize the reliability of the model, calibration was performed by simulating ^{137}Cs dispersion following the Chernobyl accident in the biotic and abiotic components of the costal marine environment. The initial radiocesium fallout was set as a homogenous deposition of 30 kBq m^{-2}. An additional monthly, exponentially decreasing, contamination burden from the open sea towards the Gulf has been also considered, due to the Black Sea water influence in the hydrology of the region. The initial generic values of cesium migration parameters for reservoir-type segments of MOIRA model are reported in Table 33, while the model's input values for the main morphological and hydrological features are illustrated in Table 34. The calibration was performed by comparing the results of model with the available empirical data and, consequently, modifying the values of the appropriate parameters, within established limits from the relevant literature.

The calibrated values of mixing ratio between marine segments, sedimentation rate and transfer parameters for ^{137}Cs are given in Table 35. For ^{90}Sr, where empirical data were not available, default model values for reservoir-type compartments were assumed. Figures 40–43 show the predicted concentrations of the calibrated model in comparison with the empirical concentrations of ^{137}Cs in water, sediment, fish and mussels for a period of 25 years since the initial deposition. Considering the complexity of the environment, the model limitations and simplifications, the measurements' uncertainties, spatial dispersion and sampling conditions, the results are satisfactory with a divergence of expected values less than 1 order of magnitude. An exception is the predicted concentration in sediment, where the greater disagreement is attributed to the fact that completely different coastal and deep sediments characteristics (sedimentation ratios, composition, radionuclide deposition etc.) cannot be integrated into a single compartment. Nevertheless, actual sediment concentrations are not critical to the exercise goals.

TABLE 33. DEFAULT RADIONUCLIDES' MIGRATION VALUES FOR THE RESERVOIR-TYPE SEGMENTS OF MOIRA MODEL

Parameter	**Unit**	**^{137}Cs**	**^{40}Sr**
Radionuclide migration velocity to sediment (v)	m s^{-1}	1.0E-06	3.5E-07
Migration rate to deep sediment (K_{ds})	s^{-1}	1.2E-08	–
Migration rate from bottom sediment (K_{sw})	s^{-1}	1.5E-08	1.5E-08
Incremental depth, accounting for the quick radionuclide interaction in the water-sediment interface layer (h_{Δ})	m	6	0
Transfer coefficient from catchment (ε)	m^{-1}	0.2	0.2

TABLE 34. MAIN MORPHOLOGICAL CHARACTERISTICS OF THE HYDROLOGICAL FEATURES INCLUDED IN THE MODEL

Compartment number	**Description**	**Average depth (m)**	**Average length (km)**	**Average width (km)**	**Average flux (m^3 month^{-1})**	**Catchment area (km^2)**
1	Gallikos River	0.49	65	0.03	3.09E+07	9.30E+02
2	Axios River	1.29	388	0.08	2.64E+08	2.37E+04
3	Loudias River	0.67	130	0.04	6.10E+07	1.00E+03
4	Aliakmon River	0.71	322	0.05	6.97E+07	9.25E+03
5	Pinios River	1.04	216	0.07	1.64E+08	1.08E+04
m.1	East. Outer Thermaikos Gulf	72.5	67.3	22.7		7.50E+02
m.2	East. Inner Thermaikos Gulf	16.32	17.4	7.8		3.00E+01
m.3	Thessaloniki Gulf	40.37	14.5	19.3		
m.4	Weast. Inner Thermaikos Gulf	31.23	16.4	9.4		
m.5	Weast. Outer Thermaikos Gulf	81.2	67.3	25.6		

TABLE 35. CALIBRATED VALUES OF MODEL PARAMETERS IN THE THERMAIKOS GULF

Parameter	**Unit**	**Value**	
Mixing coefficient between marine segments	m^3 s^{-1}	10	
Sedimentation rate	m month^{-1}	0.0003	
		^{137}Cs	**^{90}Sr**
Bioaccumulation factor (fish)	kg^{-1} m^3	0.1	0.0095 (Model calculation)
Bioaccumulation factor (mussels)	kg^{-1} m^3	0.03	0.0095 (Model calculation)
Excretion rate factor (fish)	month^{-1}	0.35	0.012 (Default)
Excretion rate factor (mussels)	month^{-1}	0.058	0.012 (Default)

TABLE 36. AGE DISTRIBUTION OF THE HUMAN POPULATION FROM THE MUNICIPALITIES SURROUNDING THE THERMAIKOS GULF AND THE FISH PRODUCTIVITY IN EACH MARINE COMPARTMENT

Marine compartment	**Population (persons)**			**Fish production (kg y^{-1})**	
	0–5 years	**6–15 years**	**>16 years**	**Fish**	**Mussels**
1	5224	3527	55 860	10 116 901	
2	3083	2062	31 141	247 713	
3	76 043	53 391	812 982	217 342	
4	14 429	9594	147 443	422 918	6 551 750
5	32 317	21 707	320 524	12 243 426	3 527 865

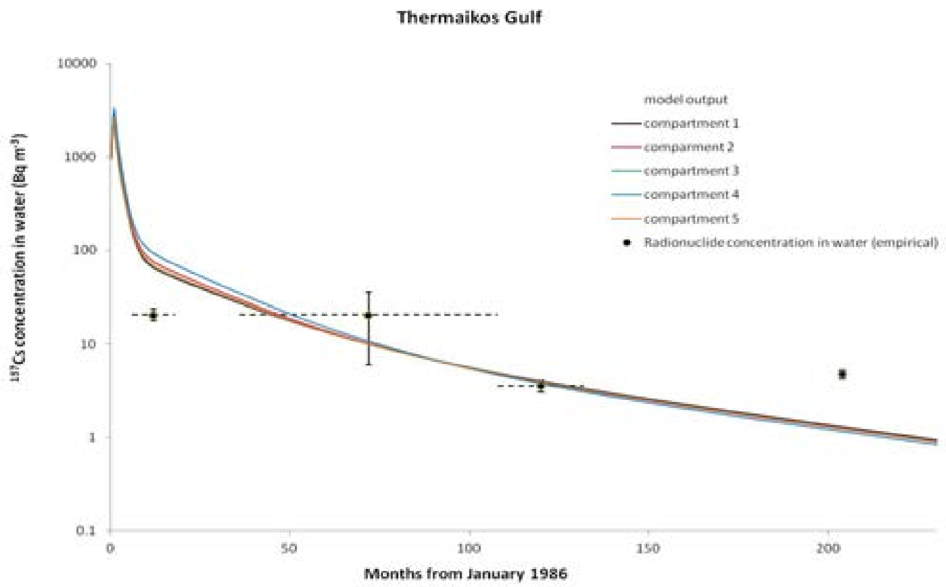

Compartment 1–5: Eastern Outer Thermaikos, Eastern Inner Thermaikos, Thessaloniki Gulf, Western Inner Thermaikos and Western Outer Thermaikos Gulf, respectively (see Figure 82 in Appendix IV).

FIG. 40. Calibrated model results and experimental data of ^{137}Cs concentrations in the waters of the Thermaikos Gulf marine compartments, due to the deposition following the Chernobyl accident.

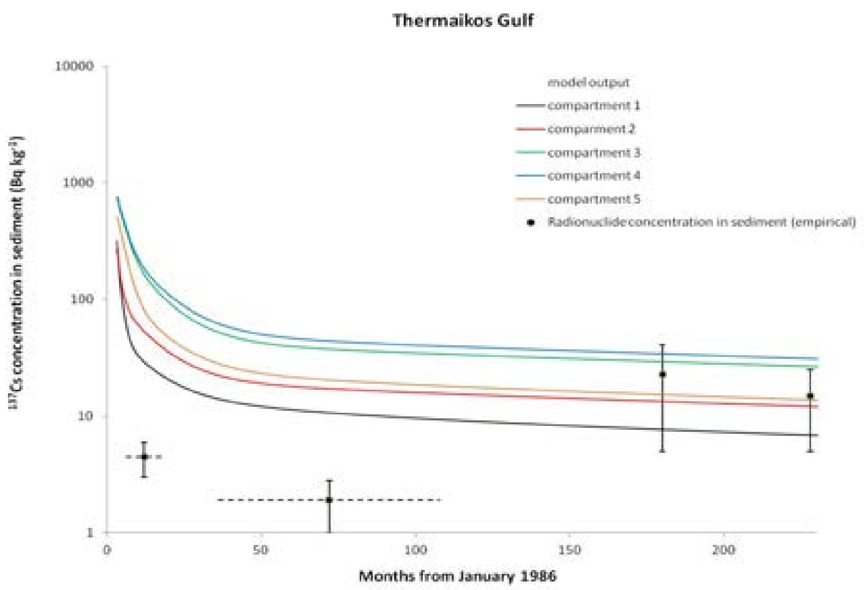

Compartment 1–5: Eastern Outer Thermaikos, Eastern Inner Thermaikos, Thessaloniki Gulf, Western Inner Thermaikos and Western Outer Thermaikos Gulf, respectively (see Figure 82 in Appendix IV).

FIG. 41. Calibrated model results and experimental data of ^{137}Cs concentration in the sediment of the Thermaikos Gulf marine compartments, due to the deposition following the Chernobyl accident.

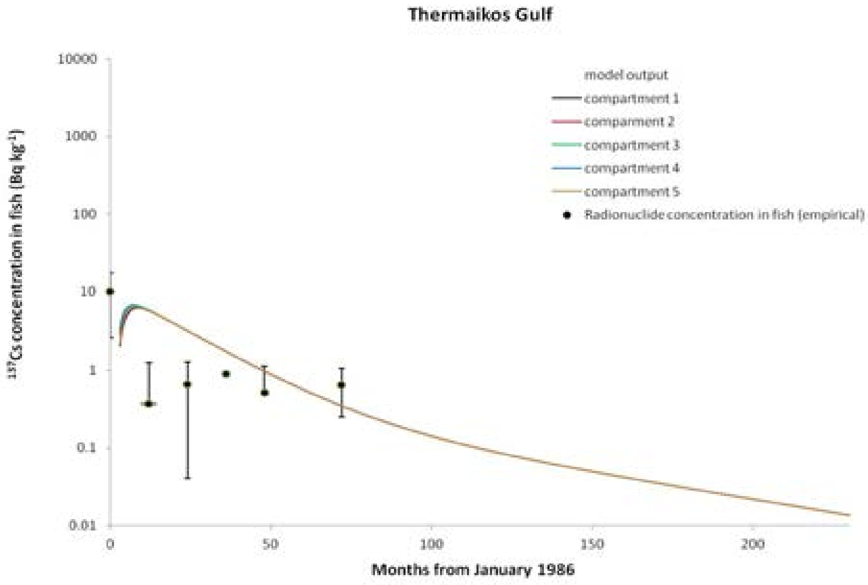

Compartment 1–5: Eastern Outer Thermaikos, Eastern Inner Thermaikos, Thessaloniki Gulf, Western Inner Thermaikos and Western Outer Thermaikos Gulf, respectively (see Figure 82 in Appendix IV).

FIG. 42. Calibrated model results and experimental data of ^{137}Cs concentration in the fish of the Thermaikos Gulf marine compartments, due to the deposition following the Chernobyl accident.

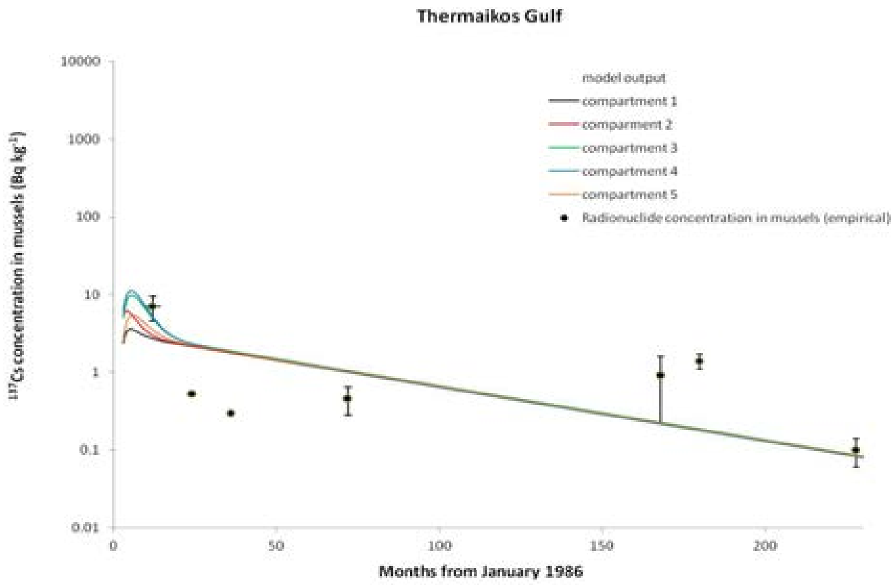

Compartment 1–5: Eastern Outer Thermaikos, Eastern Inner Thermaikos, Thessaloniki Gulf, Western Inner Thermaikos and Western Outer Thermaikos Gulf, respectively (see Figure 82 in Appendix IV).

FIG. 43. Calibrated model results and experimental data of ^{137}Cs concentration in the mussels of the Thermaikos Gulf marine compartments, due to the deposition following the Chernobyl accident.

Once the model was calibrated, the additional social and environmental data were included. The population age and spatial distribution along the coast, as well as the fish and mussels productivity are shown in Table 36. The model was then implemented for 2 scenarios of instantaneous deposition of 1000 Bq m^{-2} of ^{137}Cs and ^{90}Sr radionuclides. Figures 44–47 depict the evolution of dose rates to the population, the doses to fish and the doses to different age groups, for the 2 radionuclides after the deposition. The same results are summarized in Tables 37, along with the environmental sensitivity results presented in Table 38, as the measure of the predicted effect (e.g. the dose) divided by the deposition pulse of 1000 Bq m^{-2}.

8.2.5. Uncertainly analysis

The analysis includes only the radiological effect from the marine pathway (fish and mussel ingestion, external irradiation from the sea), in terms of the dose rate to biota respect to the spontaneous initial deposition for the first, second and tenth years after the contamination. More specifically, the analysis focuses on the total collective dose, which is the sum of the external dose and the dose for the marine food intake. These 2 doses are directly and exclusively, in the modelling frame, related to the concentration of radionuclide in water and in fish; and should be interpreted as the uncertainty indicators for these components. Additionally, the total dose to different population groups (babies, children and adults), the maximum doses to critical individual and to fish were also considered in the uncertainty analysis.

The uncertainty in the final results is mainly attributed to the selection of radionuclide transfer parameters. From the model calibration the uncertainty for ^{137}Cs is considered to be less than 1 order of magnitude in all the calculations, while for ^{90}Sr this value is expected to be more than 1 for the water concentrations predictions and even greater for the fish and mussels activity concentrations, due to the error distribution from the model calculations and the additional uncertainty induced by the bioaccumulation factors. Environmental conditions have significant effects on the reliability of the results. The assumption of a stationary annual water circulation pattern especially enhances the water concentration uncertainty in the long term, while the hydrology of the coastal marine environment is strongly dynamic and unpredictable. On the other hand, sedimentation processes have little effect on the final doses, even though the sediment concentrations can have greater uncertainty in the model predictions.

8.2.6. Discussion

The analysis showed that the main contribution in the total collective dose to the population is the fish intake for adults. ^{90}Sr and ^{137}Cs environmental sensitivity factors are of the same order of magnitude (Table 38). In the first year the value for cesium is slightly enhanced, compared to the one for strontium. However, over time the contamination effect from strontium becomes more important, while the dose rate increases significantly in contrast with dose rate for caesium which decreases slowly with the time. The dominant ^{90}Sr effect, from an environmental sensitivity point of view, is also shown in the maximum dose to critical individuals, where the values for the 2 radionuclides are of the same order of magnitude in the first year, but after 1 decade the difference is significantly greater.

The external dose, corresponding to the concentration radionuclides in water and in shore sediments, slowly decreases for ^{137}Cs, while it is almost constant for ^{90}Sr. This trend can be explained by the fact that the contribution of ^{90}Sr from the catchments of rivers flowing into the Gulf is higher than for ^{137}Cs. The dose from fish intake, corresponding to the concentration of radionuclides in fish, can be explained by accounting for the long term accumulation of ^{90}Sr in fish bones compared to the fast turnover of ^{137}Cs in fish flesh. The high content of potassium and the consequent low value of the bioaccumulation factor lead to low levels of ^{137}Cs concentrations in fish, while persistent levels of contamination for ^{90}Sr indicate higher sensitivity in long term. This fact is clearly depicted in the evolution of the maximum dose rate to fish for the 2 radionuclides (Figure 46).

Different meteorological condition have negligible effect on the model predictions; thus seasonality was absent from the analysis. The seasonal behaviour of the radionuclides is mainly due to thermal stratification of the water column. Due to the shallow water depth and the high mixing rate throughout the year, the thermocline of the water column in the Gulf is almost stationary and fixed. Thus, the predators (pelagic fish) of the region essentially move through the entire water column and seasonal differences in radionuclide activity concentrations are not noticeable in fish contamination.

In conclusion, it is important to note that in this exercise pathways other than the marine one have been excluded. Effects from other pathways are expected to be much more significant, not only because of the direct terrestrial pathways (food consumption, external irradiation from the soil), but also from the long term influence of the freshwater aquatic pathways (drinking water consumption, irrigation), due to the agricultural production in the wide catchments of the region.

TABLE 37. DOSE RATES TO MAN AND BIOTA FROM ^{137}Cs AND ^{90}Sr

Doses rates (mSv y^{-1})	**Age (years)**	**^{137}Cs**			**^{90}Sr**		
		1st year	**2nd year**	**10th year**	**1st year**	**2nd year**	**10th year**
Max. dose to critical ind.(mSv y^{-1})		7.23E-04	2.02E-04	8.84E-06	8.76E-03	4.62E-03	1.85E-03
Total collective dose		5.76E-02	1.92E-02	9.96E-04	2.62E-02	4.08E-02	2.91E-02
(a) External dose		1.42E-02	4.38E-03	2.74E-04	4.49E-03	4.54E-03	2.06E-03
(b) Dose fr. intake fish		4.33E-02	1.48E-02	7.22E-04	2.17E-02	3.64E-02	2.71E-02
Max. dose to fish (mGy y^{-1})		3.83E-03	2.41E-03	7.49E-04	1.72E-03	2.45E-03	1.69E-03
Total dose (Sv y^{-1})	0–5	7.39E-08	5.10E-08	1.36E-08	5.98E-08	1.15E-07	1.08E-07
	6–15	1.85E-07	1.25E-07	3.41E-08	1.26E-07	2.43E-07	2.15E-07
	>16	3.32E-07	2.29E-07	5.88E-08	1.56E-07	2.54E-07	1.87E-07

TABLE 38. ENVIRONMENTAL SENSITIVITY ANALYSIS FOR ^{137}Cs AND ^{90}Sr

Measure of the effect	**Age (years)**	**Sensitivity=Measure of the effect/1000 Bq m^{-2}**					
		^{137}Cs			**^{90}Sr**		
		1st year	**2nd year**	**10th year**	**1st year**	**2nd year**	**10th year**
Max. dose to critical ind.(mSv y^{-1})		7.23E-07	2.02E-07	8.84E-09	8.76E-06	4.62E-06	1.85E-06
Total collective dose		5.76E-05	1.92E-05	9.96E-07	2.62E-05	4.08E-05	2.91E-05
(a) External dose		1.42E-05	4.38E-06	2.74E-07	4.49E-06	4.54E-06	2.06E-06
(b) Dose fr. intake fish		4.33E-05	1.48E-05	7.22E-07	2.17E-05	3.64E-05	2.71E-05
Max. dose to fish (mGy y^{-1})		3.83E-06	2.41E-06	7.49E-07	1.72E-06	2.45E-06	1.69E-06
Total dose (Sv y^{-1})	0–5	7.39E-11	5.10E-11	1.36E-11	5.98E-11	1.15E-10	1.08E-10
	6–15	1.85E-10	1.25E-10	3.41E-11	1.26E-10	2.43E-10	2.15E-10
	>16	3.32E-10	2.29E-10	5.88E-11	1.56E-10	2.54E-10	1.87E-10

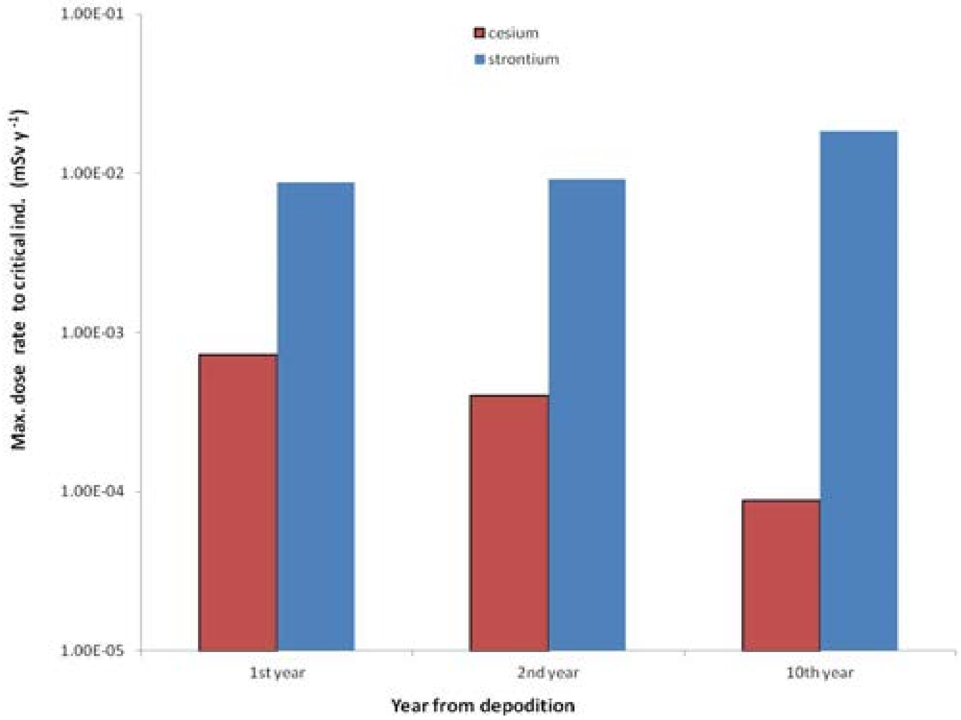

FIG. 44. Maximum dose rates to critical adult individual due to the marine pathways.

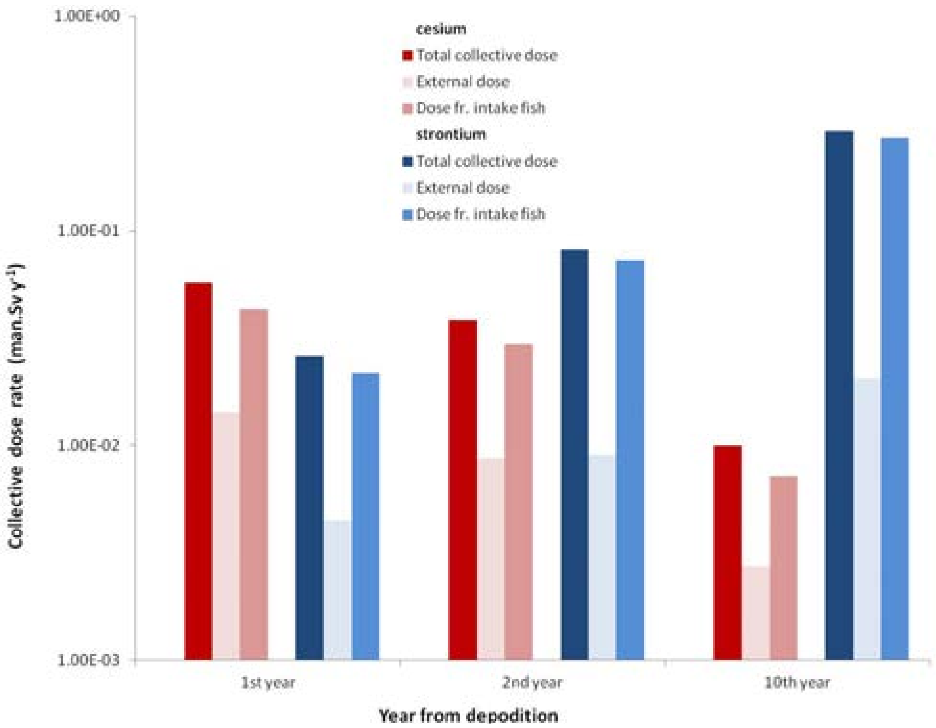

FIG. 45. Collective dose rates to the population along with the marine pathways contribution.

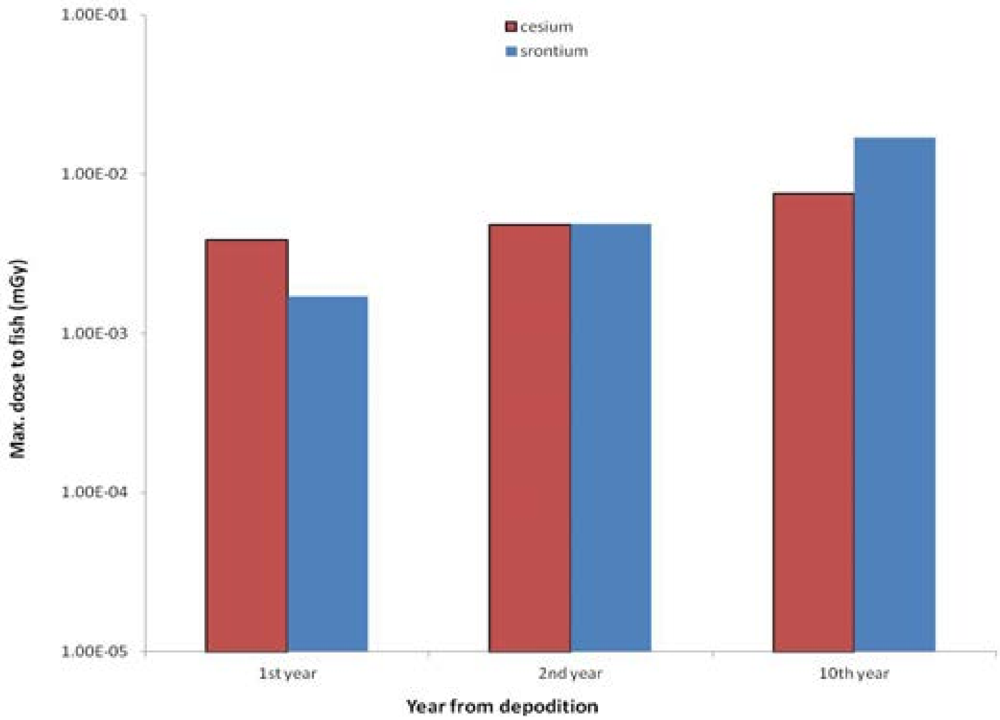

FIG. 46. *Maximum dose rates to fish from* ^{137}Cs *and* ^{90}Sr.

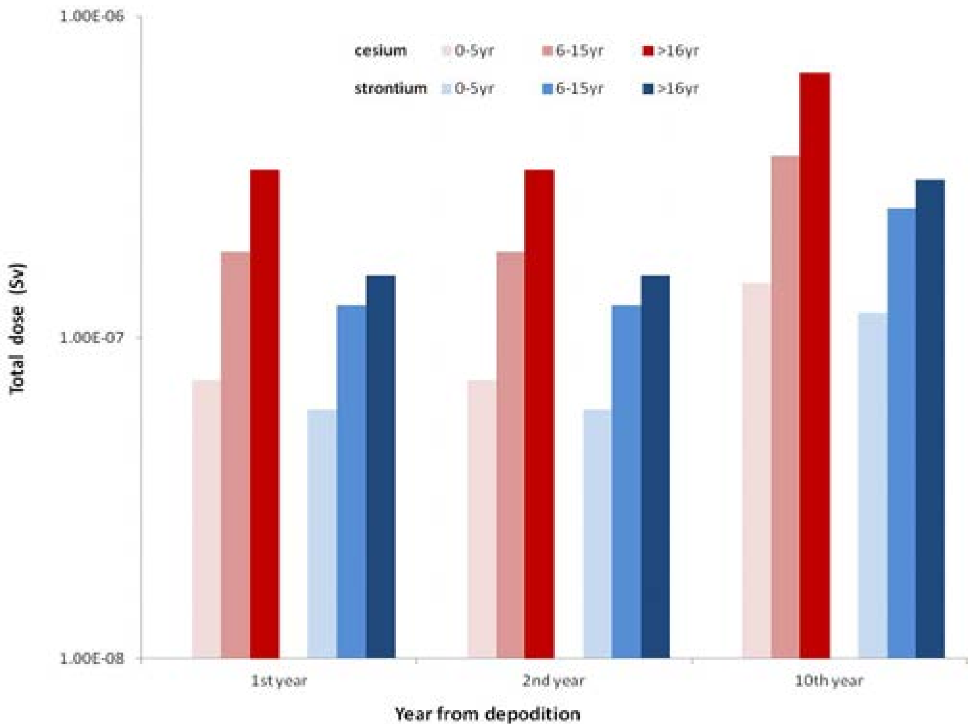

FIG. 47. *Total doses to different age groups of the population from* ^{137}Cs *and* ^{90}Sr *versus time.*

8.3. NORTHERN SEAS

Scenario type: coastal marine waters
Scenario location: Shallow coastal waters of the Northern Seas
Short name: NorthCoast

8.3.1. Model description

Name of model: the NRPA compartment model

Brief description of the model: The box model developed at NRPA uses a modified approach for compartmental modelling [82–84] which allows for dispersion of radionuclides over time. The box structures for surface, mid-depth and deep water layers have been developed based on a description of polar, Atlantic and deep waters in the Arctic Ocean and the Northern Seas (only the surface box structure is shown in Figure 48). Site-specific information for the boxes are partially generated from the 3D hydrodynamic model NAOSIM [85, 86].

The box model includes the processes of advection of radioactivity between compartments, sedimentation, diffusion of radioactivity through pore water in sediments, resuspension, mixing due to bioturbation, particle mixing and a burial process for radionuclides in deep sediment layers. Radioactive decay is calculated for all compartments. The contamination of biota is further calculated from the known radionuclide concentrations in filtered seawater in the different water regions. Doses to the population are calculated on the basis of seafood consumptions, in accordance with available data for seafood catches and assumptions about human diet in the respective areas [87, 88].

In the present report the doses to man are calculated for the ingestion pathway because when comparing the contribution of the dose to man from seafood ingestion with external exposure, one finds the ingestion pathway clearly dominates [88–90].

The NRPA compartment model can additionally calculate the dose rates to biota. Dose rates to biota are developed on the basis of calculated radionuclide concentrations in marine organisms, water and sediment, using dose conversion factors [83, 91].

8.3.2. Application of the model to the particular scenario

The results of the present report correspond to a release scenario, which has been developed under the course of the EMRAS II Programme [92] where a single deposition of 1000 Bq/m^2 of radionuclides ^{137}Cs, ^{90}Sr, ^{131}I and ^{239}Pu is released into all marine regions. The radionuclide concentrations have been calculated for seawater (filtered and unfiltered), fish, molluscs, crustaceans and seaweeds; the radiation doses, during the 1st year, 2nd year and 10th year after releases of radionuclides, have been calculated for adults and children of 1 and 10 years of age.

8.3.2.1. Selected radionuclides

Table 39 shows that the values of the sediment distribution coefficients and concentration factors for biota vary greatly for selected radionuclides in the marine environment. It is necessary to note that sediment distribution coefficient is one of the key parameters describing water-sediment interactions, while concentration factors describe the process of radionuclide bioaccumulation by marine organisms [81].

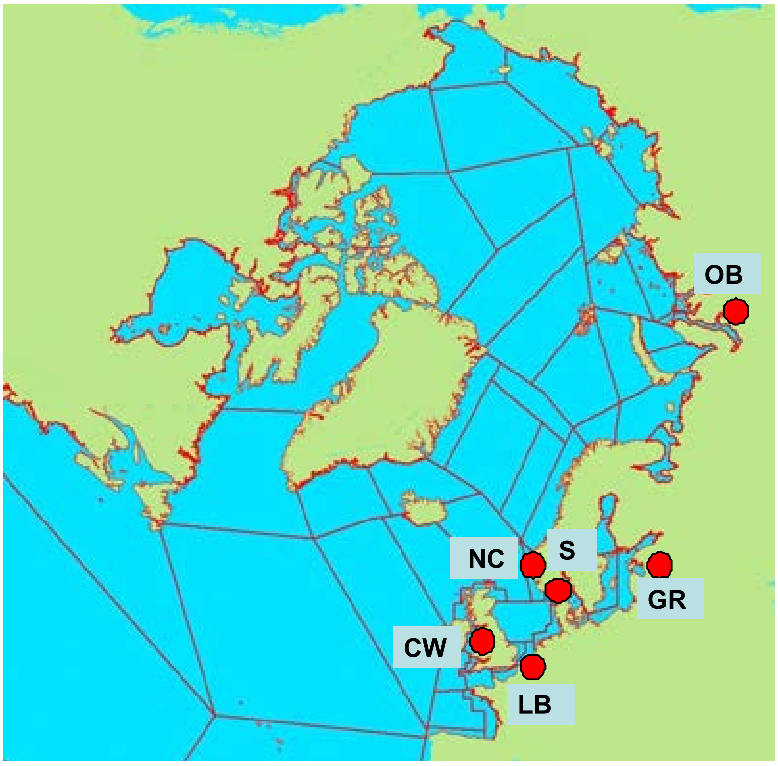

FIG. 48. The surface structure of the NRPA box model and location of the selected marine regions: the Cumbrian waters of the Irish Sea (CW), the Lyme Bay on the English Channel (LB), the North Sea of the Norwegian coasts (NC), the Skagerrak (S), the Gulf of Riga on the Baltic Sea (GR), and the Ob Bay on the Kara Sea (OB).

TABLE 39. SEDIMENT DISTRIBUTION COEFFICIENTS (m^3t^{-1}) AND CONCENTRATION FACTORS FOR BIOTA (m^3t^{-1})

Parameter	^{137}Cs	^{90}Sr	^{131}I	^{239}Pu
Sediment distribution coefficients	4000	8	70	10 0000
Concentration factors for fish	100	3	9	100
Concentration factors for crustaceans	50	5	3	200
Concentration factors for molluscs	60	10	10	3000
Concentration factors for seaweeds	50	10	10 000	4000

TABLE 40. ENVIRONMENTAL PARAMETERS OF THE COASTAL REGIONS: VOLUME (VOL), DEPTH (h_d), SUSPENDED SEDIMENT LOAD (SSL) AND SEDIMENTATION RATE (SR)

Region	VOL (m^3)	h_d (m)	SSL (t m^{-3})	SR (t m^{-2} y^{-1})
CW	3.80E+10	2.80E+01	1.0E-05	6.0E-03
LB	2.01E+11	3.95E+01	3.0E-06	1.0E-04
NC	9.20E+12	1.56E+02	6.0E-06	1.0E-04
S	6.78E+12	2.10E+02	1.0E-06	5.0E-03
GR	4.05E+11	2.30E+01	1.0E-06	5.0E-04
OB	3.19E+11	1.10E+01	5.0E-05	1.0E-03

8.3.2.2. Selected marine regions

Calculations were carried out for 6 marine coastal environments: Cumbrian waters of the Irish Sea (CW), Lyme Bay on the English Channel (LB), North Sea off the Norwegian coasts (NC), Skagerrak (S), the Gulf of Riga on the Baltic Sea (GR), and Ob Bay on the Kara Sea (OB). The selected marine regions are shown in Figure 48. Environmental parameters of the selected regions are shown in Table 40.

8.3.2.3. Seafood consumption

Seafood consumption corresponds to the results published by Smith and Jones [93] for the population of the coastal regions. Selected seafood consumptions for adults and children of 1 and 10 years of age are shown in Table 41.

8.3.3. Results and discussion

8.3.3.1. Concentration of radionuclides in seafood

The typical relationship between maximum and average concentrations of radionuclides in different foodstuffs, during 1 year after deposition is shown in Table 42. It is necessary to note that the dynamics of the concentration of radionuclides in seafood can vary widely depending on the specific radionuclide and the environmental conditions of the marine environments, as it is shown in Figure 49.

8.3.3.2. Calculations of doses to man

Results of the calculations show that for all regions the radiation doses for adults are significantly higher than doses calculated to children of 1 and 10 years of age. This is primarily due to low seafood consumption of children, which turns out to be a more important factor than the increase of dose conversion factors for children. Further, the doses calculated for the first year dominate the doses of the second and tenth year after the release of radionuclides. This is true for all selected regions. These results could be explained by redistribution of radionuclides with time between surface water and deep water compartments, as well as the sedimentation and burial processes. Typical results for the dose distributions of ^{137}Cs and ^{239}Pu for different ages and during different times are shown in Figure 50.

Therefore, the calculation of the doses to adults during the first year after radionuclide deposition is the most interesting for this modelling. Figure 51 shows doses to adults for the 4 radionuclides ^{131}I, ^{137}Cs, ^{90}Sr, and ^{239}Pu from different types of seafood for the Cumbrian Waters. The doses were calculated for the first year after deposition. Figure 51 clearly indicates that dose from ^{131}I is strongly dominated by seaweed consumption (98% of the total dose), fish and molluscs consumption significantly dominate doses from ^{137}Cs and ^{239}Pu (72% and 59% of the total doses, respectively). A dose from ^{90}Sr is dominated by fish and molluscs consumption (68% of the total dose), while doses from fish and molluscs are approximately equal.

Results of simular dose calculations for all coastal environments are shown in Figure 52. Results show the differences of radioecological sensitivity between different marine regions for different radionuclides and points of interest. The highest doses were found for the Ob Bay location for ^{131}I, ^{137}Cs and ^{90}Sr, while the highest dose for ^{239}Pu is found for the Gulf of Riga. It is important to note that the assumed level of seafood consumption has been the same for all coastal environments. It is obvious that doses for each marine region in Figure 51 are strongly dependent on radionuclide speciation. For example, the region distribution of the ^{239}Pu doses in Figure 52 differs significantly from other radionuclides. Further, the doses for the same radionuclide vary greatly in different marine environments. Such differences could be explained by the complexity of the processes of radionuclide dispersion and bioaccumulation, which can progress differently in different marine locations. Therefore, it could be interesting to define and analyze which model parameters play a key role in the evaluation of environmental sensitivity.

TABLE 41. SELECTED SEAFOOD CONSUMPTION (kg y^{-1})

Seafood	Adult	Child 10 years	Infant 1 year
Fish	51	10.2	2.5
Crustacean	17	2.25	0
Molluscs	14	3.5	0
Seaweeds	5	0	0

TABLE 42. MAXIMUM (M) AND AVERAGE (A) CONCENTRATION OF RADIONUCLIDES IN SEAFOOD IN THE OB BAY (OB) AND THE CUMBRIAN WATERS (CW), BQ KG-1 FRESH WEIGHT

Region	Seafood	^{137}Cs		^{90}Sr		^{131}I		^{239}Pu	
		M	A	M	A	M	A	M	A
OB	Fish	9.1	2.9	0.27	0.12	0.82	0.077	1.5	0.25
	Crustacean	4.5	1.4	0.45	0.20	0.27	0.026	3.0	0.50
	Molluscs	5.5	1.7	0.91	0.40	0.91	0.086	45.5	7.5
	Seaweeds	4.5	1.4	0.91	0.40	909	85.6	60.6	10.0
CW	Fish	3.6	1.7	0.11	0.067	0.32	0.031	1.8	0.22
	Crustacean	1.8	0.85	0.18	0.11	0.11	0.010	3.6	0.44
	Molluscs	2.1	1.0	0.36	0.22	0.36	0.034	55.6	6.7
	Seaweeds	1.8	0.85	0.36	0.22	357	33.9	71.4	8.9

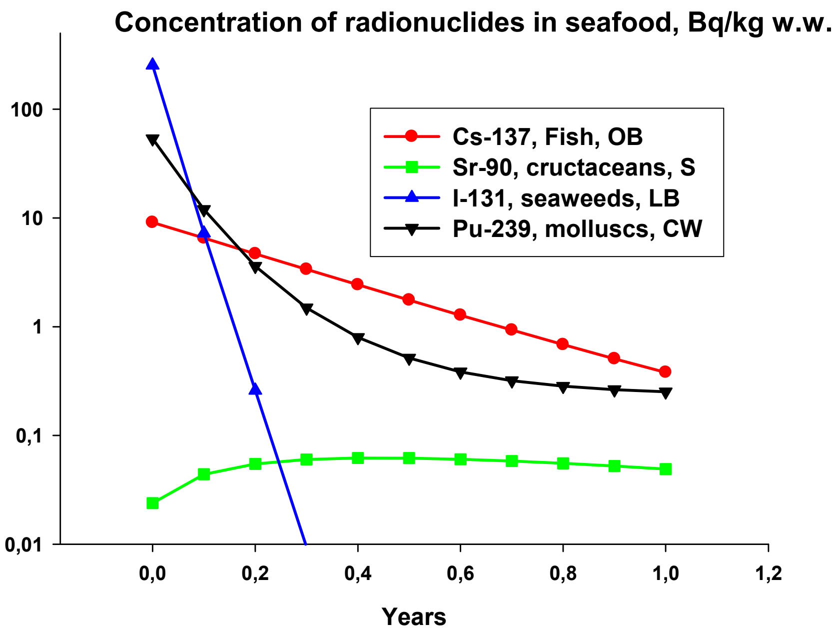

FIG. 49. Dynamic of the concentration radionuclides in seafood in the Ob Bay (OB), Skagerrak, Lyme Bay (LB) and Cumbrian waters (CW), Bq kg^{-1} fresh weight.

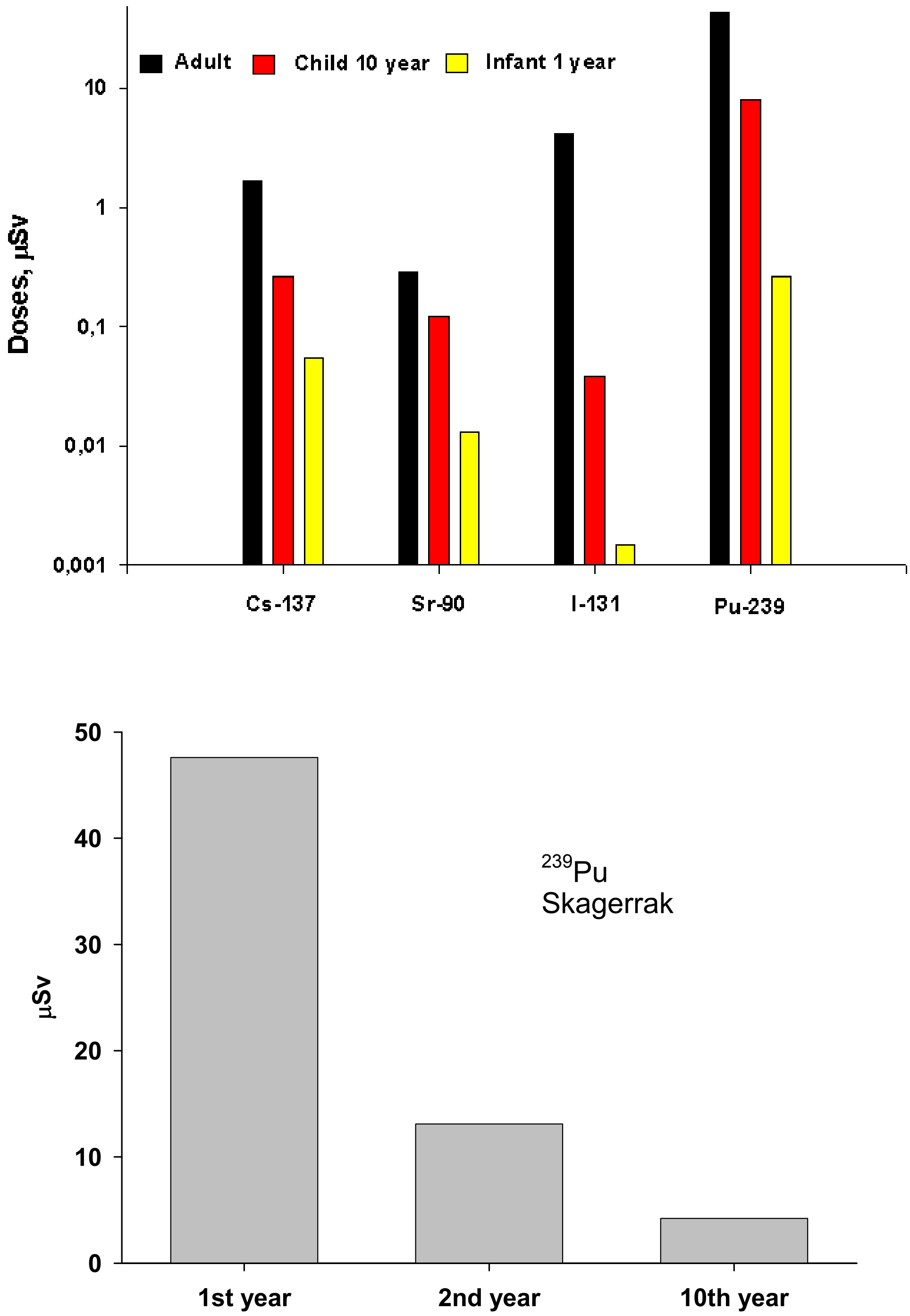

FIG. 50. Doses (µSv) for different age from ^{137}Cs in the Cumbrian waters (top), and during different times from ^{239}Pu for adult in the Skagerrak (bottom).

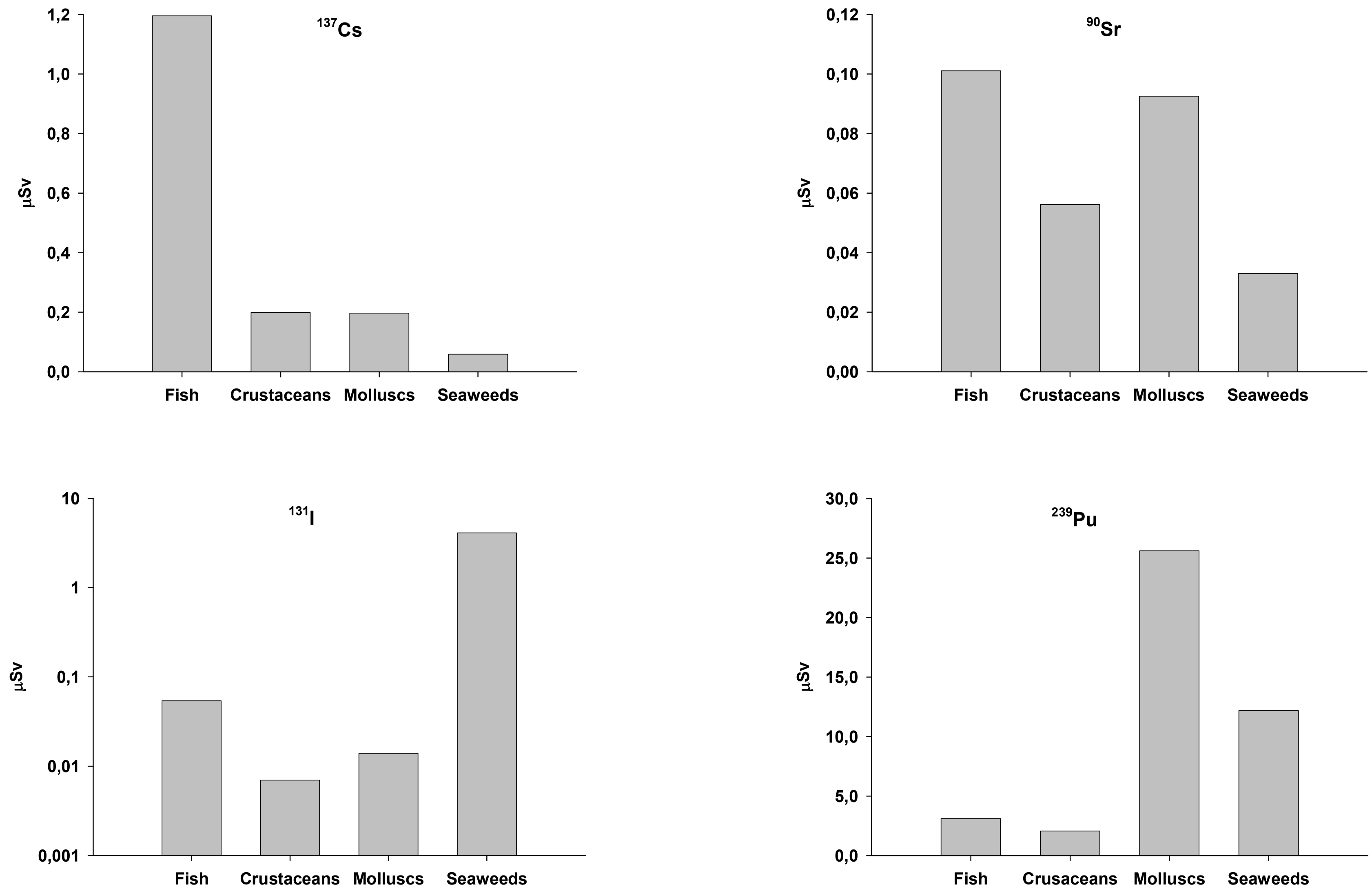

FIG. 51. Doses (µSv) from 1 year of consumption of ^{131}I, ^{137}Cs, ^{90}Sr, and ^{239}Pu in fish, crustaceans, molluscs, and seaweed from Cumbrian waters.

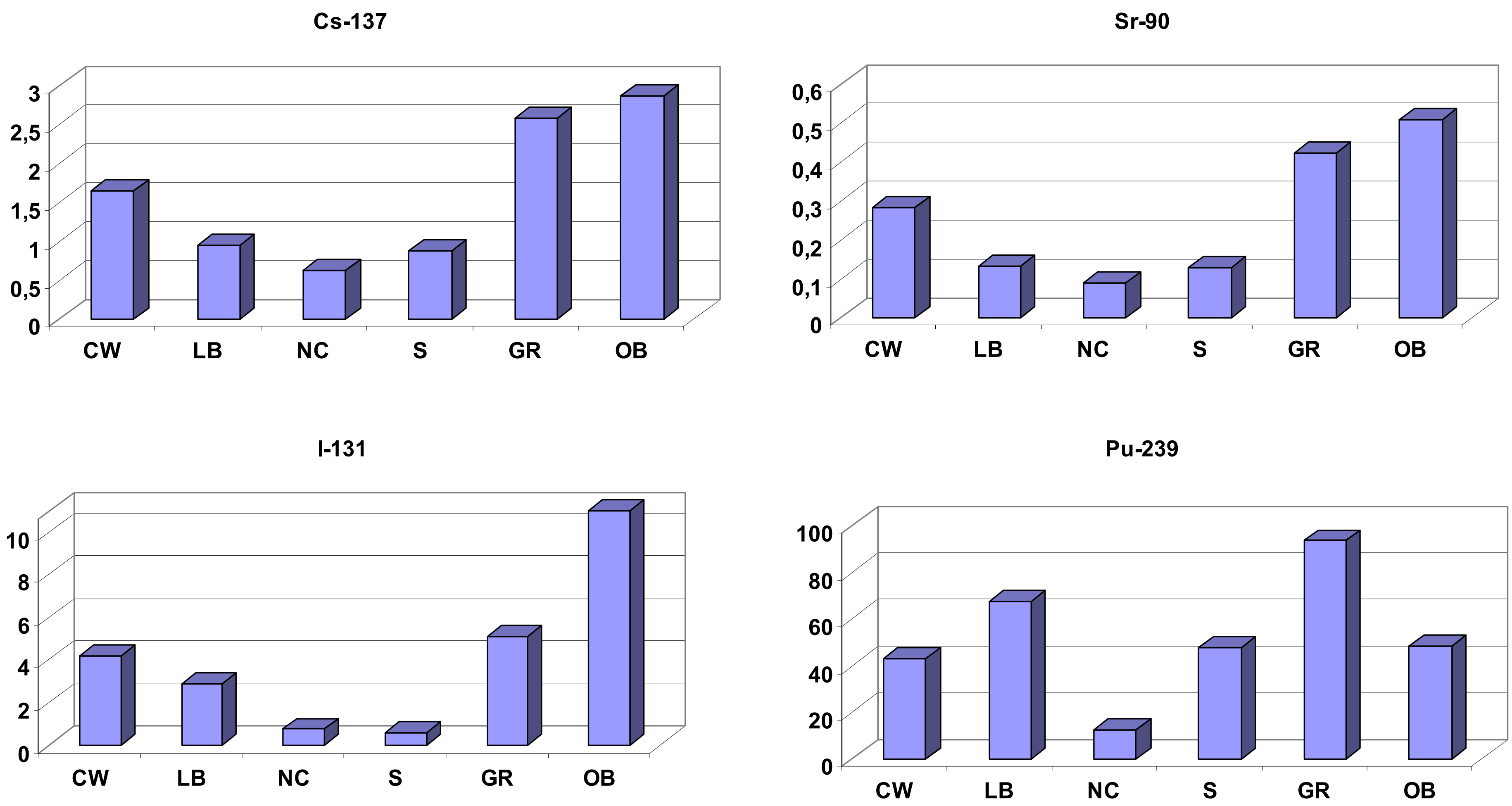

FIG. 52. Doses in μSv from 1 year of the same consumption of ^{131}I, ^{137}Cs, ^{90}Sr, and ^{239}Pu in seafood for locations: Cumbrian waters (CW), Lyme Bay (LB), Norwegian coastal current (NC), Skagerrak (S), the Gulf of Riga (GR) and Ob Bay (OB).

8.3.4. Sensitivity/uncertainly analysis

It is obvious that the calculation of doses presented in Section 8.3.3 comes up against the problem of complexity and the need for a large set of parameters. The sensitivity analysis of the model parameters can contribute to the process of defining which parameters can play a key role in the evaluation of environmental vulnerability.

On the basis of results and discussion in Section 8.3.3, the doses to adults for the first year after radionuclide deposition have been used for the sensitivity analysis of the model parameters.

The sensitivity parameter analysis has been provided on the basis of the local sensitivity index $S^{(L)}$ [94]:

$$S^{(L)}(P) = \left(\frac{dV^{(S)}}{dP} \right)_{P_0} \frac{P_0}{V_0^{(S)}}, \tag{12}$$

where $V^{(S)}$ and P correspond to state variables (for example, doses to man) and parameters which are under evaluation respectively; P_0 and $V_0^{(S)}$ correspond to the basic values of the parameter P and the state variable $V^{(S)}$. In the present paper the values for P_0 and $V_0^{(S)}$ correspond to results presented in Section 8.3.3.

In the present study the following parameters have been considered: parameters describing the dispersion of radionuclides between water compartment as advection rates (fl), where parameter "fl" corresponds to maximum water exchange for the evaluated compartment and adjacent compartments; parameters describing water-sediment interactions as sediment reworking rate (R_W), pore-water turnover rate (R_T), sediment distribution coefficient (K_d), suspended sediment load in water column (SSL), sedimentation rate (SR) and molecular diffusion coefficient (D); and finally, radionuclide concentration factors for seafood describing the bioaccumulation process (CF).

Low and high absolute values of the local sensitivity index, $S^{(L)}$ correspond to low and high sensitivity of the state variables to the evaluated parameters. Further, positive/negative values of $S^{(L)}$ corresponds to the increase/decrease of the state variable when the evaluated parameter increases.

Results of the calculations indicates that doses to adults for all radionuclides and marine locations have very low sensitivity (the absolute values of $S^{(L)}$ are very low) to the molecular diffusion coefficient (D) and pore-water turnover rate (R_T).

Further, a sensitivity analysis of model parameters for ^{131}I indicate that only 1 parameter, namely the concentration factor for seaweeds has a high value of the sensitivity index of ($S^{(L)}$ = 0.99). Calculations for all other parameters show very low values of sensitivity indexes for this radionuclide. Such results can be potentially explained by the characteristics of ^{131}I, which has a short half-life (8 days, approximately), low sediment distribution coefficient for shallow waters (70 $m^3\ t^{-1}$) and very high concentration factor for seaweeds (10^4 Bq kg^{-1}). In a similar manner, all calculations for ^{90}Sr indicate very low values of the sensitivity index for all parameters describing water-sediment interactions, which can be explained by the lowest Kd value for ^{90}Sr in the present set of radionuclides (8 $m^3\ t^{-1}$)

Results of calculations of the local sensitivity index for the advection rates, fl, ^{137}Cs, ^{90}Sr and ^{239}Pu are shown in Table 43. Results in Table 44 show that doses to man from ^{137}Cs and ^{90}Sr are more sensitive to the process of water exchange than doses from ^{239}Pu. Similar, the Lim Bay is much less sensitive to this process than, for example, the Ob Bay. The highest sensitivity index in Table 43 corresponds to the Ob Bay location for ^{90}Sr.

TABLE 43. ABSOLUTE VALUES OF THE LOCAL SENSITIVITY INDEX FOR THE ADVECTION RATES, FL, FOR OB BAY ON THE KARA SEA (OB), CUMBRIAN WATERS OF THE IRISH SEA (CW), LYME BAY ON THE ENGLISH CHANNEL (LB), SKAGERRAK (S), THE GULF OF RIGA ON THE BALTIC SEA (GR) AND NORTH SEA OFF THE NORWEGIAN COASTS (NC)

Locations	OB	CW	LB	S	GR	NC
^{137}Cs	0.26	0.10	0.06	0.21	0.10	0.22
^{90}Sr	0.39	0.16	0.06	0.21	0.13	0.23
^{239}Pu	0.11	0.02	0.04	0.12	0.00	0.15

TABLE 44. ABSOLUTE VALUES OF THE LOCAL SENSITIVITY INDEX FOR SOME PARAMETERS DESCRIBING THE PROCESS OF WATER–SEDIMENT INTERACTIONS: SEDIMENT REWORKING RATE (RW), SEDIMENT DISTRIBUTION COEFFICIENT (K_d), SUSPENDED SEDIMENT LOAD IN WATER COLUMN (SSL), SEDIMENTATION RATE (SR)

Locations	Parameter	OB	CW	LB	S	GR	NC
^{137}Cs	Rw	0.19	0.11	0.06	0.08	0.17	0.07
^{239}Pu	Rw	0.33	0.23	0.39	0.28	0.33	0.18
^{137}Cs	K_d	0.21	0.22	0.06	0.09	0.21	0.07
^{239}Pu	K_d	0.07	0.27	0.36	0.20	0.37	0.13
^{239}Pu	SSL	0.39	0.13	0.04	0.04	0.04	0.00
^{239}Pu	SR	0.11	0.16	0.01	0.29	0.06	0.00

TABLE 45. ABSOLUTE VALUES OF THE LOCAL SENSITIVITY INDEX FOR CONCENTRATION FACTORS FOR FISH (CFf), CRUSTACEANS (CF_c), MOLLUSCS (CF_m) AND SEAWEEDS (CF_s)

Parameter	^{137}Cs	^{90}Sr	^{131}I	^{239}Pu
CF_f	0.72	0.36	0.01	0.07
CF_c	0.12	0.20	0.00	0.05
CF_m	0.12	0.33	0.00	0.60
CF_s	0.04	0.12	0.99	0.28

The absolute values of the local sensitivity index for the parameters describing the process of water–sediment interactions are relatively high for ^{137}Cs and ^{239}Pu (Kd values for ^{137}Cs and ^{239}Pu are $4 \cdot 10^3$ and $1 \cdot 10^5$, respectively). Results of calculations are shown in Table 43 (values for the sensitivity index for parameters SSl and SR are very low for ^{137}Cs and they are not shown in Table 44).

Water-sediment interaction is a complicated process arising from combinations of many parameters. Nevertheless, results in Table 45 show that doses to man from ^{239}Pu are, mainly, more sensitive to the process of water–sediment interactions than doses from ^{137}Cs. It is also interesting to note that values of the sensitivity indexes in Table 43 are significantly higher for the marine regions with low depth as the Ob Bay (OB) and the Cumbrian Waters (CW) than for regions with relatively high depth as the North Sea off the Norwegian coasts (NC). Values of the depth for these regions are 11 m, 28 m and 156 m, correspondently.

Further, sediment reworking rate (R_W), sediment distribution coefficient (K_d), suspended sediment load in water column (SSL) and depth of the water column are used in defining the process of particle mixing under water sediment interaction description. This means that the process of particle mixing dominates the water-sediment interactions for radionuclides with relatively high K_d which means that doses to man from ^{239}Pu and ^{137}Cs are sensitive to this process.

Doses to man are calculated on the basis of the same seafood consumption in all evaluated regions. Therefore, sensitivity indexes for the concentration factors (CF) will be the same for all environments. Results of calculations are shown in Table 45.

Results of calculations in Table 45 show that according to the present assumption about seafood consumption, the doses for all selected regions are sensitive to the parameters describing the process of bioaccumulation of radionuclides to biota. Some concentration factors are especially significant, namely, for ^{137}Cs (fish), for ^{239}Pu (molluscs) and for ^{131}I (seaweeds).

9. COMPARISONS AND DISCUSSIONS

A comparison of the most significant results from each of the model calculations is given in Table 46. The primary basis for comparison used here is the highest dose to an adult member of the critical group during the first year for each of the radionuclides ^{137}Cs, ^{90}Sr and ^{131}I. This is the one feature that is consistently calculated by all of the models. Table 46 also shows the highest concentrations of these radionuclides in various food items that are making the greatest contribution to the adult dose.

9.1. AGRICULTURAL AND ALPINE SCENARIOS

Three separate models were applied to the agricultural scenario:

- The CHERPAC model, developed for eastern Canada;
- JRODOS, applicable to a western European temperate environment; and
- An Alpine model, specific to the mountainous region of Central Europe.

A comparison of doses to adult members of the most affected group are shown in Figure 53 for the 3 radionuclides – ^{137}Cs, ^{90}Sr, and ^{131}I. For ^{137}Cs, CHERPAC predicted a result that was about 3 times as high as that from JRODOS. On the other hand, the ^{90}Sr and ^{131}I predictions were basically similar from both CHERPAC and JRODOS. It is unlikely that the ^{137}Cs discrepancy was due to actual regional differences since climate, agricultural practices and food consumption patterns are broadly similar in eastern Canada and central Europe. It is more likely that the assumptions and parameter values used with CHERPAC are more conservative than those used with JRODOS. The peak milk (657 Bq/L vs 153 Bq/L) and beef (4674 Bq/kg vs 180 Bq/kg) concentrations predicted using CHERPAC were considerably higher than those using JRODOS (see Table 46). Due to time constraints, the reasons for the differences in the predictions of CHERPAC and JRODOS were not fully investigated, but generally speaking, CHERPAC uses more conservative assumptions and parameter values than JRODOS. For example, CHERPAC assumes that dairy cow's complete diet is from contaminated grass, and that the cow eats 74 kg grass every day, 30% of the ingested material is transferred into a cow's body burden and 0.5% of the body burden is transferred into cow's milk. CHERPAC assumed that people living in the agricultural ecosystem were self-sufficient with respect to the agricultural products whereas JRODOS allowed for seasonal variation in the fraction of total diet obtained from local sources.

Since the Alpine model used parameters that were basically similar to JRODOS, it is likely that the lower values are due to real differences between temperate and Alpine environments.

All agricultural models generally agree that ^{137}Cs leads to higher activity concentrations and doses than ^{90}Sr. A ground deposition of 1000 Bq/m^2 can cause high activity concentrations in leafy vegetables, lamb, milk and beef. Regional variations in the diet (e.g. higher consumptions of lamb) can cause significant increases in the ingestion dose. Doses from ^{90}Sr and ^{131}I are higher for infants in all scenarios considered as compared to adults or 10 years old children. In case of ^{137}Cs, the doses for adults are slightly higher than for infants.

Generally doses from agricultural products were found to be highest from radionuclide deposition in late summer because all plants are at their peak growth and are assumed to have been ingested fresh after the deposition event. The dose is higher if the deposition occurs in dry conditions rather than during heavy rain, because radionuclides adhere better to dry plant leaves.

TABLE 46. COMPARISON OF RESULTS FROM ALL THE MODELLING EXERCISES, BASED ON A DEPOSITION OF 1000 Bq/m^2 FOR EACH RADIONUCLIDE

Scenario location	Model	Max dose (μSv/y) to adult in 1st year			Max concentration (Bq/kg) in food items, 1st year			
		^{137}Cs	^{90}Sr	^{131}I	Food item	^{137}Cs	^{90}Sr	^{131}I
Agricultural								
Canada-temperate	CHERPAC	1914	280	51	Milk Beef Leafy veg.	657 4674 690	174 270 691	215 1.7 351
Europe-temperate	FDMT-RODOS	646	273	44	Milk Beef Leafy veg.	153 180 1800	91 3.3 800	240 2.5 2500
Europe-alpine	ECOSYS	280	110	20	Milk Beef Winter wheat Leafy veg. Berries	64.6 134 65.6 467 81.5	38.6 – 21.4 467 10.7	71.7 – – 448 23.5
Forest and Arctic Tundra								
Ontario forest	CHERPAC	13	0.45	0.5	Mushrooms Deer Birds	46 20 44	55 1.2 2.6	31 1.7 3.7
Northern Saskatchewan	IMPACT	288			Caribou Moose Mallard Beaver	281 20 557 20689	0.34 0.05 0.03 0.43	0.26 0.22 0.24 0.75
Canadian tundra	Arctic Model	189			Caribou Moose Berries	586 21.3 40.6		
Freshwater aquatic								
Norway	MOIRA–PLUS	2.9	420		Water Fish	0.039 39	0.24 2.3	
Italy	MOIRA–PLUS	2	150		Water Fish	0.009 1.8	0.011 <0.01	
Northern Saskatchewan	IMPACT	222	16	8	Water Fish	0.67 2335	0.67 1.33	0.67 4
Ontario	CHERPAC	17	0.06	0.48	Water Fish	0.18 130	0.2 0.15	0.11 1.2
Coastal marine								
Nordic seas	NRPA box model	2.86	0.51	10	Fish Crustaceans Seaweeds	10	0.8	>100
NE Aegean Sea. Greece	NTUA 3D model	1.21			Pelagic fish	3.52		
Thermaikos Gulf, Greece	MOIRA–PLUS	0.72	8.8					

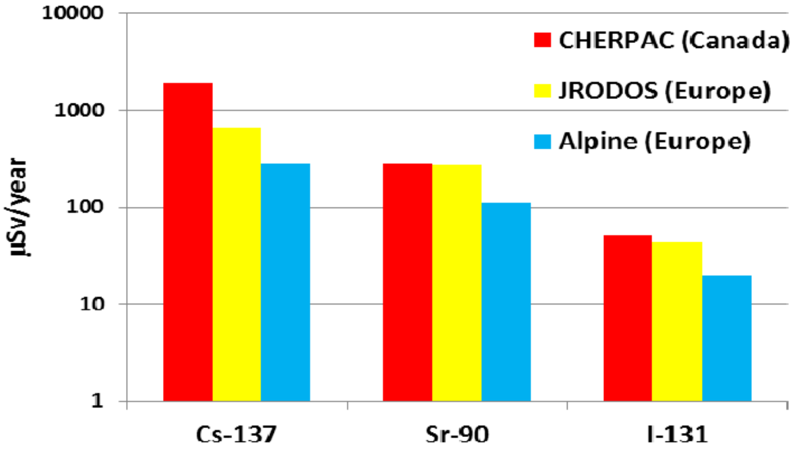

FIG. 53. Comparison of first year adult dose predictions from the agricultural models.

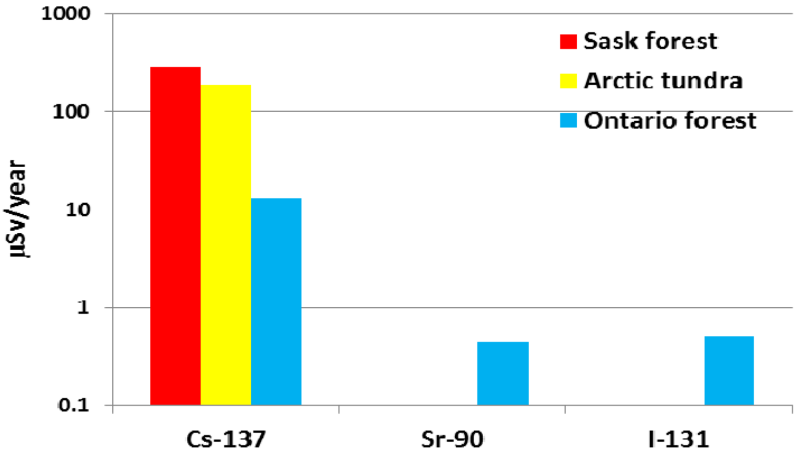

FIG. 54. Comparison of first year adult dose predictions from the temperate forest and arctic tundra models.

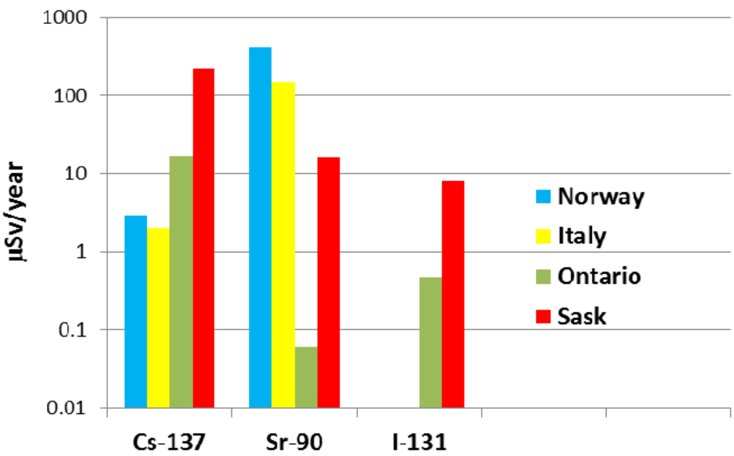

FIG. 55. Comparison of first year adult dose predictions from the freshwater aquatic models.

9.2. TEMPERATE FOREST AND ARCTIC TUNDRA ENVIRONMENTS

Three models were applied to the temperate forest and arctic tundra environments:

- CHERPAC model, adapted to a forest setting in Ontario;
- IMPACT model for a forest setting in northern Saskatchewan;
- An Arctic model for the tundra region of northern Canada.

The description of the IMPACT model in Section 6.2 does not distinguish between terrestrial forest and aquatic environments, since the goal was to measure the total effect on hunting and food gathering society from both terrestrial and aquatic pathways. For comparison purposes here the effects of IMPACT have been separated into terrestrial and aquatic components. A comparison of results from the 3 models is set forth in Figure 54.

It is apparent that doses from ^{137}Cs dominate the impact in forest and tundra environments. The higher doses in northern Saskatchewan and arctic regions compared to Ontario are due mainly to the lichen → caribou → human food chain, which is important in northern Canada but less so in the more temperate region of Ontario. The Arctic model gave a ^{137}Cs concentration in caribou that was about twice as high as the IMPACT model (see Table 46). However, this effect was offset by the IMPACT assumption of a higher consumption of caribou meat.

The ^{90}Sr doses are lower than those from ^{137} Cs because the uptake of ^{90}Sr from the animal GI tract is only fractional and because ^{90}Sr tends to concentrate in the bones and teeth of the animals whereas ^{137}Cs is more or less uniformly distributed throughout the muscle tissues and organs which are consumed by humans. The impact of ^{131}I is very minimal because of its short half-life and because of the absence of fresh leafy vegetables and local milk production in forested or tundra regions of Canada.

9.3. FRESHWATER LAKE ENVIRONMENTS

Three different models were applied to the freshwater environments:

- MOIRA PLUS (lakes in Norway and Italy);
- CHERPAC (an Ontario lake);
- IMPACT (a lake in northern Saskatchewan).

^{137}Cs tends to dominate the doses in the northern Canadian environment, mainly due to fish consumption. Bioconcentration factors in freshwater fish can range up to several thousand. (Note the high ^{137}Cs concentration in fish from the Saskatchewan lake shown in Table 46). The concentration of a radionuclide in water is, to a first approximation, inversely proportional to the height of the water column. The Saskatchewan lake was assumed to have a mean depth of only 1.5 m whereas the Ontario lake had a mean depth of 5 m. Lake Øvre Heimdalsvatn in Norway Lake Bracciano in Italy have mean depths of 4.7 m and 165 m respectively. These differences are reflected in the ^{137}Cs doses of Figure 55 although other factors, e.g. fish production and consumption, come into play.

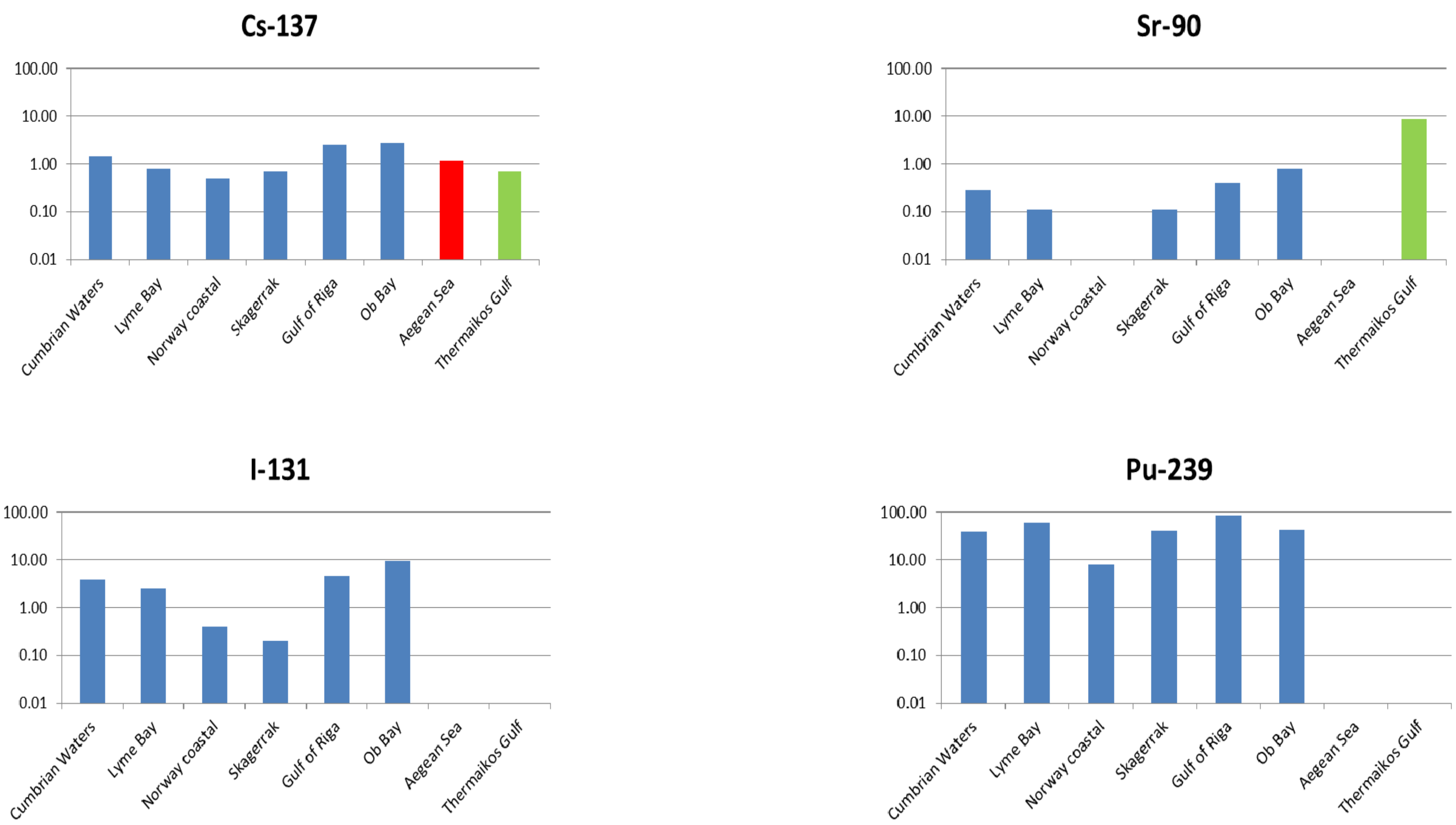

FIG. 56. Comparison of first year adult dose predictions (μSv) from the coastal marine models.

Northern Seas NE Aegean Sea Thermaikos Gulf

All the marine coastal results have been plotted on a common logarithmic scale to facilitate comparison between different radionuclides and different locations. ^{131}I and ^{239}Pu doses were calculated only for the northern seas.

The lakes in Norway and Italy show high ^{90}Sr doses, because MOIRA PLUS assumes that lake water is used to irrigate crops. The concentrations of ^{90}Sr in lake water are more persistent than those of ^{137}Cs because of a lower sediment/water distribution coefficient. In a sense this is really a dose contribution from an agricultural environment. In the environments considered in northern Canada, agricultural practices are virtually absent.

The Ontario and Saskatchewan lakes show a very small dose contribution to the 8 day ^{131}I, mainly as a result of water consumption.

9.4. COASTAL MARINE ENVIRONMENTS

Three different modelling efforts were applied to the coastal or shallow marine environments:

- The NRPA box model, which considered 6 locations in northern seas;
- MOIRA PLUS, which was adapted to Thermaikos Gulf in the Mediterranean;
- Northeast Aegean Sea model.

The results are compared in Figure 56.

The doses from ^{137}Cs in coastal marine locations are generally much lower compared to other scenarios. This can be attributed to the greater depth of water and degree of mixing by ocean currents in the marine environments. Furthermore, the uptake of ^{137}Cs by fish is much less in salt water because of competition from natural potassium. All 3 radionuclides – ^{137}Cs, ^{90}Sr, and ^{131}I – show higher results in the shallower depths of Ob Bay and Cumbrian Waters.

Although the radionuclide ^{239}Pu was considered only in the NRPA box model, it appears to have the greatest impact in the marine locations. ^{239}Pu is strongly taken up by molluscs, which are an important source of food for humans. ^{131}I doses are also elevated in marine scenarios due to the uptake of iodine by edible seaweeds.

The ^{137}Cs doses from Thermaikos Gulf and northeast Aegean Sea fall in the same range as results from the northern seas. However, the ^{90}Sr dose Thermaikos Gulf is an order of magnitude higher compared to the northern seas. Thermaikos Gulf receives a large amount of water from rivers and the MOIRA approach used here allows for ^{90}Sr input from the river catchment areas. Also, concentrations of ^{90}Sr in water (and consequently fish) tend to be more persistent than ^{137}Cs.

9.5. COMPARISON OF DIFFERENT ENVIRONMENTS.

Comparisons of model predictions across the various environments are summarized in Figures 57–59 for the 3 radionuclides ^{137}Cs, ^{90}Sr, and ^{131}I.

Overall, the highest doses are due to ^{137}Cs. The ^{137}Cs doses in Figure 57 are arranged roughly in order of decreasing value across the different environments. The dose from ^{137}Cs during the first year to an adult member of the critical group can thus be taken as a good indicator of environmental sensitivity, as defined in Section 2. The sensitivity is highest in agricultural settings followed by forest environments, where the pathway lichens → grazing animals → humans dominates. The sensitivity is less in freshwater aquatic environments and least in marine environments. (The higher ^{137}Cs value in the Saskatchewan lake is due to the assumed shallow depth of the lake, i.e. 1.5 m.) The chief contributor to ^{137}Cs doses in marine environments is fish consumption, but uptake is suppressed due to competition with natural ^{40}K in sea water.

The ^{90}Sr doses are lower, but still elevated in agricultural environments. The high ^{90}Sr values for the Norwegian and Italian lakes are due to the assumption in the MOIRA methodology that lake water is being used to irrigate crop lands. In the Saskatchewan and Ontario lakes, no assumptions were made about the use of the water for irrigation. In these cases the ^{90}Sr doses were primarily due to fish consumption.

In most environments the first year doses from ^{131}I are lower than those from ^{137}Cs or ^{90}Sr by 1–2 orders of magnitude. Annual doses from ^{131}I are limited by its short half-life (8.05 days). However ^{131}I becomes important in marine environments because of enhanced uptake by seaweeds. Also, as the NRPA box model shows, Pu^{239} doses become significant in marine settings due to enhanced uptake by molluscs.

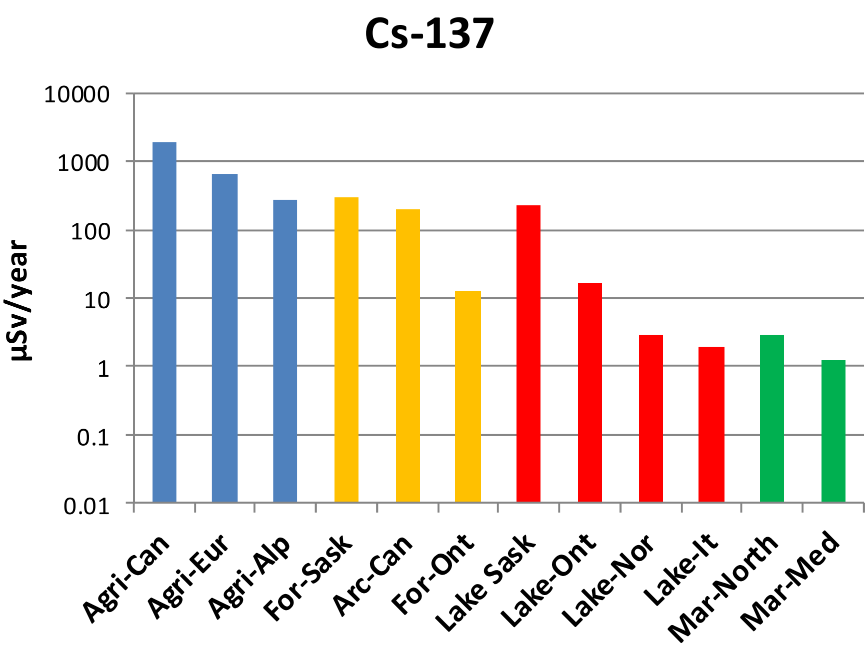

FIG. 57. Adult doses during the first year for the various environments from ^{137}Cs.

Agricultural Forest Freshwater aquatic Coastal marine
All results are plotted on a common logarithmic scale to facilitate comparisons.

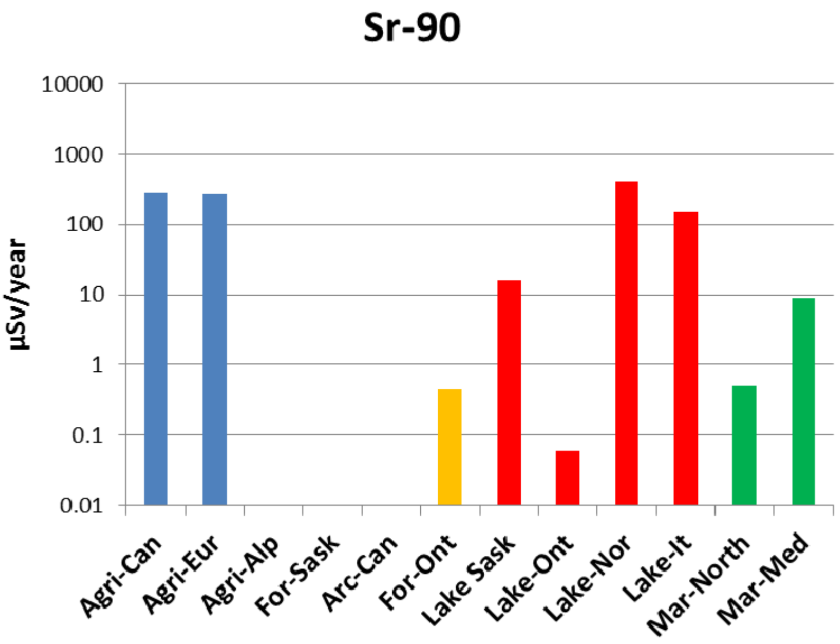

FIG. 58. Adult doses during the first year for the various environments from ^{90}Sr.

Agricultural Forest Freshwater aquatic Coastal marine
All results are plotted on a common logarithmic scale to facilitate comparisons.

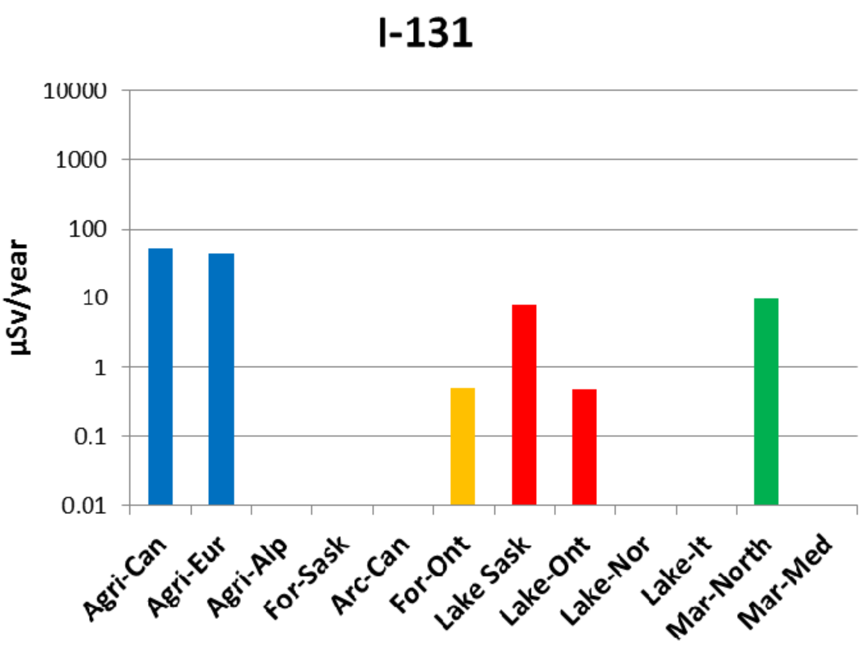

FIG. 59. Adult doses during the first year for the various environments from ^{131}I.

Agricultural Forest Freshwater aquatic Coastal marine
All results are plotted on a common logarithmic scale to facilitate comparisons.

10. CONCLUSIONS AND RECOMMENDATIONS

This report has demonstrated the usefulness of environmental modelling exercises in identifying the sensitivities of different environments to radionuclide contamination in an accident situation. The exercises can also provide rudimentary systems for ranking the sensitivities of different types of environments.

The adult dose during the first year from ^{137}Cs has been shown to be a particularly useful indicator of sensitivity. The ^{137}Cs doses dominate in most environments, with the highest values obtained for agricultural settings, following by temperate forests, freshwater bodies, and then coastal marine locations. However, there are situations where consideration of other radionuclides can add additional information. For instance ^{90}Sr and ^{131}I may have greater impacts on children and infants, particularly through the grass → cow → milk pathway. In certain scenarios, ^{90}Sr in water may be important, because of its persistence in the solution phase. In the coastal marine environments, ^{131}I uptake may be significant from edible seaweeds, whereas ^{239}Pu may be important from consumption of molluscs.

With regard to sensitivity factors, we have seen that seasonal differences perhaps contribute the greatest degree of variability and uncertainty in all the environmental settings considered here except coastal marine. Depth of the water body is very important in both freshwater aquatic and shallow marine environments. In human dose assessments, the greatest variability factor is the assumed consumption rate of a contaminated food item. For this reason, radionuclide concentrations in major food items and drinking water should be used as supplementary indicators of sensitivity.

Overall, satisfactory agreement has been demonstrated between different modelers although there were some inconsistencies. The overall goal of these exercises was not necessarily to achieve uniformity of results, but rather to account for the differences in terms of underlying model assumptions.

The Working Group recognized that a comparison of sensitivities across different environments is a very broad topic, and there were many other issues that could have been addressed. Given the limited resources of our group, we have focused on problems that could be resolved within the given time frame. However, we have identified a number of areas that could be fruitfully explored by future Working Groups.

- **Other environments** could be considered, such as tropical rain forests and semi-arid environments. This would require input from experts who have experience with these environments.
- **Other radionuclides** could be considered, for example – tritium, actinides and transuranic elements. It was felt that the 3 radionuclides – ^{137}Cs, ^{90}Sr, and ^{131}I –covered a reasonable range of conditions and that other isotopes of these elements could easily be added, since different isotopes of the same element would presumably exhibit the same environmental behaviours.
- **Other species or abiotic components** of the environment. This was clearly beyond the scope of the present Working Group, but could be profitably taken up by other Working Groups.

— **Collective doses** were not considered here, but could easily be added. All that would be needed is the total food production per unit area (e.g. per km^2) in a given environment. Models could be used to calculate the contamination of each food item in Bq/kg from an assumed deposition density of e.g. 1000 Bq/m^2. The collective dose then becomes:

$$\textit{Collective dose (person-Sieverts/km}^2\textit{/year) = concentration in food item (Bq/kg)} \times \textit{food production (kg/km}^2\textit{/year)} \times \textit{dose coefficient (Sv/Bq).}$$

The only assumption here is that all of the food produced per km^2 in 1 year is consumed by somebody somewhere. This eliminates the uncertainty of individual consumption amounts and the size and extent of an affected population. Collective doses from different environments could be easily compared with one another, based only on total food contamination per unit area per year.

APPENDIX I. MAPS SHOWING ALL MODELLING SITES

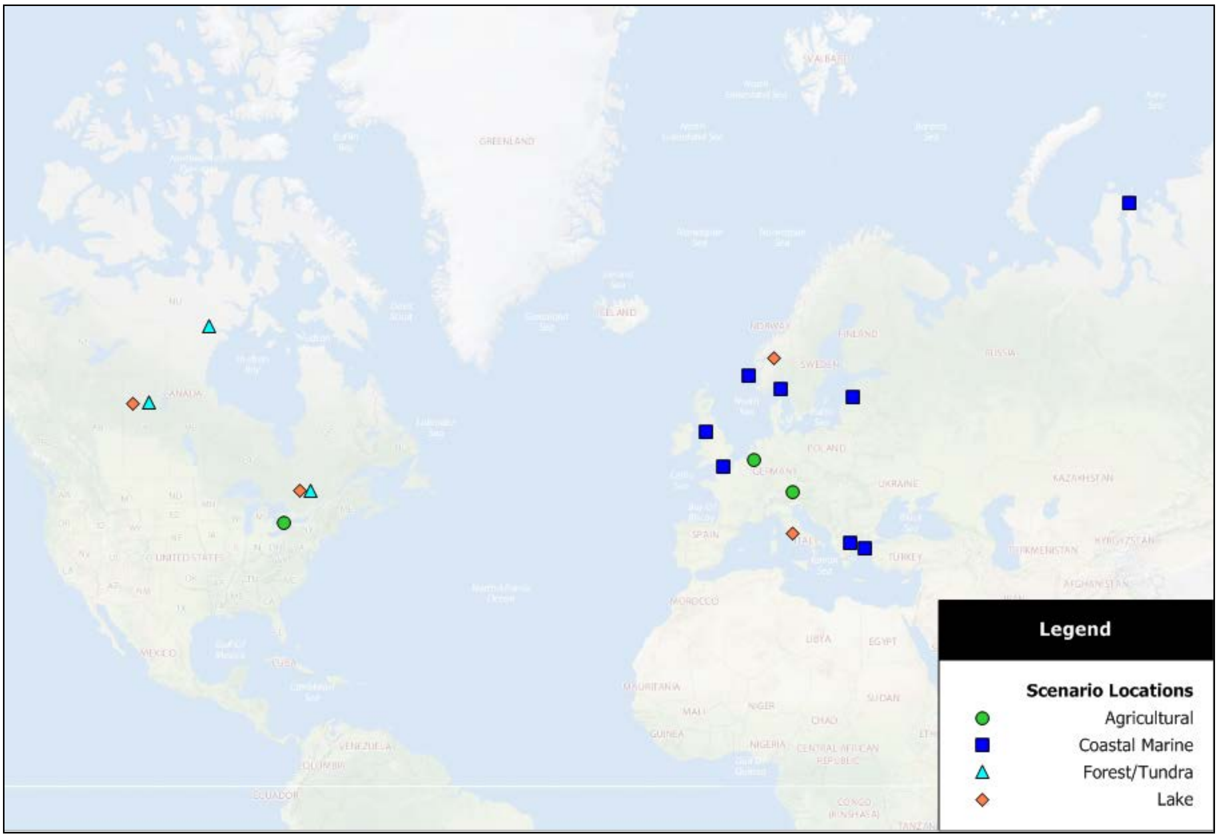

FIG. 60. Worldwide distribution of modelling sites considered in this report.

The European sites are described in more detail in Figure 61. The Canadian sites are described as follows: The agricultural site in southern Ontario and the forest and lake sites in northern Ontario were modelled by CHERPAC (Sections 5.1, 6.1, and 7.2). The forest and lake sites in northern Saskatchewan were modelled by IMPACT (Section 6.2). The tundra site in the high Arctic was modelling by a Health Canada caribou model (Section 6.3).

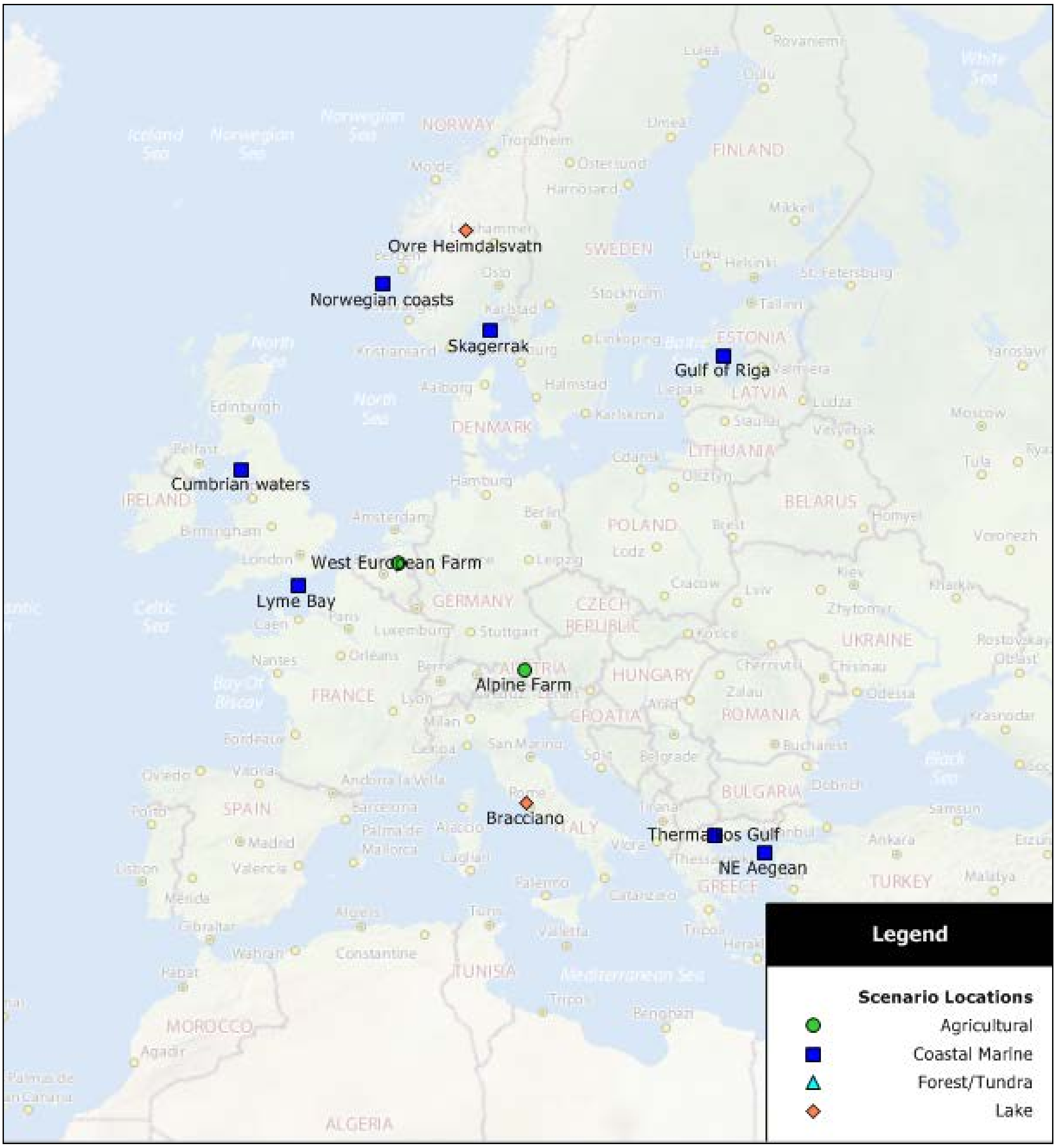

FIG. 61. Detailed map of European sites considered in this report.

The West European Farm was modelled by JRODOS (Section 5.2) and the Alpine Farm by the Alpine model (Section 5.3). Lake Øvre Heimdalsvatn in Norway and Lake Bracciano in Italy were modelled by MOIRA-PLUS (Section 7.1). The coastal marine site for the NE Aegean was modelled by the NTUA model (Section 8.1) and that for Thermaikos Gulf was modelled by a modified MOIRA PLUS (Section 8.2). The other coastal marine sites were modelled by the NRPA box model (Section 8.3).

APPENDIX II. SUPPLEMENTARY DATA FROM JRODOS

In Section 5.2 it was stated that a sandy soil and a July release date produced (with few exceptions) the highest activity concentrations in food products. Results for other release dates and soil types, as well as some comparisons between different soil types, are presented here in Tables 47 and 48. The ratio of activity concentrations for a release on 1 May corresponding to clay and sandy soil types, respectively, is depicted in the Figures 62 and 63 for ^{90}Sr and ^{137}Cs.

The dose estimates in Section 5.2 were based on a standard RODOS diet. For comparison we present in Figures 64–68 the ingestion doses based on the Belgian dietary consumption for all 3 radionuclides and in the first and second years after deposition.

TABLE 47. MAXIMUM AND AVERAGE CONCENTRATIONS OF RADIONUCLIDES IN DIFFERENT FOODSTUFFS AND FEEDING STUFFS FOR YEAR 1(Bq/kg FRESH WEIGHT)

(a) Soil type: clay; release date 1 May

Product	^{137}Cs Maximum Year 1	^{137}Cs Average Year 1	^{131}I Maximum Year 1	^{131}I Average Year 1	^{90}Sr Maximum Year 1	^{90}Sr Average Year 1
Cow's milk	1.36E+02	2.60E+01	1.61E+02	5.62E+00	8.47E+01	1.42E+01
Beef	1.79E+02	7.65E+01	2.16E+00	1.51E-01	3.26E+00	1.60E+00
Pork	4.32E+01	2.54E+01	7.05E-04	2.19E-05	1.09E-02	5.39E-03
Chicken	3.25E+00	1.92E+00	1.68E-03	5.18E-05	8.78E-02	2.05E-03
Lamb	1.27E+03	5.46E+02	2.36E+00	1.74E-01	3.69E+00	2.08E+00
Fruit Vegetables	4.24E+01	1.99E+01	3.14E-02	1.53E-03	1.11E+00	3.91E-01
Leafy Vegetables	1.46E+03	6.50E+01	1.64E+03	3.06E+01	1.46E+03	6.51E+01
Root Vegetables	3.18E+01	1.93E+01	2.16E-02	1.08E-03	3.64E-01	2.85E-01
Winter Wheat	9.84E+00	7.31E+00	4.21E-03	3.53E-04	4.63E-01	3.44E-01
Potatoes	5.86E-02	4.36E-02	1.96E-07	1.87E-08	2.28E-01	1.70E-01
Grass	1.33E+03	6.93E+01	2.00E+03	3.55E+01	1.33E+03	5.99E+01

(b) Soil type: clay; release date 20 November

Product	^{137}Cs Maximum Year 1	^{137}Cs Average Year 1	^{131}I Maximum Year 1	^{131}I Average Year 1	^{90}Sr Maximum Year 1	^{90}Sr Average Year 1
Cow's milk	3.67E+00	9.74E-01	6.87E-01	2.89E-03	9.85E-01	1.14E-01
Beef	7.75E+00	2.98E+00	2.52E-03	7.82E-05	2.28E-02	1.14E-02
Pork	2.90E+00	3.75E-01	1.06E-03	3.28E-05	1.40E-02	1.55E-03
Chicken	4.05E+00	2.73E-01	2.52E-03	7.76E-05	1.13E-01	1.96E-03
Lamb	3.20E+01	1.14E+01	2.01E-03	6.25E-05	1.70E-02	8.82E-03
Fruit Vegetables	1.05E-02	3.46E-03	1.47E-12	1.32E-13	3.88E-02	1.29E-02
Leafy Vegetables	1.87E+03	1.74E+02	2.45E+03	5.62E+01	1.87E+03	1.74E+02
Root Vegetables	1.72E-02	5.67E-03	2.59E-13	2.32E-14	1.68E-01	5.56E-02
Winter Wheat	3.57E-02	1.19E-02	9.82E-13	8.34E-14	2.08E-01	6.91E-02
Potatoes	2.60E-02	8.60E-03	1.64E-13	1.53E-14	1.03E-01	3.41E-02
Grass	2.94E+03	2.82E+02	8.08E+03	1.87E+02	2.94E+03	2.64E+02

(c) Soil type: sandy; release date 1 May

Product	^{137}Cs		^{90}Sr		^{131}I	
	Maximum Year 1	**Average Year 1**	**Maximum Year 1**	**Average Year 1**	**Maximum Year 1**	**Average Year 1**
Cow's milk	1.37E+02	2.65E+01	8.56E+01	1.55E+01	1.70E+02	5.91E+00
Beef	1.80E+02	7.79E+01	3.30E+00	1.73E+00	2.27E+00	1.59E-01
Pork	4.38E+01	2.57E+01	1.10E-02	6.33E-03	7.42E-04	2.31E-05
Chicken	3.33E+00	1.96E+00	8.87E-02	2.50E-03	1.77E-03	5.45E-05
Lamb	1.29E+03	5.54E+02	3.73E+00	2.18E+00	2.48E+00	1.83E-01
Fruit Vegetables	4.28E+01	2.01E+01	1.51E+00	6.97E-01	3.03E-02	1.48E-03
Leafy Vegetables	1.47E+03	6.57E+01	1.47E+03	6.65E+01	1.72E+03	3.22E+01
Root Vegetables	3.22E+01	1.96E+01	9.52E-01	7.45E-01	2.27E-02	1.14E-03
Winter Wheat	1.01E+01	7.50E+00	8.21E-01	6.10E-01	4.44E-03	3.73E-04
Potatoes	1.68E-01	1.25E-01	3.76E-01	2.80E-01	5.32E-06	5.06E-07
Grass	1.35E+03	7.04E+01	1.35E+03	6.37E+01	2.10E+03	3.73E+01

(d) Soil type: sandy; release date 20 November

Product	^{137}Cs		^{90}Sr		^{131}I	
	Maximum Year 1	**Average Year 1**	**Maximum Year 1**	**Average Year 1**	**Maximum Year 1**	**Average Year 1**
Cow's milk	3.74E+00	1.00E+00	9.93E-01	2.18E-01	7.25E-01	3.06E-03
Beef	7.92E+00	3.06E+00	4.63E-02	2.10E-02	2.66E-03	8.26E-05
Pork	2.93E+00	3.90E-01	1.41E-02	1.65E-03	1.12E-03	3.47E-05
Chicken	4.08E+00	2.78E-01	1.14E-01	2.02E-03	2.66E-03	8.19E-05
Lamb	3.27E+01	1.17E+01	3.39E-02	1.57E-02	2.13E-03	6.60E-05
Fruit Vegetables	1.64E-02	5.43E-03	2.11E-01	7.00E-02	1.53E-12	1.37E-13
Leafy Vegetables	1.89E+03	1.76E+02	1.89E+03	1.76E+02	2.59E+03	5.94E+01
Root Vegetables	3.13E-02	1.03E-02	4.24E-01	1.41E-01	6.77E-13	6.06E-14
Winter Wheat	1.06E-01	3.52E-02	3.67E-01	1.22E-01	4.14E-12	3.51E-13
Potatoes	7.44E-02	2.47E-02	1.69E-01	5.59E-02	4.41E-12	4.12E-13
Grass	2.97E+03	2.84E+02	2.97E+03	2.68E+02	8.53E+03	1.97E+02

TABLE 48. MAXIMUM AND AVERAGE CONCENTRATIONS OF RADIONUCLIDES IN DIFFERENT FOODSTUFFS AND FEEDINGSTUFFS FOR YEAR 2, (Bq/kg FRESH WEIGHT)

(a) Soil type: clay; release date 1 May

Product	^{137}Cs		^{90}Sr		^{131}I	
	Maximum Year 2	**Average Year 2**	**Maximum Year 2**	**Average Year 2**	**Maximum Year 2**	**Average Year 2**
Cow's milk	2.71E+01	1.40E+00	1.49E+01	1.78E+00	N/A	N/A
Beef	8.86E+01	1.13E+01	1.92E+00	6.41E-01		
Pork	4.30E+01	1.96E+01	7.76E-03	4.79E-03		
Chicken	3.22E+00	1.53E+00	1.06E-03	1.02E-03		
Lamb	6.59E+02	5.62E+01	2.72E+00	4.92E-01		
Fruit Vegetables	2.50E+01	4.17E+00	4.90E-01	1.48E-01		
Leafy Vegetables	2.63E-02	2.49E-02	9.27E-02	8.97E-02		
Root Vegetables	2.39E+01	4.00E+00	3.56E-01	3.41E-01		
Winter Wheat	9.67E+00	2.46E+00	4.54E-01	4.36E-01		
Potatoes	5.77E-02	5.35E-02	2.25E-01	2.15E-01		
Grass	1.71E+00	8.99E-01	3.08E+00	2.98E+00		

(b) Soil type: clay; release date 20 November

Product	^{137}Cs		^{90}Sr		^{131}I	
	Maximum Year 2	**Average Year 2**	**Maximum Year 2**	**Maximum Year 2**	**Maximum Year 2**	**Average Year 2**
Cow's milk	2.53E+00	1.32E+00	6.64E-01	4.31E-01	N/A	N/A
Beef	8.31E+00	4.60E+00	8.37E-02	5.93E-02		
Pork	4.13E-02	4.01E-02	9.49E-04	9.14E-04		
Chicken	1.18E-02	1.16E-02	4.80E-04	4.72E-04		
Lamb	3.05E+01	1.62E+01	5.88E-02	3.74E-02		
Fruit Vegetables	1.04E-02	9.95E-03	3.85E-02	3.76E-02		
Leafy Vegetables	1.21E-02	1.15E-02	4.28E-02	4.15E-02		
Root Vegetables	1.70E-02	1.63E-02	1.67E-01	1.62E-01		
Winter Wheat	3.55E-02	3.41E-02	2.07E-01	2.01E-01		
Potatoes	2.57E-02	2.47E-02	1.02E-01	9.95E-02		
Grass	2.45E+00	7.37E-01	1.42E+00	1.38E+00		

(c) Soil type: sandy; release date 1 May

Product	^{137}Cs		^{90}Sr		^{131}I	
	Maximum Year 2	**Average Year 2**	**Maximum Year 2**	**Average Year 2**	**Maximum Year 2**	**Average Year 2**
Cow's milk	2.77E+01	1.66E+00	1.72E+01	3.24E+00	N/A	N/A
Beef	9.08E+01	1.22E+01	2.20E+00	8.51E-01		
Pork	4.36E+01	1.99E+01	9.45E-03	6.38E-03		
Chicken	3.31E+00	1.60E+00	1.88E-03	1.81E-03		
Lamb	6.70E+02	5.97E+01	2.93E+00	6.14E-01		
Fruit Vegetables	2.53E+01	4.23E+00	8.71E-01	5.08E-01		
Leafy Vegetables	7.53E-02	7.12E-02	8.61E-01	8.31E-01		
Root Vegetables	2.42E+01	4.07E+00	9.30E-01	8.84E-01		
Winter Wheat	9.92E+00	2.63E+00	8.06E-01	7.69E-01		
Potatoes	1.66E-01	1.54E-01	3.70E-01	3.53E-01		
Grass	2.12E+00	1.28E+00	6.38E+00	6.12E+00		

(d) Soil type: sandy; release date 20 November

Product	^{137}Cs		^{90}Sr		^{131}I	
	Maximum Year 2	**Average Year 2**	**Maximum Year 2**	**Average Year 2**	**Maximum Year 2**	**Average Year 2**
Cow's milk	2.75E+00	1.44E+00	1.82E+00	1.12E+00	N/A	N/A
Beef	9.04E+00	5.03E+00	2.27E-01	1.53E-01		
Pork	1.22E-01	1.19E-01	1.68E-03	1.61E-03		
Chicken	3.50E-02	3.44E-02	8.47E-04	8.33E-04		
Lamb	3.31E+01	1.78E+01	1.57E-01	9.47E-02		
Fruit Vegetables	1.62E-02	1.56E-02	2.09E-01	2.03E-01		
Leafy Vegetables	3.47E-02	3.29E-02	3.97E-01	3.83E-01		
Root Vegetables	3.10E-02	2.97E-02	4.21E-01	4.09E-01		
Winter Wheat	1.05E-01	1.01E-01	3.65E-01	3.55E-01		
Potatoes	7.37E-02	7.08E-02	1.67E-01	1.63E-01		
Grass	2.65E+00	9.14E-01	2.94E+00	2.82E+00		

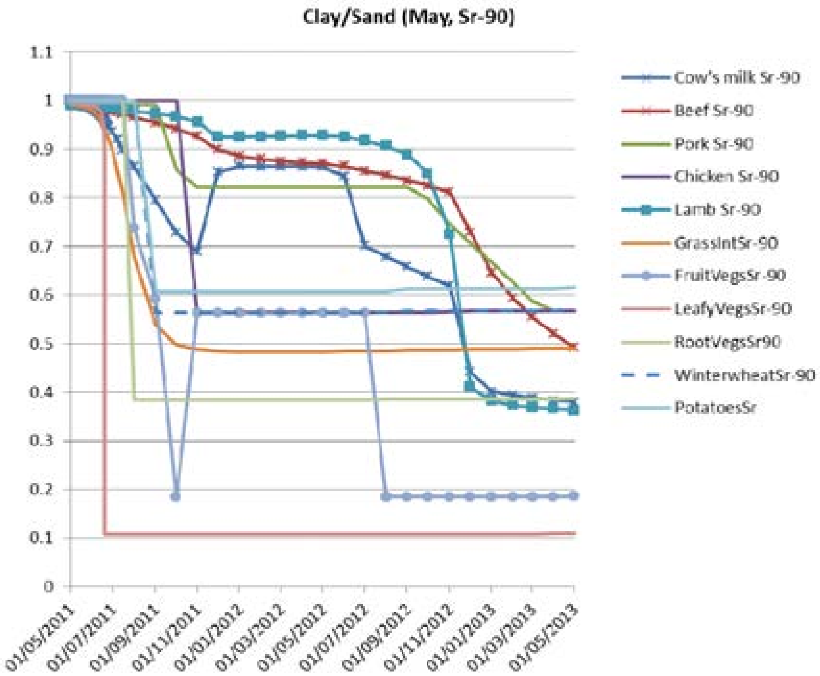

FIG. 62. Clay to sand ratios of activity concentrations in various food products for ^{90}Sr, for a release on 1 May.

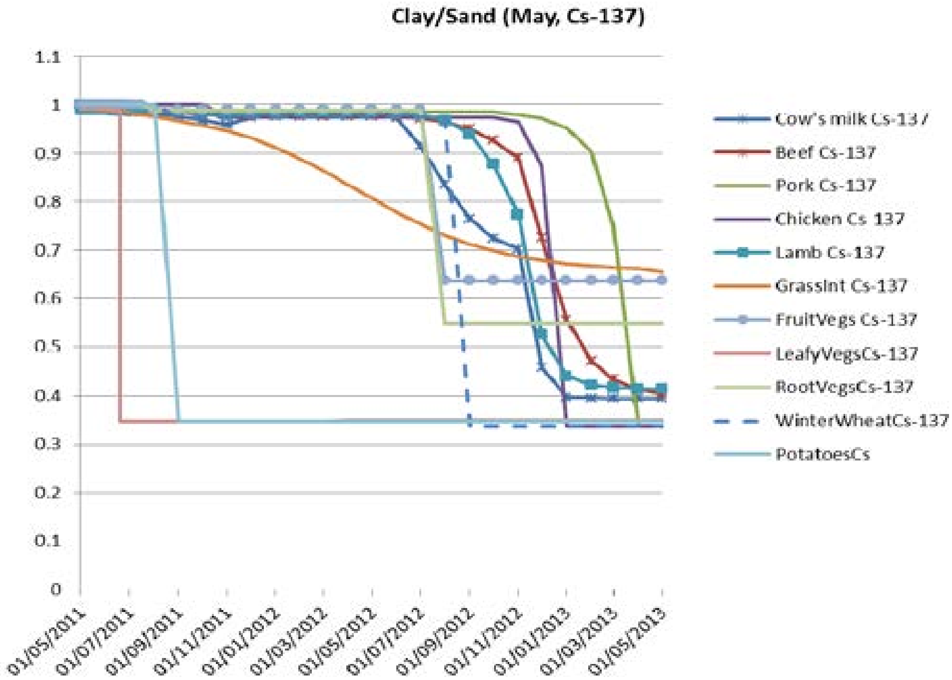

FIG. 63. Clay to sand ratios of activity concentrations in various food products for ^{137}Cs, for a release on 1 May.

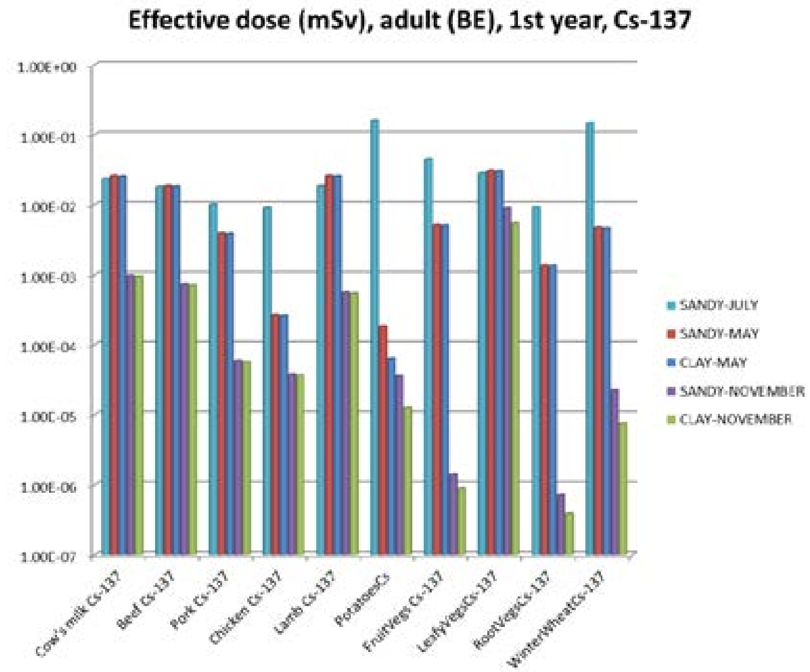

FIG. 64. Effective dose from ingestion of various food products for ^{137}Cs in the first year after deposition for various release times and soil types; Belgian diet.

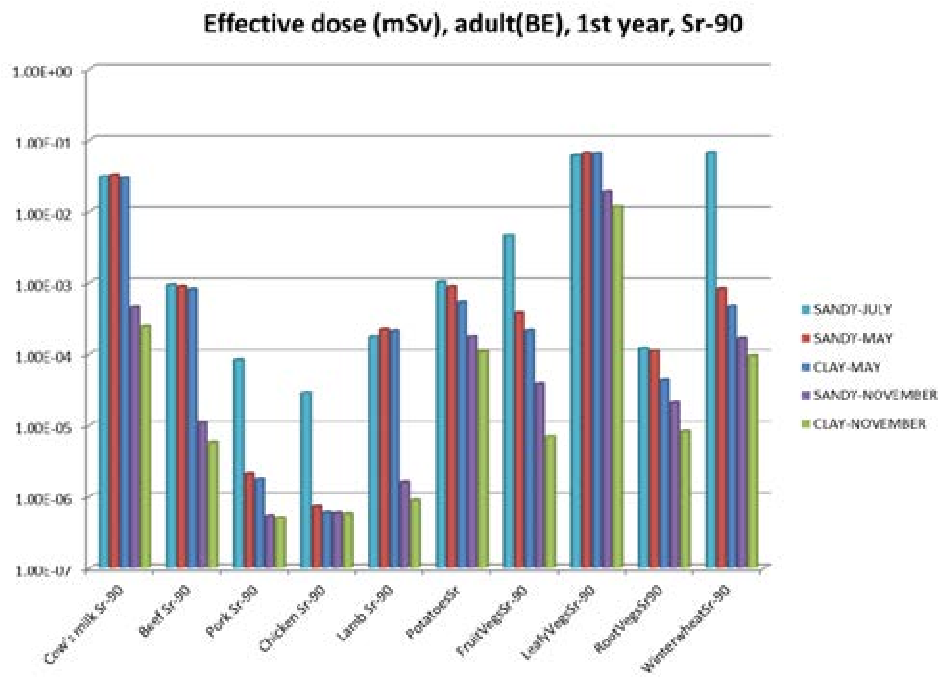

FIG. 65. Effective dose from ingestion of various food products for ^{90}Sr in the first year after deposition for various release times and soil types, Belgian diet.

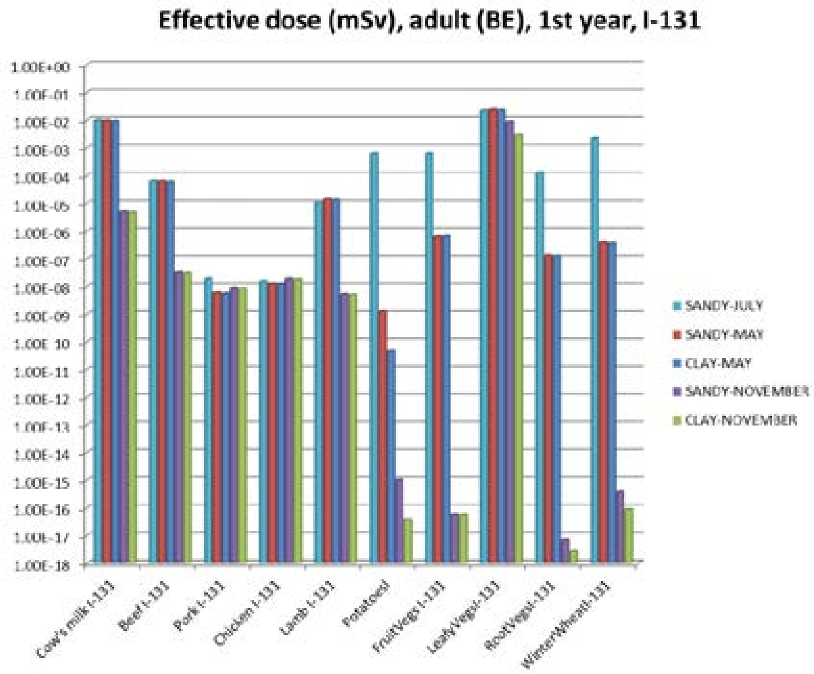

FIG. 66. Effective dose from ingestion of various food products for ^{131}I in the first year after deposition for various release times and soil types; Belgian diet.

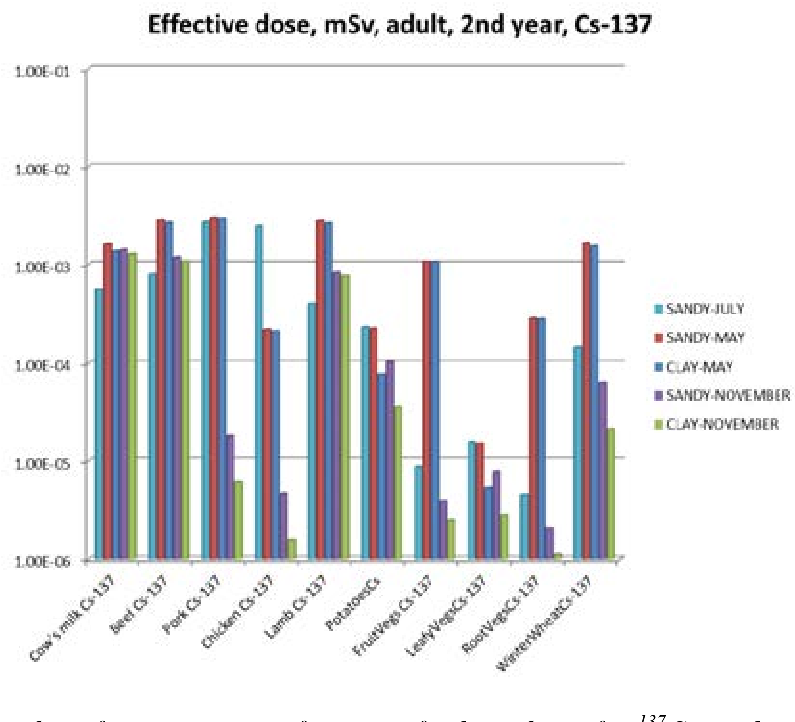

FIG. 67. Effective dose from ingestion of various food products for ^{137}Cs in the second year after deposition for various release times and soil types; Belgian diet.

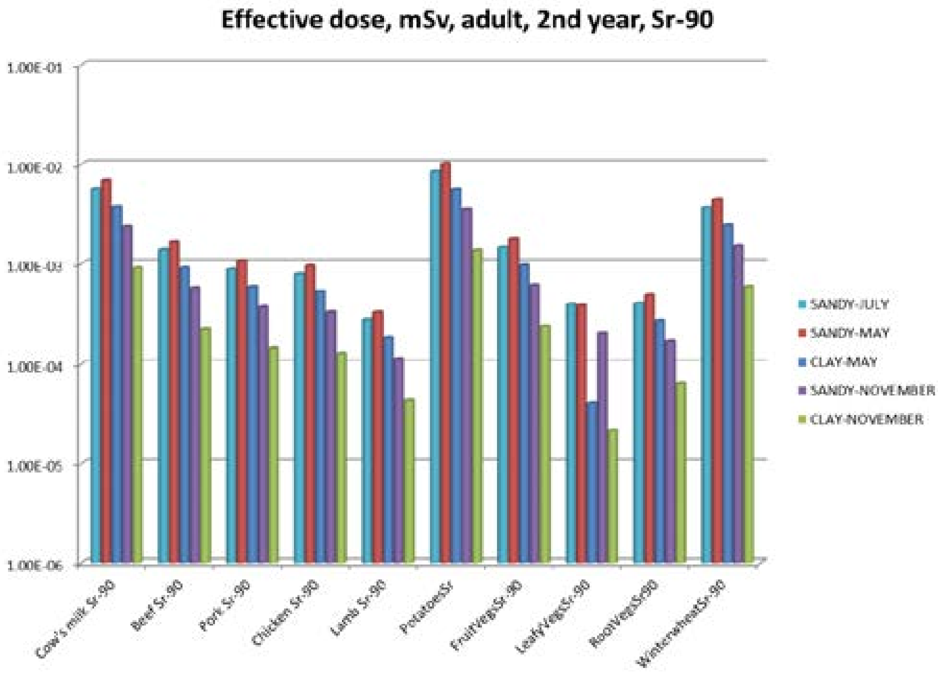

FIG. 68. Effective dose from ingestion of various food products for ^{90}Sr in the first year after deposition for various release times and soil types; Belgian diet.

APPENDIX III. SUPPLEMENTARY DATA FROM THE ALPINE SCENARIO

The description of seasonal variations in the Alpine Scenario of Section 5.3 was based mainly on the radionuclide ^{137}Cs and on an August date for deposition. Contamination with the radionuclides ^{90}Sr and ^{131}I and other release dates (1 February, 15 May and 1 November) are presented here in Figures 69–78.

The analysis of exposure pathways in Section 5.3 was carried out only for the radionuclide ^{137}Cs. For completeness, Figures 79 and 80 show the contributions of the different exposure pathways to the total dose for the radionuclides ^{90}Sr and ^{131}I.

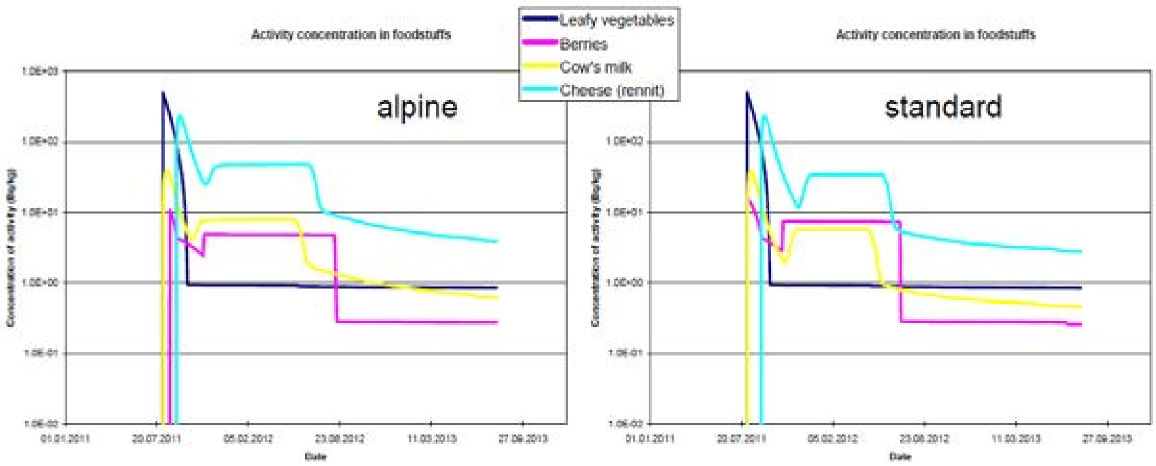

FIG. 69. ^{90}Sr contamination of selected foodstuff, dry deposition only.

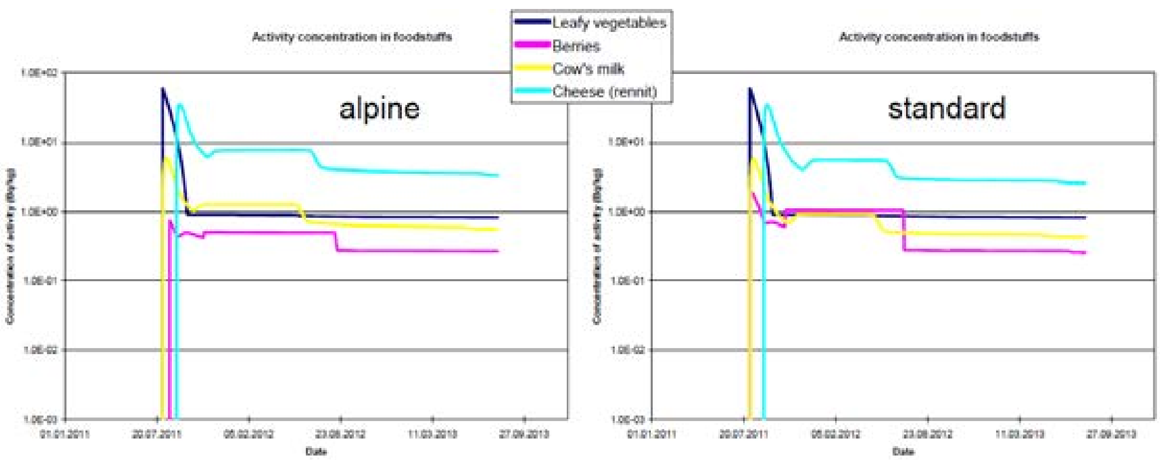

FIG. 70. ^{90}Sr contamination of selected foodstuff, wet deposition only.

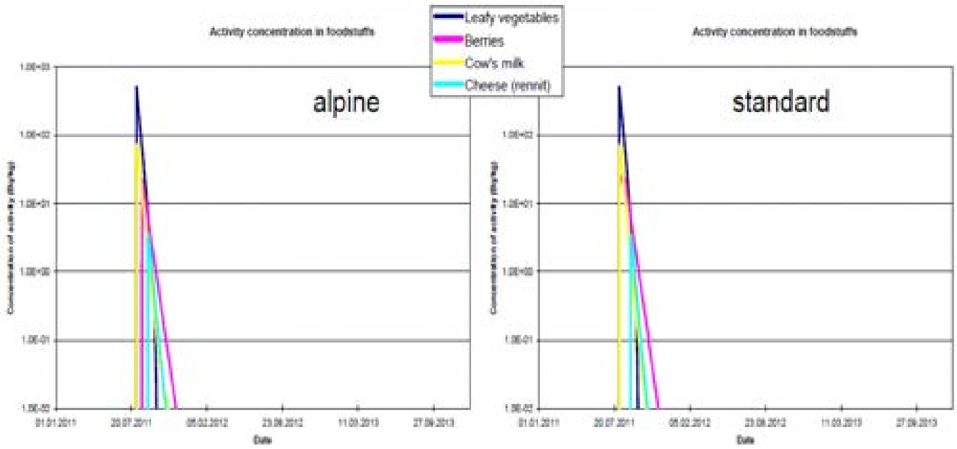

FIG. 71. ^{131}I contamination of selected foodstuff, dry deposition only.

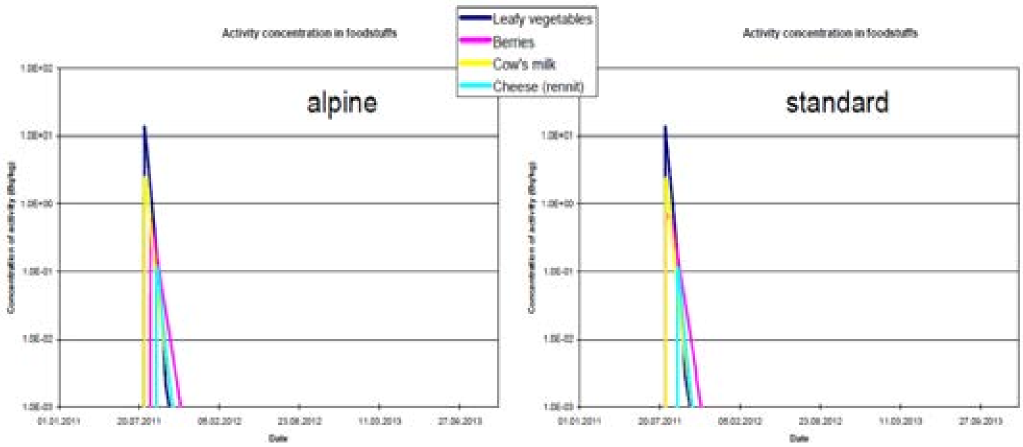

FIG. 72. ^{131}I contamination of selected foodstuff, wet deposition only.

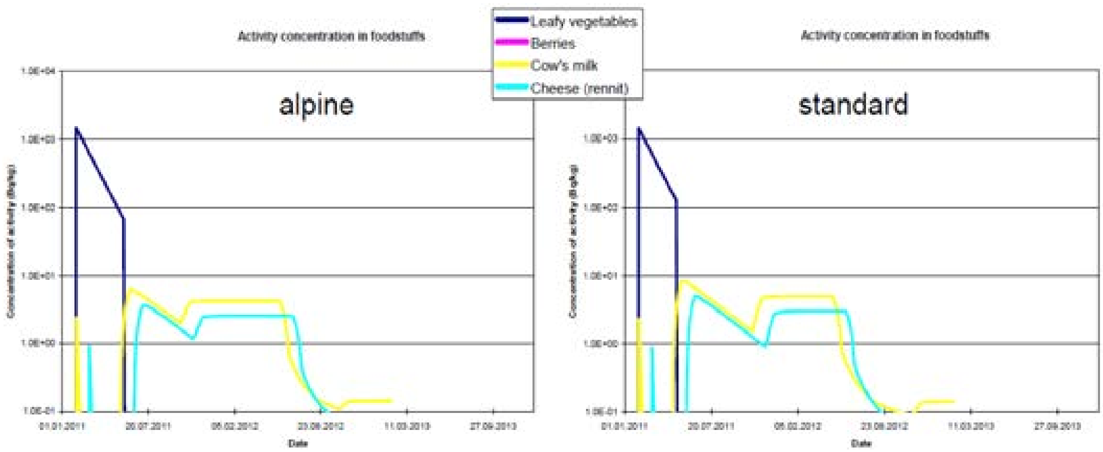

FIG. 73. ^{137}Cs contamination at the release date 1 February, dry deposition only.

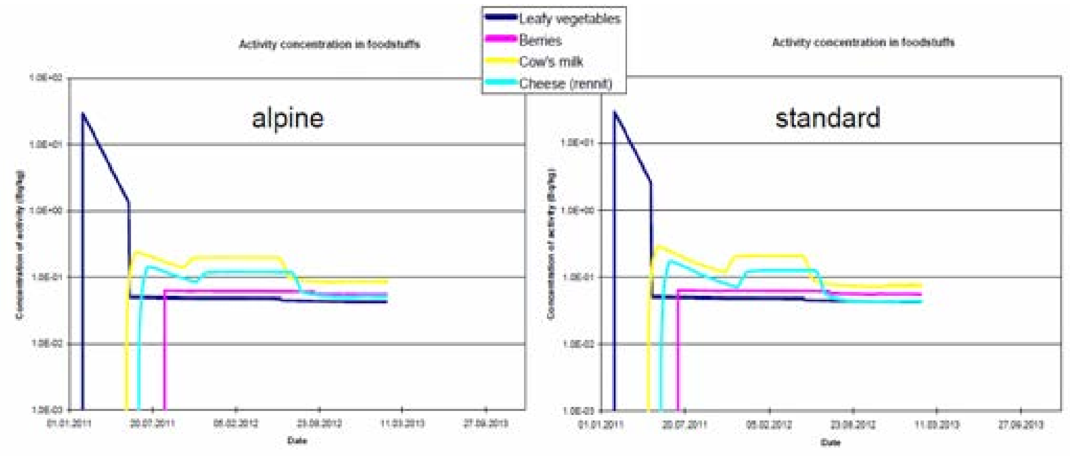

FIG. 74. ^{137}Cs contamination at the release date 1 February, wet deposition only.

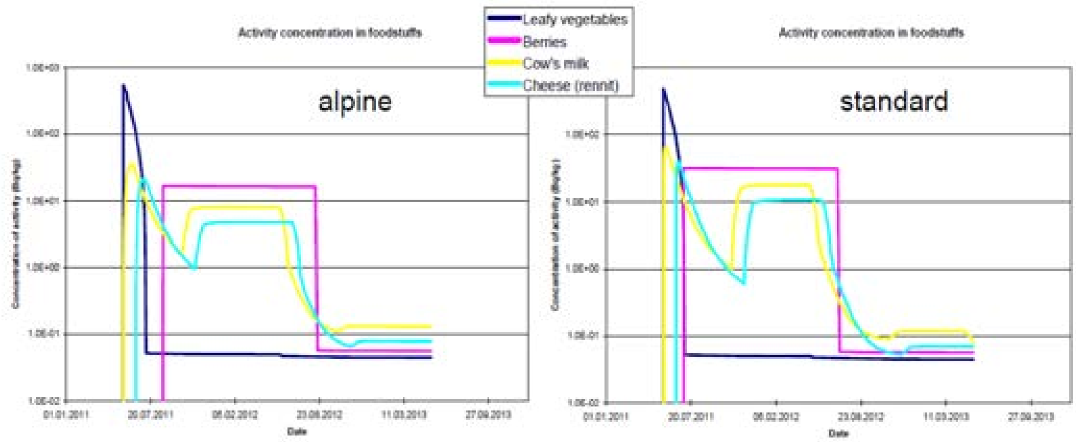

FIG. 75. ^{137}Cs contamination at the release date 15 May, dry deposition only.

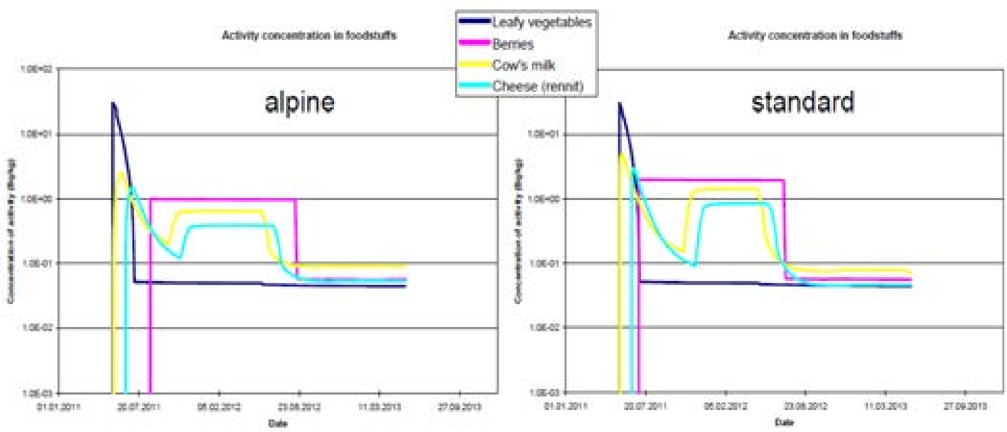

FIG. 76. ^{137}Cs contamination at the release date 15 May, wet deposition only.

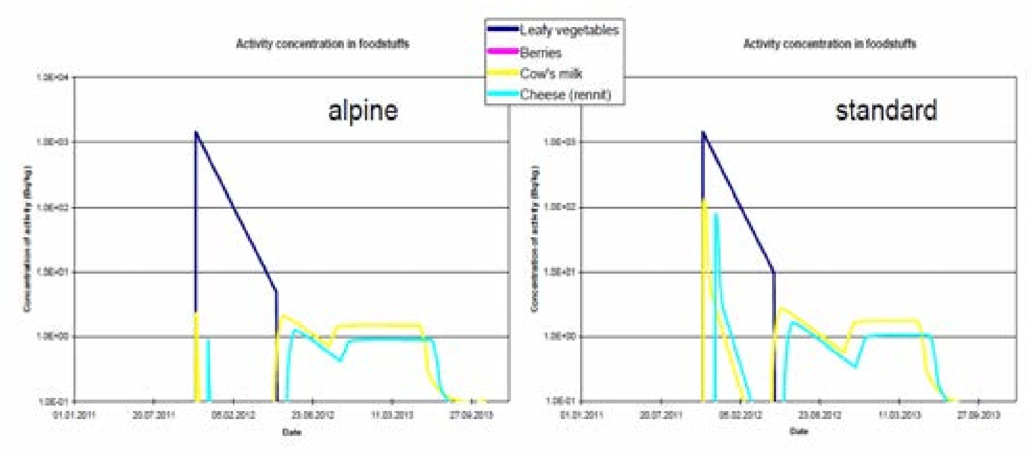

FIG. 77. ^{137}Cs contamination at the release date 1 November, dry deposition only.

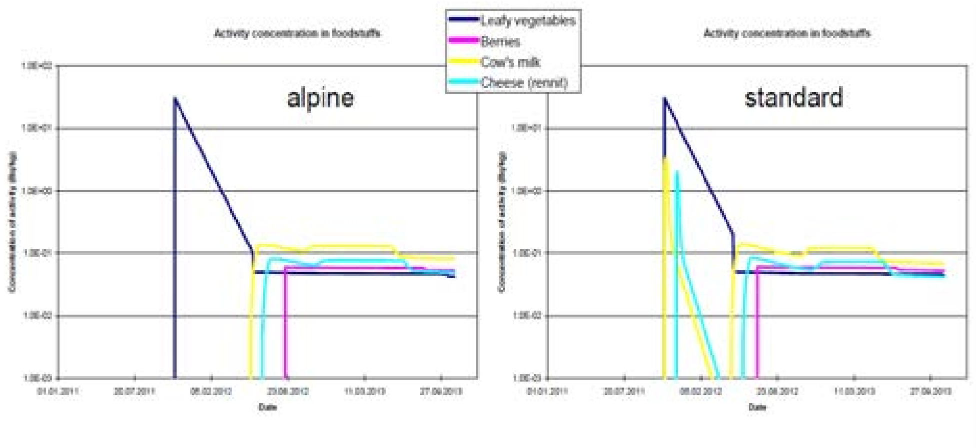

FIG. 78. ^{137}Cs contamination at the release date 1 November, wet deposition only.

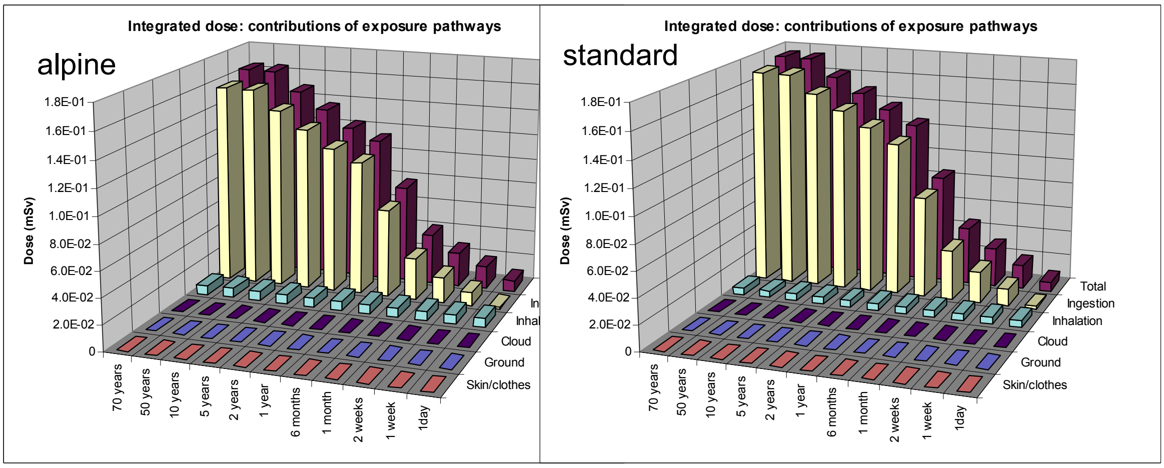

FIG. 79. Contribution of the different exposure pathways to total dose for dry deposition of ^{90}Sr in summer time (August).

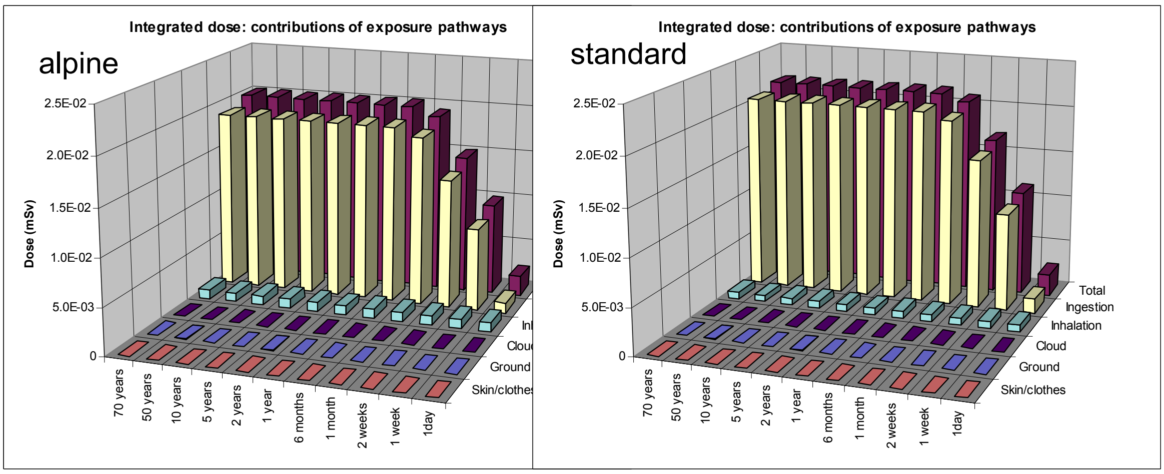

FIG. 80. Contribution of the different exposure pathways to total dose for dry deposition of ^{131}I in summer time (August).

APPENDIX IV. SUPPLEMENTARY DATA FROM THE THERMAIKOS GULF SCENARIO

IV.1. STUDY AREA

Thermaikos Gulf is located at the northwestern continental margin of the Aegean Sea and includes an extended shelf area bounded approximately by the 150 m isobath, with narrow shelf areas towards the east (Chalkidiki Peninsula) and to the west (Greek mainland). In the south, it communicates with the deep Sporades basin, while to the north there is a shallow area (Thessaloniki Gulf), with depths less than 20m and an opening of about 10 km toward the Gulf. Five major rivers are the main sources of freshwater, nutrients and sediment to the Gulf: the neighboring rivers Axios, Loudias, Aliakmon and, the smaller, Gallikos rivers to the north and the Pinios River further south.

The Gulf is part of the coastal system that belongs to the southern flank of the Alpine orogenic belt, located within the humid, mesothermal climatic zone and within an essentially tideless marine environment. Thermaikos coastal system is characterized by significant spatial and temporal heterogeneity, in terms of water mass and sediment transfer from land to the continental shelf and to the deep ocean basin; the formation and evolution of the coastal zone, in relation to land–air–ocean interaction processes; and various socio-economic aspects of the region and their impact on the natural environment.

The overall basin general circulation is influenced by coastal dynamics and the interaction with larger-scale Aegean flows, mainly Black Sea water masses flowing through the Dardanelles Straits. The tides in the region are comparatively small with a mean range of 0.25 m and consequently wind plays a major role in driving the circulation within the Gulf [95].

Wind stress is a major circulation forcing mechanism that greatly affects the transport and fate of the river-borne waters and materials. The region commonly experiences strong winds (>10 m/s) blowing from the north/northwest, which is a characteristic of the Aegean and Eastern Mediterranean seas. These winds often exhibit significant diurnal variation, blowing strongly during the day and abating at night. Field observations suggest a general anti-clockwise eddy in the northern Thessaloniki Bay area under normal meteorological conditions, a fact that can be attributed to the freshwater rivers' flow out of the Gulf along the western coastal boundary [96].

The transfer of matter is governed by the interaction between land and sea, in form of plume dynamics, as the rivers are the primary sources of low-salinity waters, sediments and nutrients. The wind-induced hydrodynamic circulation is of particular importance because the enclosed character of the area makes it susceptible to pollution problems. Wastewater enters the Gulf in the form of untreated domestic and industrial sewage from the city of Thessaloniki, while the rivers contribute significantly to the pollution loadings of nitrogen and phosphorus since they drain intensively cultivated valleys. Measurements of the water quality indicate levels of microbiological pollution in the innermost part of the Gulf, where bathing and fishing are forbidden, and jeopardizing the tourist and local shellfish industries.

The seabed within the Gulf of Thermaikos is composed of a mixture of clastic sand and mud. Sand is usually deposited around the river mouths and the shore, while silt and clay-sized materials are deposited further offshore, while Manning's roughness coefficient can be considered constant at a value of 0.03 throughout region [97].

IV.2. DATA SET UP

In order to perform the appropriate modelling exercise a number of data were collated, manipulated, modified or calculated in order to form the necessary model's input dataset. These data include oceanographic, meteorological, topological, biological, hydrological, radiological and sociological information from the area of interest. They were retrieved from scientific literature reviews, national and open access international project databases (HCMR Poseidon-LAS, NOAA NESDIS,NASA ISCCP D2, ECMWF Re-Analyis), national authorities archives (National Statistical Survey of Greece, the Greek Ministry of Environment, Institute of Geology and Mineral Exploration) and experimental survey measurements or modelling results provided from researchers of the Hellenic Centre for Marine Research, after personal contact.

Some of the main quantitative information concerning the topology, the hydrology, the climatology and the biota of the study area, essential for the formation of a mathematical model describing the radioecological processes and their evolution in space and in time, are presented in figures and tables later in the report.

IV.3. MODEL SET UP

In order to perform the risk scenario exercise an appropriate model had to be applied. Several environmental assessment models have been released for the evaluation of the radiological impact of actual and potential releases of radionuclides to the environment. The implemented model, though, has to be validated for its reliability of the predictions, by comparison with measured values in the environment or by comparing with the predictions of other models. For this reason a number of projects have been launched to validate this kind of models for predicting the behaviour of radioactive substances in the environment. The International Atomic Energy Agency (IAEA) has been organizing programmes of international model testing since the 1980's and several state-of-the-art models have been assessed, particularly in the frame of the EMRAS (Phase I) Programme. A specific part of this work was the validation of models for predicting the behaviour of radionuclides in the freshwater environment and coastal areas, resulting in a list of specialized radioecological models [98].

In this work, the available environmental models were examined in detail and the most suitable for the case of shallow costal marine scenario was selected. The ENEA's model MOIRA-PLUS Decision Support System was found to be the most appropriate in the framework of the projects requirements, where emphasis is given in the ecology and the biota relations of the study area. However, certain model modifications had to be made in order to be compatible with the peculiarities of the marine environment.

IV.3.1. Structure

MOIRA-PLUS is a model-based computerized decision support system (DSS) for management support to identify optimal remedial strategies for restoration of radionuclide contaminated aquatic ecosystems and drainage areas [56]. The model can be implemented either as a whole using the interface program of the model or by independently applying the sequence of appropriate sub-models. In this work, the second method was chosen, for greater control and interference with the calculation algorithms.

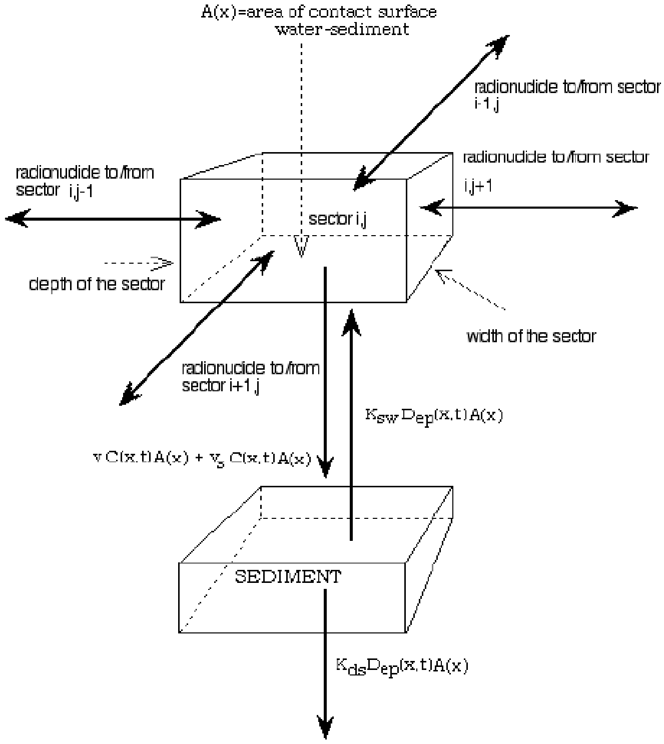

FIG. 81. Structure of the sub-model for predicting the behaviour of radionuclide within the systems "water column – bottom sediment".

The structured set of MOIRA codes implemented in this exercise, covering the basic processes of radionuclides dispersion in abiotic and biotic components in complex basins, includes:

- HYDRO (hydrological module): sub-code simulating the temporal behaviour of the hydrological and morphologic parameters of a complex water body;
- CAT (catchment module): sub-code simulating the migration of the pollutant from the catchment to the aquatic system;
- MIGRA sub-code simulating the migration of a pollutant through the abiotic components of the aquatic system;
- BIOT sub-code simulating the migration of a pollutant from the abiotic components of the aquatic system to the fish species;
- DOSE4B sub-code calculating the doses to the human population and to fish for ^{137}Cs and ^{90}Sr.

The basic concept of the model lies in is the horizontal parameterization of the examined water body in up to 20 sectors. Different vertical sub-components can be included simulating the water column and sediment vertical diversion. Each compartment is then treated as unique element in the subsequent calculations of the average radiological contamination (Bq m^{-3}), taking into account the radionuclide transfer between the compartments, the water sub-compartments, the water column with the sediment and the surface water with the atmosphere.

Specific customization of MOIRA-PLUS had to be made, in order to simulate the movement of masses of water through different segments. Additionally, appropriate environmental constants had to be introduced in all sub-models in order to describe the swallow marine environment scenario. The water balance equation in each segment was finally calculated simple by the formula:

$$B_i + \sum_{1;j \neq i}^{N} k_{ij}\varphi_j - \varphi_{i_i} = 0 \tag{13}$$

where:

B_i is the balance, in the generic sector *i*, between the evaporation, the precipitation and the water discharged by rivers or from other external water sources;

φ_j is the total flux of water that flows out of the sector *j(i)*; and

k_{ij} is the proportion of this total flux that flows from sector *j* to *i ≠j*.

Consequently, in each elementary compartment all the dominant mechanisms are been considered for the description of the radionuclide's behaviour in the water body and the seabed, through the equation:

$$\frac{\partial C(x,t)}{\partial t} = \frac{1}{l(x)h_{eff}(x)}\frac{\partial}{\partial x}\left[C_T(x,t)F(x,t)\right] + \frac{R(x,t)}{l(x)h_{eff}} - \frac{vC(x,t)}{h_{eff}} - \frac{v_s C(x,t)}{h_{eff}} + \frac{K_{sw}D_{ep}(x,t)}{h_{eff}} - \lambda C(x,t) \tag{14}$$

where:

C(x,t) is the radionuclide concentration in water (dissolved form, Bq m^{-3}) at point *x* and time *t*;
l(x) is the width of the watercourse (m);
heff(x) is the effective depth of the watercourse(m) [99];
$C_T(x,t)$ is the radionuclide concentration in water (total radionuclide dissolved and particulate form) (Bq m^{-3});
F(x,t) is the water flux(m^3 s^{-1});
R(x,t) is the contribution from the catchment (Bq per meter of water course per unit time);
v is the deposition velocity of radionuclide (dissolved form) from the water column to sediment (m s^{-1});
v_s is the deposition velocity of radionuclide (particulate form) due to sedimentation (m/s);
K_{sw} is the contaminant migration rate from sediment to water (re-suspension) (s^{-1});
l is the radioactive decay constant (s^{-1});
D_{ep} is the contaminant deposit in bottom sediment (Bq m^{-2});
K_{ds} is the contaminant migration rate from bottom sediment to deep sediment (s^{-1}); and
f is the ratio between the total contaminant concentration in water and the contaminant concentration in dissolved form (dimensionless).

IV.3.2. Implementation

The study area has been parameterized in 5 river segments and 5 marine segments, mainly according to the hydrological characteristics of the Gulf and the fish production. One segment was used for the simulation of the Thessaloniki Gulf with small water circulation (seg. n°8), significant water income from Gallikos River and no fish production; 2 for the Inner Thermaikos Gulf (seg. n°7; 9) characterized by an almost constant cyclonic eddy, dense fresh water flux (seg. n°9) and significant fish production mainly from the mussels cultivations in the Aliakmonas and Axios rivers estuaries; and 2 for the Outer Thermaikos Gulf (seg. n°6; 10) with the main fishing production, large variation in the water circulation due to Black Sea water incomes and a temporal cyclonic eddy feature.

IV.3.3. Input data

The required input for each compartment included in the model involves:

Environmental data

- Compartments morphology (mean depth, width and length) and topology (catchment areas, total surface area and position – latitude/longitude);
- Climatology (precipitation, evaporation and temperature);
- Water chemistry (Ca, K, suspended mater and total phosphorus concentrations, pH);
- Seabed type (acidic, basic, precambrian, sedimentary, metamorphosed) and soil composition (clay, sand, loam and organic composition);
- Water flow and circulation (rivers mean fluxes, catchment area runoff, open sea inflow and outflow, magnitude of current fluxes).

Biota data

- Human population density (n° of persons per prefecture) and their age distribution (0–5, 6–15, 15 < years old);
- Human population diet (fish consumption) and habits (boating, shoring, swimming and recreational sea use time per person);
- Fish classification (prey, predators) and production (fishing, fish farm production).

The aforementioned data were sufficient to form the hydrology model of the region. Monthly average atmospheric temperatures are shown in Figure 84. The compartments' morphological and catchment area data were calculated externally with GIS techniques or retrieved from the literature [100]. The main monthly rivers influxes and the rest catchment runoff in each compartment were retrieved from experimental data for the period 1997–1998 in the literature (Tables 49 and 50). Uniform mean monthly precipitation and evaporation data for all the compartments were calculated from climatology prediction maps for the last 5 years (Table 51; NASA ISCCP D2 and ECMWF Re-Analysis). The absolute open sea water flux income/outcome in the Gulf and the circulation, in form of water balance ratios between the compartments, were calculated based on 1 year (2008) Aegean Sea hydrodynamic model data (Poseidon system, HCMR) of the 3D velocity field grid with a horizontal resolution of 1/30° and 24 sigma layers along the vertical with a logarithmic distribution near the surface and the bottom [101]. An appropriate algorithm was developed in order to calculate the mean monthly absolute flux volume ($m^3\ m^{-2}\ s^{-1}$) in the compartments border-surfaces. Consequently, the flux ($m^3\ month^{-1}$) from the open sea (Black Sea water) and the total outflow from the Gulf in the boundary marine compartments (seg. n°6 and n°10) could be calculated; and the percentage flux between every compartment was derived.

For the human population data have an influence zone of 30–60 km near-shore area according the land morphology and population habits was assumed, while for the recreational use the MOIRA-PLUS default values for the specific coordinates were used, taking into account the inhabitant's age distribution in each compartment (Table 52). Values for the mean fish production from the last 20 years were classified into 2 groups (Figure 85), including the mussels aquafarm production near the main rivers exits and all the other fishing catches (Table 53) according the volume of each compartment, within the regions fishing is allowed.

The mean sedimentation values were retrieved from published model estimates, calibrated with experimental data. The Ca and K concentrations were calculated based on the mean salinity value of the compartments over a 10 years period and the compartments' suspended matter was also retrieved from literature model predictions based on field measurements (Figure 85). The standard values of the radionuclides (^{137}Cs and ^{90}Sr) migration and transfer coefficients in the marine environment, as well as bioconcentration factors of the fish groups were used (IAEA and ICRP guidelines).

IV.3.4. Calibration

For the radiological dispersion calibration of the model, literature and unpublished data of radiocesium concentration in water and sediment from Thermaikos region were collected. According various terrestrial measurements and estimations of the total ^{137}Cs fallout in the surrounding regions of the Thermaikos Gulf after the Chernobyl accident in 1986 vary from 24–35 kBq m^{-2} [75, 102]. These values are in agreement with model predictions of the Aegean Sea ^{137}Cs deposition, which estimate that Thermaikos Gulf was the most contaminated marine environment in Greece after the Chernobyl accident, with fallout value ranging between 20 and 40 kBq m^{-2} [73]. Within the years 1990–2005, a number of field measurements were performed mainly by the Institute of Oceanography, HCMR; and the Institute of Nuclear Technology and Radiation Protection, NCNR "Demokritos" [103], providing concentration values also for mussels and fishes. In Table 54 all the available current data of ^{137}Cs concentrations in the biotic and abiotic elements of the Thermaikos marine environment are summarized.

The variation in time of cesium concentration in the water of the Gulf is strongly affected by the higher concentrations in the Black Sea water masses. These water masses circulate inside the Gulf, entering to the Aegean Sea from the Dardanelle Straits. The horizontal variety of sediments core concentrations depends on the vicinity to rivers estuaries. In these estuaries elevated concentrations have been recorded, due to the wash off of cesium from the catchment areas. The vertical variations along the same core samples can be attributed to the sedimentation processes and the soil characteristics of the seabed at the sample points.

The annual ^{137}Cs influx after the Chernobyl accident from the Black Sea water circulation into the Thermaikos Gulf was calculated as the fraction of the total concentration at the upper 50 m of water income from Dardanelles Straits [104] towards the North Aegean sea. The estimated concentrations in the waters entering the Agean Sea from the Dardanelles straights are illustrated in Figure 87.

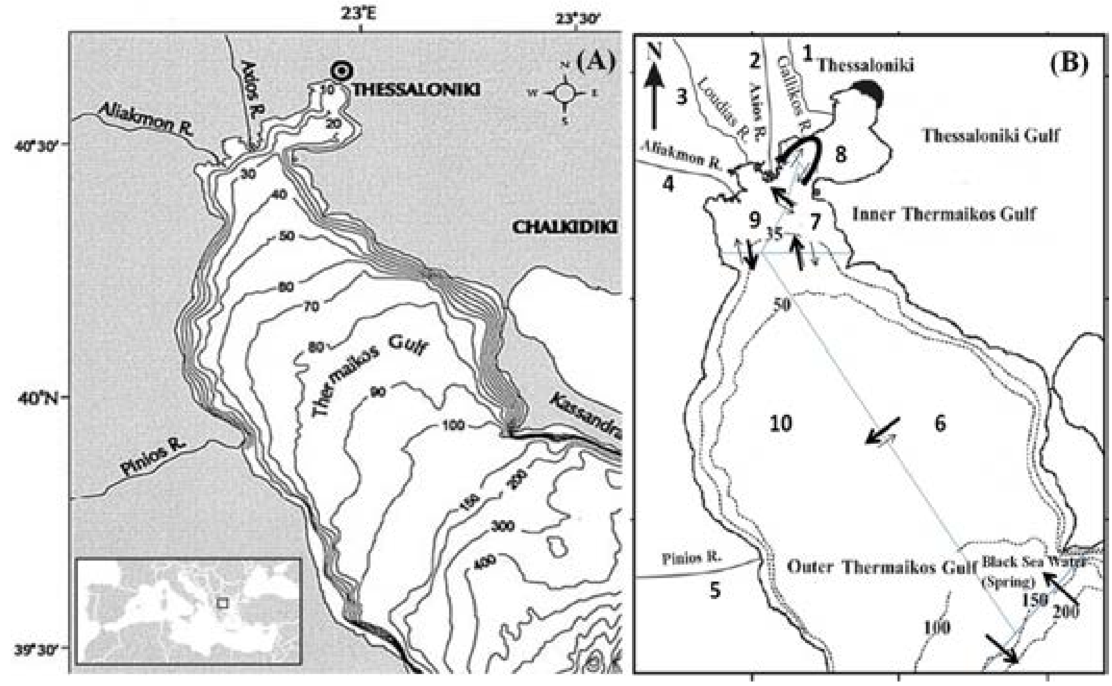

FIG. 82. (A) The Gulf of Thermaikos located at the North Aegean Sea (NE Mediterranean); (B) Box-model of the 5 river and 5 marine segments of Thermaikos Gulf, up to 150 m isobaths line, included in the simulation with the main water flux structures considered in the model.

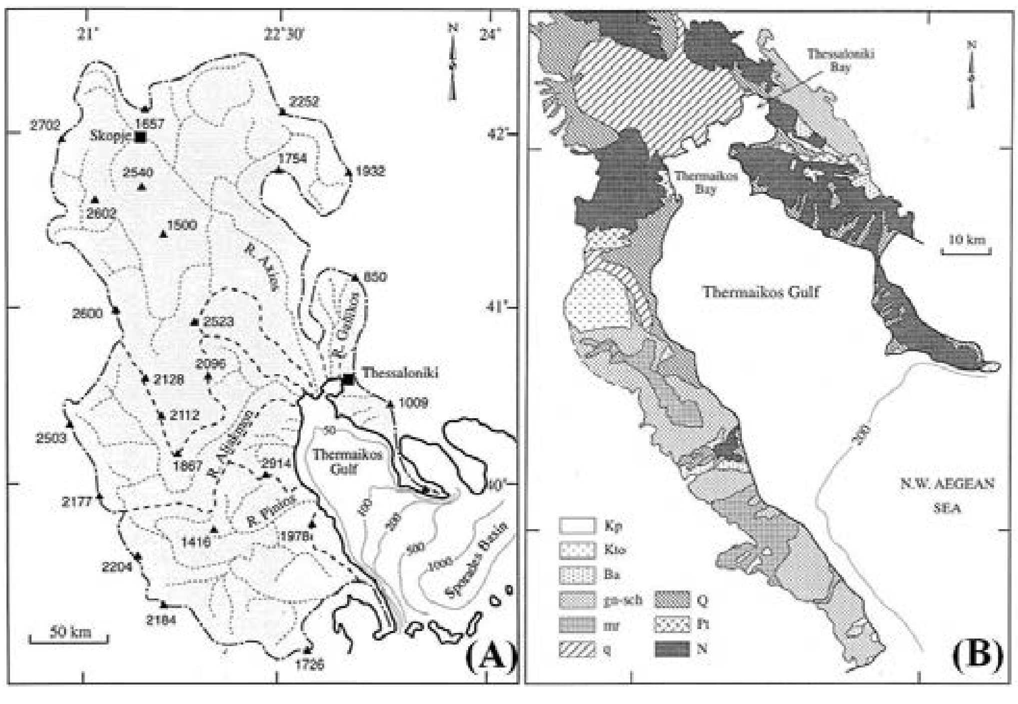

FIG. 83. (A) Geographical map showing the Thermaikos Gulf Coastal System, NW Aegean Sea, eastern Mediterranean (The Times Atlas of the World, 1994); (B) Lithology of the coastal zone region of Thermaikos Gulf (based upon geotectonic map by IGME, 1989).

TABLE 49. MEAN MONTHLY VALUES FOR WATER AND SEDIMENT DISCHARGES OF THE MAIN RIVERS TO THERMAIKOS GULF FOR THE PERIOD SEPTEMBER 1997 – SEPTEMBER 1998 (METROMED PROJECT DATA, HCMR)

Month	Axios	Loudias	Aliakmon	Pinios
		Water discharge (m^3/s)		
September	38	23	34	10
October	108	17	25	20
November*	166	27	29	136
December	223	37	33	252
January	174	35	79	65
February	150	14	97	62
March	155	12	32	80
April	97	40	11	31
May	85	35	37	58
June	11	11	10	6
July	0.5	11	10	12
August	1.5	16	17	10
September	57	18	22	20
		Sediment discharge (g/s)		
September	368	163	200	26
October	30	9	13	14
November*	5985	146	324	97 500
December	11 939	284	636	195 000
January	6651	0	635	500
February	1390	0	0	1555
March	5967	428	388	6214
April	4406	888	179	115
May	1203	70	74	1787
June	1364	96	282	1708
July	12	0	184	116
August	62	352	344	130
September	693	118	200	188

* Due to lack of data for November, the average value between October and December was used.

TABLE 50. AVERAGE BIOGEOCHEMICAL COMPOSITION OF THE MAIN RIVERS WATER [105]

Component	Axois	Aliakmon	Pinios	Gallikos
Ca (mval/l)	2.7	2.7	3.1	3.1
Mg (mval/l)	0.8	1.3	1.5	1.0
Na (mval/l)	0.8	0.2	0.3	1.4
K (mval/l)	0.1	0.1	0.1	0.1
Cl (mval/l)	0.4	0.2	0.3	0.6
SO_4 (mval/l)	0.7	0.3	0.3	0.6
NO_3 (mg/l)	4.9	3.1	4.3	3.7
PO_4 (mg/l)	1.6	0.2	0.3	0.1
SiO_2 (mg/l)	10.1	10.2	13.1	10.3
DO (%)	98.7	104.9	99.7	114.3
DOC (mg/l)	1.4	1.6	1.5	2.3
POC (mg/l)	0.5	0.5	1.1	0.1
Cu (ppb)	4.8	9.3	–	–
Pb (ppb)	4.5	2.0	2.5	1.0
Ni (ppb)	20.0	18.3	18.5	17.0

TABLE 51. AVERAGE MONTHLY ATMOSPHERIC TEMPERATURE FROM 4 METEOROLOGICAL STATIONS AT THE NORTH AEGEAN SEA AND AVERAGE MONTHLY PRECIPITATION (MM) FROM THESSALONIKI METEOROLOGICAL STATION FOR THE PERIOD 2002–2008 (HELLENIC NATIONAL METEOROLOGICAL SERVICE)

Month	2006	2007	2008	2009	2010
January	39	4.6	19.2	68.8	10.6
February	30.6	15.8	17	4.2	89.8
March	30.4	14.6	10.4	45.4	27.2
April	51	9.4	64.4	17.6	22.2
May	20.8	53.4	21.8	11.4	40.8
June	0	40.2	12	41	48.6
July	37.4	0	9.6	4.8	45.4
August	5.6	42.8	0	98.6	0
September	42.2	26.4	69.2	14.6	10
October	58.4	52.8	23.2	28.4	150.4
November	22.6	40	15.4	24.4	25.2
December	24.6	12.8	50.6	91.2	20

TABLE 52. POPULATION AGE STRUCTURE FROM THE 2001 CENSUS IN NORTH GREECE AND THE PREFECTURE OF THESSALONIKI (NATIONAL STATISTICAL SURVEY OF GREECE)

Location	Total	0–14	15–24	25–39	40–54	55–64	65–79	>80
Thessaloniki	363 987	45 387	63 450	84 584	70 665	39 660	50 004	10 237
North Greece	3 540 691	554 609	506 833	780 882	687 181	415 953	504 044	91 189

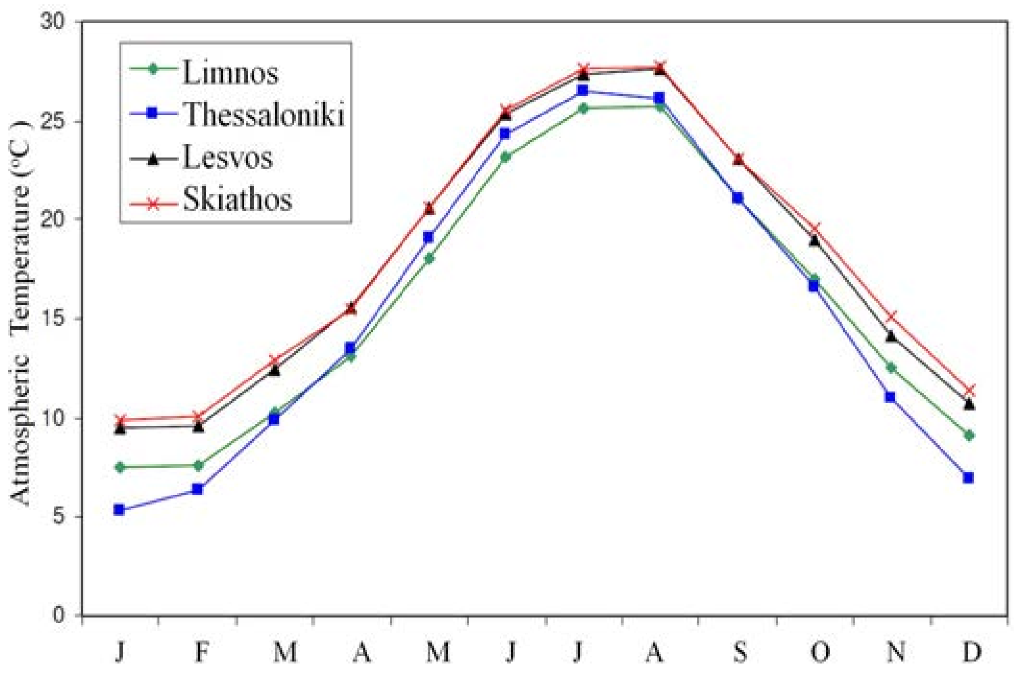

FIG. 84. Monthly average atmospheric temperatures in the Thermaikos Gulf region.

TABLE 53. CLASSIFICATION OF THE ANNUAL FISH PRODUCTION (TONES) IN THE THERMAIKOS GULF FOR THE YEAR 2008 (NATIONAL STATISTICAL SURVEY OF GREECE)

Fish						**Molluscs**	
Hake	581.8	Pickerel	79.4	Pilchard	1374.5	Flying squid	106.4
Thornback ray	48.7	Black bream	38.5	Horse mackerel	522	Common squid	41.9
Stone bass	2.9	Blotched pickerel	24	Black sea bream	16.8	Poulp	34.8
Gurnard	36.8	Large eyed dog's teeth	26.6	Scorpion fish	30.8	Cuttle fish	762.9
Black-mouthed godfish	17	Red mullet	165.9	Mackerel	55.1	Octapus	489.5
Anchovy	3247.7	Croaker	1.7	Dog fish	5.5		
Sole	406.3	Daouki	46.9	Couch's sea bream	119.7	**Crustaceans**	
Bogue	105.4	Swordfish	22.2	Dog's teeth	25.8	Lobster	4
Bluefish	41.8	Bonito	15.7	Dusky sea perch	1.1	Common prawn	215.4
Garfish	33.8	Sprat	35.5	Tune fish	42.2	Shrimp (common)	20.9
Brill	1.1	Anglerfish	161.8	Blotched pickerel	166.2	Crab	33.6
Tub fish	18.9	Couch's whiting	80.4	Red sea bream	22	Crayfish	31.7
Common grey mullet	1187.1	Rassa	0.9	Common sea bream	20.1		
Shapper	9.6	Grouper	1.1	Gilt sardine	1530.8	**Bivalvia**	
Club mackerel	375.8	Skipjack	0	Comber	1.9	Warty venus	227.1
Goatfish	325.8	Guitarfish	5.2	Eel	3.7	Mussel	154.3
Bass	416.1	Goldline	36.4	John dory	16.1	Oyster	5.7
Red bream	34.9	Jack mackerel	40	Others (Fish)	4175.8	Bay scallop	4.5
Yellowtail	18.8	White bream	14.4			Others (Pelecipoda)	169.7

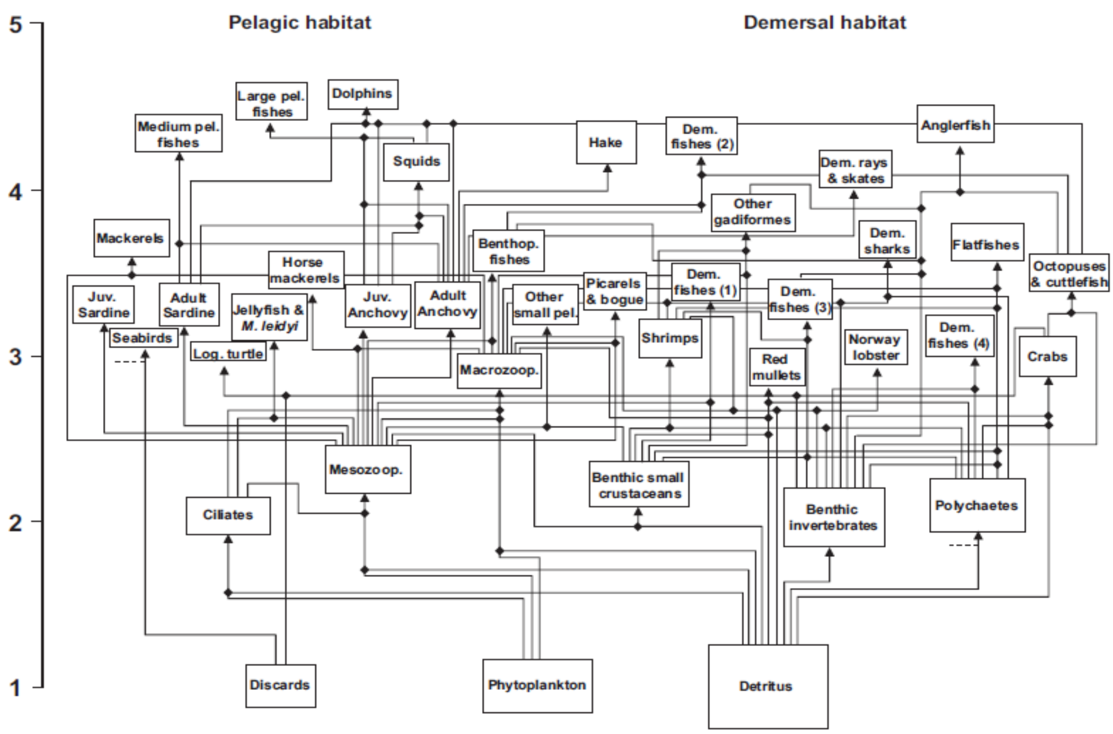

FIG. 85. Flow diagram of the N. Aegean Sea organized into 40 functional groups according to trophic level and pelagic or demersal habitat. Links indicate flows >10% for each group [75].

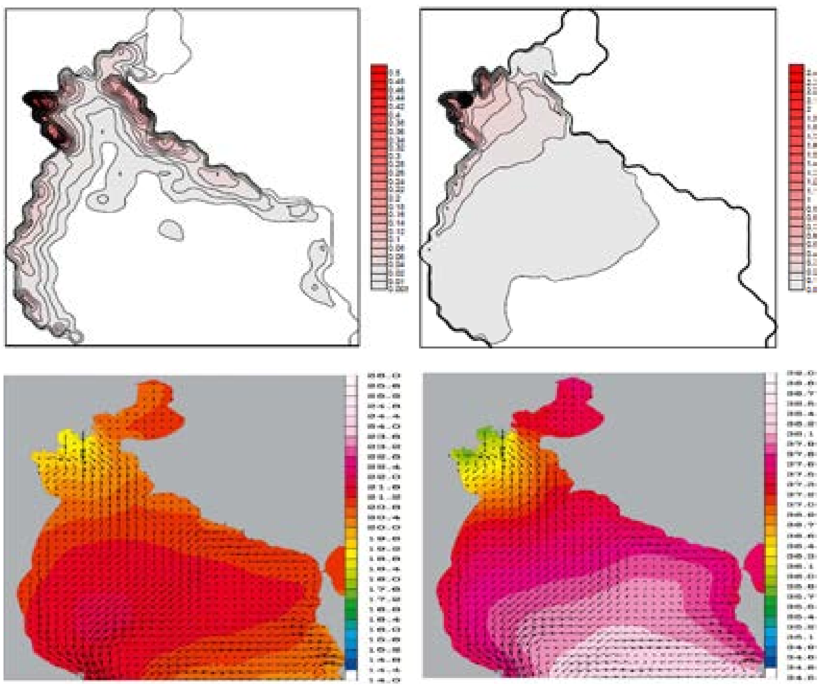

FIG. 86. Model computed (i) mean annual, depth averaged concentration of the SPM in mg l^{-1} (top right); (ii) sedimentation thickness of the layer of deposited matter in mm (top left); (iii) near-surface annual averages of velocities with temperature in ^{o}C (bottom left); and (iv) salinity in psu (bottom right) after the 1 year simulation period [106].

TABLE 54. EMPIRICAL DATA OF ^{137}CS CONCENTRATION IN WATER, SEDIMENT, FISH AND MUSSELS IN THERMAIKOS GULF

Sampling Location	Date	Concentration ($Bq\ kg^{-1}$ or $Bq\ m^{-3}$)			Type	Reference
		Average	Min.	Max.		
Weststern Thermaikos Gulf	2004–2006	0.1	0.07	0.13	mussels	Thebaultt et al., [107]
	May 2000	1.4	1.11	1.69	mussels	Katsiki & Florou, [108]
Thermaikos Gulf	1999–2001	0.92	0.24	1.6	mussels	Florou et al., [109]
North Agean Sea	1986–1987	7.1	5.3	8.9	mussels	
	1984–1985	0.68	0.58	0.78	mussels	
	1988–1995	0.46	0.18	0.74	mussels	
Agean Sea	1985	0.63	–	–	mussels	Pappuci & Delfanit, [110]
	1987	0.55	–	–	mussels	
	1988	0.53	–	–	mussels	
	1989	0.3	–	–	mussels	
	1985	0.93	0.31	1.55	fish	
	1987	0.37	0.06	1.24	fish	
	1988	0.66	0.31	1.28	fish	
	1989	0.9	-	-	fish	
	1990	0.51	0.31	1.13	fish	
NorthEast Agean Sea	1984–1985	0.34	0.27	0.41	fish	Florou, [111]
	1986	10.14	2.69	17.59	fish	
	1987–1995	0.65	0.28	1.02	fish	
	1984–1985	2.42	2.08	2.76	sediment	
	1986–1987	4.54	2.55	6.53	sediment	
	1988–1995	1.88	0.92	2.84	sediment	
Thermaikos Gulf	2005	15	5	30	sediment	Evangelou et al., [112]
	2007	25	5	35	sediment	
Thessaloniki Gulf	2006	41	22	22	sediment	Tsabaris et al., [113]
Inner Thermaikos Gulf	Sept. 2001	38	34	41	sediment	Karagiorgis et al., [114]
Outer Thermaikos Gulf	Sept. 2001	20	5	35	sediment	
NorthEast Agean Sea	1984–1985	2.7	2.42	2.98	water	Florou, [111]
	1986–1987	20.7	17.9	23.5	water	
	1988–1995	20.7	6	35.4	water	
Thessaloniki Gulf	2009	5.7	2.1	14.7	surf water	Florou et al., [115]
NorthEastern Agean Sea	Dec. 2005	5.5	4.6	7.3	surf water	Evangeliou et al., [116]
	June 2006	10.3	8.5	12.8	surf water	
Eastern Mediteranian	1995–1997	3.6	3.3	4	surf water	Delfanti et al., [117]
Outer Thermaikos (Katerini)	2003	4.8	4.5	5.1	surf water	Tsabaris, [118]

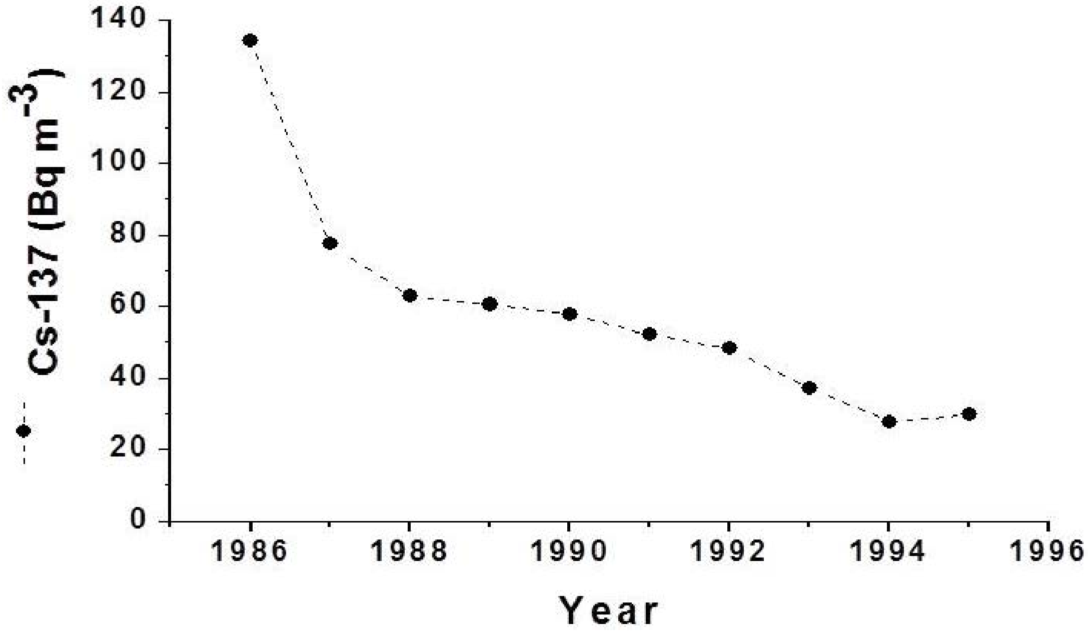

FIG. 87. ^{137}Cs concentration in the Black Sea water masses entering the Thermaikos Gulf versus time.

REFERENCES

[1] HÅKANSON, L., BRITTAIN, J. E., MONTE, L., BERGSTRÖM, U., HELING, R., Modelling of radiocesium in lakes – Lake sensitivity and remedial strategies, J. Env. Rad. **33** (1996) 1–25.

[2] AARKROG, A., Environmental studies on radioecological sensitivity and variability with special emphasis on the fallout nuclides ^{90}Sr and ^{137}Cs, Risø-R-437, Risø National Laboratory, (1979).

[3] HOWARD, B.J., The concept of radioecological sensitivity, Rad. Prot. Dos. **92** 1–3 (2000) 29–34.

[4] SHAW, G., ROBINSON, C., HOLM, E., FRISSEL, M.J., CRICK, M., A cost-benefit analysis of long-term management options for forests following contamination of ^{137}Cs, J.Env. Rad. **56** (2001) 185–208.

[5] BUCKLEY, R.C., Environmental sensitivity mapping – what, why and how, Env. Geo. and Health **4** (1982) 151–155.

[6] UNITED NATIONS, Glossary of Environmental Statistics, Studies in Methods, Series F, No. 67, New York (1997).

[7] INTERNATIONAL ATOMIC ENERGY AGENCY, Evaluating the Reliability of Predictions made using Environmental Transfer Models, Safety Series No. 100, IAEA, Vienna (1989).

[8] BIOMOVS II, Guidelines for uncertainty analysis, BIOMOVS II Technical Report No. 1, Swedish Radiation Protection Institute, Stockholm (1993).

[9] IMAN, R.L., SHORTENCARIER, M.J.A., FORTRAN 77 Program and user's guide for the generation of Latin Hypercube and random samples for use with computer models, NUREG/CR-3624, Sandia National Laboratories, Albuquerque, NM (1984).

[10] IMAN, R.L., SHORTENCARIER, M.J., JOHNSON, J.D., A FORTRAN 77 Program and user's guide for the calculation of partial correlation and standardized regression coefficients, NUREG/CR-4122 (SAND85-0044), Sandia National Laboratories, Albuquerque, NM (1985).

[11] INTERNATIONAL ATOMIC ENERGY AGENCY, Handbook of Parameter Values for the Prediction of Radionuclide Transfer in Terrestrial and Freshwater Environments, Technical Reports Series No. 472, IAEA, Vienna (2010).

[12] INTERNATIONAL ATOMIC ENERGY AGENCY, Quantification of Radionuclide Transfers in Terrestrial and Freshwater Environments for Radiological Assessments, IAEA-TECDOC-1616, IAEA, Vienna (2009).

[13] MÜLLER, H., PRÖHL, G., The role of seasonal, climatic and meteorological conditions in modifying nuclear accidents consequences, The Influence of Seasonal Conditions on the Radiological Consequences of a Nuclear Accident (Proc. NEA Workshop, Paris, 1989) OECD/NEA, Paris (1989).

[14] WRIGHT, S.M., HOWARD, B.J., STRAND, P., NYLEN, T., SICKEL, M.A.K., Prediction of ^{137}Cs Deposition from Atmospheric Nuclear Weapons Tests within the Arctic, Env. Pollut. **104** 1 (1999) 131–143.

[15] CHOUHAN, S.L., SCHEIER, N.W., PETERSON, S.R., CHERPAC, an environmental transport code, and its predictions of environmental sensitivities in agricultural and forest ecosystems, Radioprotection, **46** 6 S515–S520, EDP Sciences, DOI: 10.1051 / radiopro / 20116784s (2011).

[16] CHOUHAN, S.L., NSENGIYUMVA, D., BOURGOUIN, P., BENSIMON, D., SCHEIER, N.W., Comparison of Atmospheric Dispersion, (CSA-ERM and MLCD) and Food-Chain (CHERPAC and AgriCP) Models Among Themselves and Against Gentilly Data, Canadian Radiation Protection Annual Conference, Halifax, Canada (2012).
[17] CHOUHAN, S.L. SCHEIER. N.W., CHERPAC Version 2.0 Program Abstract, Theory Manual, User's Manual, Design Description, Verification Report, Validation Report and Version Tracking Record, AECL Draft Report 153-112320-SDAL-001 (In preparation).
[18] PRÖHL, G., "Interception", Quantification of Radionuclide Transfers in Terrestrial and Freshwater Environments for Radiological Assessments, IAEA-TECDOC-1616, IAEA, Vienna (2009) 29–43.
[19] HOWARD, B., BERESFORD, N.A., BARNETT, C.L., FESENKO, S., "Transfer to animals' Quantification of Radionuclide Transfers in Terrestrial and Freshwater Environments for Radiological Assessments, IAEA-TECDOC-1616, IAEA, Vienna (2009) 267–307.
[20] SANZHAROVA, N., FESENKO, S., REED, E., "Processes governing radionuclide transfer to plants", Quantification of Radionuclide Transfers in Terrestrial and Freshwater Environments for Radiological Assessments, IAEA-TECDOC-1616, IAEA, Vienna (2009) 123–138.
[21] VIDAL, M., RIGOL, A., GIL-GARCÍA, C.J., "Soil-radionuclide interactions", Quantification of Radionuclide Transfers in Terrestrial and Freshwater Environments for Radiological Assessments, IAEA-TECDOC-1616, IAEA, Vienna (2009) 71–102.
[22] STREBL, F., LETTNER, H., HUMBER, A.K., BOSSEW, P., "Radionuclide transfer in alpine ecosystems", Quantification of Radionuclide Transfers in Terrestrial and Freshwater Environments for Radiological Assessments, IAEA-TECDOC-1616, IAEA, Vienna (2009) 397–401.
[23] CALMON, P., THIRY, Y., ZIBOLD, G., RANTAVAARA, A., FESENKO, S., ORLOV, O., "Radionuclide transfer in forest ecosystems", Quantification of Radionuclide Transfers in Terrestrial and Freshwater Environments for Radiological Assessments, IAEA-TECDOC-1616, IAEA, Vienna (2009) 333–380.
[24] PALSSON, S.E., SKUTERUD, L., FESENKO, S., GOLIKOV, V., "Radionuclide transfer in Arctic ecosystems", Quantification of Radionuclide Transfers in Terrestrial and Freshwater Environments for Radiological Assessments, IAEA-TECDOC-1616, IAEA, Vienna (2009) 381–396.
[25] MONTE, L., BRITTAIN, J.E., HÅKANSON L., HELING, R., SMITH, J.T., ZHELEZNYAK, M., Review and assessment of models used to predict the fate of radionuclides in lakes, J. Env. Rad. **69** (2003) 177–205.
[26] MONTE, L., BRITTAIN, J.E., HÅKANSON, L., SMITH, J.T., VAN DER PERK, M., Review and assessment of models used to predict the migration of radionuclides from catchments, J. Env. Rad. **75** (2004) 83–103.
[27] MONTE, L. BRITTAIN, J.E., HÅKANSON, L., SMITH, J.T., BOYER, P. LEPICARD, S., Review and assessment of models used to predict the migration of radionuclides through rivers, J. Env. Rad. **79** (2005) 273–296.
[28] IOSJPE, M., Evaluation of the environmental parameters controlling the vulnerability of the coastal marine regions, Radioprotection **46** 6 (2011) S289-S293.

[29] INTERNATIONAL COMMISSION ON RADIOLOGICAL PROTECTION, Age-Dependent Doses to Members of the Public from Intake of Radionuclides: Part 5, Compilation of Ingestion and Inhalation Coefficients, ICRP Publication 72, Elsevier (1996).

[30] CANADIAN STANDARDS ASSOCIATION, Guidelines for Calculating Derived Release Limits for Radioactive Material in Airborne and Liquid Effluents for Normal Operation of Nuclear Facilities. Standard CAN/CSA-N288.1-M87, CSA, Rexdale, ON (1987).

[31] MÜLLER, H., GERING, F., PRÖHL, G., Model Description of the Terrestrial Food Chain and Dose Module FDMT in RODOS PV6.0. RODOS(RA3)-TN(03)06 (2006). Available at: http://www.rodos.fzk.de/Documents/Public/HandbookV6/Volume3/FDM_Terra.pdf

[32] EHRHARDT J., The RODOS system: decision support for off-site emergency management in Europe, Rad. Prot. Dos. **73** 1–4 (1997) 35–40.

[33] IEVDIN, I., TRYBUSHNYD., ZHELEZNYAK, M., RASKOB, W., RODOS re-engineering: aims and implementation details, Radioprotection **45** 5 (2010) S181–S189.

[34] MÜLLER, H., PRÖHL, G., ECOSYS-87: A Dynamic Model for Assessing Radiological Consequences of Nuclear Accidents, Health Physics **64** 3 (1993) 232–25.

[35] BASE, C.F., SHARP, R.D., A proposal for estimation of soil leaching and leaching constants for use in assessments models, J. Env. Quality **12** (1983) 17–28.

[36] MÜLLER, H., GERING F., PRÖHL, G., Model Description of the Terrestrial Food Chain and Dose Module FDMT in RODOS PV4.0, Report RODOS(WG3)-TN(99)17, Forschungszentrum, Karlsruhe (2000).

[37] MÜLLER, H., GERING F., PRÖHL G., Model Description of the Terrestrial Food Chain and Dose Module FDMT in RODOS PV6.0, Report RODOS(WG3)-TN(03)06, Forschungszentrum, Karlsruhe (2003).

[38] SDOUZ, G., PACHOLE, M., Food chain data customization for decision support systems in Austria, Second European IRPA Congress on Radiation Protection, 15–19 May 2006, Paris, France (2006).

[39] LETTNER H., BOSSEW P., STREBL F., ^{137}Cs und ^{90}Sr Verteilung auf Almen der Salzburger Hohen Tauern und Aktivitätskonzentrationen in Lebensmitteln, Salzburg (2003) (in German).

[40] CANADIAN STANDARDS ASSOCIATION, Guidelines for calculating derived release limits for radioactive material in airborne and liquid effluents for normal operation of nuclear facilities, CAN/CSA N288.1-08, Mississauga, ON (2008).

[41] INTERNATIONAL ATOMIC ENERGY AGENCY, Generic Models for Using in Assessing the Impact of Discharges of Radioactive Substances to Environment, Safety Reports Series No. 19, IAEA, Vienna (2001).

[42] NATIONAL COUNCIL ON RADIATION PROTECTION AND MEASUREMENTS, Screening Models for Releases of Radionuclides to Atmosphere, Surface Water and Ground, NCRP Report No. 123I, Bethesda, MD (1996).

[43] ECOMETRIX INCORPORATED, Derived Release Limits Guidance. COG-06-3090R2-1 (2008).

[44] ENVIRONMENT CANADA, National Climate Data and Information Archive, Canadian Climate Normals 1971–2000, Key Lake Saskatchewan, EC (2011). Available at: http://climate.weatheroffice.gc.ca/climate_normals/results_e.html?stnID=3377&prov=&lang=e&dCode=4&dispBack=1&StationName=key_lake&SearchType=Contains&province=ALL&provBut=&month1=0&month2=12
[45] ECOMETRIX INCORPORATED, Key Lake Project: Environmental Risk Assessment (2005).
[46] ECOMETRIX INCORPORATED, Key Lake Extension Project Ecological and Human Health Risk Assessment (2012).
[47] HANSON, W., ^{137}Cs concentrations in northern Alaskan Eskimos, 1962–79: Effects of ecological, cultural, and physical factors, Health Phys. **42** 4 (1982) 433-447.
[48] RAMZAEV, P.V., MIRETSKIY, G.M., TROITSKAYA, M.N., Features of the USSR Territory around the Novaya Zemlya Nuclear Test Site, Report to the Soviet-Finnish meeting of experts, Moscow, 28 February, (1991).
[49] HOFMANN, W., ATTARPOUR, N., LETTNER, H., TURK, R., ^{137}Cs concentrations in lichens before and after the Chernobyl accident, Health Phys. **64** 1 (1993) 70–73.
[50] DIETERICH, R.A., MORTON, J.K., Reindeer Health Aid Manual, US Department of Agriculture, AFES Misc. Pub 90-4 CES 100H-00046 (1990).
[51] ÅHMAN, B., Modelling radiocaesium transfer and long-term changes in reindeer, J. Env. Rad. **98** (2007) 153–165.
[52] HOLLEMAN, D.F., LUICK, J.R., WHITE, R.G., Lichen intake estimates for reindeer and caribou during winter, J. Wildlife Manage. **43** 1 (1979) 192–201.
[53] SKUTERUD, L., PEDERSEN, Ø., STAALAND, H., RØED, K. H., SALBU, B., LIKEN, A., HOVE, K., Absorption, retention and tissue distribution of radiocaesium in reindeer: effects of diet and radiocaesium source, Rad. Env. Biophys. **43** 4 (2004) 293–301.
[54] TRACY, B.L., KRAMER, G.H., A method for estimating caribou consumption by northern Canadians, Arctic **53** (2000) 42–52.
[55] MACDONALD. C.R., ELKIN, B.T., TRACY, B.L., Radiocesium in caribou and reindeer in northern Canada, Alaska and Greenland from 1958 to 2000, J. Envi. Rad. **93** (2007) 1–25.
[56] MONTE, L., BRITTAIN, J.E., GALLEGO, E., HÅKANSON, L., HOFMAN, D., JIMÉNEZ, A., MOIRA-PLUS: A decision support system for the management of complex fresh water ecosystems contaminated by radionuclides and heavy metals, Computers and Geosciences **35** (2009) 880–896.
[57] HÅKANSON, L., Modelling Radiocesium in Lakes and Coastal Areas – New Approaches for Ecosystem Modellers, 1st Edition, Kluwer Academic Publishers, Dordrecht (2000) 215.
[58] HÅKANSON, L., PETERS, R.H., Predictive Limnology, 1st Edition, SPB Academic Publishing, Amsterdam (1995) 464.
[59] MONTE, L., A generic model for assessing the effects of countermeasures to reduce the radionuclide contamination levels in abiotic components of fresh water systems and complex catchments, Env. Mod. and Software **16** (2001) 669–690.
[60] INTERNATIONAL ATOMIC ENERGY AGENCY, Modelling of the transfer of radiocaesium from deposition to lake ecosystems, Report from the VAMP Aquatic Working Group, IAEA-TECDOC-1143, IAEA, Vienna (2000).

[61] STRAND, P., BØE, E., BERTEIG, L., BERTHELSEN, T., STRAND, T., TRYGG, K., HARBITZ, O., Whole-body counting and dietary surveys in Norway during the first year after the Chernobyl accident, Rad. Prot. Dos. **27** (1989) 163–171.
[62] MONTE, L., HÅKANSON, L., PERIAÑEZ, R., LAPTEV, G., ZHELEZNYAK, M., MADERICH, V., ANGELI, G., KOSHEBUTSKY, V., Experiences from a case study of multi-model application to assess the behavior of pollutants in the Dnieper-Bug estuary, Eco. Mod. **195** (2006) 247–263.
[63] STRAND, T., STRAND, P., BAARLI, J., Radioactivity in foodstuffs and doses to the Norwegian population from the Chernobyl fall-out, Rad. Prot. Dos. **20** (1987) 211–220.
[64] SALBU, B., BJØRNSTAD, H.E., BRITTAIN, J.E., Fractionation of Cs-isotopes and 90-Sr in snowmelt run-off and lake waters from a contaminated Norwegian mountain catchment, J. Rad. Nuc. Chem. **156** (1992) 7–20.
[65] PSALTAKI, M.G., FLOROU, H. MARKATOS, N.C., A model of the behaviour of Caesium-137 in Marine Environment (A Finite-Volume Method Implementation), Proc. of the 1st WSEAS International Conference on Finite-Differences-Finite Elements-Finite Volumes, Malta, 11–13 September (2008) 74–78.
[66] PSALTAKI, M., FLOROU, H., TRABIDOU, G., MARKATOS, N.C., Modelling and the assessment of anthropogenic impacts on marine ecosystems, Book of Abstracts of the 2nd International Conference on "Environmental Management , Engineering Planning and Economics (CEMEPE) and SECOTOC Conference, Mykonos, 21–26 June (2009) 83.
[67] PSALTAKI, M., MARKATOS, N., Implementing the Finite-Volume method in simulating the behaviour of pollutants in marine environment, Proc. of the 4th IASME/WSEAS International Conference on CONTINUUM MeCHANICS (CM'09), Cambridge, UK, 24–26 February (2009) 187–199.
[68] PSALTAKI, M., FLOROU, H., TRABIDOU, G., MARKATOS, N.C., Modelling and assessment of pollutant impact on marine environments, 2nd WSEAS International Conference on Computer Engineering and Applications (CEA '10), Harvard University, Cambridge, USA, 27–29 January (2010) 176–180.
[69] PAPADIMITRAKIS J., PSALTAKI M., CHRISTOLIS M., MARKATOS N.C., Three dimensional oil spill modelling for coastal waters, J. Marine Env. Eng. **7** 4 (2005) 249–260.
[70] PAPADIMITRAKIS, J., PSALTAKI, M., CHRISTOLIS, M., MARKATOS, N.C., Simulating the fate of an oil spill near coastal zones, Env. Mod. Software **21** 2, Elsevier (2006) 170–177.
[71] PETRIDOU, E., TRICHOPOULOS, D., DESSYPRIS, N., FLYTZANI, V., HAIDAS, S., KALMANTI, M., Infant leukaemia after in utero exposure to radiation from Chernobyl. Nature **382** 6589 (1996) 352–353.
[72] SIMOPOULOS, S.E., Soil sampling and ^{137}Cs analysis of the Chernobyl fallout in Greece, Applied Radiation and Isotopes **40** 7 (1989) 607–613.
[73] KRITIDIS, P., FLOROU, H,. Radiological impact in Greece of the Chernobyl accident – A 10-y retrospective synopsis, Health Physics **80** 5 (2001) 440–446.
[74] OLSON, D.B., KOURAFALOU, V.H., JOHNS, W.E., SAMUELS, G., VENEZIANI, M., Aegean surface circulation from a satellite-tracked drifter array, J. Phys. Ocean. **37** (2007) 1898–1917.

[75] TSAGARAKIS, K., COLL, M., GIANNOULAKI, M., SOMARAKIS, S., PAPACONSTANTINOU, C., MACHIAS, A., Food-web traits of the North Aegean Sea ecosystem (Eastern Mediterranean) and comparison with other Mediterranean ecosystems, Estuarine, Coastal and Shelf Science **88** (2010) 233–248.

[76] HOFMAN, D., MOIRA-DSS architecture, model integration and user interface design, In: Pahl-Wostl, C., Schmidt, S., Rizzoli, A.E., Jakeman, A.J. (Eds.), Complexity-and Integrated Resources Management, Transactions of the Second Biennial Meeting of the International Environmental Modelling and Software Society, IEMSS, Manno, Switzerland (2004) 1–5.

[77] MONTE, L., VAN DER STEEN, J., BERGSTRÖM, U., GALLEGO DIAZ, E., HÅKANSON, L., BRITTAIN, J.E., The project MOIRA: a model based computerised system for management support to identify optimal remedial strategies for restoring radionuclide contaminated aquatic ecosystems and drainage areas – Final Report, ENEA RT/AMB/2000/13 (2000).

[78] HÅKANSON, L., SAZYKINA, T., A blind test of the MOIRA lake model for radiocesium for Lake Uruskul, Russia, contaminated by fallout from the Kyshtym accident in 1957, J. Env. Rad. **54** (2001) 327–344.

[79] INTERNATIONAL COMMISSION ON RADIOLOGICAL PROTECTION, 1990 Recommendations of the ICRP, Annals of the ICRP, Publication 60, Pergamon Press, Oxford (1991).

[80] MONTE, L., Customisation of the decision support system MOIRA-PLUS for applications to the marine environment, J. Env. Rad. **102** (2011) 1112–1116.

[81] INTERNATIONAL ATOMIC ENERGY AGENCY, IAEA, Sediment Distribution Coefficients and Concentration Factors for Biota in the Marine Environment, Technical Reports Series No. 422, IAEA, Vienna (2004).

[82] IOSJPE, M., BROWN, J., STRAND, P., Modified approach for box modelling of radiological consequences from releases into marine environment, J. Env. Rad. **60** 1–2 (2002) 91–103.

[83] IOSJPE M., Environmental Modelling: Modified Approach for Compartmental Models, In: Radionuclides in the Environment (Eds. P.P. Povinec, J.A. Sanchez-Cabeza), Rad. in Env. **8** (Series Editor: M.S. Baxter) (2006) 463–476.

[84] IOSJPE, M., KARCHER, M., J., GWYNN, I., HARMS, R., GERDES, R., KAUKER, F., Improvement of the dose assessment tools on the basis of dispersion of the ^{99}Tc in the Nordic Seas and the Arctic Ocean, Radioprotection **44** 5 (2009a) 531–536.

[85] KÖBERLE, C., GERDES, R., Mechanisms determining the variability of Arctic Sea ice conditions and export, J. Clim. **16** (2003) 2843–2858.

[86] KARCHER, M., KAUKER, F, GERDES, R. HUNKE, E., ZHANG, J., On the dynamics of Atlantic Water circulation in the Arctic Ocean, J. Geophys. Res. **112**, C04S02, DOI:10.1029/2006JC003630 (2007).

[87] NIELSEN, S.P., IOSJPE, M., STRAND, P., Collective Doses to Man from Dumping of Radioactive Waste in the Arctic Seas, Sci. Total Env. **202** 1–3 (1997) 135–147.

[88] INTERNATIONAL ATOMIC ENERGY AGENCY, Modelling of the Radiological Impact of Radioactive Waste Dumping in the Arctic Seas, IAEA-TECDOC-1330, IAEA, Vienna (2003).

[89] EUROPEAN COMMUNITY, The Radiological Exposure of the Population of the European Community from Radioactivity in the Mediterranean Sea, Project ''MARINA-Med'', In: Radiation Protection Series **69**, EC XI-094/93, EC (1994).

[90] IOSJPE, M., REISTAD, O., AMUNDSEN, I.B., Radioecological consequences of a potential accident during transport of spent nuclear fuel along an Arctic coastline, J. Env. Rad. **100** (2009b) 184–191.
[91] BROWN, J.E., HOSSEINI, A., BØRRETZEN, P., THØRRING, H., Development of a methodology for assessing the environmental impact of radioactivity in Northern Marine environments, Mar. Pollut. Bull. **52** 10 (2006) 1127–1137.
[92] INTERNATIONAL ATOMIC ENERGY AGENCY, Environmental Modelling for Radiation Safety (EMRAS II), Working Group 8, Environmental Sensitivity: Documents, IAEA, Vienna (2011). Available at: http://www-ns.iaea.org/projects/emras/emras2/working-groups/working-group-eight.asp?s=8
[93] SMITH, K., JONES, A., Generalised habit data for radiological assessment, NRPB Report W41 (2003).
[94] JØRGENSEN, S.E., Fundamentals of ecological modelling, Dev. Env. Mod. **19**, Elsevier (1994).
[95] LYKOUSIS, V., ROUSSAKIS, G., ALEXANDRI, M., PAVLAKIS, P., PAPOULIA, I., Sliding and regional slope stability in active margin: North Aegean Trough (Mediterranean), Marine Geology **186** 3–4 (2002) 281–298.
[96] LATINOPOULOS, P.D., KRESTENITIS, Y.N. ,VALIOULIS, I.A., A decision analysis approach to a coastal pollution problem: the sewage system of the City of Thessaloniki (Greece), Proc. of the 1st Int. Conf. on Environmental Problems in Coastal Regions (Eds. A.J. Ferrante and C.A. Brebbia), Computational Mechanics Publications, Southampton (1996) 11–21.
[97] BALOPOULOS, E.T., Circulation and mixing in the water masses of the N.W. Aegean Sea, Noting effects of waste disposal in Thermaikos Gulf, PhD Thesis, University of Wales, (1982).
[98] INTERNATIONAL ATOMIC ENERGY AGENCY, Testing of Models for Predicting the Behaviour of Radionuclides in Freshwater Systems and Coastal Areas, Report of the Aguatic Working Group of EMRAS Theme 1, EMRAS TECDOC, IAEA, Vienna (2012). Available at: http://www-pub.iaea.org/MTCD/publications/PDF/TE_1678_CD/Reports/Theme_1_WorkingGroup4(Aquatic)/TestingofModelsforPredictingtheBehaviourofRadionuclidesinFreshwaterSystemsandCoastalAreas.pdf
[99] MONTE, L., A simple formula to predict approximate initial contamination of lakewater following a pulse deposition of radionuclide, Health Physics **68** (1995) 397–400.
[100] POULOS, S.E., CHRONIS, G.TH., COLLINS, M.B., LYKOUSIS, V., Thermaikos Gulf Coastal System, NW Aegean Sea: an overview of waterrsediment fluxes in relation to air–land–ocean interactions and human activities, J. Marine Sys. **25** (2000) 47–76.
[101] KORRES, G., LASCARATOS, A., HATZIAPOSTOLOU, E., KATSAFADOS, P., Towards an Ocean Forecasting System for the Aegean Sea, The Global Atmosphere and Ocean System **8** 2–3 (2002) 191–218.
[102] SIMOPOULOS, S.E., AGELOPOULOS, M.G., Deposition measurments in Europe after the Cernobyl accident and comparison with the Greek NTUA data set, In: Workshop on the Long term follow up of the Chernobyl Disaster, Athens, Greece, 6–8 December (1991) 157–171.
[103] FLOROU, H., KRIRIDIS, P., The dispersion of ^{137}Cs in the Aegean Sea, Radiochimica Acta 66/67 (1994) 415–417.

[104] EGOROV, V.N., POVINEC, P.P., POLIKARPOV, G.G., STOKOZOV, N.A., GULIN, S.B., KULEBAKINA, L.G., OSVATH, I., ^{90}Sr and ^{137}Cs in the Black Sea after the Chernobyl NPP Accident: Inventories, balance and tracer applications, J. Env. Rad. **43** 2 (1999) 137–155.

[105] SKOULIKIDIS, N., Significance evaluation of factors controlling river water composition, Env. Geol. **22** (1993) 178–185.

[106] KOURAFALOU, V.H., SAVVIDIS, Y.G., KRESTENITIS, Y.N., KOUTITAS, G.C., Modelling studies on the processes that influence matter transfer on the Gulf of Thermaikos (NW Aegean Sea), Continental Shelf Research **24** (2004) 203–222.

[107] THÉBAULT, H., RODRIGUEZ Y BAENA, A.M., ANDRAL, B., BARISIC, D., ALBALADEJO, J.B., BOLOGA, A.S., ^{137}Cs baseline levels in the mediterranean and black sea: A cross-basin survey of the CIESM mediterranean mussel watch programme, Marine Poll. Bull. **57** 6–12 (2008) 801–806.

[108] KATSIKI, V. A., FLOROU, H., Study on the behaviour of the heavy metals Cu, Er, Ni, Zn, Fe, Mn and ^{137}Cs in an estuarine ecosystem using mytilus galloprovincialis as a bioindicator species: The case of thermaikos Gulf, Greece, J. Env. Rad. **86** 1 (2006) 31–44.

[109] FLOROU, H., CHALALOU, CH., LYKOMITROU, CH., MADOPOULOU M., Enviromental radioactivity monitoring in Greece: present knowledge and planned study, In: Mediterranean Mussel Watch – Designing a regional program, Marseilles, CIEM Workshop Series No. 15 (2002) 63–66.

[110] PAPUCCI, C., DELFANTI, R., 137 Caesium distribution in the eastern mediterranean sea: Recent changes and future trends, Sci. Total Env. 237–238 (1999) 67–75.

[111] FLOROU, H., ^{137}Cs inventory in abiotic component and biota from the aegean and ionian sea – Greece, Chemistry and Ecology **1** 2(4) (1996) 253–258.

[112] EVANGELIOU, N., FLOROU, H., SCOULLOS, M., A preliminary study of particle dynamics in the water column of Saronikos Gulf, Greece, by using Th-234/U-238 disequilibrium approach, Desalination and Water Treatment, **13** 1–3 (2010) 290–302.

[113] TSABARIS, C., KAPSIMALIS, V., ELEFTHERIOU, G., LAUBENSTEIN, M., KABERI, H., PLASTINO, W., ^{137}Cs geochronology in Thessaloniki Gulf sediments, Greece, J. Env. Earth Sci., DOI: 10.1007/s12665-012-1530-5 (2012).

[114] KARAGEORGIS, A.P., KABERI, H., PRICE, N.B., MUIR, G.K.P., PATES, J.M., LYKOUSIS, V., Chemical composition of short sediment cores from Thermaikos Gulf (Eastern Mediterranean): Sediment accumulation rates, trawling and winnowing effects, Continental Shelf Research **25** 19–20 (2005) 2456–2475.

[115] FLOROU, H., NICOLAOU, G., EVANGELIOU, N., The concentration of ^{137}Cs in the surface of the greek marine environment, J. Env. Rad. **101** 8 (2010) 654–657.

[116] EVANGELIOU, N., FLOROU, H., BOKOROS, P., SCOULLOS, M., Temporal and spatial distribution of ^{137}Cs in eastern mediterranean sea. horizontal and vertical dispersion in 2 regions, J. Env. Rad. **100** 8 (2009) 626–636.

[117] DELFANTI, R., KLEIN, B., PAPUCCI, C., Distribution of ^{137}Cs and other radioactive tracers in the eastern mediterranean: Relationship ot the deepwater transient, J. of Geo. Res. C. Oceans, **108**:9 (2003) 9–10.

[118] TSABARIS, C., Unpublished data, Personal Communication (2009).

CONTRIBUTORS TO DRAFTING AND REVIEW

Barabash, S.	EcoMetrix Incorporated, Canada
Berkovskyy, V.	International Atomic Energy Agency
Brittain, J.E.	University of Oslo, Norway
Carini, F.	Università Cattolica del Sacro Cuore, Italy
Chouhan, S.L.	Atomic Energy of Canada Limited, Canada
Eleftheriou, G.	National Technical University of Athens, Greece
Iosjpe, M.	Norwegian Radiation Protection Authority, Norway
Markatos, N.C.	National Technical University of Athens, Greece
Monte, L.	Italian National Agency for New Technologies, Energy and Sustainable Economic Development, Italy
Psaltaki, M.	National Technical University of Athens, Greece
Scheier, N.W.	Atomic Energy of Canada Limited, Canada
Shen, G.	EcoMetrix Incorporated, Canada
Tracy, B.L.	(Retired, Formerly of) Health Canada, Canada
Tschiersch, J.	Helmholtz-Zentrum München GmbH, Germany
Turcanu, C.	Belgian Nuclear Research Centre, Belgium

LIST OF PARTICIPANTS

Barabash, S.	EcoMetrix Incorporated, Canada
Berkovskyy, V.	International Atomic Energy Agency
Bodor, K.	Atomic Energy Research Institute, Hungary
Brittain, J.E.	University of Oslo, Norway
Camps, J.	Belgian Nuclear Research Centre, Belgium
Carini, F.	Università Cattolica del Sacro Cuore, Italy
Chouhan, S.L.	Atomic Energy of Canada Limited, Canada
El Kadi Abderrezzak, K.	Electricité de France, France
Eleftheriou, G.	National Technical University of Athens, Greece
Florou, H.	National Center for Scientific Research “Demokritos”, Greece
Földi, A.	Atomic Energy Research Institute, Hungary
Howard, B.J.	Centre for Ecology and Hydrology, United Kingdom
Iosjpe, M.	Norwegian Radiation Protection Authority, Norway
Monte, L.	Italian National Agency for New Technologies, Energy and Sustainable Economic Development, Italy
Mothersill, C.	McMaster University, Canada
Muikku, M.	Radiation and Nuclear Safety Authority, Finland
Outola, I.	Radiation and Nuclear Safety Authority, Finland
Parache, V.	Institut de Radioprotection et de Sûreté Nucléaire, France
Proehl, G.	International Atomic Energy Agency
Psaltaki, M.	National Technical University of Athens, Greece
Saizar Rodríguez, A.	Dirección Nacional de Medio Ambiente, Uruguay
Seymour, C.	McMaster University, Canada
Shen, G.	EcoMetrix Incorporated, Canada
Strebl, F.	Austrian Institute of Technology GmbH, Austria
Sweeck, L.	Belgian Nuclear Research Centre, Belgium
Tracy, B.L.	(Retired, Formerly of) Health Canada, Canada
Tschiersch, J.	Helmholtz-Zentrum München GmbH, Germany
Turcanu, C.	Belgian Nuclear Research Centre, Belgium
Vandenhove, H.	Belgian Nuclear Research Centre, Belgium
Varga, B.	Hungarian Agricultural Authority, Food and Feed Safety Directorate, Hungary
Willrodt, C.	Bundesamt für Strahlenschutz, Germany
Ytre-Eide, M.	Norwegian Radiation Protection Authority, Norway

EMRAS II Technical Meetings, IAEA Headquarters, Vienna

Vienna, Austria: 19–23 January 2009, 25–29 January 2010, 24–28 January 2011

Interim Working Group Meetings, EMRAS II, Working Group 8

Piacenza, Italy: 1–2 July 2010
Brussels, Belgium: 27–28 September 2011

International Atomic Energy Agency
Vienna
ISBN 978–92–0–112610–8
ISSN 1011–4289